DOTTORATO DI RICERCA IN INGEGNERIA CIVILE PER L'AMBIENTE ED IL TERRITORIO
XVI Ciclo - Nuova Serie (2014-2017)
DIPARTIMENTO DI INGEGNERIA CIVILE, UNIVERSITÀ DEGLI STUDI DI SALERNO

THE EFFECTS OF ROOTS ON THE HYDRO-MECHANICAL BEHAVIOR OF UNSATURATED PYROCLASTIC SOILS

GLI EFFETTI DELLE RADICI SUL COMPORTAMENTO IDRO-MECCANICO DEI TERRENI PIROCLASTICI PARZIALMENTE SATURI

ING. VITTORIA CAPOBIANCO

Relatore:
PROF. ING. LEONARDO CASCINI

Coordinatore
PROF. ING. FERNANDO FRATERNALI

Correlatori:
PROF. ING. SABATINO CUOMO
ING. VITO FORESTA

In copertina: sezione del terreno piroclastico permeato da radici

THE EFFECTS OF ROOTS ON THE HYDRO-MECHANICAL BEHAVIOR OF UNSATURATED PYROCLASTIC SOILS

Finito di stampare il 01/03/2018

INDEX

FIGURE INDEX

TABLE INDEX

NOTATIONS

AEV	Air Entry value
a	Intercept of *(q-p')* enveloping equation
$a_{r,i}$	Cross section of single root
A_r	Rooted area
A_s	Soil cross section
B	Bare soil
C	Control series
c	Empirical parameter for *RAR* fitting equation
C	Integrated cohesion
Cr	Root cohesion
Cs	Soil cohesion
C/N	Carbon/Nitrogen ratio
D	Drying test
D	Duration of W test
d_i	Root diameter
e	Void ratio
e_0	Initial void ratio
e_{ini}	Initial void ratio at 3rd stage of growth
ET	Evapotranspiration
f	Empirical parameter for *RAR* fitting equation
FBM	Fiber Bundle Model
Fi (Δx)	Maximum pull out force allowed in the root belonging to i
FS	Factor of Safety
F_{tot}	Total force in the bundle
Gs	Specific Gravity
i	Index for diameter class
j	Index of the weakest root still unbroken in FBM
k	Soil hydraulic conductivity
(k-s)	Soil conductivity curve
k'	Parameter depending on θ and ϕ'
LAI	Leaf Area Index
M	Stress ratio of *(q-p')* enveloping equation

Ms	Dry mass of the root-permeated soil sample
N	Nutrient series
N	Diameter classes
n	Porosity
n_0	Initial porosity
n_i	Number of roots belonging to i-class diameter
n_{ini}	Initial porosity at 3rd stage of growth
n_{max}	Maximum number of roots
n_{min}	Minimum number of roots
NPK	Nitrogen, Phosphorous, Potassium
NV	No-vegetated
$n(z,d_i)$	Number of roots with diameter d_i
p'	Mean effective stress
Pf	Probability of failure
PWP	Pore Water Pressure
q	Deviatoric stress
$(q\text{-}p')$	Enveloping equation at critical state
q_{fbare}	Deviatoric stress at critical state for bare soil
$q_{frooted}$	Deviatoric stress at critical state for rooted soil
R	Reconstituted
RAI	Root Area Index
RAR	Root Area Ratio
$RARmax$	Maximum RAR
$RARn$	RAR of the root class diameter
RBM	Root Bundle Model
RH	Daily Relative Humidity
RM	Root dry biomass
RMD	Root Mass density
RVD	Root Volume Density
s	Matric soil suction
s_0	Initial soil suction
Sr	Saturation degree
SWCC	Soil Water Characteristic Curve
T_e	Daily external temperature
Tn	Normal component of root tensile strength
Tr	Root single tensile strength

Tr,n	Tensile strength of root class
Ts	Daily soil temperature
Tt	Tangential component of root tensile strength
TX	Triaxial test
U	Undisturbed
v	Specific volume
v_{cons}	Specific volume after consolidation process
V	Vegetated
V	Total volume of root-soil sample
VA	Vegetated block A
VB	Vegetated block B
VC	Vegetated block C
VD	Vegetated block D
Vr	Total volume occupied by roots
VWC	Volumetric Water Content
W	Wetting Test
w	Gravimetric water content
z	Depth of rooted soil
z_{max}	Maximum root depth
α	Empirical constant for Tr law
β	Empirical constant for Tr law
γd	Bulk density
γd_{cons}	Bulk density after consolidation process
γ_r	Root density
Δx	Displacement of the bundle
$\Delta s<0$	Soil suction reduction during W test
$\Delta s>0$	Daily suction increment during D test
ε_{coll}	Volumetric collapse
θ	Volumetric water content
θs	Saturated volumetric water content
$(\theta\text{-}s)$	Soil water characteristic curve
θ	Angle between the deformed root and initial vertical root
σ	Vertical stress
τ_f	Final shear strength
ϕ	Integrated friction angle
ϕ'	Internal friction angle

ABSTRACT

Pyroclastic soils are widely diffused all over the world and they are characterized by high porosity and an open metastable internal structure. In situ they usually cover the shallowest layers of slopes in unsaturated conditions. As consequence, they are often involved in rainfall induced flow-like landslides triggered, during the rainy season, by water infiltration in unsaturated pyroclastic soils on steep slopes. The rain water infiltration leads to the volumetric collapse of the metastable structure in unsaturated conditions, and to liquefaction in fully saturated conditions. Once triggered, the propagating mass can reach great distances and cause many damages when it impacts with structures or infrastructures. These damages can be count as loss of life and economic damages.

As risk mitigation measures for these rainfall induced flow-like landslides, structural and passive control works such as dissipative basins and/or brindles have been usually adopted over the centuries.

An alternative sustainable risk mitigation measure can be represented by bio-engineering techniques, since they use natural elements such as woods or vegetation for stabilizing slopes prone to failure.

The effectiveness of bio-engineering practices depends firstly on the soil properties. This aspect was investigated by carring out an experimental study on the effect of soil nutrients on the plant growth and how this is reflected on the soil hydraulic response. It was found that nutrient availability in soil enhance the plant growth, particularly the root number, and this increases the effectiveness of the vegetation on induced soil suction during evapotranspiration.

After this preliminary study, the hydro-mechanical behavior of pyroclastic soils (widely known as rich in nutrients) permeated by roots of perennial graminae, typically used for controlling surface erosion, was investigated.

From drying (Evapotranspiration) and wetting (Infiltration) test results it can be claimed that the presence of roots influences mostly the shallowest layers of the soil (up to 1.2 m). In particular, during drying the effect of roots on induced soil suction is highlighted in dry season, when

air temperatures are high and the vegetation is florid. On the other hand, during wetting, the presence of roots tends to delay the water infiltration, even if the magnitude of suction reduction depends on the initial condition.

Oedometer tests provided original insigths on the role of roots on the internal structure of these collapsible soils. In particular, it was found that during root growth, the soil structure tends to reduce its porosity and this is reflected into a reduction of the collapsibility of the root permeated soil during wetting in unsaturated condition.

Shear strength of rooted soil, performed trough consolidated drained and undrained triaxial tests, show that the presence of roots increases both total cohesion and the internal friction angle, proportionally with the root biomass in the soil. Moreover, consolidate triaxial test results in undrained conditions showed that during post-failure stage the presence of roots reduces drastically the increment of pore water pressures avoiding the probability of static liquefaction of the material.

All those insights allow having a basic framework to design further experimental investigations in order to consider this technique a sustainable risk mitigation measure in unsaturated pyroclastic soils of the Campania region.

RINGRAZIAMENTI

Vorrei esprimere un sincero grazie alle persone che ho avuto vicino in questi tre anni di dottorato e senza le quali non sarei qui oggi.

Al mio tutor Prof. Leonardo Cascini, che sin dal primo giorno mi ha trasmesso il suo amore per la geotecnica e ha accettato la mia sfida con grande entusiasmo e passione. Senza la sua fiducia non avrei avuto il coraggio di "buttare il cuore oltre l'ostacolo" e appassionarmi alla ricerca, raggiungendo importanti traguardi e tante soddisfazioni.

Al Prof. Sabatino Cuomo, pronto a chiarire i miei dubbi geotecnici e ad aiutarmi a migliorare. Senza le sue battute e la sua pungente ironia non avrei affrontato le difficoltà con la giusta leggerezza.

Al mio maestro della sperimentazione l'Ing. Vito Foresta, persona leale e sincera con cui ho condiviso gioe e dolori di questo dottorato. Senza la sua preparazione, disponibilità, e talvolta il suo sforzo fisico, sarei certamente annegata negli abissi del laboratorio.

Agli strutturati del laboratorio di Geotecnica, i prof. Settimio Ferlisi, Dario Peduto, Michele Calvello, presenze costanti e punti di riferimento per qualsiasi necessità.

Un pensiero va a Mauro Forte e alla sua simpatica solarità, senza la quale i giorni passati al laboratorio non sarebbero stati gli stessi.

Agli assegnisti di ricerca e ai dottorandi, a tutti e ad ognuno di loro va il mio più sentito grazie per i piacevoli giorni passati insieme. Con affetto ricorderò le chiacchierate davanti a un "buon" caffè, i discorsi filosofici, i dubbi e le preoccupazioni che abbiamo condiviso durante questi tre anni.

Ringrazio di cuore il prof. Ng e tutto il suo gruppo per avermi accolto in un ambiente positivo e stimolante in cui ho avuto modo di imparare tanto durante il mio periodo di ricerca a Hong Kong. Grazie a Rafa, collega e amica, e a tutti gli amici che hanno allietato i miei mesi lontano da casa.

Grazie a Ilaria, con la quale ho condiviso la maggior parte dei traguardi accademici. Ricorderò con affetto e con un velo di nostalgia come eravamo e come, con sacrificio, impegno e tanta determinazione, siamo cresciute e maturate insieme durante questi anni. Gioisco due volte oggi per il nostro traguardo, con la speranza di poterne condividere ancora tanti insieme.

Un grazie a quello che è de "Il classico dell'amicizia", il gruppo degli amici di una vita e per la vita. Grazie ad Annalisa e Ilaria, una la mia ala, l'altra il mio grillo parlante. E grazie a Sofia e Chiara, semplicemente le mie sorelle.

A ki da sempre ha creduto in me, spesso più di me. Con cuore e ragione mi ha sostenuto nei momenti negativi, rendendo unici quelli positivi.

Alla mia famiglia, nonna Sofia, Michele e i miei genitori. I pilastri della mia vita. Grazie per avermi supportato nelle scelte, anche quando non condivise, dimostrando sempre sincero amore e grande fiducia. Spero di avervi resi fieri di me.

ABOUT THE AUTHOR

Vittoria Capobianco graduated in July 2014 in Environmental Engineering at University of Salerno with 110/110 cum laude. As part of the PhD activities, she performed soil suction and volumetric water content monitoring of soil permeated by roots in 1D physical model directly constructed at University of Salerno for the PhD purposes.
Within the PhD research, she perfomed conventional laboratory tests, on bare soils and rooted soils to investigate the effect of roots on collapsibility and the soil shear strength.
Part of the research was conducted at Hong Kong University of Science and Technology, where she improved her knowledge on bio-engineering investigation and conducted an experimental study on the effect of nutrients in soil on plant growth and the induced soil hydraulic response. During the period abroad, she attended the "Unsaturated Soil Mechanics and Engineering" course and passed the final written examination.

Vittoria Capobianco consegue nel Luglio 2014 la laurea specialistica in Ingegneria per l'Ambiente e il Territorio persso l'Università di Salerno con votazione 110/110 e lode. Nell'ambito del Corso di Dottorato realizza un modello fisico 1D in vera grandezza presso l'Università di Salerno per il monitoraggio dei valori di suzione e contenuto d'acqua dei terreni permeati da radici.
Nel corso della sperimentazione, conduce test di laboratorio convenzionali su provini di terreno con radici e senza radici per investigare l'effetto delle radici sulla collassabilità e sulla resistenza al taglio.
Parte dell'attività di ricerca è stata svolta presso l'Hong Kong University of Science and Technology, dove ha condotto uno studio sperimentale sull'effetto della presenza di nutrienti nel suolo sulla crescita delle piante e di conseguenza sulla risposta idraulica dei terreni radicati. Durante il periodo all'estero, ha seguito il corso di "Meccanica dei terreni parzialmente saturi" passando l'esame scritto finale.

1 INTRODUCTION

Some unsaturated soils having high porosity are known as "metastable" soils, because they can show irreversible volumetric collapse due to wetting under a constant mean effective stress.
Among them, pyroclastic soils produced by volcanic eruptions, are worldwide diffused and form shallow deposits of thickness up to few meters along the slopes rounding the volcanic areas.
As examples, pyroclastic soils covering mountainous basins of around 3000 km^2 in Southern Italy (Campania region), due to the volcanic activities of Somma-Vesuvius, are typically in unsaturated conditions and show a very open structure, which induces to volumetric collapse when suction is reduced due to rainfall infiltration.
Rainfall induced flow-like landslides systematically occur in these soils, as confirmed by the catastrophic events recorded in the last decades. These are caused by the most likely triggering mechanisms during the rainy season, such as the volumetric collapse due to wetting in unsaturated conditions and the consequent static liquefaction in saturated conditions.
Since the Middle Age landslide risk mitigation measures adopted in Campania region are mostly characterized by passive control works, which allow to the triggering of the unstable mass and reduce the risk by intercepting the flow during its propagation (brindle, channeling) or in the deposition zone (dissipative basins). However, these mitigation measures are expensive, environmental impactful and require frequent maintenance.
On the other hand, among the active control works (aimed to avoid the triggering of the unstable mass) bio-engineering techniques can represent an alternative and sustainable choice for unsaturated pyroclastic covers.
Among them, the use of living plant materials, established by conventional seeding or live planting, is widely diffused to treat sites where surface stability and erosion problems arise.
The aim of this PhD thesis is to provide a contribution on the study of the effectiveness of using indigenous grasses (*graminae* species), which develop roots up to 2 m of depth, in unsaturated pyroclastic soils as

natural-based solution for slopes affected by rainfall induced flow-like landslides.

In particular, in Chapter 2 general features and geotechnical characteristics of pyroclastic soils, with a focus on those of Campania region, are discussed. The monitoring data of soil suction regimes in four test sites are collected from literature contributions and compared with seasonal trends of suction proposed by Cascini et al. (2014).

Chapter 3 introduces flow-like landslides and how they are classified in literature, highlighting the characteristics of debris flows and hyperconcentrated flows which seasonally occur in Campania region.

The triggering stage, failure and postfailure stage are described to better understand the typical mechanisms in which pyroclastic soils are involved due to rainfall. Then, a brief description of the ancient and recent risk mitigation measures and their limitations are discussed.

In Chapter 4 the bio-engineering practices for reinforcing the hydro-mechanical behavior of unsaturated soils are introduced and the experimental study conducted at Hong Kong University of Science and Technology on the effect of a rich nutrient soil on the effectiveness of vegetation on inducing soil suction is explained. The contents of this Chapter have been published as technical note contribution (Ng et al., 2018 in press).

Chapter 5 introduces the experimental study conducted at University of Salerno with the description of the physical model used for the investigation on the effect of vegetation, specifically roots, on the hydro-mechanical behavior of unsaturated pyroclastic soils.

Chapter 6 explaines the results obtained during the experimental investigation on the hydro-mechanical response of vegetated pyroclastic soils to atmospheric stresses (evapotranspiration and rainfall infiltration). Some of the contents of this Chapter have been published in a note within the IARG 2017 conference (Capobianco et al., 2017).

Chapter 7 deals with the effects of the presence of roots on the collapsibility of unsaturated pyroclastic soils through standard oedometer tests conducted on both rooted soils and bare soils.

Finally, in Chapter 8 the contribution of roots on increasing the soil shear strength is investigated with standard isotripically consolidated drained and undrained triaxial tests. The experimental mechanical parameters are compared with those computed by the W&W model for predicting the root cohesion in soil during shear. Then, conclusions of research are outlined and further developments are proposed.

2 PYROCLASTIC SOILS

Why do people live close to volcanoes?
Volcanos are widespread all over the world and it is well known the devastating potential of lava flows, pyroclastic flows and heavy falls of ash, which are produced during volcanic eruption, over lands, structures and infrastructures developed around the volcano.
Nevertheless, many volcanic regions are highly populated since volcanic ash soils are widely recognized as rich in nutrients which makes lands fertile, encouraging the agricultural activities.
In the middle of 20th century volcanic ash soils received global recognition among soil scientists and in 1960 they were also identified for the first time in an international system of soil classification.
In the last decades the attention of scientific literature was focused on pyroclastic soils, whose physical and mechanical features are hereafter discussed mainly with reference to pyroclastic soils originated by Campi Flegrei and Somma-Vesusius eruptions in Campania region (southern Italy).

2.1 GENERAL FEATURES

2.1.1 Origin

Pyroclastic soils are produced by volcanic eruptions and they are distributed exclusively in areas where active or at least recently extinct volcanoes are located.
During an explosive eruption the magma rises from the mantle through the vent until the crust of the earth, with a subsequent explosion where magma is expelled either as lava or ash.
Lava is the semi-fluid non-explosive effusive rock that spills over the volcano surface, and when cooled forms tube like structures that run down the sides of the volcano by adding a new layer of igneous rock which covers the volcanoes cone.

Ashes consist on fragments of rocks, minerals and volcanic glass which are ejected by the eruption column. The height of the eruption column provides the explosiveness of the event (Fig. 2.1), in particular the higher the eruption column height, the larger the explosiveness. In relation to this factor, starting from the lower explosiveness, the Hawaiian, Strombolian, Vulcanian, and Plilian eruption types are defined in literature (Schmincke, 2004).

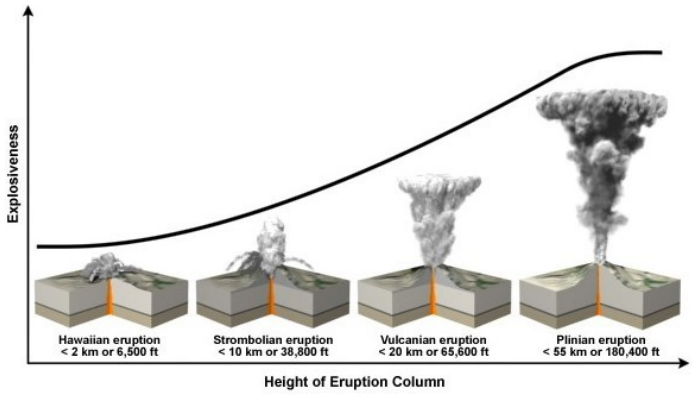

Figure 2.1 Relative explosiveness and Resulting height of eruption for different eruption types (US Geological Survey)

The ash clouds formed by the eruption column can extend around volcanic areas depending on several factors: grain size of fragments, wind speed and direction, and eruption type. The grain size of fragments typically decreases with distances (Fig. 2.2). Larger and heavier rock fragments fall down in the area close to the volcano, and progressively smaller and lighter fragments are transported farther from the volcano by wind (Johnston, 1997).

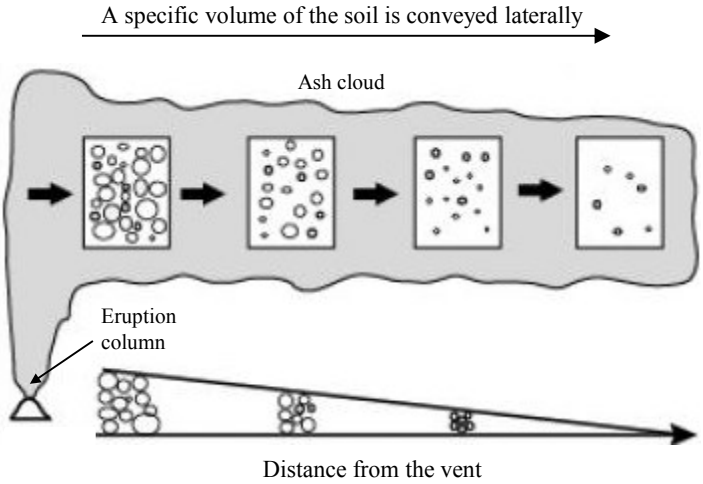

Figure 2.2 Schematic of ash clouds with mean particle size of ashes decreasing from the source of eruption (Johnston, 1997, modified)

Wind speed and direction during eruption strongly affect the dispersal pattern of volcanic ashes in the atmosphere and the dispersion of air fall deposits on the ground: significant change in wind directions within the same eruption event produces a complex dispersal pattern of pyroclastic deposits around the volcanic area. High wind speed can carry small volcanic ashes particles along great distance, as happened during the 2008 eruption of Chaitén in Chile: the ash cloud ejected by eruption column blew 1000 kilometers (620 miles) across Patagonia to Argentina, reaching both the Atlantic and Pacific coasts (Watt et al., 2009).
In the volcanic area, distribution and thickness of pyroclastic deposits of each eruption are quantified through the isopach lines, which are usually in form of ellipses and with elongation in the downwind direction. The dispersal axis of deposits is defined by the direction of elongation away from the vent. Figure 2.3 shows the isopach lines map of the 2008 eruption of Chaitén (Chile) and the dispersion of the ash clouds until the Argentina coast during the first week of eruption.

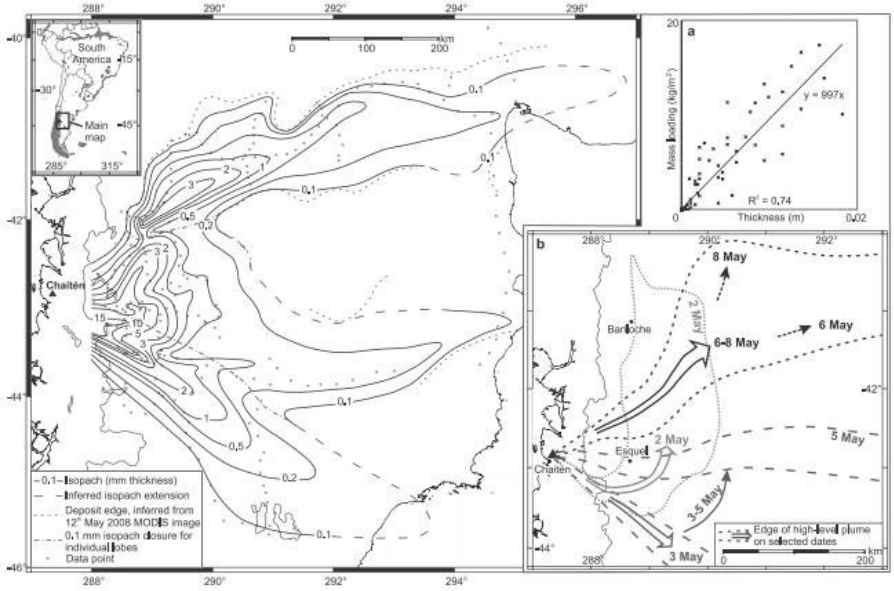

Figure 2.3 Isopach lines of the Chaitén distal ash deposit and thickness. a) Ashfall mass loading against thickness. b) plume dispersal over Argentina during the first week of eruption (Watt et al., 2009).

Among the pyroclastic products, bombs and blocks are fragments greater than 64 mm, while small debris such as scoria, pumice and ashes can be distingished depending on their grain size, composition and weigth.

Bombs and blocks are ejected respectively as incandescent lava fragments with aerodinamic shape and solid fragments with angular shape. Scoria and pumice are both ejected as highly porous fragments because of vescicles and holes formed by the gas dissolved in magma during eruption with different specific gravity (pumice is ligther than scoria and is not able to sink in water). The fragments smaller than 2 mm are usually named ashes (Fig. 2.4).

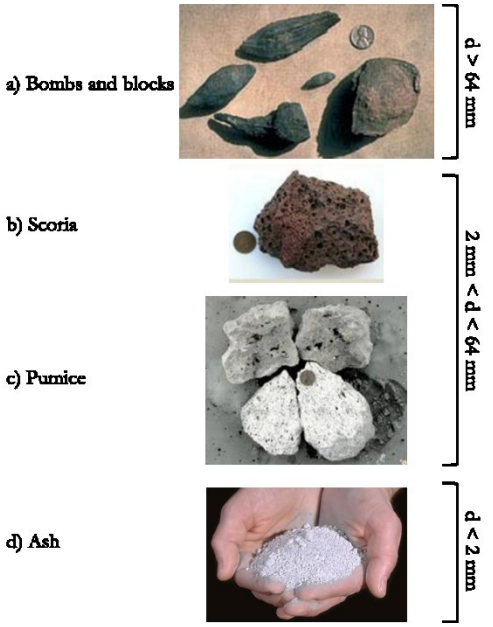

Figure 2.4 Size of eruption pyroclastic ejecta: a) bombs and blocks, b) scoria, c) pumice, d) ash.

2.1.2 Geographic distribution and land use

Volcanic ash soils, also called Andisols in US Soil Taxonomy (Soil Survey Staff, 1999) cover 124 million hectares, which means that they represent the 0.84% of the world's land surface (Leamy, 1984). They are widespread all over the world, covering the volcanic regions where active and recently extinct volcanoes are located.

Ashy soils derived by active volcanoes is distributed along the main borders of tectonic plates such as the Philippine Islands, Indonesia, Pacific Island in Asia, the Rift valley trough Yemen, Ethiopia, Rwanda and Burundi, or Cameroon and Kenya in Africa, the Circum-Pacific Ring of fire in western American coast. Some other regions where pyroclastic soils cover the hillsides around volcanoes are located in Southern Italy in Europe, New Zeland, and Japan, western provinces of China, Arizona, southern portion of British Columbia and Alberta of Canada (Fig. 2.5). Considering the worldwide distribution of active volcanoes, the majority of pyroclastic soils cover tropical regions (Takahashi & Shoji, 2002).

Despite the active volcanos eruption's hazard, human population living in volcanic regions is extremely dense because pyroclastic soils are widely

recognized as important resource for agricultural activities, especially for upland crop production. Many agricultural regions of the world are located near active or dormant volcanos (Shoji et al., 1993a) since, during each eruption, an intermittent addition of volcanic ash rich in nutrients is generated providing a renew of the soil fertility status. The 27% of the total agricultural land use in Japan consists on cultivated volcanic ash soils (Takahashi & Shoji, 2002), in Indonesia the most densely populated areas are found near volcanoes, in Italy the mount Etna region represents around the 7% of the whole land of Sicily but contains more than 20% of the population of the island, because of the Etna-related factors of fertile soils and a reliable freshwater supply (Duncan et al., 1981). In Campania region of Italy, more than 600,000 people live exposed to the Vesuvius eruption risk, and cultivate the volcanic lands with grapes, vegetables, orange and lemon trees, herbs, flowers and tomato.

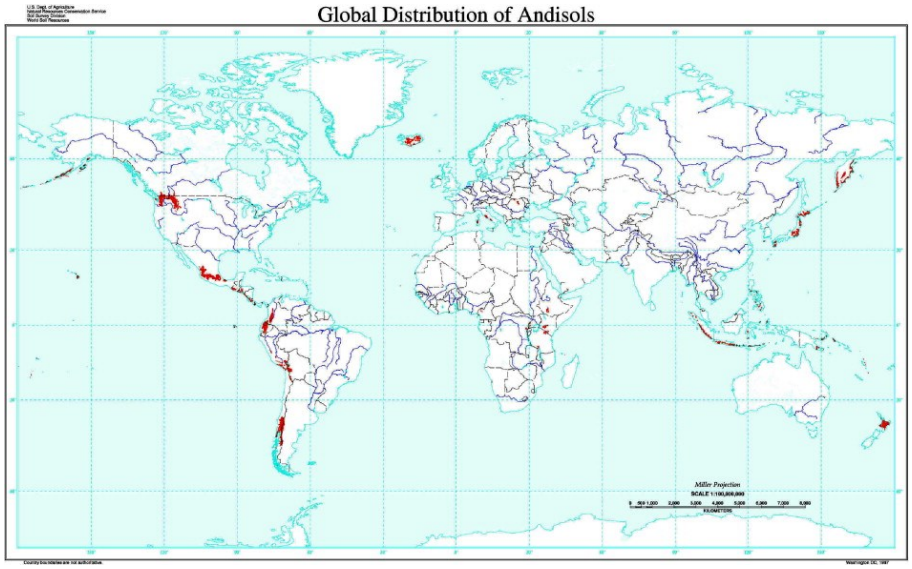

Figure 2.5 Worldwide distribution of volcanic ash soils (Andisols) according to World Soil Resources Staff, 1999 (Dahlgren et al., 2004).

The volcanic areas represent high natural hazard zones for two main reasons: the volcanic eruption hazard is related to volcano activity, and the shallow landslides hazard is usually greatly enhanced by the geomorphological features of hillsides and the hydro-mechanical

properties of pyroclastic deposits involved in landslides, as discussed in depth in the following sections for the case of pyroclastic soils in Campania region (Italy).

2.2 PYROCLASTIC SOILS IN CAMPANIA REGION

2.2.1 Origin and diffusion

Many areas of Campania region (southern Italy) are covered by pyroclastic soils produced by the past volcanos eruptions (Rolandi et al., 1998). In particular two main volcanic districts are distinguished in the so called "Campania Volcanic Zone" (CVZ): the Somma-Vesuvius district and the subordinated Campi Flegrei district with Ischia, Procida and Roccamonfina.
The Campi Flegrei depression volcanic zone is the older district of the area and is the result of two main episodes of subsidence: the older Campanian Ignimbrite caldera and the younger Neapolitan Yellow Tuff caldera formation. Inside the caldera more then seventy active eruptive centers were located (Budetta et al., 1993; Orsi et al., 1996; Rolandi et al., 2003) and intense fumarolic and hot spring activities are still frequent. The Campi Flegrei activities were studied by many authors in the past (Dellino et al., 2001, 2004; Fedi et al., 1991, 2004; Piochi 2005; Signorelli 2001). The pyroclastic soils produced by Campi Flegrei during the IV cycles of activities cover the Neapolitan area in either dissolved and litihified conditions. The products of the I cycle (> 35,000 years from now) are widespread all over the area; the Ignibrite campana (known as Tufo Grigio Campano), produced by the pyroclastic flow during the II cycle of eruptions (35,000-30,000 years from now), cover the Piana Campania site with thicknesses between 50-60 m; the Tufo stratified and Tufo Giallo Napoletano, the latter produced as pumices and lithic fragments, were the results of the III cycle of erutpions (18,000 – 10,000 years from now); the IV cycle of eruptions (10,000 years from now – 1538) produced pyroclastic loose products consisting of pumice, lapilli and ash (pozzolana).
The inactive volcanic apparatus of Roccamonfina had its last eruption more then 500.000 years from now. The diameter of the cone extends for 25 km and is located in the northern part of Campania region. Many

remarks of its past activities are reported in literature (Giordano 1998, Cole 1992, 1993; Vacca et al., 2003), while seismic movements and fresh water springs are still frequent.
Somma-Vesuvius is a moderate size (1281 m a.s.l.) volcano as the result of the older caldera Mt. Somma and the formation of the recent Vesuvius cone (Rolandi et al., 1998) that grew within the caldera after the AD 79 Pompei eruption (Fig. 2.6).

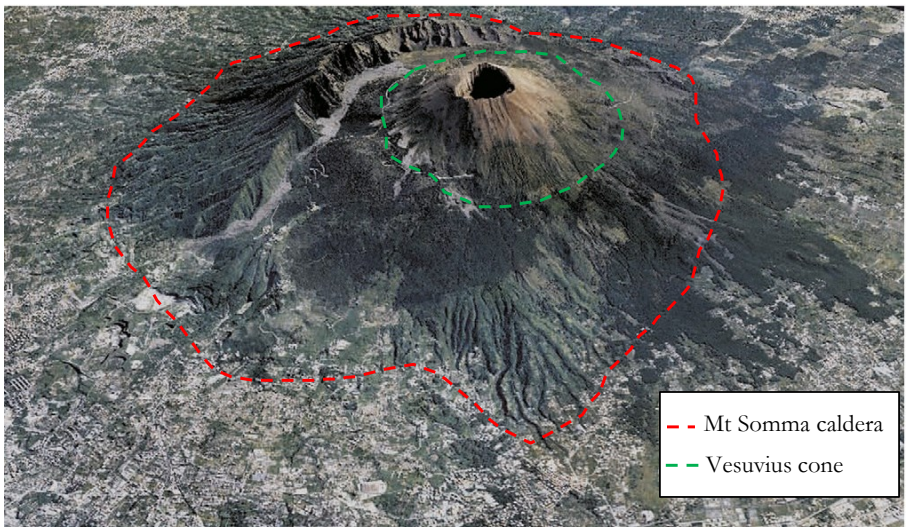

Figure 2.6 Vesuvius cone and Mt. Somma caldera (courtesy of Lab. Grafica e Immagini, INGV-Roma; Cioni et al., 2008 modified).

Vesuvius volcano is famous all over the world for the eruption of AD 79, which destructed the ancient Romanic city of Pompei. An accurate and suggestive description of this catastrophic event was reported by the Latin author Plinius in two letters to his friend, the historian Publius Cornelius Tacitus. The activities of the volcano started with the most ancient Plinian eruption (18,300 years BP) known as "Basal Pumice" eruption that caused the caldera formation, followed by three high-magnitude plinian eruptions called respectively Mercato (8000 years BP.; Rolandi et al., 1993a; Cioni et al., 1999b), Avellino (3800 years BP.; ; Lirer et al., 1973; Rolandi et al., 1993b; Cioni et al., 2000) and Pompei (AD 79) Pumice eruption (Lirer et al., 1973; Sigurdsson et al., 1985; Cioni et al., 1995).

Two subordinate eruptions occurred respectively in the 472 (Pollena) and 1631 (Principe et al., 2004), after that the activities became explosive with low intensity until the last eruption occurred in the 1944 (Cioni et al., 1999b; Arrighi et al., 2001).
Currently the Somma-Vesuvius is the only active volcano of the European mainland, and is one of the dangerous volcanos in the world because of the extremely dense population living around the volcanic cone. In order to enhance the emergency planning and the risk reduction, recently hazard assessment of new possible eruption scenarios were carried out (Todesco et al., 2002; Cioni et al., 2008; Gurioli et al., 2013).

2.2.2 Geological and Stratigraphical settings

The soil produced in Campania region from Somma-Vesuvius and Campi Flegrei eruption activities are distributed around the interested area either in dissolved and lithified conditions.
The area around Naples consists of lithified and dissolved pyroclastic soils originated by Campi Flegrei past activities, which appear very different in degree and type of alteration, even if they have similar composition, grain size, age and pre-eruptive environment.
On the other hand, the area covered by the pyroclastic deposits, originated from the Vesuvius past activities, is here presented with a brief summary about some features of the soils and their stratigraphical settings.
The pyroclastic deposits produced by Somma-Vesuvius were heterogeneously distributed in Campania region (southern Italy) according to the axes of dispersion reported in Fig. 2.7 in relation with the main plinian eruptions occurred (Cascini et al., 2008a). They covered three main geoenvironmental contexts: carbonate bedrock (A1, A2 in Fig. 2.7) around Sarno mountains, Monti Lattari and Monti Picentini, tuff and lava deposits (B in Fig. 2.7) located around the volcano and Caserta, and flysh and terrigenous bedrock (C in Fig. 2.7) in north east side (Calcaterra et al., 2004; Cascini et al., 2005). Pyroclastic soils covering carbonatic bedrock of Campania region are those which were mostly studied because in the years have been widely recognized as prone to landslide triggering induced by rainfall, as is discussed in depth in Chapter 3.

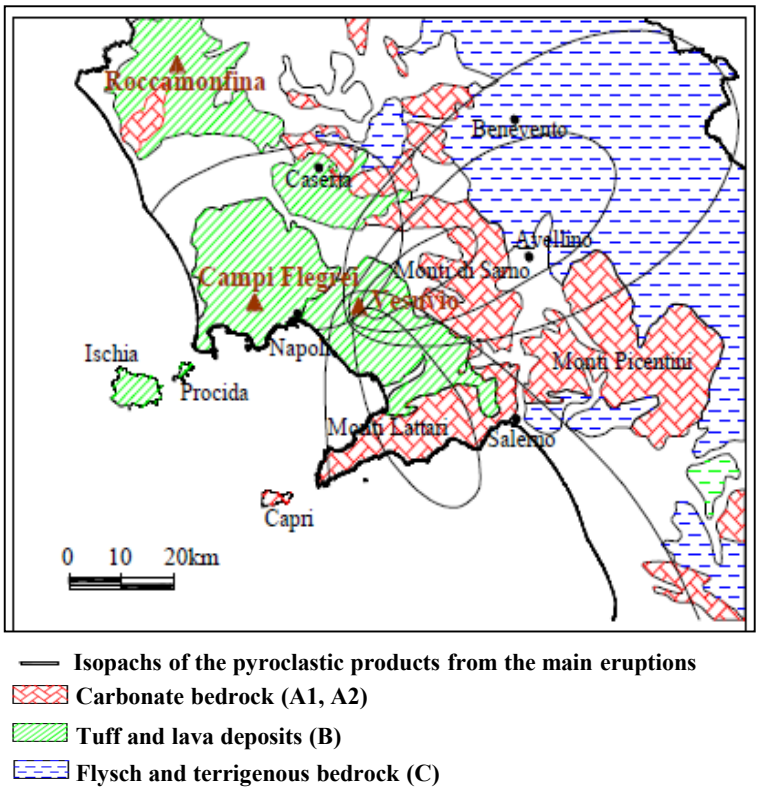

Figure 2.7 Geological map and dispersion of pyroclastic deposits produced by the main Somma-Vesuvius eruptions. Isopachs of the pyroclastic products from the main eruptions (Cascini et al., 2008a, modified)

Many authors investigated the recent thickness and distribution of pyroclastic deposits at different scales. At regional scale the isopach lines (Fig. 2.8) show the geographic distribution and the thickness range of deposits varying between 4 and 7 meters around the Sarno mountains, in east direction and 2 meters around Lattari Mountains, in south-east direction (Rolandi et al., 2000).

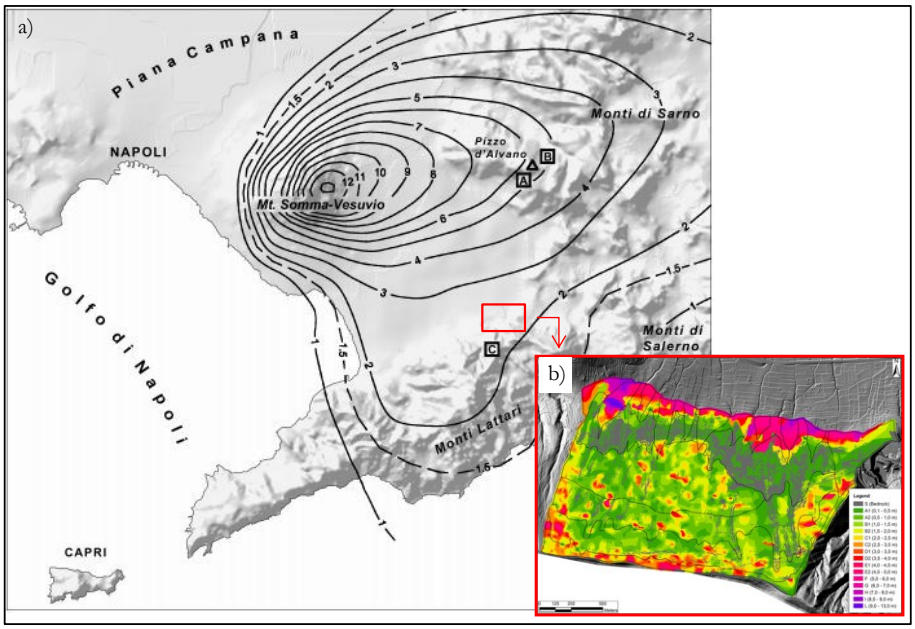

Figure 2.8 a) Isopach lines map of the Recent Pyroclastic Complex (Rolandi et al., 2000) (isopachous lines of the eruptions. The red rectangle represents the Mount Albino massif; b) Pyroclastic deposits thickness map of Mount Albino massif (Ferlisi et al., 2015).

Recently, an advanced thickness map at basin scale of pyroclastic deposits on Mount Albino massif (Fig. 2.9), located at the south-east side of the volcanic area, was carried out through an integrated analysis of data achieved via in-situ investigations and results of laboratory tests (De Chiara 2014; Ferlisi et al., 2015). This map showed thickness varying between 0.5 m in the flat zones through 4.0 m of deposits collected inside the concavities (zero order basins) until 9.0 m of deposits in the colluvial zones at the toe of the slope.

Stratigraphic successions of pyroclastic deposits were investigated from many authors in different test sites of the Somma-Vesuvius district, in particular Cervinara site (Olivares et al., 2002, 2004; Damiano, 2004; Damiano et al., 2012), Monteforte Irpino site (Di Crescenzo et al., 2007; Nicotera et al., 2008; Pirone et al., 2015) and Pizzo d'Alvano site (Bilotta et al., 2005).

Cervinara mountain basin (41°01'13.5"N, 14°36'52.0"E) was widely investigated from some authors after the debris avalanche occurred on December 1999 (Fiorillo et al., 2001). Pyroclastic covers in Cervinara

site, observed from a typical stratigraphical section constructed by Lampitello (2004) as result of several vertical investigations (Fig. 2.9), consist on ash layers alternating with pumiceous soil layers, sometimes mixed with weathered soil derived from the carbonatic bedrock. The soil layer directly in contact with the carbonatic bedrock is weathered fine-graded ashy soil.

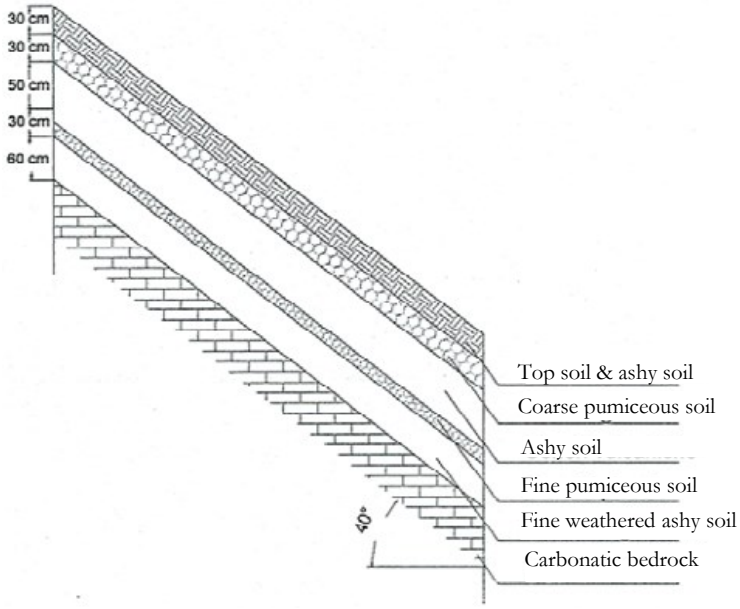

Figure 2.9 Typical stratigraphical section of Cervinara test site (Lampitiello 2004, modified)

From field investigation of pyroclastic deposits in Monteforte Irpino test site (40°53'26.7"N, 14°42'52.4"E), it can be concluded that the stratigraphical succession is represented by a series of soil layers quite parallel to the ground surface. This sequence of soil layers is due to the different eruption occurred in the past as described in depth in section 2.2.1. Starting from the ground surface the sequence consists of 1) topsoil, 2) weathered and humified ashy soil, 3) pumices originated from the Avellino eruption; 4) palaeosoil consisting of weathered volcanic ashes; 5) pumices originated from the Ottaviano eruption; 6) palaeosoil consisting of weathered volcanic ashes; 7) volcanic sand; 8) highly weathered fine-grained ashy soil (Fig. 2.10).

Papa (2008) investigated the grain size distributions of the above mentioned soil layers, demonstrating a limited scatter and thus a uniformity of soil deposits.
First two shallow layers (soil 1 and 2) have a similar grain size distribution although the layer 1 is quite finer; the soil layer 4 is well graded

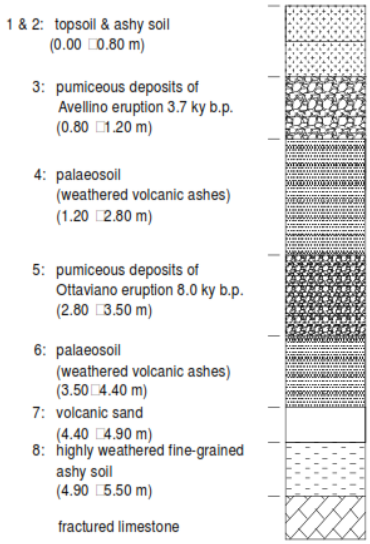

Figure 2.10 Typical stratigraphical profile of Monteforte Irpino test site (Nicotera et al., 2008)

ranging from sand to silt with a small clay fraction; finally layer 3, 5 and 7 are made of pumiceous and sand deposits and they are described as quite uniform coarse-grained materials, in particular soil 3 is a gravel, soil 5 a coarse sand, while soil 7 is silty sand.
Investigations on the typical stratigraphic sections of Pizzo d'Alvano Massif (Fig. 2.8a) were carried out after the rainfall-induced flow-like landslides occurred on May 1998, where many damages and loss of life were recorded in the urbanized areas located at the toe of the slope. Several flow-like landslides reached four villages located at four sides of the massif, respectively Bracigliano at East, Quindici at North, Sarno at South and Siano at South-East. Figure 2.11 shows the typical stratigraphic sections of the sites involved during the events of May 1998 (Cascini & Sorbino, 2003).

In Bracigliano site (Fig.2.11a) the stratigraphy is quite homogeneous due to the presence of a thick layer of ashy soil without any sequence of pumiceous layers originated by different eruptions. On the other hand, stratigraphic profiles of the other investigation sites show pomiceous soil layers at different depths among the main ashy layers (Fig. 2.11b,c,d), with a stratigraphic configuration similar to those observed for Cervinara and Monteforte Irpino sites.

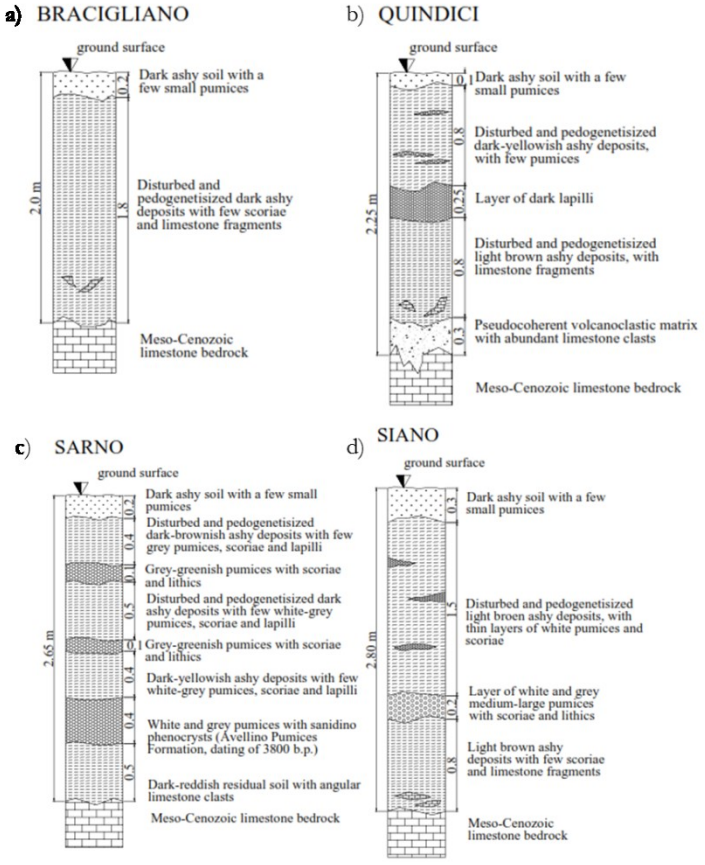

Figure 2.11 Typical stratigraphic sections of the investigation sites (Cascini & Sorbino, 2003)

2.2.3 Physical properties

As previously mentioned, in this study the attention is focused on pyroclastic soils produced by Somma-Vesuvio eruptions and distributed on carbonatic bedrock (A1 in Figure 2.7) around the mountains of Campania region.
To this aim, the principal physical properties of these soils investigated in the recent years, are collected and discussed below.
Ashy soils are extremely porous and thus they are considered loose soils. The grain size distribution mostly depends on the eruption they belong and the consequent deposition process. Nevertheless in many cases two main litotypes can be distinguished. Bilotta et al. (2005) classified the ashy soils, on the basis of detailed analysis of grain-size distribution (Fig. 2.12) and statistical distribution of physical and mechanical properties of samples collected on Pizzo d'Alvano, in two main classes called 'A' and 'B' .

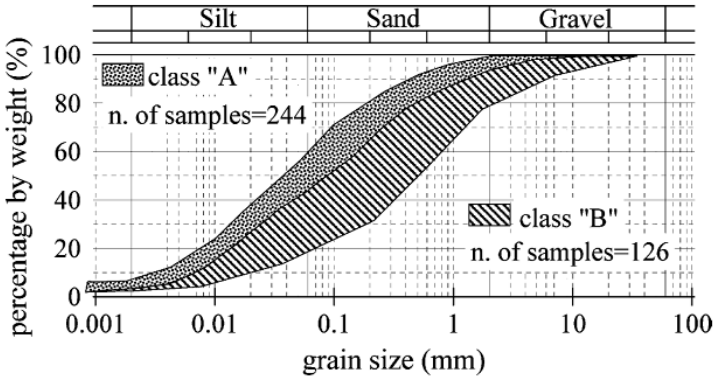

Figure 2.12 Ashy soils collected on Pizzo d'Alvano: range of the grain size distribution (Bilotta et al., 2005).

Mean values of the main soil physical properties of the ashy soils are reported in Table 2.1.

Table 2.1 Range of main physical properties (Bilotta et al., 2005).

	G_s		n_a		γ (kN/m^3)		γ_d (kN/m^3)	
Soil class	Min	Max	Min	Max	Min	Max	Min	Max
A	2.33	2.59	0.63	0.74	8.88	14.40	6.58	9.50
B	2.45	2.70	0.53	0.69	9.20	16.59	5.71	12.32

In general, class 'A' includes ashy soils with a finer grain size distribution, higher porosity values and lower specific gravity values than class 'B'.
On the basis of stratigraphical settings of most of the pyroclastic soil covers along slopes (Revellino et al., 2004; Bilotta et al., 2005; Cascini et al., 2008; Ferlisi et al., 2016), it was observed that generally coarser ashy soils of class 'B' form the superficial layers (1 – 2 m) and overlay those of class 'A', with presence of some interbedded pumice layers.

2.2.4 Chemical composition

Volcanic soils, and in general Andisoils, are widely recognized as rich in minerals. The primary minerals are volcanic glass, phenocrystal, feldspar, silica minerals and all the iron and magnesium-rich minerals together with minor content of allophone-like materials, imogolite, zeolite, non-crystalline silicate clays. Their aluminium-rich elemental composition, the highly reactive nature of their colloidal fractions and their high surface area result in unique chemical properties. Chemical and mineralogical characteristics are reflected in their physical properties and biological activities and affect positively the utilization of these soils for agricultural purposes. The striking accumulation of organic C and N in these soils is indicated by comparing the organic C (Carbon) and N (Nitrogen) contents between Andisols and other mineral soils.
C/N ratio (Carbon/Nitrogen) is the parameter commonly used to describe the cultivability of soils and that of cultivated Andisols (C/N =14) is higher than other mineral soils (C/N=11) (Nanzyo et al., 1993).
Generally such soils exhibit pH ranging from 5 to 7 (weak acid range). These features change during the soil formation process and also due to eventual weathering phenomena. In particular, formation of non-crystalline materials and accumulation of organic matter are the dominant pedogenic processes occurring in most soils formed in volcanic materials (Shoji et al., 1993; Ugolini & Dahlgren, 2002). Time and climate combine to determine the relative degree of weathering and pedogenetic development. Moreover, in some cases, intermitted additions of volcanic ash restart the soil developmental processes, maintaining such soils in relatively stable chemical conditions.
In conclusion, Campania region is widely known as "Campania Felix" because of these fertile soils, which have been used for agricultural purposes since the V century B.C. thank to their chemical characteristics favorable for planting such as nuts, chestnuts, vineyards (Unger, 1953).

2.3 SUCTION AND MECHANICAL PROPERTIES OF VESUVIAN SOILS

2.3.1 Soil suction regime

Soil suction is one of the stress-state variables used to understand soil-atmospheric interaction and to model the hydraulic behavior of unsaturated slopes. Rainwater infiltration and Evaporation are the main processes regulating the suction in shallow layers of unsaturated soils. Rainfall infiltration is the mechanism that induces significant drops in suction and the consequent reduction of the shear strength of the soil which eventually causes the slope failure (Anderson and Sitar 1995; Alonso et al. 1996).

On the other hand, evaporation is the process that generally increases suction due to the exiting water fluxes from the ground surface. Generally the evaporation is much smaller than rainfall especially during rainy seasons, when most of the instabilities evolving in flowslides occur (Cascini et al., 2014). In geotechnical boundary value problems, rainfall infiltration and evaporation represent the boundary conditions for determining soil-atmospheric interaction and, in most of cases they are extremely simplified. Sometimes, evapotranspiration replaces the evaporation when a vegetation cover is present.

The majority of mountainous areas around the volcanic zones of Campania region, are characterized by steep slopes covered by pyroclastic soils in unsaturated conditions.

The unsaturated conditions, as mentioned before, are guaranteed by the continuous soil-atmosphere interactions typically observed in the shallowest layers of the ground. Since the pyroclastic deposits typically form covers ranging from 1 to 5 meters of thickness, these soils are usually in unsaturated conditions.

The knowledge of soil suction values in the unsaturated zones is useful to better understand the hydrological processes occurring in field during the time and consequently to distinguish the seasonal fluctuations due to the metereological forcing (rainfall infiltration or evaporation).

In the last years some authors monitored the soil suction variations in unsaturated pyroclastic covers of Campania region, in different test sites where past rainfall-induced landslides occurred.

The test sites selected, as abovementioned, are those where stratigraphical investigations and thus the geotechnical characterization of the soil were carried out: they were Cervinara, Monteforte Irpino and Pizzo d'Alvano test sites.
The test site selected in Cervinara for the hydraulic regime monitoring (Olivares et al., 2003, Damiano et al., 2012), was located near the source area of the debris avalanche occurred in December 1999. Several laboratory tests on undisturbed and remodeled samples were conducted for soil hydraulic characterization (Damiano et al., 2012), while in-situ monitoring consisted on soil suction and rainfall intensity over 4 years (from 2001 to 2004). Starting from 2005, volumetric water content variations were also measured until the 2007.
Soil suction regime was monitored along the four main pyroclastic layers between the top soil and the carbonatic bedrock (Fig. 2.9). They found the general conclusion relative to the seasonal fluctuations characterizing the suction regime over yearly time scale. Furthermore, considering a thickness of the pyroclastic cover investigated of almost 2 meters, they found that during spring and summer the highest suction value recorded in the deepest layer is about 30% less than that attained in the shallowest ones. One more interesting observation over the yearly time scale is that the suction trend delayed with increasing depth: during autumn, peak suction is reached in the deepest layer, but starting from February it decreases.
Comegna et al. (2016) continued to collect data of soil suction, rainfall intensity and volumetric water content on Cervinara test site, for a better understanding of the hydrological processes which involve unsaturated pyroclastic soils in Campania region. In particular they studied the effect of rainfall events on the short term and long term hydrological response of soil. The monitoring time period was around 2 years and the seasonal suction trends recorded within the long term period (one year) were consistent with those observed by other authors in different slopes of Campania region covered by pyroclastic soils (Cascini and Sorbino 2003; Evangelista et al. 2008; Pirone et al. 2015; Cascini et al. 2014). On the other hand, a single rainfall event can cause, within the short term period, a drop of soil suction at shallowest depth and a delayed suction reduction at greater depths due to infiltration process after the rainfall event. Furthermore, in the short term period it was observed that the reduction in suction due to a single rainfall event is strictly related to the initial soil suction and also to the rainfall duration and intensity.

Pirone et al. (2015) investigated the suction regime of unsaturated pyroclastic cover in Monteforte Irpino test site, with stratigraphic features (Fig. 2.10) similar to those recognized in the source area of the flow-like landslides occurred in May 1998 at Pizzo d'Alvano Massif.
The test site has been extensively investigated both through laboratory testing and field monitoring for an hydraulic characterization of soil and its hydraulic behavior (Papa 2008; Papa et al. 2008, 2013; Nicotera et al. 2010; Pirone and Urciuoli 2012).
In-situ monitoring consisted in soil suction, volumetric water content and climatic measurements, such as rainfall intensity, wind speed, temperature and relative humidity, over three years (from 2008 to 2010), and the measurements are still on going.
Soil suction regime was monitored through tensiometers located at different depths in the main pyroclastic layers (except for the coarser pumiceous layers) with a frequency of three measurements per month. It was observed that the suction, and also the volumetric water content, showed at all the depths a seasonal fluctuation on the yearly time scale due to seasonal factors, while only the top layer appeared to be affected by a single rainfall event, and it showed a quite small fluctuation. The suction trends were consistent with those observed for the other test sites previously mentioned. Furthermore, they identified the most critical periods for slope stability by observing the seasonal trends of both matric suction and volumetric water content, which clearly reduced their amplitude with increasing depth. From a spatial analysis of hydraulic heads (along a specified section of the test site), they individuated the period of the year from December to April as the worst for slope stability, because the groundwater flow is one-dimensional, vertical and oriented downwards.
Cascini & Sorbino (2003) investigated the soil suction regime in pyroclastic covers of Pizzo d'Alvano Massif, where the May 1998 catastrophic events occurred, in order to evaluate the contribution of soil suction knowledge in the analysis of the flowslide triggering. The monitoring time period was from 1999 to 2002 and the measurements were carried out in four test sites selected (Bracigliano, Siano, Sarno, Quindici, as showed in the stratigraphical settings in Figure 2.11). From the data collected, the monthly average of soil suction over the years was obtained and significant differences were not observed for soil suction values measured in the four different sites, except for the exposure of

the slopes to the solar radiation, which slightly influenced the suction values measured.
Cascini et al. (2014), from a detailed analysis of the rainfall and soil suction measurements in Campania region collected over ten years by the authors abovementioned, distinguished qualitatively two main period of the years, respectively rainy period and dry period, where soil suction can show different values (Tab. 2.2).

Table 2.2 Typical time trends of soil suction in pyroclastic covers on carbonatic bedrock in Campania region (Cascini et al. 2014).

	Oct	Nov	Dec	Jan	Feb	Mar	Apr	May	Jun	Jul	Aug	Sep
season *	Autumn			Winter			Spring			Summer		
rainfall *	rainy period								dry period			
suction **	high	medium		low					very high			high

Within the two main periods of the year, four seasons were distinguished with reference to the soil suction values recorded: from January to May suction is low and usually less than 10 kPa, in summer (June-August) suction is very high and usually more than 30 kPa, at the end of summer (September-October), suction ranges from 20 kPa to 30 kPa and the rainy period starts, while, in the last period of the year (November-December) suction decreases again to typical values from 10 kPa to 20 kPa.
Starting from this qualitative seasonal analysis, the average seasonal suction values and their fluctuations recorded over the years for the main four test sites of Campania region at different depths were summarized (Tab. 2.3) in order to have an overview of the hydraulic response of pyroclastic soils on yearly scale (Capobianco et al., 2017).
The average seasonal suction values were calculated in four different ranges of depth (0.2-0.4 m; 0.4-0.6 m; 0.8-1.3 m; 1.3-2.0 m), which are the range of depths investigated in the experimental study conducted within this PhD research on the hydraulic response of root-permeated pyroclastic soils, as discussed in depth in Chapters 5-6.

Table 2.3 Average seasonal suction measured in pyroclastic covers of Campania region (*slope exposure: N-S-W-E). (Capobianco et al. 2017, modified).

Site	Monitoring period	Depth (m)	Average seasonal suction (kPa)				References
			September-October	November-December	January-May	June- August	
-	-	-	20-30	10 – 20	<10	>30	*Cascini et al. (2014)*
Pizzo d'Alvano (SW*)	Nov 1999 Aug 2002	0.2 – 0.4	28.7 ± 0.3	13.8 ± 2.5	12.9 ± 2.9	29.1 ± 4.6	*Cascini & Sorbino (2003)*
		0.4 – 0.6	25.9 ± 1.6	13.7 ± 3.0	11.0 ± 1.0	26.7 ± 4.1	
		0.8 – 1.3	23.5 ± 0.2	19.3 ± 3.6	11.5 ± 1.4	25.3 ± 5.9	
		1.3 – 2.0	23.2 ± 3.1	24.7 ± 3.8	12.9 ± 2.8	22.4 ± 4.4	
Cervinara (N -NE)	Nov 2001 Mar 2007	0.2 – 0.4	no data	no data	no data	no data	*Damiano et al. (2012)*
		0.4 – 0.6	28.9± 13.8	6.7 ± 1.2	7.9 ± 1.7	33.5 ± 13.1	
		0.8 – 1.3	31.5 ± 9.4	6.6 ± 0.8	9.4 ± 2.2	27.5 ± 9.3	
		1.3 – 2.0	48.9 ± 0.0	33.0 ± 7.1	9.5 ± 2.3	31.9 ± 14.3	
Monteforte Irpino (N-NE)	Apr 2008 Oct 2010	0.2 – 0.4	27.2 ± 8.3	6.7 ± 1.0	8.4 ± 3.3	39.1 ± 16.5	*Pirone et al (2015)*
		0.4 – 0.6	27.7 ± 7.6	6.2 ± 1.4	7.1 ± 3.0	34.9 ± 15.8	
		0.8 – 1.3	no data	no data	no data	no data	
		1.3 – 2.0	30.8 ± 1.3	14.1 ± 7.9	5.3 ± 1.0	16.7 ± 7.0	
Cervinara (N -NE)	Jan 2011 Jan 2012	0.2 – 0.4	no data	no data	no data	no data	*Comegna et al. (2016)*
		0.4 – 0.6	no data	14.5 ± 4.0	10.8 ± 2.0	30.8 ± 7.8	
		0.8 – 1.3	no data	12.8	10.5 ± 1.5	30.4 ± 7.7	
		1.3 – 2.0	37.6 ± 29.0	32.4 ± 1.7	7.8 ± 1.1	41.5 ± 19.5	

It can be observed that during the period from January to May suction values at all the depths are quite similar, around 10 kPa and show small fluctuations due to the small thermal excursions during the winter season. From June to August the suction values are very high in the shallowest depths and generally tend to decrease with depth even their values is always more than 20 kPa. The suction fluctuations in this period of the year are very high because of the increase of temperature from June to August together with high thermal excursions, in fact they vary between a minimum of 4.1 kPa recorded in Pizzo d'Alvano site up to 19.5 kPa recorded in Cervinara site. The suction starts to decrease in September and October at the shallowest depths because of the beginning of the rainy period and the reduction of temperatures, while in deepest layers the peak suction is reached due to the suction trend delayed, as previously discussed. The period of the year between November and December is still characterized by a reduction of suction at the shallowest depths with a delay at the higher depths. The suction fluctuations in this period are quite small and similar to those recorded in the first period of the year (January – May) since in the rainy period a more stable hydraulic condition is guaranteed along all the depths.

2.3.2 Hydraulic properties

The hydraulic characterization of unsaturated soils is determined by the relationship between the matric suction (s) and both volumetric water content (θ) and soil hydraulic conductivity (k). These relationships are know as Soil Water Characteristic Curves (SWCCs), alternatively Soil Water Retention Curve (θ-s) and Soil Conductivity Curve (k-s), and they describe the water exchanges between soil and environment respectively due to drying and wetting cycles, trough the measurement of the hydraulic parameters of soil. The drying curve represents the loss of water from the soil during desaturation process due to evaporation, while the wetting curve corresponds to the adsorption of water during the saturation of the soil. Figure 2.13 shows a typical drying (blue curve) and wetting (dashed magenta curve) SWCCs for suction ranged from 0.1 kPa and 1e6 kPa (typical suction range for silty soil).
The slope of the curve represents the rate of water taken up (adsorption) or released by the soil (loss of water) as a result of a change in the pore water pressure.

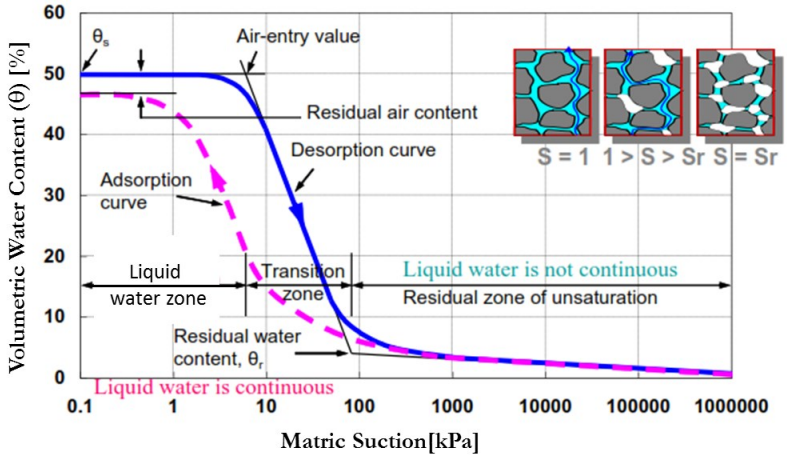

Figure 2.13 Typical Soil Water Characteristic Curve for silty soil (Fredlund & Xing 1994, modified).

SWCC can be generally divided into three zones, namely the boundary effect zone, also known as: i) liquid water zone, the soil is still in saturated conditions; ii) the transient zone where the soil is partially

saturated and a small change in soil suction is required to remove water from the soil, and iii) residual zone, where a significant change in soil suction is required to remove additional water from the highly unsaturated soil (Vanapalli et al., 1998; Fredlund et al., 2001). The Air-entry value (AEV) separates the boundary effect zone and the transition zone. AEV is defined as the minimum air pressure required for air to infiltrate or de-saturate the saturated soil, and depends the pore-size of the soil. The residual water content is the water content of the soil at the beginning of the residual zone, where the SWCCs are the same for both drying and wetting cycles.

Besides that, the difference between the drying and the wetting SWCC is termed as hydraulic hysteresis. The reasons of the hysteretic behaviour of unsaturated soils subjected to drying and wetting is due to the non-uniform pore-size distribution in soil (Hillel et al., 1972) or the difference of contact angle upon drying and wetting process (Fredlund and Rahardjo, 1993). Any swelling, shrinkage and aging of unsaturated soil would alter soil structure, results in hydraulic hysteresis in soil water retention capabilities. All drying and wetting curves inside the hysteresis are considered as scanning curves and they represent secondary or intermediate drying/wetting curves and only approximate the primary drying/wetting retention curves (Fig. 2.13), corresponding respectively to a drying process starting from perfectly saturated, and a wetting process starting from the residual soil hydraulic condition.

When the soil suction is related to the unsaturated permeability of the soil, the SWCC is also called permeability function, and is strictly related to the SWCC in terms of volumetric water content.

Some authors investigated on hydraulic properties of pyroclastic soils of Campania region and concluded that they exhibit water retention properties typical of coarse-grained materials characterized by low AEV and a complete drying reached at just 100 kPa.

In this paragraph only the hydraulic properties of pyroclastic soils collected in Pizzo d'Alvano tests site are reported, because it is the soil type investigated in this study.

Sorbino and Foresta (2002) investigated the hydraulic properties of undisturbed specimens taken from Pizzo d'Alvano by conducting laboratory tests such as Suction Controlled Oedometer (SCO), Volumetric Pressure Plate Extractor (VE), and Richard Pressure Plate (PP). SWCCs in terms of matric suction vs saturation degree (S_r) have been carried out for both pyroclastic soils 'A' and 'B' (Bilotta et al., 2005)

for different net vertical stress applied (Fig. 2.14), by using the equation suggested by Van Genuchten (1980).

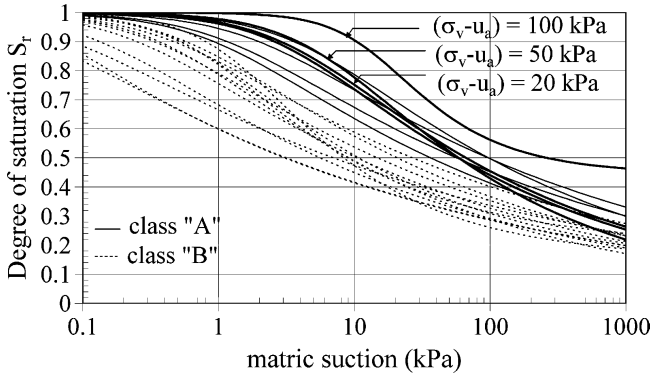

Figure 2.14 Soil Water Characteristic Curve for pyroclastic soils of Pizzo d'Alvano (Bilotta et al., 2005).

It was observed that the shape of SWCC of class 'B' soils is flatter and characterized by degree of saturation values lower than those observed for class 'A' soils. By converting the SWCC in terms of matric suction and VWC, it was observed that soil belonging to class 'A' showed an AEV higher than that for class 'B' soils and this is reflected in a different grain size distribution (Corey, 1994).
Other authors investigated the hydraulic properties of pyroclastic soils by introducing an innovative experimental technique to determine rapidly and reliably both SWCC and permeability function of undisturbed natural soil samples from the test site (Papa, 2008; Nicotera et al., 2010).

2.3.3 Collapsibility

Pyroclastic soils of Campania region are usually in partially saturated conditions, as discussed previously, and the open structure of these soils (high porosity) induces a collapsible behavior when suction is reduced due to rain water infiltration. The open structure is typical of volcanic products because of their deposition process usually occurred through rain and wind which facilitate this process. Despite they had nil cohesion during deposition, during the years they were slightly cemented by sulphate crystals or by finer particles which filled the pore spaces, so the structure is stable thank to the atmospheric humidity (de Vallejo, 2005).

A collapsible soil is any unsaturated soil that goes through a radical rearrangement of particles and great loss of volume upon wetting with or without additional loading (Dudley, 1970).
Many authors investigated the effect of both additional loading and reduction in suction on the collapsibility of pyroclastic soils of Campania region, through standard oedometer tests (Bilotta et al., 2006; Lancellotta et al., 2012) and suction controlled oedometer tests (Nicotera et al., 1998; Bilotta et al., 2008). In particular, the collapsible behavior of pyroclastic soils belonging to class 'A', the finest soils classified by Bilotta et al. (2005), has been widely investigated because in field they showed a very high porosity ranged between 63% and 74%.
In order to investigate the effect of saturation on volumetric collapse, Bilotta et al. (2006) conducted suction-controlled oedometer tests under different net vertical stresses. Starting with an initial degree of saturation, at fixed net vertical stress, the soil sample was saturated through flooding water within the cell and the vertical deformation after flooding corresponded to soil collapse. They observed that collapse upon wetting occurred in any case, also when vertical net stress applied was very low.
On the other hand, in order to investigate the effect of loads in unsaturated conditions on volumetric collapse, Bilotta et al. (2008) conducted suction-controlled oedometer tests under an imposed value of suction. By adopting the double oedometric procedure they compared results obtained in saturated conditions with those obtained in suction controlled oedometer tests.
The difference of vertical deformation between the specimens with imposed suction and the saturated specimens were attributed to soil collapse.
In unsaturated conditions, magnitude of collapse was strictly dependent on the initial suction value and the initial specific volume of specimen, in particular soil collapse was higher with increasing in suction value. The collapse increased with increasing in stress level up to 160 kPa, after that the collapse tends to decrease as the overburden stress increases. Moreover, for a fixed level of suction, in undisturbed specimens the entity of collapse was higher than that observed in reconstituted specimens because in these latter cases it was impossible reproducing the natural aggregates and bridges between particles typical of metastable pyroclastic soils (Lancellotta et al., 2012). Pyroclastic soils belonging to class 'B', which were used in this study, showed a collapsible behavior similar of class 'A' soils (Lancellotta et al., 2012). However, laboratory

tests on class 'B' pyroclastic soils are still very scarce and a laboratory campaign aimed to the investigation of collapsibility of these soils was conduced and discussed in depth in Chapter 7. Test results have been compared with results obtained from collapsible tests on rooted soils to quantify the effect of roots on soil aggregation and thus on reduction in collapsibility of these soils.

2.3.4 Shear strength

Many authors in recent years investigated on shear strength parameters of pyroclastic soils in Campania region in both saturated and unsaturated conditions (Olivares & Picarelli, 2001; Olivares & Picarelli, 2003; Bilotta et al., 2005; Picarelli et al., 2006; Migliaro, 2008). Olivares & Picarelli (2003) conducted both drained and undrained tests on undisturbed saturated samples from some of these pyroclastic soils with highly metastable structure. For these soils, the measured stress paths showed a contractive behavior in drained tests, while positive induced excess pore pressures were observed in undrained tests. Moreover, the undrained stress-strain curve evidences the unstable behavior of soil that is characterized, after the peak of strength, by a progressive shear strength decrease due to a continuous pore pressure increase.
Migliaro (2008) performed both triaxial compression drained and undrained tests and confirmed their contractive behavior in drained conditions, strictly dependent on initial specific volume and if they are reconstituted or not. In particular, reconstituted specimens showed a reduction in contractive behavior. On the other hand, for undrained conditions, decreasing in shear strength after the peak confirmed the increasing in pore water pressure, which can lead to static liquefaction. Both triaxial tests in drained and undrained conditions for reconstituted specimens of class 'B' soils have been conducted in this experimental study, as discussed in depth in Chapter 8. These results are compared with triaxial test results obtained from reconstituted soil used for the filling of the experimental column, and from which undisturbed rooted samples have been taken.

3 SLOPE INSTABILITY IN CAMPANIA REGION AND RISK MITIGATION MEASURES OVER THE CENTURIES

Rainfall induced landslides of the flow-type systematically occur in shallow pyroclastic soils of Campania region. This Chapter firstly provides a brief review of landslide classifications. Then, the slope instability types typically occurring in Campania region are introduced and the relationship between in situ soil suction and rainfall conditions are discussed, since they represent the triggering factors of these phenomena.
Finally, a brief description of mitigation measures realized in Campania region from the Middle Age to the beginning of XX century and the most frequent mitigation measures, applied after the catastrophic events occurred in May 1998, are introduced.

3.1 FLOW-LIKE LANDSLIDES

3.1.1 General classification systems

Flow-like landslides are very complex phenomena usually composed of mixtures of air, steam, water and solid fractions of different natures such as fractural rocks, sand, silts including loess and volcanic ashes, sensitive and stiff fissured clays and organic soils (Hungr et al., 2001). Since these phenomena are characterised by very complex features, many contributions have been proposed during the time in order to establish a general classification system (Hungr et al., 2001; Hutchinson 2003).
Varnes (1978) classified the phenomena on the base of the type of both movement and material involved. This classification was later improved by adding the velocity reached by the landslide body in the paroxysmal stage of the motion (Cruden & Varnes, 1996).

Hutchinson (1988) focused on landslides morphology, mechanism, material and rate of movement. Within this classification system, the flow-like phenomena, the mass transport phenomena and mass movement phenomena were distinguished on the base of the water content value and unit weight of the mixture. In particular, debris flows are characterised by sediment concentration by weight of more than 80% and unit weight higher than 2 t/m^3. Smaller values are characteristic of the mass transport phenomena such as hyperconcentrated flows and streamflow.
Costa (1988) classified flow-like landslides in water floods, hyperconcentrated flows and debris flows on the base of the rheology (shear strength and bulk density), fluid type and sediment concentration. In particular, water floods are those with the lowest sediment concentration (0.4-20% by volume), whereas hyperconcentrated flows and debris flows are made of respectively 20-47% and 47-77% of sediment concentration by volume.
Coussot and Meunier (1996) reviewed this classification on the basis of physical characteristics and mechanical behavior of flow-like landslides, while Hutchinson (2003) improved his previous classification by identifying four types of flow-type landslides. Perticularly, this author grouped these phenomena into two different categories depending on the involved material: flow-type landslides in granular materials (debris flows, flow slide and rock avalanche) and flow-type landslides in cohesive material (mudslides). Finally, Hungr et al. (2001 and 2012) detailed these factors providing a detailed and comprehensive classification system based on four basic elements: material, water content, special conditions and velocity.
Considering that the phenomena occurring inside the pyroclastic soils of the Campania region can be essentially classified as debris and hyperconcentrated flows, according to the classification systems previously summarized, hereafter the attention is focused on the main characteristics of these phenomena, which are analyzed from a mechanical point of view.

3.1.2 Debris flows

Debris flows belong to landslides of the flow-type and are characterized by a very rapid to extremely rapid surging flows of saturated non-plastic debris (plasticity index < 5% in sand and finer fractions) in a steep

channel with a strong entrainment of material and water along their flow path. Hungr et al. (2012) distinguishes debris flows from other landslides since they periodically occur on established paths, usually gullies and first or second order drainage channels.
Debris flows are triggered by rainfall usually during a period of heavy rainfall or melting snow, with peak discharge up to 40 times greater than those of extreme floods (Hungr et al., 2001). The high discharge is recognized to be responsible for greater flow depth, higher velocity, higher impact loads and the ability to move large boulders.
The flow may be initiated by a slide, debris avalanche or rock fall from a steep bank, or by spontaneous instability of the steep stream bed, carrying heavy water flow. As discussed in the next sections, in some loose saturated soils in undrained conditions, in post-failure stage during shearing, the increase of pore water pressure, which can not freely dissipate, leads to the annulment of mean effective stresses. This process is known as static liquefaction and leads the unstable mass to evolve into a flow during the propagation stage.
The materials involved are loose unsorted materials ranging from clay to blocks of several meters in diameter, produced by mass wasting processes (colluvium), weathering (residual soils), glacier transport, or unsorted anthropogenic waste (Hungr et al., 2001) and sometimes organic materials such as trees and timber (Swanston, 1974). The thickness of the material in motion ranges from few meters to a maximum of twenty meters.
Once soil material begins to move in a steep channel, the flowing masses start to incorporate the material lying along the slope (Sassa, 1985), hence greatly increasing of the solid fraction concentration that approximately reaches 80% by volume.
Debris flows measured velocity ranges between 3 and 12 m/sec and, exceptionally, velocities of about 30 m/sec and even more have been measured (Hutchinson, 1988) with travel distances up to several kilometres.

3.1.3 Hyperconcentrated flows

Hyperconcentrated flows are sediment transport phenomena characterized by very rapid flow of water, heavily charged with debris, in a steep channel (Hung et al., 2012). Hyperconcentrated flows are also known in scientific literature as intermediate flows (Bull, 1964), cohesive

or turbulent mudflows (Kurdin, 1973; Gagoshidze, 1969), type III and IV sediment flows (Lawson, 1982), mud floods (Committee on Methodologies for Predicting Mudflow Areas, 1982) or debris floods (Hungr et al., 2001).

They are the result of erosion phenomenon performed by the volumes of water in motion or when debris flows lose coarse sediment on the ground surface through dilution and selective deposition.

These phenomena commonly occur in semiarid and arid regions, as results of very intense hurricanes where the basins are steep, hillslopes are eroded, channel banks are fragile, and channel beds are unreinforced and erodible (Gerson, 1977; Laronne et al., 1994). Moreover, in scientific literature there are many others documented triggering mechanisms including: lake-breakout floods (Rodolfo et al., 1991; O' Connor et al., 2002), hillslope and channel erosion during intense rainstorms (Beverage and Culbertson, 1964; Major et al., 1996; Pierson et al., 1996), glacier-outburst floods (Maizels, 1989), inputs of large sediment volumes to water floods by landslides (Kostaschuk et al., 2003) and dilution and/or selective deposition at the heads and tail of debris flows (Pierson, 1986; Pierson and Scott, 1985; Cronin et al., 2000).

The material involved is characterized by a solid concentration by volume ranging from 20% to about 47% (Costa, 1988) and it can be transported in the form of massive surges, leaving sheets of poorly sorted debris ranging from sand to cobbles or small boulders.

Hyperconcentrated flows are common in pyroclastic soils recently impacted by explosive eruption, as those covering mountainous basins of Campania region. They are often generated by rainfall events of high intensity and short duration that determine the development of sudden river flooding, with peak discharge comparable to that of a water flood.

Hyperconcentrated flows usually develop impact forces less than those related to debris flows and, consequently, they are characterized by a lower risk to life and to properties (resulting from flooding and burying of the objects impacted by the flow). Moreover, hyperconcentrated flows can occur in much larger river catchments, with greater hydrologic flood discharges which are magnified by heavy sediment loads.

3.2 SEASONAL EFFECTS OF RAINFALL ON SLOPE INSTABILITIES IN CAMPANIA REGION

Campania region has long been affected by rainfall-induced slope instabilities that often involve large areas from which the propagation of flow-like phenomena can occur and cause many damages in terms of loss of life and economic losses along their run-out.
Cascini et al. (2014) analyzed the slope instability events occurred in the past and their triggering factors, in order to gain further insight into the analysis and forecasting of future events. This study highlighted that the homogenous geological context called A1 (Fig. 2.7), characterized by pyroclastic soils covering carbonatic bedrock and extending for around 1,400 km^2 , has been the most affected by past events, with more than 1900 recorded casualties from 1640 to the present (Cascini et al. 2008b). Within the geological context A1, the shape of mountain basins and slope morphology were analyzed and two main types of basins have been recognized: the first group with high order of drainage networks, and the second with low order of drainage network. The thickness of pyroclastic covers in all these basins affected by instability phenomena usually depends on the volcanic eruptions and isopach lines and it can reach up to 5 m.
The main types of flow-like phenomena occurred in past have been summarized in Table 3.1 on the base of the initiation processes and the consequent propagation stages.

Table 3.1 Main slope instabilities in Campania Region (Cascini et al., 2014, modified)

Initiation		**Propagation**
Erosion phenomena		Hyperconcentrated flows
First time shallow slides	Flow slides	Debris flows
	Debris avalanches	Debris avalanches/ debris flows

The temporal-spatial distribution of critical rainfall influences the triggering of flow-like phenomena. Moreover, the relationship between soil suction and rainfall intensity and duration is the key factor to

forecast the triggering of flow-like landslides. This is introduced in previous Chapter and established by Cascini et al. (2014) through Table 3.2, relating the slope instability types to the periods of the year.

Table 3.2 Interpretation of slope instability types based on rainfall, suction and historical data (Cascini et al., 2014).

	Oct	Nov	Dec	Jan	Feb	Mar	Apr	May	Jun	Jul	Aug	Sep
Rainfall *	Rainy							Dry				
Pa - cumulative antecedent (mm)	*Pa* < 200	200 < *Pa* < 500		*Pa* > 500								
Pe - critical 48 hours rainfall event (mm) *	*Pe* > 120	120 > *Pe* > 60		*Pe* < 60								
typical suction range **	high	medium		low					very high			high
some events ***	1910, 1954, 1966 (Lattari mounts)	1999 (Cervinara town)		January 1841 (Gragnano town), March 1924 (Lattari mounts), May 1998 (Pizzo d'Alvano massif),					August 1935 (Gragnano town)			2010 (Atrani town)
Period	1	2		3					4			1

* Data from Rossi and Chirico (1998)
** Data from Cascini and Sorbino (2004)
*** Data from Mete and Del Prete (1999), Cascini et al. (2008b) and Bovolin (2012)

They found that the years could be divided in 4 periods, depending on suction values and rainfall intensities. In particular, in periods 1 and 4 mostly erosion phenomena occur, typically turning into hyperconcentrated flows, bein generated by rainfall events of high intensity and short duration during a peiod in which the highest soil suction values are recorded. In period 3, i.e. when the soil suction attains the lowest values, first-time shallow slides (i.e. flowslides or debris avalanches) are triggered by low intensity and long duration rainfall infiltrating the slopes, later propagating as debris flows or debris avalanches. Springs from bedrock (Cascini et al. 2008a) have been recognised in this period as another key triggering factor of shallow slides (Cascini et al. 2005a, 2008a; Di Crescenzo and Santo 2005) as well as trackways and cut slopes widely diffused within these mountain basins (Fiorillo et al. 2001; Guadagno et al. 2005). Finally, in period 2 both classes of slope instabilities may occur since local erosion phenomena and small-size, first-time, shallow slides may be triggered.
Considering that this thesis is aimed to analyze the role of vegetation in the prevention of shallow landslides induced by rainfall, next section provides further details on characteristics and mechanisms recorded in Campania region as described in the literature.

3.3 FAILURE AND POST-FAILURE STAGES

Rainfall induced shallow pyroclastic deposits have been recorded in Central America (Capra et al., 2003), New Zealand (DeRose, 1994, Ekanayake and Philipps 2002) and in South Italy; (Cascini 2004). After triggering, these soils experiment a complex kinematic behavior expressed by failure, post-failure and propagation stages of landslide (Fell et al. 2000; Hungr et al. 2001; Pastor et al. 2002; Leroueil 2004). Failure and post-failure stages occur inside the source area, whereas the propagation stage includes the movement of soil mass from the source area to the deposition area.
Triggering mechanisms as well as failure and post-failure stages are hereafter reviewed from the scientific literature available on the events that in the past affected the pyroclastic soils of Campania region.

3.3.1 Triggering mechanisms

Triggering mechanisms of shallow landslides in pyroclastic soils can be strongly affected by several factors during a rainfall event. Cascini et al. (2008), referring to the flow-like landslidesoccurred on May 1998 all over the Pizzo d'Alvano Massif, individuate six different first failure stage, named M1–M6 (Fig. 3.1), taking into account the geomorphological, the hydrogeological features of the massif and the anthropogenic factors.
The most frequent triggering mechanisms were those related to M1 (Fig. 3.1), M2 (Fig. 3.1b) and M3 (Fig. 3.1c) source areas. M1 source areas are located inside colluvial hollows associated to zero order basins (Dietrich et al., 1986; Guida, 2003) affected by convergent sub-superficial groundwater circulation inside the pyroclastic deposits and by temporary springs from the bedrock.
The source areas M2 (Fig. 3.1b) are triangular shaped with an upper crown not too wide and the downslope enlarging. They lay in the upper open slopes and are associated to outcropping or buried bedrock scarps. These instability phenomena enlarged at the base of bedrock scarps, as a consequence of the impacting forces mainly in correspondence to springs from karst conduits.

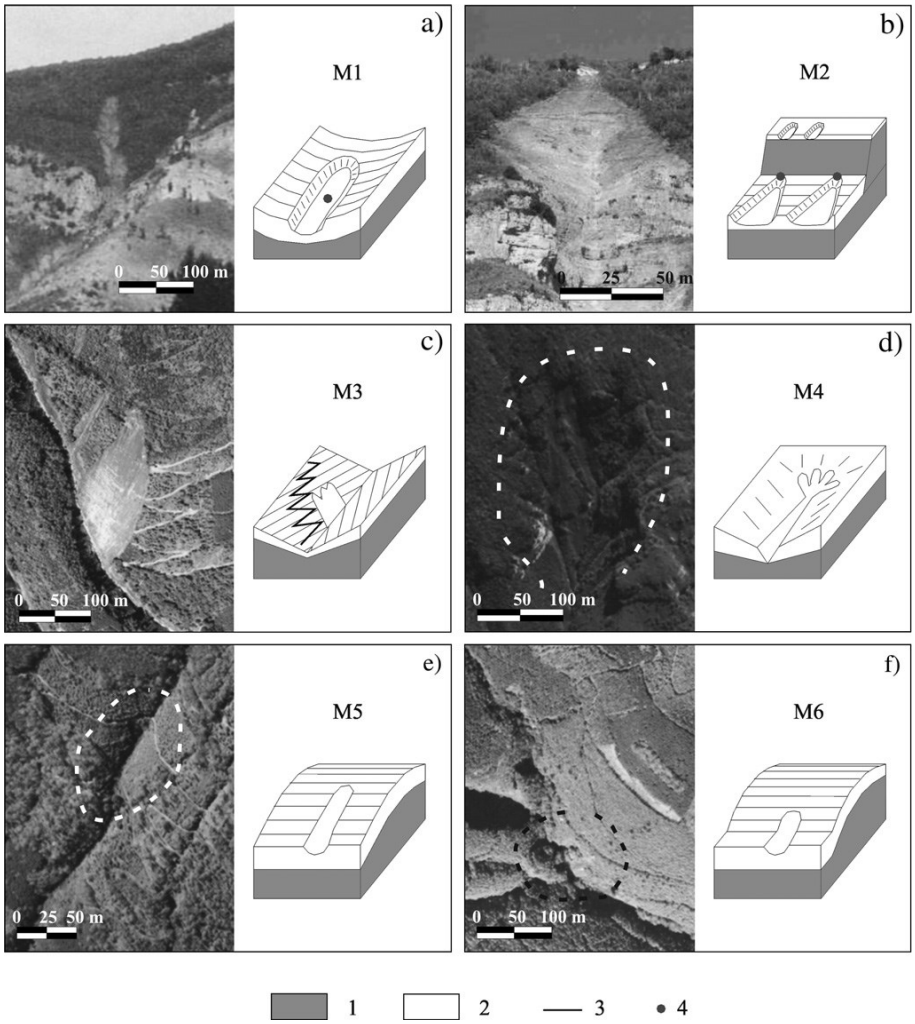

Figure 3.1 Schematic of the typical source areas for the May 1998 flow-like mass movements (Cascini et al., 2008).

The source areas M3 (Fig. 3.1c) show compound planforms that, based on in-situ evidence, can be related to overlapping and/or laterally enlarging local slope instabilities strictly connected to man-made tracks that allow the concentration of superficial waters towards singular portion along the hillslopes.

Finally, the source areas named M4, M5 and M6 originated instability phenomena not having a particularly magnitude as well described in Cascini et al. (2008).
The areal distribution of the landslide triggering areas are shown in fig. 3.26 highlighting that trhey are essentially located more or less at the some altitude all over the massif. This to attest the role played by springs from the karst conduits that in this part of the slope has been recognized (Cascini et al., 2005).

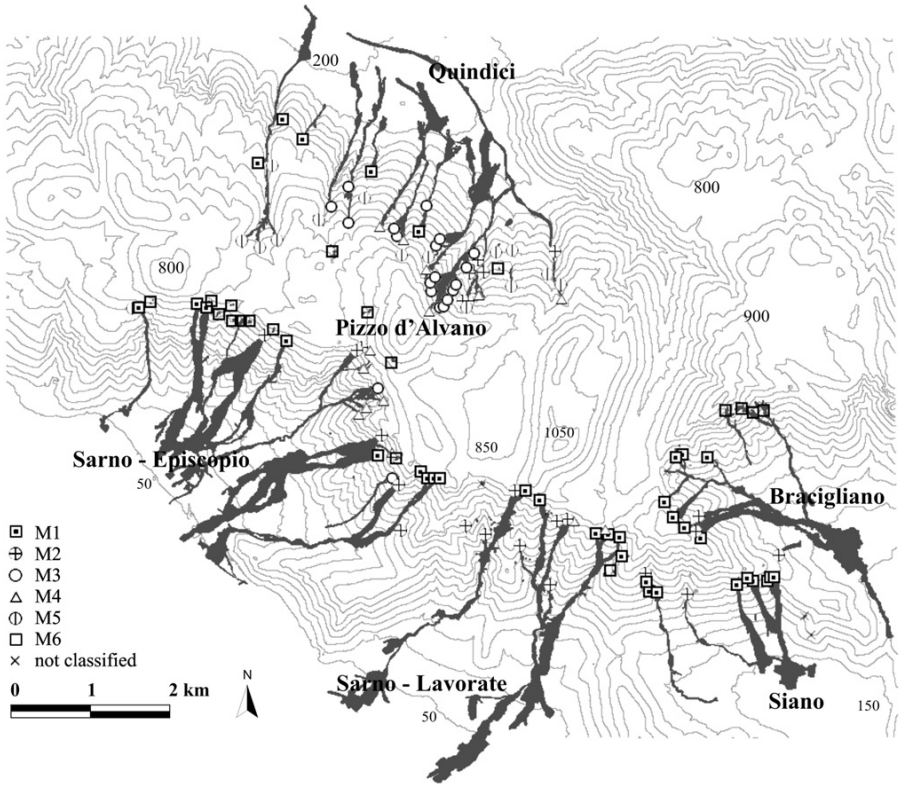

Figure 3.2 Distribution of typical source areas for the 1998 flow-like mass movements (Cascini et al., 2008).

3.3.2 From slide to flow

Once defined the typical source areas, it is of interest distinguishing among three stages which are respectively failure, post-failure and propagation stage.

The failure stage occurs inside the landslide source area of the slope and it is strictly related to the increase in pore water pressure due to rainfall infiltration process, and/or spring from bedrock and this stage typically occurs in drained conditions.
Post-failure stage, which leads to the acceleration of the failed mass after failure, is mostly attributed to the development of total or partial undrained conditions able to produce high pore water pressure during shearing. In particular, volumetric collapse occurs for loose unsaturated soils, as discussed in the scientific literature (Yasufuku et al. 2005; Bilotta et al., 2006; Olivares and Damiano, 2007), and observed in constant shear drained triaxial tests upon wetting (Anderson and Riemer 1995; Dai et al. 1999; Chu et al. 2003; Olivares and Damiano 2007).
For saturated loose soils, this process is associated with a volume reduction causing, in undrained conditions, a significant increase of the pore-water pressure that cannot freely dissipate. As consequence during shearing the soil static liquefaction can be induced, as observed in triaxial tests conducted by Lade (1992), Yamamuro and Lade (1998), Chu et al. (2003) since the increasing in pore water pressure leads to an annulment of mean effective stresses (Wang et al., 2002; van Asch et al., 2006; Olivares and Damiano, 2007). This phenomenon was found to be significant for soils with low density (Iverson 2000; Wang and Sassa 2001), fine grain size (Wang and Sassa 2003), low hydraulic conductivity (Iverson et al. 1997; Lourenco et al. 2006), and subjected to high deformation rate (Iverson et al. 1997).
A comprehensive scheme of failure and post-failure stages (Fig. 3.3) is provided by Cascini et al. (2010) referring to mechanism M1 (Fig. 3.1a). Within the slides (Fig. 3.3b), soil mechanical behavior in drained conditions is controlled by the hydrologic response up to the failure onset. During failure stage, drained conditions remain for both loose and dense soils and resisting forces decrease up to become equal to driving forces ($t=t_1$). During the post-failure stage small accelerations develop ($t>t_1$). The same process in loose saturated soils lead to a volume reduction of the soil. During post-failure stage, when the soil is in partially or totally undrained conditions, so the pore-water pressure cannot freely dissipate, the flowslide occurs (Fig. 3.3d). In particular, catastrophic failure occurs in point A (Fig. 3.3a) when porewater pressures build up and the soil follows a stress path 0 to 1, which means that soil can not sustain the deviatoric stress and great accellerations develop ($t>t1$).

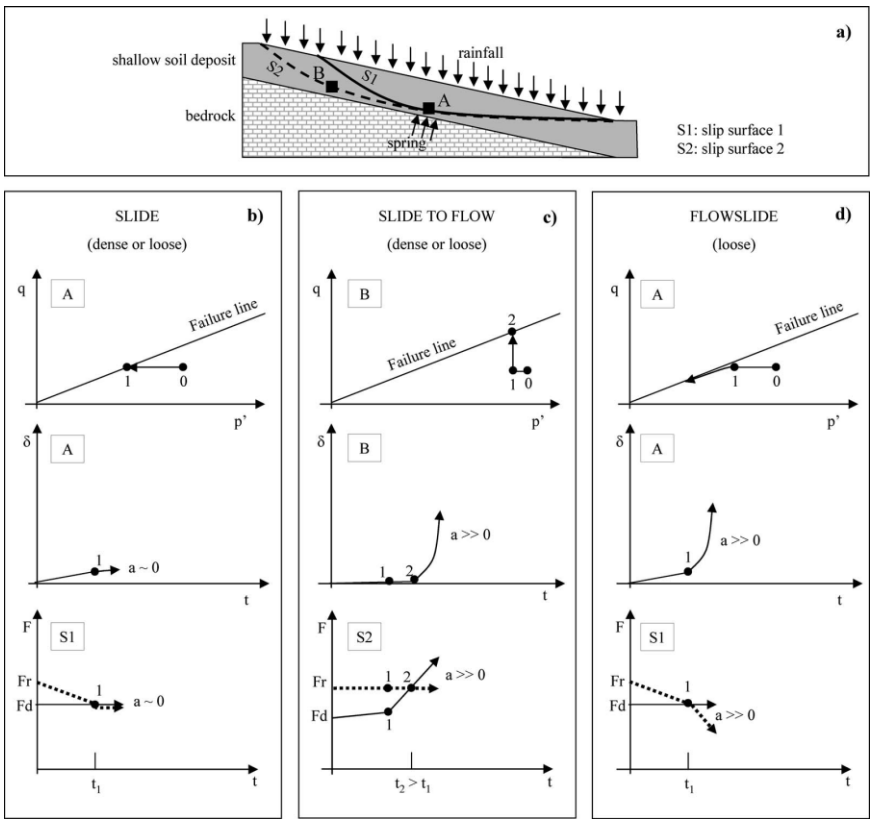

Figure 3.3 Reference schemes adopted for the shallow landslides induced by rainfall directly infiltrating the slope surface and spring from the bedrock (Cascini et al. 2010).

A slide can turn into a flow after a decreasing in the shear strength due to local hydraulic boundary conditions that can lead to fail the portion of the slope corresponding to the spring zone. Above this zone (Point B in Fig. 3.3a), the mobilized shear stresses increase, both in loose and dense soils, due to the unbalanced driving forces along an upslope potential slip surface and a further slide can occur. The latter is characterized by a high initial acceleration and it consequently turns into a flow.
The pore water pressure increment during failure is different between the flowslide (Fig. 3.3d) and the slides turning into flow (Fig. 3.3c).
Porewater pressures reach the highest values at Point A due to both rainfall and local hydraulic boundary conditions such as spring from

bedrock, while the lowest values at Point B above the spring zone is related only to the rainfall. This means that the pore water pressure values at failure can be negative at Point B as showed in Figure 3.3c and thus slides turning into flow can also occur in portions of the slope characterized by unsaturated conditions.

The type of failure is also important. In Figures 3.3b,c drained failure occurs at the critical state line and conversely, fully or partially undrained conditions take place in post-failure stage for very loose materials (Fig. 3.3d). The failure in drained condition can be of localized type (Pastor et al., 2002, 2004), while that occurring in undrained condition is of diffuse type (Darve and Laouafa 2000; Fernandez Merodo et al., 2004).

Most of the above findings on the post-failure stage are obtained through observation of laboratory tests such as isotropically/anisotropically consolidated undrained triaxial tests (Chu et al. 2003; Eckersley 1990) and constant shear drained triaxial tests (Chu et al. 2003). On the other hand, the direct measurement of pressures and displacements in real slopes is rare and is only possible for monitored sites during the occurrence of landslides or for artificially induced failure in real slopes without the repeatability of the measurements.

Flume tests are also reproduced in order to measure the pore water pressure increasing during failure and post-failure stages (Eckersley 1990). However these experiments are expensive and as they reproduce the real processes at a greatly reduced scale they may be irrespective of the full-scale slope behaviour, even if Nevertheless, downward rainfall infiltration from ground surface and/or downwards–upwards water spring from the bedrock to the tested soil layer can be well analyzed (Lourenco et al. 2006). Centrifuge tests have been recently introduced to reproduce stress levels similar to those experienced by a real slope and to study the post-failure stage during shearing. In particular, Take et al. (2004) found that the transition from slide to flow is caused by local failures producing a variation in the slope geometry, which are related to transient localized pore-water pressures that are not associated with the development of undrained conditions, but originated from the combination of particular hydraulic boundary conditions and stratigraphical settings. Moreover, the experimental results highlighted that the transition from slide to flow can occur both for loose and dense soils and it can also correspond to decreasing pore-water pressures during the post-failure stage. These findings have been confirmed also by

other researchers through small-scale flume tests (Lourenco et al. 2006) or centrifuge tests (Lee et al. 2008; Ng 2009).

3.4 RISK MITIGATION MEASURES

3.4.1 Ancient hydrogeological mitigation measures

Hydrogeological risk management in Campania region started very early. Lavecchia (1999) writes that after the year 1000 the landscape transformation, reclamation and remediation were performed by monasteries and abbeys, and all these operations have been intensified during the age of the Municipalities and during the Reinassance.
It was widely recognized that in those centuries the Campania region was affected by landscape problems. In particular, during the intense rainfall events, the debris were transported trought the riverbeds of the mountains up to the piedmont areas, compromising the safety of the villages and the urban centers located at the toe of the slopes. This led to the formation of many swampy zones in correspondence of the flat area of the Campania region.
The typology of the actions aimed to reduce landscape problems and their temporal distribution have been summarized in Figure 3.4 for a period going from the year 1000 up to the XIX century, corresponding to the Italian State Unity (Sacco, 2015).
The prevailing operations adopted since the 1300 belong to hydraulic works (e.g. channelling) aimed to allow the use of natural resources (e.g. water).
The most famous channeling system is represented by Regi Lagni, designed by the architect Domenico Fontana in the late Sixteenth century (Fiengo, 1988), which involved many sectors of Campania Region, starting from the southern boundary (Avellino province) and extending along the provinces of Naples and Caserta for a total of 110'000 ha.
However, the efficiency of this new channeling system was turned out to be scarce since no maintenance actions for stabilizing the embankments were adopted. As consequence, the debris produced by the surface erosion along the embankments were collected in the channels and many flow inoundations affected the arounding villages (Cibelli, 2014).

In order to reduce these effects, from 1749 under the rules of the House of Bourbon in Naples, an improvement of the channeling system was conducted. Many drainage systems and open ditches have been realized to guarantee the outflow of the water to the sea. Moreover restoration works have been conducted such as the plantation of different rows of poplars plants along the embakments. Regulatory actions had been already introduced by the 'Universitas of Quindici' (1703) such as the prohibition of dragging the cut chestnut for the huge damages and flow inoundation induced by the abovementioned dragging. Restoration works continued during the years and the creation of a cultivation system characterized by regular agricultural lots alternated by channels.

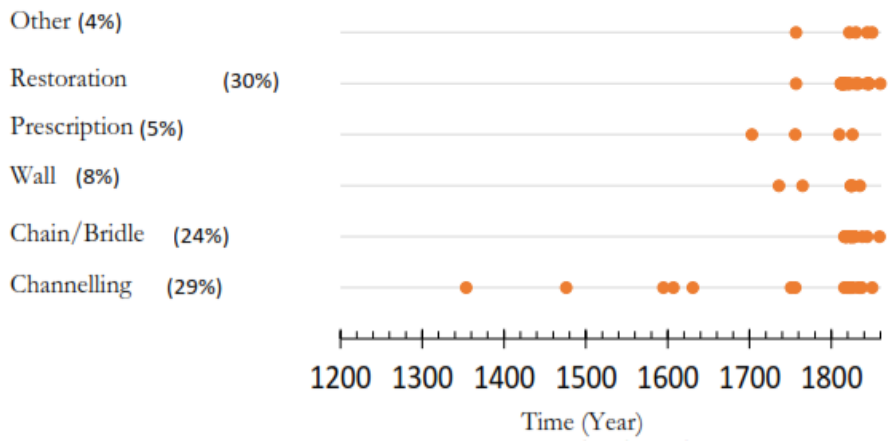

Figure 3.4 Typical landscape measures carried out from the Middle Age to the Italian State national Unity (Sacco, 2015).

During the 1855 the General Administration of Land Reclamation (Amministrazione Generale delle Bonifiche) has been established. This latter provided many actions in all the South Italy (two Sicilies Kingdom), in particular in the area of Naples and Volla, as well as the Somma-Vesuvius area.

The first attentions for the vegetation regarded the prohibition in cutting chestnuts and woods or brushes because they were already recognized to be natural reinforcement for soil and to contrast the water floods.

Starting from this period, many bio-engineering control (i.e. woods, brushes) works have been realized in order to reduce the slope inclination of the embankments or to improve the slope stabilization and

to realize new artificial channels (Fig. 3.5a) of 100 km of length linked with Regi Lagni. Moreover, for the next 60 years many other works have been realized such as 210 km of reverbed roads with related chutes, bridles (Fig. 3.5b), and 35 storage basins.

Figure 3.5 Examples of a) artificial reverbed channel and b) brindle with 4 steps realized during the XIX century (Cibelli, 2014).

After the eruption of 1906 many ahsy soils were produced and transported along the slopes by the rainfall occurred after the explosion. Most of the channels were completely covered by debris and many flow inoundations caused damages to the arounding cities. As consequence, from 1907 new operations such as forest and hydraulic works were started and the recovery of the ancient channels was conducted. From the Seventies, no more maintenance actions on these works have been guaranteed and the complex system of mitigation measures constructed during the last centuries was forgot. Only after the recent catastrophic events these ancient mitigation measures were rediscovered and their efficiency was confirmed. Indeed, the land transformation related to its use from the XIV up to XVIII century was locally time-tested in several territories (Cacini, 2008) regarding the consequences in terms of loss of human life.

In addition, the effectiveness of the channeling and drainage systems realized by the Bourbons was credited during the emergency management after the May 1998 events, when the Operational Unit 2.38 identified among the urgent risk mitigation measures the recovering of part of the drainage network located in the municipalities affected by landslides (Cascini, 2006). Is important to highlight that for the first time

this Operational Unit, after the catastrophic event of 1998, proposed a zoning of mountain areas which could be involved or not in landslide triggering. This latter represents a fundamental prerequisite for an integrated design of passive control works with measures introduced in the next section.

3.4.2 Recent landslide risk mitigation measures

Landslide consequence can be reduced through landslide mitigation measures, which can be divided into two categories: active and passive measures (Picarelli and Urcioli, 2006; Evangelista et al., 2008), in relation to whether the mitigation measures "actively" pursue an improvement of the stability of slope, or they "passively" intercept the run out when movement actually occurs, protecting the elements at risk.
In particular, Ambrozic et al. (2009) defined as active those measures acting to reduce the hazard (through reducing the probability of triggering through stabilization and/or by reducing subsequent ground movement through barriers or containment) and as passive those measures which reduce the vulnerability (i.e. reducing the consequences of failure). Within the passive works Lo (2000) introduced those which do not involve directly engineering and can include land-use regulation, education and landslide warnings, while Van Dine (1996) described control structure works for the reduction of consequences of debris flows. On the other hand, active measurements involve engineering works and normally comprise upgrading works on the slope aiming to reduce the probability of failure.
Bridles, dissipation basins and protection works for the exhibited properties, belong to structural passive mitigation measures and they all require information about mass of volume involved and its discharge, velocity, as well as the run out distance (distance that the mass will travel), and thus the expected deposition area (where the mass will stop).
On the other hand, in order to design the active control works the spatial distribution of slope instabilities and volumes involved are required.
Vaciago (2013) within the SafeLand project summarized advantages and disadvantages of active an passive control works.
In Campania region, after the catastrophic event of May 1998 many landslide mitigation measures have been conducted because it was widely recognized that pyroclastic covers are systematically affected by the triggering of debris flows.

Passive control works have been preferred to active ones and 20 dissipation basins, 120 brindles and 26 km of channeling have been constructed for a predicted volume of 1 million m^3 (Versace et al., 2008). Figure 3.6 shows the view from the top of the piedmont area of Pizzo d'Alvano, where the May 1998 events occurred and the location of one dissipation basin of about 176000 m^3 (Fig. 3.6b) and one brindle 5 m high along the channeling system (Fig. 3.6c).

Figure 3.6 a) view from top of the dissipation basin at piedmont of Pizzo d'Alvano (where the May 1998 debris flows occurred) and particular of the b) dissipation basin and c) brindle.

These passive control works required an expensive construction and still they represent a great impact with the environment. Moreover, a frequent maintenance is currently required since debris, garbage and wild vegetation can cover them over the time and reduce drastically their effectiveness.

3.5 CONCLUDING REMARKS

Pyroclastic soils are systematically affected in Campania region by rainfall induced flow-like landslides. Particularly, debris flows are triggered during rainy season due to the rainfall with low intensity infiltrating the slopes in correspondence of low soil suction values in the soil cover, while hyperconcentrated flows occur during dry season due to intense rainfall impacting and eroding dry soil.

Since the Middle Age in Campania region hydraulic channels aimed to avoid river inundations and/or to collect meteoric water have represented the most frequent ancient risk mitigation measures to reduce the impact of hyperconcentrated flows. During the centuries, particularly in the period when the Bourbons ruled in Naples, a complex hydraulic system was constructed and after that many active actions (such as vegetative restoration, woods, brushes) have been conducted along the embankments as well as brindles and storage basins for the collection of debris were constructed at the piedmont areas of the slopes.
Similar mitigation measures (dissipative basins, brindles etc.) were built up after the events occurred in the Campania region on May 1998, even though they do not represent a sustainable choice considering that 212 municipalities are affected in this region by similar phenomena.
Bio-engineering techniques, which use indigenous plants on slopes susceptible to failure, can be an alternative and/or an integration to passive control works in Campania region as well as in many other part of the World.
The attention for the vegetation since the Middle Age regarded the landscape transformation, reclamation and remediation. Over the centuries restoration actions and the laws for the prohibition in cutting chestnuts and woods of brushes were adopted because the threes have always been recognized to provide a positive effect on slope stabilization, in particular in contrasting the erosion phenomena which lead to the propagation of hyperconcentrated flows.
On the other hand, since the effect of vegetation on hydro-mechanical behavior of pyroclastic soils and on the consequential triggering of debris flows is still not well understood, in next Chapters the experimental investigation conducted during the PhD research project is described and discussed in depth with conclusions achieved.

4 BIO-ENGINEERING TECHNOLOGY

In this Chapter the bio-engineering technology using exclusively vegetation for slope stability is discussed in depth. General features, such as bio-engineering practices and vegetation species are described as well as plant traits and plant indexes usually measured in geotechnical field.
In addition, the influence of soil properties on the effectiveness of bio-engineering technique is discussed and the experimental program conducted during Ph.D. research at Hong Kong University of Science and Technology on the effect of soil nutrient on plant growth and thus hydraulic response of soil is deeply described.

4.1 GENERAL FEATURES

4.1.1 Bio-engineering practices

Bio-engineering for slope stabilization is the use of living plant materials, established by conventional seeding or live planting, to treat sites where surface stability and erosion problems arise (Morgan & Rickson, 2003).
The main goal of erosion control is to protect the face of the slope and to strengthen subsurface parts, typically by interlocking soil particles with a complex matrix of roots.
Is widely recognized that vegetation intercepts rain, by reducing the impact energy of rain drop to the soil preventing splash erosion and consequently slowing down the surface runoff. The main consequence of the rain interception by vegetation would be the reduction of infiltration rate in soil, as investigated by some authors in the past for grass species and tree species (Pollen-Bankhead & Simon, 2010; Ng et al., 2013; Leung et al., 2015).
Furthermore, the use of vegetation (grasses, shrubs and trees) has been recently recognized as sustainable and environmentally friendly engineering practice also for stabilizing shallow slopes and landfill covers

(Greenwood et al., 2004; Cazzuffi et al., 2006; Sinnathamby et al., 2013) through hydro-mechanical reinforcement on root-permeated soil.

This natural bio-engineering technique has received recently worldwide attention due to its relatively low cost, aesthetic and environmental value, as well as sustainability (Coppin et al. 1990; Gray and Sotir 1996; Goldsmith et al. 2014; Bo et al. 2015).

The stability of slopes is dependent on the ratio of driving forces and the strength of the soil-root system. Despite the weight of vegetation growing on the slope accounts for a part of the driving forces, according to Simon & Collison (2002), root-permeated soil makes up a composite material that has an enhanced strength, because of the tensile strength of the fibrous roots of trees and herbaceous plants, which gives an additional cohesion to the composite soil. Site trials investigations have been carried out in the past to quantify the reinforcing capability of plant rooting systems, with regard to their use as a means of improving slope stability (Yim et al, 1988; Campbell et al, 2008). However, it is difficult to ensure the lateral spread and depth of a root system within a soil mass in practice. The mechanical contribution of roots on shear strength of composite soil is discussed in depth in the following sections.

The main planting techniques widely used in bio-engineering practices are the hydroseeding or the direct pit planting of young trees.

Hydroseeding technique (Fig. 4.1a), usually aimed to erosion control, consists on applying a mixture of different quantities of seeds, wood fibre, fertilizer, depending on the soil and environment conditions, together with stabilizing emulsion by using an hydro mulch equipment, to temporarily protect exposed soils from erosion by water and wind (Albaladejo et al., 2000; Vaciago 2013). On the other hand, pit planting consists on direct transplant of young sprouts in pits excavated in soil (Fig. 4.1b). For this latter technique the species should have a root system that penetrates to the required depth to create favorable conditions for root growth and thus stability.

The planting techniques can be also combined together, where bio-engineering slope works with hydroseeding and pit planting of native species seedlings has been realized in man-made slope in Hong Kong.

The selection of planting techniques is affected by site conditions such as the availability of soil, water and light to support the successful establishment and growth of plants (GEO, 2011).

Figure 4.1 Examples of planting techniques: a) Aerial Hydroseeding (http://www.ericksonaircrane.com/hydroseeding.php), b) pit planting of grasses in Nepal.

Engineering practices for slope stabilization when living plant materials are combined with other mechanical materials, such as woods, non biodegradable control mats, gabions, are properly called bio-technical (Fig. 4.2), where both biological and mechanical complements must work together in an integrated and complementary manner (Gray & Sotir 1996).

Figure 4.2 Schwandrübi scree slope (left) in 1978 before the application of gabions and hydroseeding, and (right) after the heavy rainstorm in August 2005 (source: left Forestry Service of Nidwalden; right WSL).

4.1.2 Vegetation types and plant traits

The selection of vegetation type (i.e. grasses, shrubs and trees) depends on the bio-engineering purpose: grass cover is increasingly considered as a sustainable means of reducing the coefficient of erodibility of soil (Zhu & Zhang, 2016) and enhancing durability of soil slopes (Borja & White, 2010), while tree species with high transpiration, rather then grasses, was found more effective in decreasing soil moisture and increasing induced soil suction (Garg et al., 2015a).

Another factor influencing the selection and thus the effectiveness of vegetation types is the environmental context where they grow, such as the climate conditions, so, wherever feasible, a native vegetation is preferred (Gray & Leiser, 1982; Schiechtl & Stern, 1996).

In tropical and subtropical areas like Hong Kong, and in many parts of Asia, such as Vietnam, India, and Malaysia, including in Japan, *Schefflera heptaphylla* (Fig. 4.3a) tree species, also known as Ivy Tree, is widely used in bio-engineering practices because of its significant ornamental and ecological value for slope rehabilitation and reforestation (GEO, 2011) and is drought tolerant (Hau & Corlett, 2003).

Among grass species *Cynodon dactylon* (Fig. 4.3b), perennial species native to tropical America and widespread in subtropical areas of the world, together with *Zoysia Matrella* (Fig. 4.3c), were recently recommended for

soil bio-engineering in Hong Kong, because of their high root density which controls the extent to which roots alleviate soil erosion (Zhu & Zhang, 2016).

Among "perennial graminae" grass species, *Chrysopogon zizanioides* (Fig. 4.3d), commonly known as *Vetiver*, has been widely used for bio-engineering purposes in many tropical and sub-tropical countries in South East Asia, China, Africa, South America, as well as warmer parts of the United States, Australia and Europe.

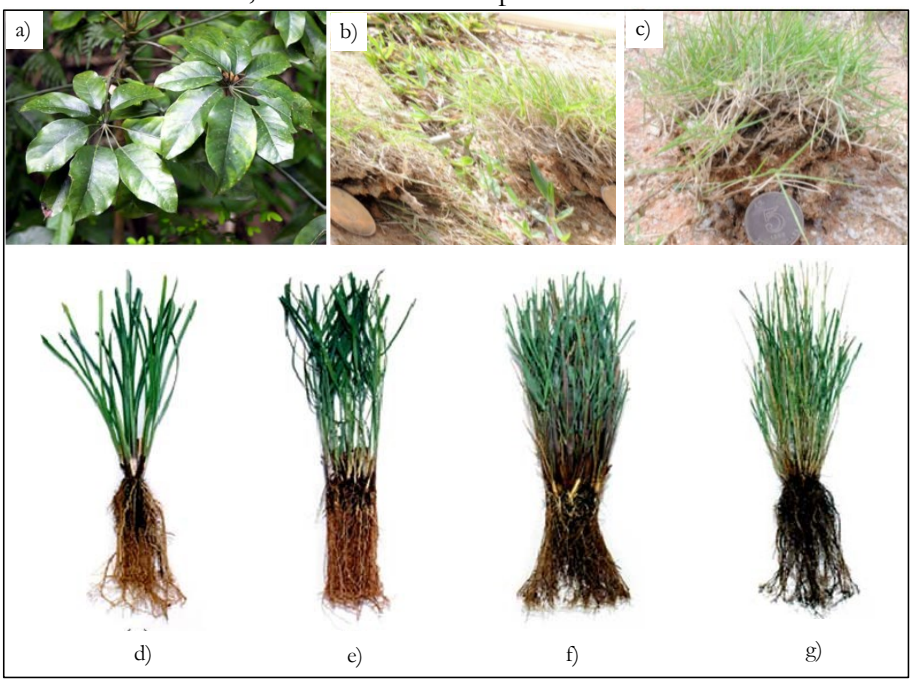

Figure 4.3 Main vegetation types studied for bio-engineering. Tree species: a) Schefflera Heptaphylla (GEO, 2011); Grass species: b) Cynodon dactylon and c) Zoysia Matrella (Zhu & Zhang, 2016), d) Vetiver, e) Pangrass, f) Eragrass and g) Elygrass (Cazzuffi et al., 2006).

Vetiver, together with other "perennial graminae" grass species such as *Pangrass* (Fig. 4.3e) native to North America, *Eragrass* (Fig. 4.3f), native to south Africa and *Elygrass* (4.3g), found in southern east Europe, has been recently introduced also in Mediterranean areas, in south Italy, for erosion control and superficial instability of shallow slopes surrounding a new thermoeletrical station under construction (Cazzuffi et al., 2006).

The effectiveness of the vegetation on improving hydro-mechanical properties of soil was recently indirectly quantified by measuring the main plant traits.
It has been well-recognized that plant transpiration and the associated induced soil suction is manly controlled by the percentage of radiant energy intercepted by leaves, the number of stomata as well as the stomatal conductance (Ritchie, 1972; Kelliher et al., 1995; Hetherington and Woodward, 2003).
It is therefore common to monitor the Leaf Area Index (*LAI*), which is a dimensionless index for a single plant defined as the ratio of the total leaf area to the projected area of canopy of an individual plant on the soil surface in horizontal plane (Watson, 1947), to indirectly have information about induces soil suction in soil by plant transpiration (Fig.4.4a).
This index can be measured through different methods (He et al., 2007), for example by using a proper plant canopy analyzer (Ramírez García et al., 2012) or by analyzing, through image software, digital images of the surface of leaf blades from the sampling area (Garg et al., 2015b, 2015c).
Root area index (*RAI*) is defined as the ratio of total root surface area for a given depth range to the circular cross-sectional area of soil in the horizontal plane (Francour & Semroud, 1992). *RAI* can be also measured by analyzing digital images, after the sampling of the root structure (Fig. 4.4b), through image software (Ng et al. 2016), as discussed in depth in the following section.

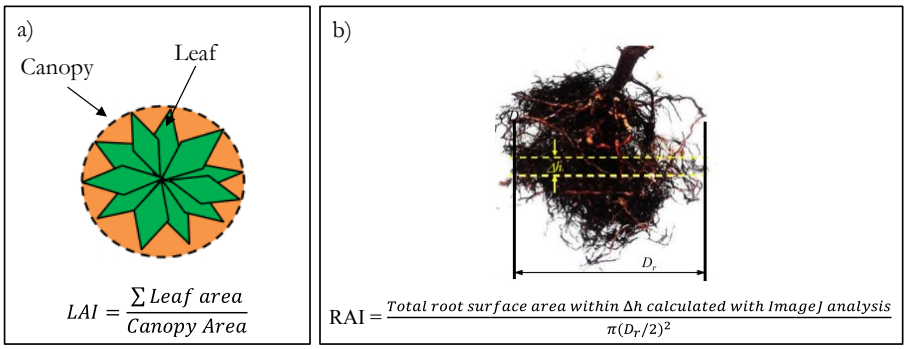

Figure 4.4 a) Schematization of Leaf Area Index image calculation (Gadi et al., 2016, modified); b) Root structure sampled for RAI analysis (Leung et al., 2015, modified).

The biomass of shoot and roots of the plants were recently used as indicators of the effectiveness of the vegetation species used in increasing induced soil suction during evapotranspiration. The biomass is referred to the dry mass of each part of the plant (i.e. root biomass is the dry mass of the total roots in the soil, shoot biomass is the dry mass of the total leaves of the plant).

Recent experimental studies observed that the induced soil suction is positively correlated to leaf area index (*LAI*), root area index (*RAI*) (Ng et al., 2016) and root-shoot biomass ratio (Boldrin et al., 2017).

Furthermore, the erodibility of the soil was found to decrease with the increasing of Root Mass Density (*RMD*), which is described by the ratio between the dry mass of the roots and the dry mass of the root-permeated soil sample (Zhu & Zhang, 2016). In addition, root traits also influence soil shear strength (Operstein & Frydman, 2000; Mickovski et al., 2009) and plant roots could induce substantial change in soil water retention characteristics (Leung et al., 2015).

However, soil characteristics (i.e., physical composition, chemical composition (nutrient availability), pH, salinity) affect vegetation growth and hence the effectiveness of vegetation on slopes, as discussed in depth in the following sections for the case of the effects of nutrient availability in Completely Decomposed Granite in Hong Kong on vegetation growth and thus change in soil hydraulic properties.

4.2 ROOTS GROWTH IN NUTRIENT RICH PATH AND EFFECTS ON SOIL HYDRAULIC RESPONSE: THE HONG KONG CASE STUDY

4.2.1 Nutrient availability in soil on plant traits

Soil characteristic (i.e., physical composition, chemical composition (nutrient availability), pH, salinity) can affect the vegetation growth used in bio-engineering technology and thus its effectiveness. Stokes et al. (2009) schematized a typical root system growth in soil without nutrient availability compared with root system in nutrient rich path (Fig. 4.5). In soil with nutrient availability, root traits change their spatial distribution and proliferation (López-Bucio et al., 2003; Miller et al., 2003; Desnos, 2008). Previous studies on different plant species observed that roots grown in nutrient-rich patch proliferate within it by becoming longer and thinner (Farley &Fitter, 1999). This proliferation occurs by initiating new secondary order roots and root hairs around the primary or 1st order lateral roots (Hodge, 2004).

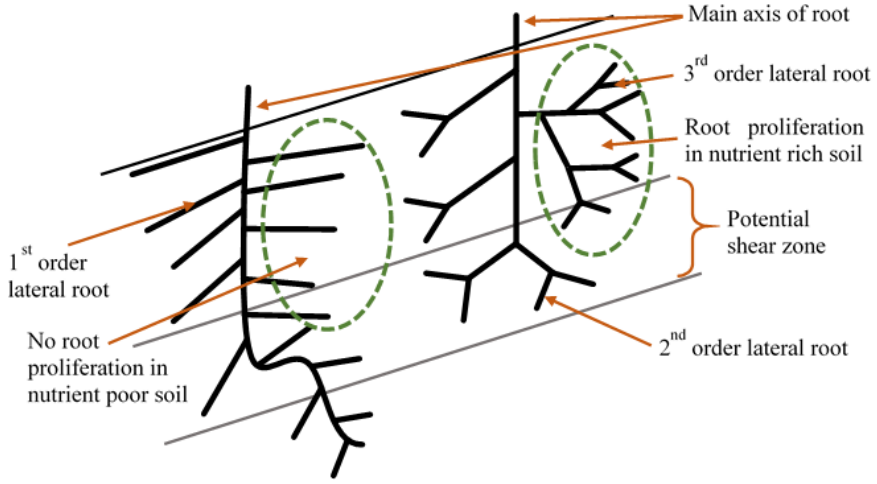

Figure 4.5 A herringbone root system with one main axis on which are borne first order lateral roots (left) and a dichotomous root system with two external root tips borne on every lateral. 2nd and 3rd order lateral (right). (Stokes et al. 2009, modified).

It is well known that fine roots have high surface area and thus are mostly responsible for water and nutrient up-take from soil (Eamus et

al., 2016). Soil with high nutrient supply usually provide healthier species in terms of growth (Arredondo & Johnson, 1999) and it was observed that root traits reflect an increased development for the entire plants (Gersani & Sanchs, 1992).
Most of these studies have been conducted for agricultural purposes and currently are rare the contributions related to the quantification of the effect of nutrient availability in soil on vegetation growth for bio-engineering purposes. In fact, plant traits can strongly change in nutrient rich path soil and thus affect its hydro-mechanical properties.
Hong Kong government, since the end of '70s, adopted landslide risk mitigation measures which include also bio-engineering practices for man-made slope stabilization (GEO, 2011). In practical bio-engineering techniques in Hong Kong, and also in other countries, an establishment period is usually contemplate (typically 12 months) within that slow release granular soil fertilizers (NPK complex fertilizer: which describes the amount of nitrogen, phosphorus, and potassium in a fertilizer) are used in order to enhance the plant growth. Field study conducted on degraded hillside grassland in Hong Kong also found that slow release NPK complex fertilizer had long-term significant effects on *Schefflera heptaphylla* (Fig. 4.3a) growth (Hau & Corlett, 2003). However, there is a lack of contribution whether nitrogen rich NPK nutrient can stimulate both shoot and root growth of plants in soil for bio-engineering purposes. Furthermore, how nutrients will affect the root proliferation in soil and how the proliferated lateral roots shown in Figure 4.5 by nutrient supply will affect induced soil suction and water retention ability is not well understood.
Within the Ph.D. program, a 6 months experimental study was conducted at Hong Kong University of Science and Technology (HKUST) in Hong Kong. The aim of the study was to improve the knowledge on the effect of soil characteristics on plant growth in bio-engineering practices and to quantify the induced hydraulic responses. In the next sections the experimental program is explained and the results obtained in terms of plant growth are discussed.

4.2.2 Test set-up and instrumentation

In this study, an atmospheric controlled laboratory experiment was carried out to quantify the effects of NPK nutrient supply on the growth of *Schefflera heptaphylla* in silty sand and its effects on induced soil suction

and water retention ability. In addition, plant traits (e.g., *LAI*, leaf number, root length, *RAI*, shoot and root biomass) were quantified and correlated with plant induced suction and soil-water retention curves were also established.

Figure 4.6 shows the schematic setup of a vegetated soil column. Six columns were constructed with inner diameter of 200 mm and outer diameter of 220 mm and a height of 400 mm. Soil was compacted in columns up-to 390 mm depth and an individual tree was transplanted at the center of six columns.

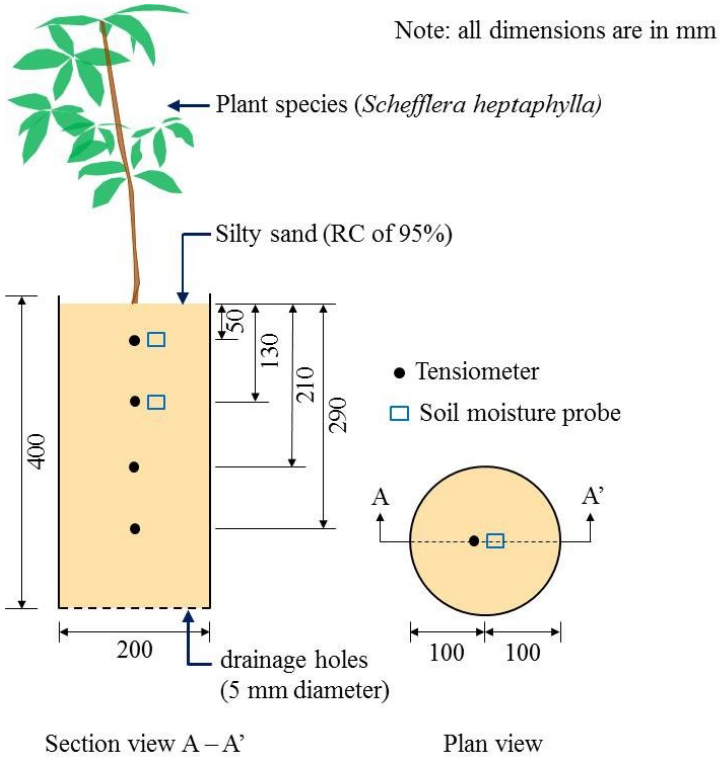

Figure 4.6 Typical schematic setup and instrumentation of a tree-vegetated column in (a) Cross section view A–A' and (b) Plan view (Ng et al., 2018 in press).

Side boundaries were impermeable, free drainage was allowed through 5 mm diameter holes at the bottom of the column and top boundary was exposed to the environment. Four miniature tip tensiometers at 50 mm, 130 mm, 210 mm and 290 mm depth (from soil surface) were installed just below the tree at the center of column.

The measurement range of suction is limited by water cavitation in tensiometer when negative pore-water pressure in soil approaches 80–90 kPa (Fredlund & Rahardjo, 1993). Soil moisture probes (SM-300) were installed at 50 mm and 130 mm depth right next to the tensiometer to monitor VWC. The purpose was also to investigate the effects of soil nutrition on root growth and occupancy in soil pores with consequent soil aggregation and changes in soil pore structure, which might affect soil water retention behaviour.
All soil columns were placed in a temperature- and humidity-controlled plant room for the whole testing period (Fig. 4.7). The daily temperature and relative humidity in the room were maintained constant at 25± 1°C and 55±5%, respectively. The light intensity provided by a cool white fluorescent lamp that was placed on top of the six soil columns was controlled to approximately 120 (μmol/m2)/s within the 400-700 nm waveband (i.e. equivalent to 5.0 (MJ/m2)/day).

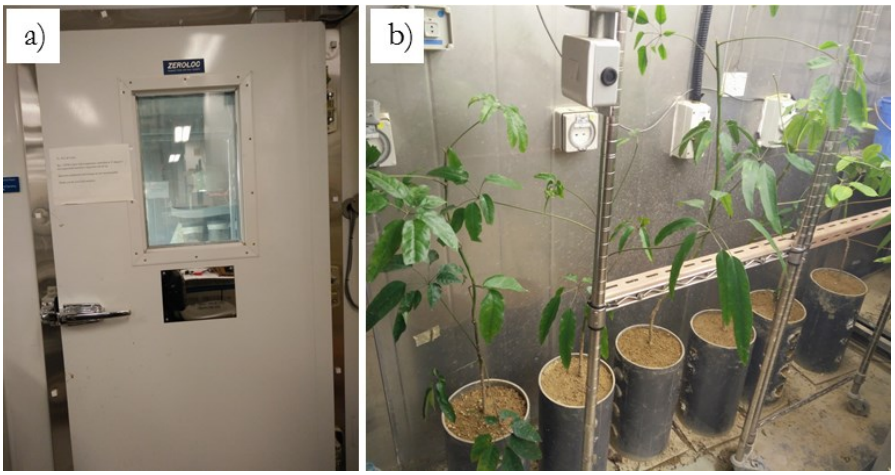

Figure 4.7 a) Environment controlled room placed inside the Geotechnical laboratory of HKUST and b) vegetated columns.

This waveband range is known to be favorable for plant photosynthesis and plant growth (Gates, 1980). Based on the atmospheric condition in the plant room, it can be estimated from the Penman equation (Penman, 1948) and Penman-Monteith equation (Allen et al., 1998) that the potential evaporation (PE) and potential evapotranspiration (PET) were 4.46 and 2.51 mm/day, respectively.

4.2.3 Soil type and preparation method

The type of soil tested in this study was completely decomposed granite (CDG), which is a poor nutrient soil commonly found in tropical and sub-tropical regions of the world such as Hong Kong and Korea. Measurements from the particle-size distribution showed that the contents of gravel, sand, silt and clay in the CDG were 19%, 42%, 27% and 12%, respectively. The plastic limit and liquid limit of CDG are 26% and 44%, respectively. According to the Unified Soil Classification System (USCS; ASTM, 2010), CDG can be classified as silty sand. Based on the results from standard proctor tests, the maximum dry density and the corresponding optimum water content (by mass) of the CDG were 1870 kg/m3 and 12%, respectively. X-ray Photoelectron Spectroscopy (XPS) analysis was used to determine atomic and mass concentration of nitrogen (N), Phosphorous (P) and Potassium (K) in CDG soil (Tab. 4.1). The CDG in each column was compacted by moist tamping at a relative compaction (RC) of 95% (corresponding to the dry density of 1777 kg/m3). Compacting to such a high RC is common for man-made slopes in countries such as the USA (TDOT, 1981) and Hong Kong (GCO, 2000). This is to design against rainfall infiltration and its induced slope instability. CDG has a field capacity of 21%, which is defined as the water content held in soil after excess water has drained away, assuming a negligible rate of water movement (Veihmeyer & Hendrickson, 1931).

Table 4.1 Atomic and mass concentration (%) of major nutrient elements (N, P, K) in CDG soil.

Major nutrient elements	Atomic concentration (%)	Mass concentration (%)
Nitrogen (N)	0.19±0.04	0.13±0.03
Phosphorous (P)	0	0
Potassium (K)	0.48±0.07	0.94±0.13

This water content corresponds to soil suction of 25 kPa. In each column, the CDG was compacted in 13 layers, with each spanning a height of 30 mm. Between each successive layer, the soil surface was scarified to provide better contact.

4.2.4 Vegetation species and nutrient type

The plant species investigated in this study was *Schefflera heptaphylla* (Fig. 4.3a), which has sharp leaves and is common in many parts of Asia including southern China, Japan, Vietnam and India (Hau & Corlett, 2003). This species is selected for testing because it has significant ornamental and ecological value for slope rehabilitation and reforestation (GEO, 2011) and is drought tolerant (Hau & Corlett, 2003). Various experiments have shown that *Schefflera heptaphylla* species is able to survive and thrive under high degree of compaction i.e., 95% (Garg et al., 2015; Leung et al., 2015). For fair comparison, tree seedlings with similar basal diameters and root depths were selected for initial transplantation. Before transplantation, the mean basal diameter (i.e. the diameter of the stem at the base of a tree) was 10±2 mm and root length was 125±10 mm. In order to consider the effects of any differences of plant characteristics on test results, three replicates were tested for each test series.

NPK (30-10-10) water-soluble nutrient was used in this study since NPK granular fertilizers have significant effect on *Schefflera heptaphylla* (Hau & Corlett, 2003). The nutrient used in this study is soluble in water so it was used with irrigation water once a week in this study. NPK rating system describes the amount of nitrogen, phosphorus, and potassium in a fertilizer. NPK ratings consist of three numbers separated by dashes (e.g., 10-10-10 or 16-4-8) describing the chemical content of fertilizers (EPA, 2003). The first number represents the percentage of nitrogen in the product; the second number, P_2O_5; the third, K_2O. Fertilizers do not actually contain P_2O_5 or K_2O, but the rating system is a conventional shorthand for the amount of the phosphorus (P) or potassium (K) in a fertilizer. A 50-pound (23 kg) bag of fertilizer labeled 16-4-8 contains 8 pounds (3.6 kg) of nitrogen (16% of the 50 pounds), 2 pounds of P_2O_5 (4% of 50 pounds), and 4 pounds of K_2O (8% of 50 pounds).

4.2.5 Test procedures

Two test series were conducted to grow plants in heavily compacted soil with and without nutrient supply and to investigate soil suction and volumetric water content (VWC). The first series was used as reference without using any nutrient in soil and the second series was conducted by supplying NPK (30-10-10) water-soluble nutrient in soil.

Bare soil was also tested in both test series as an additional reference test for the vegetated soil. For simplicity C and N represent the plants growing in nutrient poor and nutrient supplied soil, respectively (Tab. 4.2).
For each test series, three replicates of plants (total 6 plants) were grown for 6 months and suction and VWC were monitored. Every 2 days, all columns were irrigated with similar amount of water and every 8 days 3 columns were instead irrigated with NPK (30-10-10) nutrient mixed with water. NPK (30-10-10) water-soluble fertilizer was used in three vegetated soil columns after mixing 2 grams of NPK (30-10-10) fertilizer with 1 liter of water. The cumulative fertilizer used for each column over 6 months was 15 gm (corresponding to 212 kg/ha).
Since the expected root depth for all trees in this study was around 130 mm, decreasing suction values at 50 mm and 130 mm depth (monitored during irrigation by tensiometers) ensured that nutrient solution reached up to roots.

Table 4.2 Test series and ID of the columns in the experimental study conducted at HKUST.

Series	ID	Vegetation	Nutrient supply
Vegetated	C	*Schefflera heptaphylla*	No
	N	*Schefflera heptaphylla*	NPK (30-10-10)
Bare	B	No vegetation	-

At the end of 3 months and 6 months, in both series, the bare and six vegetated columns were subjected to a two-stage test. The first stage was to apply a ponding head on the surface of each column until i) suctions at all four depths decreased to 0 kPa and ii) percolation through the drainage holes at the column base was observed. At the second stage, to quantify the effects of evapotranspiration by plant-soil system on suction responses, the columns were exposed to the environment. Evapotranspiration-induced suctions were recorded by the four tensiometers. Each test was stopped when any tensiometer registered a value close to 80 kPa, which is the limit of the measurement range. The drainage holes at the bottom of all the columns remained open during the monitoring period. During the growth period, leaf area index (*LAI*) was monitored and after 6 months, plants were carefully removed from

the columns and *RAI* was determined using Image J as per procedures described in Garg et al. (2015). *LAI* was determined by image analysis using an open source software called ImageJ (Rasband, 2011). Images of individual tree leaves were captured by a high-resolution camera and then converted to binary images, based on which the leaf area can be determined.

After testing, the root area index (*RAI*) of all the plants was determined. *RAI* is defined as the ratio of total root surface area for a given depth range to the circular cross-sectional area of soil in the horizontal plane (Francour & Semroud, 1992), as introduced in the previous section (Fig. 4.4). The circular cross-sectional area of soil refers to the circular area, of which the diameter is defined by the maximum lateral spread of the root system within a given depth range. The root surface area refers to the total outside (external) surface area of all roots within a given soil volume that is defined by the cross-sectional area and the depth range. The tree roots were carefully removed from the columns and the soil attached to the roots was washed away with great care according to the standardized root washing procedures adopted by Smucker et al. (1982). Using the principle of hydro-pneumatic elutriation, roots were separated from compacted soils to minimize the destruction of small lateral roots and other fragile root structures. Root depth was determined as the deepest soil depth beyond which no root was found. Then, image analysis using ImageJ (Rasband, 2011) was conducted to determine *RAI*, following the procedures suggested by Garg et al. (2015). High-resolution images were taken 360° around the roots. All these images were combined to generate a three-dimensional (3D) image. Grids with equal pixel size (i.e. 12 pixels per unit mm of length) were superimposed on the 3D image. The total number of grids that contain roots at the given depth range was counted and hence converted into the total outside surface area of roots in mm2. Finally, *RAI* at any depth within a root zone can be determined by dividing the total outside surface area of roots at a given depth by the planar cross-sectional area of soil. In this study, *RAI* was discretized at intervals of 10 mm. The reason to provide such a discretized *RAI* is to more clearly determine the distribution of root surface area, which is shown to be important for interpreting suction (Garg et al., 2015; Leung et al., 2015). Stem, leaves and roots were weighed and oven-dried at 60° C for 24 h and again weighed to determine the dry biomass (Liang et al., 1989).

Finally, the ratio of root and shoot biomass was calculated for each plant to determine root-shoot biomass ratio. Ratio of root biomass and soil volume and ratio of root volume and soil volume for all vegetated nutrient poor and nutrient supplied soil columns are shown in Table 4.3.

Table 4.3 Normalized root biomass and root volume of the vegetated soil columns (Ng et al., 2018 in press).

Series	Root biomass (gm)/ Soil Volume (m3)	Root volume (m3)/ Soil Volume (m3)
C	775.5±195.9	0.04±0.02
N	1583.7±800	0.088±0.04

4.2.6 Effect of nutrients on plant traits

Figures 4.8a,b compare the typical plants immediately after transplantation and after 6 months of growth in nutrient poor heavily compacted soil (C series). It can be visually observed from Figure 4.8b that, without any nutrient supply, there are few leaves left and some of the leaves are turning yellow and brown which implies that the tree is not healthy. This is because nitrogen deficiency in soil reduces the chlorophyll content of the plant leaves which result in pale yellow colored leaves and likely to detach and fall (Morgan et al., 2013). During 6 months of plant growth, older leaves were turning yellow and falling from the plants which did not get any additional nutrient supply.

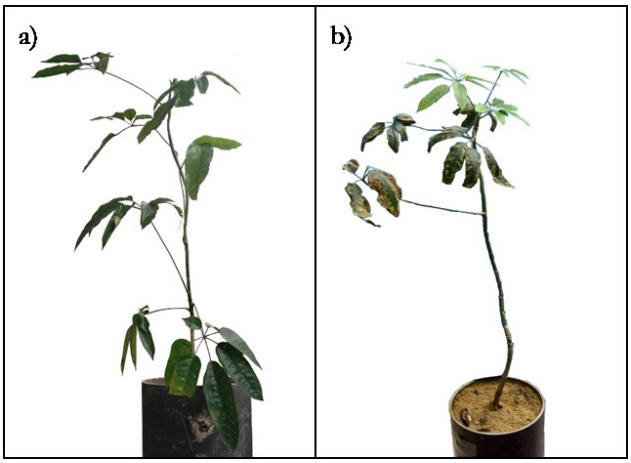

Figure 4.8Typical shoot growth of Schefflera heptaphylla in nutrient poor soil (C series) a) after transplantationand b) after 6 months of growth.

Figures 4.9a,b compare the typical plants immediately after transplantation and after 6 months of growth in nutrient supplied heavily compacted soil. From Figure 4.9b it can be observed that the amount of leaves increased and also grew bigger and greener.
However, the old and new leaves of the nitrogen rich nutrient supplied plants were comparatively bigger and greener with few fallen leaves during the typical 3 months of adaptation period after transplantation (Kitao et al. 2006).

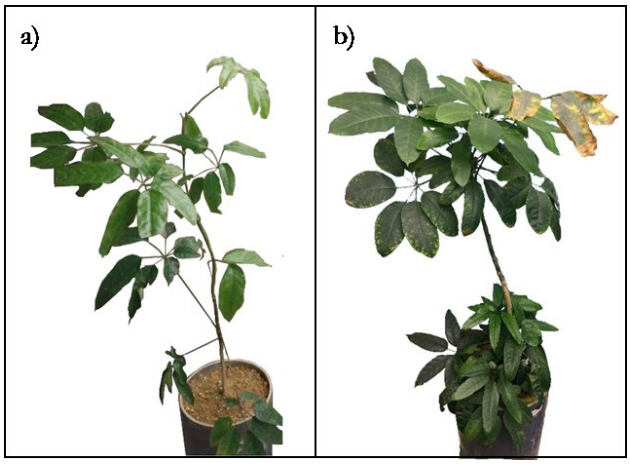

Figure 4.9 Typical shoot growth of Schefflera heptaphylla in nutrient rich soil (N series) a) after transplantationand b) after 6 months of growth.

Figure 4.10 compares the *LAI* between "C" and "N" tests. In "N" test, *LAI* increased by 350% compared to "C" test after 6 months of plant growth. Tingey et al. (1996) also found 40% increase of *LAI* using nitrogen fertilizer (100 kg N/ha) in clay-loam soil after 6 months of plant growth from ponderosa-pine seeds.

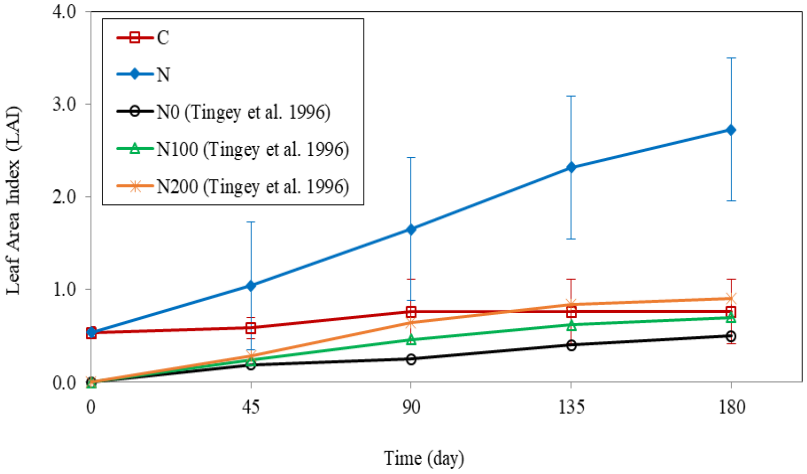

Figure 4.10 Measured changes in Leaf Area Index (LAI) of plants before transplantation and during 6 months of growth in nutrient poor soil and nutrient supplied soil ("C" represents the controlled test without nutrient supply and "N" represents the test with nutrient supply (Ng et al., 2018 *in press*).

Nitrogen-insufficiencies reduce *LAI* resulting in reduced surface light interception for photosynthesis (Cechin & Fumis, 2004).
CDG soil did not have sufficient nitrogen and is generally considered as nutrient poor soil.
However, the growth rate of leaves is larger when nitrogen-rich nutrient is present in soil because nitrogen plays significant role in chlorophyll-synthesis which stimulates plant growth resulting in larger leaves (Jasso-Chaverria et al. 2005).
Figures 4.11a,b compare the root geometry of plants growing for 6 months in nutrient poor and nutrient supplied soil, respectively. It can be visually observed from the figures that, without nutrient supply the roots are not as dense as the roots growing in nutrient supplied soil. The roots in Figure 4.11b are denser with clustered fine roots. This is because, in nutrient rich patch the roots proliferate with more 2nd order and 3rd order lateral roots as previously mentioned in Figure 4.5 (Stokes et al., 2009).

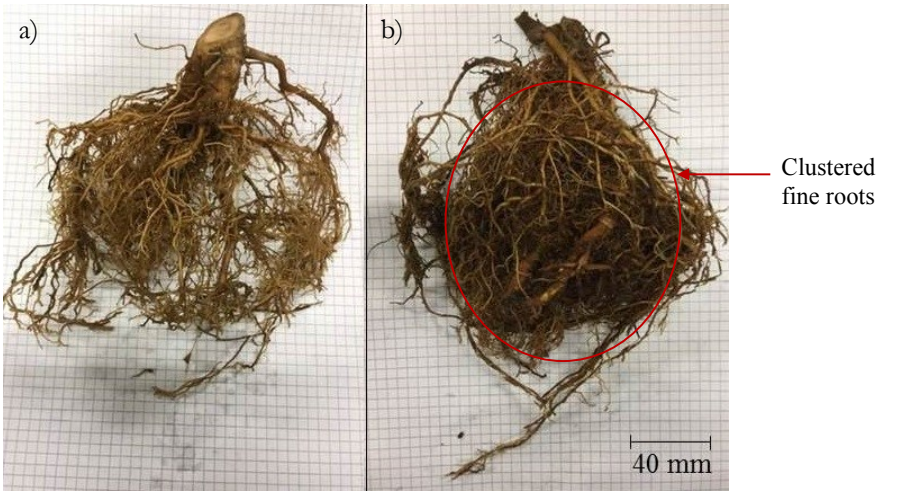

Figure 4.11 Root growth of plants after 6 months in a) nutrient poor and b) nutrient supplied soil (the sheet of paper in the background contains 5 mm× 5 mm squares) (Ng et al., 2018 in press).

Figure 4.12 compares *RAI* distributions along the root depth of plants growing in nutrient poor and nutrient supplied soil after 6 months of growth. *RAI* distributions are non-linear and parabolic in shape which is consistent with Garg et al. (2015) and Ng et al. (2016), which also used same plant species, soil type and soil density. The root surface area hence, *RAI* was larger at 70%-80% depths of root length, also observed by Garg et al. (2015) during the root distribution factor (Rdf) measurements. *RAI* difference between "C" and "N" tests was significant up to 130 mm depth (desired nutrient-rich zone) since the initial root depth was within 140 mm. Difference between peak *RAI* was about 130% implying that the total root surface area and root volume was significantly larger over a certain cross-section area and in a certain volume of soil in nutrient supplied vegetated soil columns. This is because phosphorous (P) enhances root growth, particularly lateral fine root development (Brady & Weil, 2002) which were clustered (Fig. 4.11b).

In contrast, several researches have shown contrasting responses of lateral root elongation due to soil nitrate and phosphorous concentration (Zhang & Forde, 1998; Johnson et al. 1996). Since different plants and their genes are responding to nutrient-rich soil regions in a different way, this study implies that nitrogen and phosphorous supply has significant

effects on the studied plant roots of *Schefflera heptaphylla* to stabilize bio-engineered slopes.

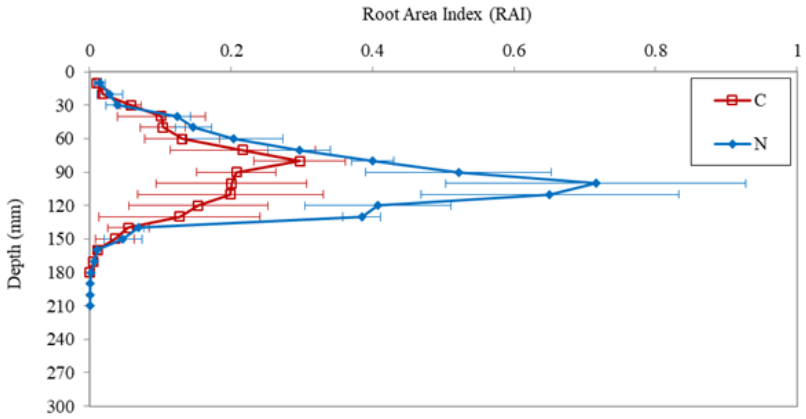

Figure 4.12 Measured changes in Root Area Index (RAI) of plants after 6 months of growth in nutrient poor and nutrient supplied soil ("C" represents the controlled test without nutrient supply and "N" represents the test with nutrient supply) (Ng et al., 2018 *in press*).

In this study, growth rate of roots was not significantly higher like the study by Gersani & Sanchs, (1992) which observed about 5 times greater relative growth of roots in the high nutrient condition than the plant roots growing without nutrients. This is because the plant roots in this study were grown in heavily compacted soil (95% RC) in this study, where the growth is generally hindered (Arrieta et al., 2009; Ng et al., 2014).

4.2.7 Effect on Soil Water Retention Ability (SWRC)

Figure 4.13 shows the drying path of soil water retention curve (SWRC) of bare, nutrient poor and nutrient supplied vegetated soil obtained by relating VWC to suction at a depth of 50 mm during drying from three replicates. Data points were scattered in a wider range in nutrient supplied vegetated soil compared to the nutrient poor vegetated soil due to the larger variation in root biomass as shown in Table 4.3 (Leung et al. 2015). Van Genuchten (1980) equation was used to fit the SWRCs and required fitting parameters are shown in Table 3. For any given suction, the rooted soils in tests "C" and "N" had noticeably greater water retention ability than the bare soil, also observed by Leung et al. (2015),

because roots can induce substantial changes in soil water retention curves.

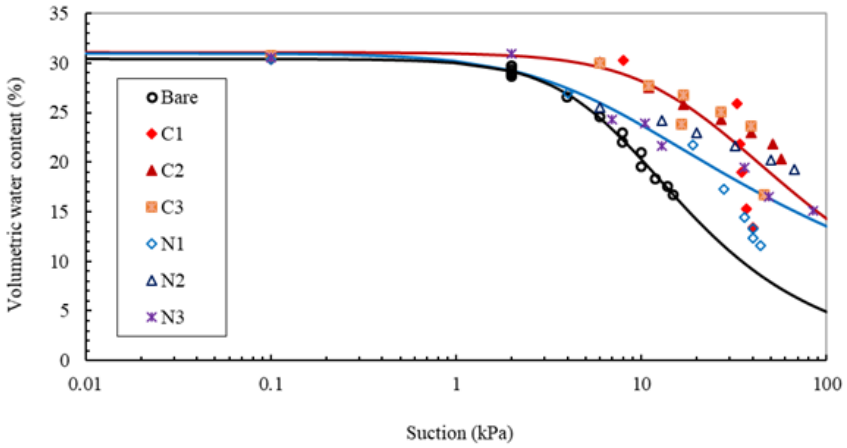

Figure 4.13 Measured SWRCs of bare and vegetated soil along the drying path in nutrient poor soil and nutrient supplied soil ("C1, C2 and C3" represent the controlled test of 3 replicates without nutrient supply and "N1, N2 and N3" represent the test of 3 replicates with nutrient supply (Ng et al., 2018 *in press*).

However, there was 5-6 kPa differences in AEV and water retention ability between "C" and "N" tests due to the 50% *RAI* difference between the roots and more than 2 times difference between normalized root volume (Table 4.3).

For any given suction, nutrient supplied rooted soils had reduced water retention ability compared to the nutrient poor rooted soil because plants grown with nutrient supply has more cluster of fine roots (Fig. 4.11b), larger root surface area hence, *RAI* (Fig. 4.12) and larger root volume. This occupied and clogged in to soil pores changing soil pore structure with consequent soil aggregation. Fine roots covered by root hairs significantly increase absorptive surface area and improve contact between roots and soil which increases occupancy in soil pores and they are the most permeable portion of a root system having the greatest ability to absorb water (McElrone et al., 2013). For a given soil water content, root occupancy in soil pore space (4% in "C" test and 8% in "N" test (Table 4.3) could reduce the diameter of soil pore throat changing pore structure and, which in turn increases suction according to capillary law (Scanlan & Hinz, 2010). Since soil water retention curve (SWRC) primarily depends on soil pore structure and its distribution

(Romero et al., 1999; Ng and Leung, 2012), soil water retention ability was different in nutrient poor and nutrient supplied vegetated soil. The drying curve is significantly impactful for geotechnical engineers in understanding crack formations in bioengineered slopes and landfill cover for vegetative layers which was emphasized and discussed by Gadi et al. (2016).

4.2.8 Effect on plant induced soil suction

Figure 4.14 shows the suction profiles along depth before and after 3 days of drying after 6 months of plant growth. Initial suctions in bare and vegetated soils were 0-2 kPa. Higher suction induced at shallow depth (50 mm) in bare and vegetated soil than deeper depths due to the hydraulic-gradient established at the soil–atmosphere interface during surface evaporation. During drying, evapotranspiration induced suction increased 26-50 kPa (at 50 mm depth) and 15-26 kPa (at 130 mm depth) in nutrient supplied vegetated soil compared to the nutrient poor vegetated soil.

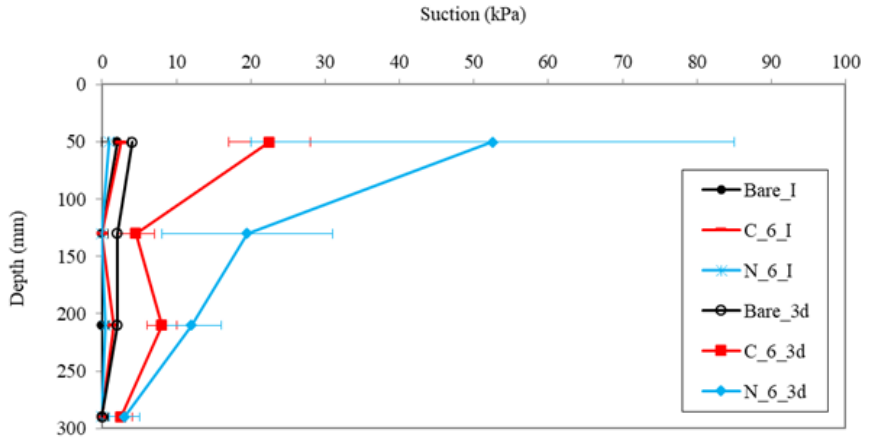

Figure 4.14 Measured suction profiles of bare and nutrient poor and nutrient supplied vegetated soils before and after 3 days drying after 6th month of plant growth ("6" represents the drying test conducted at 6th month of plants growth; I and 3d represent the initial suction in soil before drying and suction after 3 days of drying) (Ng et al., 2018 in press).

This is due to 50% (at 50 mm depth) and 138% (at 130 mm depth) larger *RAI* and 2 times larger root volume (Table 4.3)

besides 160%-200% larger *LAI* in nutrient supplied vegetated soil (Fig. 2). However, there is a variability of suction measurements in the replicates of vegetated soils which is representing the uncertainty of suction behaviour during evapotranspiration due to water uptake by roots. In fact, recent studies used probabilistic approach to analyse the stability of vegetated slopes by treating suction as a random variable (Das et al., 2018). Since a cluster of fine roots (Fig. 3-(b)), larger root surface area (Fig. 4) and larger root volume in soil (Table 4) can absorb and uptake more water and nutrient (McElrone et al., 2013; Eamus et al., 2016) and higher leaf surface area (Fig. 2) can transpire more water (Kelliher et al., 1995), induced suction in nutrient supplied vegetated soil was significantly higher. This implies that, using additional NPK nutrient can stimulate leaf and root growth significantly having long term establishment in slopes and thus higher suction can be induced in vegetated heavily compacted soil. Therefore, there would be significant impact on the performance of the infrastructure because soil shear strength will increase, soil permeability during rainfall will decrease (Ng & Menzies, 2007; Ng & Leung, 2012) and the probability of failure (P_f) will be less in the nutrient supplied treed slopes due to higher amount of evapotranspiration induced soil suction (Das et al., 2018).

4.2.9 Nutrient supply effect on correlation between plant traits and plant induced soil suction

Figure 4.15 shows the correlation of root-shoot biomass ratio with induced peak soil suction in nutrient poor and nutrient supplied vegetated soils. In both tests, higher root-shoot biomass ratio induces higher suction and correlation between root-shoot biomass ratio and induced peak suction is stronger (R^2=0.86) than the study by Boldrin et al. (2017) (R^2=0.65) because it considered 10 different kinds of plant species. Steeper correlation was observed in "N" test implying that root-shoot biomass ratio and their induced suction both were significantly higher in nutrient supplied vegetated soil. This is because increase in root-shoot ratio allow the plant to extract more water from soil (Stulen & den Hertog, 1993) and therefore, induced suction would be higher which can increase hydrologic reinforcement and reduce the probability of failure (Pf) in bio-engineered treed slopes (Das et al., 2018). This highlights the importance of considering the combined effects of both

the below- and above- ground organs on the hydrologic reinforcement to soil (Boldrin et al., 2017).

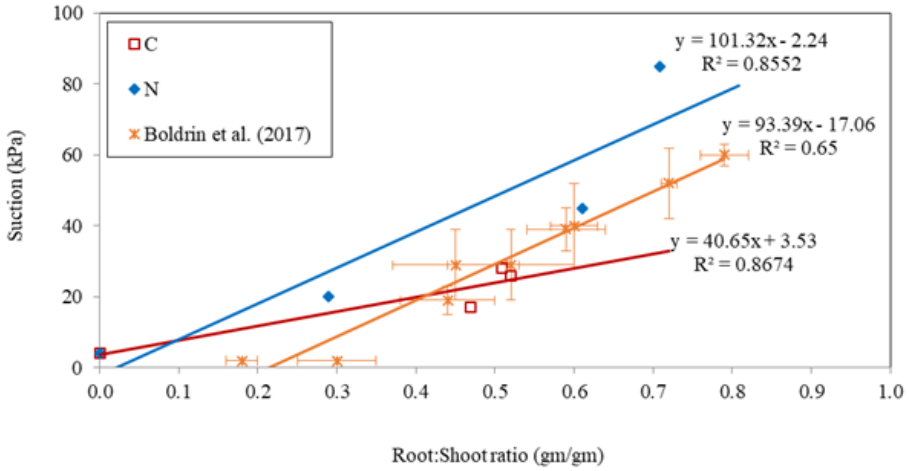

Figure 4.15 Relationship of root-shoot biomass ratio with matric suction (kPa) after 3 days of drying in nutrient poor and nutrient supplied vegetated soil after 6 months of plants growth ("C" represents the controlled test without nutrient supply and "N" represents the test with nutrient supply; Boldrin et al. (2017) used 10 different woody plant species in sandy loam soil) (Ng et al., 2018 *in press*).

4.3 CONCLUDING REMARKS

This study explores effects of NPK (30-10-10) water soluble fertilizer on *Schefflera heptaphylla* and its induced soil suction and VWC. Two test series (three replicates for each test) with and without NPK water soluble fertilizer supply in heavily compacted (95% RC) silty sand were conducted for 6 months. After 6 months, *LAI* and peak *RAI* increased by 350% and 133%, respectively and clustered fine roots and more than 2 times larger root volume were observed in nutrient supplied vegetated soil compared to nutrient poor soil. This is because nitrogen stimulates chlorophyll-synthesis providing plants with larger leaves and mediates phosphorous to be utilized by roots in soil which enable plants to grow more fine roots and thus larger root surface area. Due to occupancy in soil pores with more clustered fine roots, larger root surface area and root volume in a certain volume of soil which decreases pore diameter

with consequent soil aggregation and increases suction by capillary law, water retention ability decreased in nutrient supplied vegetated soil. Because of having larger *LAI*, *RAI*, root volume and root-shoot biomass ratio plants in nutrient supplied vegetated soil could extract, absorb and transpire more water and so 15-50 kPa (68%-173%) higher soil suction was induced after 3 days of evapotranspiration.

Since this experimental study was conducted on heavily compacted soils and suggested that the plant growth is hindered if nutrient is not supplied into the soil, this conclusion can be exported more in general to all types of soil.

Additional nitrogen rich NPK water soluble fertilizer supply during irrigation of vegetated soil could stimulate plant growth which increases plant induced soil suction that can increase shear strength, reduce permeability effectively during rainfall and reduce the probability of failure of bio-engineered treed slopes.

This means that initial soil properties can strongly affect the efficiency of plants on hydro-mechanical reinforcement, and this factor must be taken into account when a bio-engineering practice is chosen for stabilizing slopes.

5 EXPERIMENTAL INVESTIGATION ON LONG ROOT GRASS TECHNOLOGY

The Prati Armati bio-engineering technology is introduced and the general features, such as the vegetation species selected, the typical growth period and the root characteristics are discussed. These sustainable natural elements are indigenous thus they do not contrast with the arounding system by developing naturally a fibrous root system up to 2 meters of depth.
In order to contrast the surface erosion due to heavy rainfall, this technology have been already used in many geological and geomorphological contexts and examples of the main applications are exposed.
Considering that the slip surface in shallow landslides is generally located about few meters from the ground surface, this feature suggests that Prati Armati could be profitably used as an active measure to control the surface erosion and to improve the stability of the pyroclastic deposits systematically affected by rainfall induced flow-like landslides.
To this aim, in this Chapter the experimental set up constructed at the University of Salerno and the vegetation species investigated are deeply described. Finally, the observed vegetation growth in pyroclastic soils and measured root characteristics are discussed.

5.1 PRATI ARMATI TECHNOLOGY

5.1.1 General features

Prati Armati is an Italian bio-engineering technology, since 1999, which uses different type of perennial graminae species on man-made slopes to protect soil from erosion and superficial instability.
This technology includes simple fast installation without maintenance. Recent studies also supported by botanists, agronomists, naturalists and geologists, have concluded that herbaceous species can effectively

contrast erosive phenomena, even in bare and sterile soils where other common species do not succeed to vegetate (Briaud et al., 2008; Borja, & White, 2010; Zarotti, 2014; Zhu & Zhang, 2016). Moreover, these perennial graminae species, have a root system able to reach about 2 meters of depth within the first vegetative year, up to 5 meters of depth in loose soils.

They are able to grow in different litotypes, such as clay, silt, sand, gravel, flysh, and in soils with different chemical properties, such as those with lime addiction. They can adapt to different geo-environmental contexts and their climatic changes, also in dry conditions, thanks to their capability to reach the deeper zones of the soil substrate where water is available (i.e. water springs, deep aquifers).

The installation of these herbs usually is done through hydroseeding: a mixture of water, compost, vegetable fibers and seeds is spread along the surface of the affected soil by helicopter, crane or tank, depending on the position of the site (i.e. easily approachable or not).

Three main vegetative behaviors were individuated from agronomists during the first vegetative year: *microthermal* species, *meso thermal* species and *macro thermal* species. The typical temperature range where *microthermal* species likely grow is between 15°C and 20°C and the growing behavior is characterized by 2 peak of growth during the first vegetative year, the first is higher and occurs in spring season and the smaller occurs during fall season (Fig 5.1b). *Meso thermal* species grow when temperature ranges between 20°C-25°C, while *macro thermal* species require higher temperature values (25°C-30°C) and usually show only one peak growth during summer season (Fig. 5.1c).

Experimental observations on plant growth claimed that the ratio between the hypogeum part (roots) and the above part (leaves) of these plants is always very high, compared to traditional plant species (Fig. 5.1a).

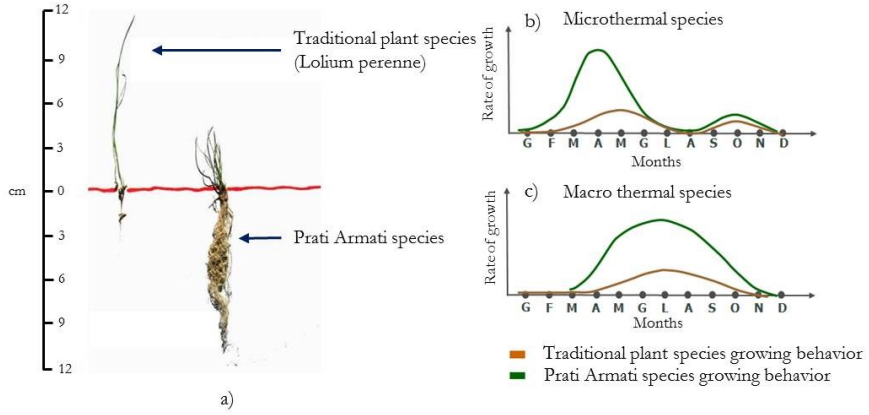

Figure 5.1 a) Example of hypogeum part (roots) and aboveground part (leaves) of traditional plant species and Prati Armati species; Qualitative behavior of b) Microthermal species and c) Macro thermal species in terms of rate of growth during the first vegetative year for traditional plant species and Prati Armati species.

Some authors carried out experimental tests on the tensile strength of several variants of perennial grass species, mainly belonging to the botanical families of graminae, such as those used by Prati Armati technology, and leguminosae (Bonfanti and Bischetti, 2001; Cecconi et al., 2015). They found extremely high values (tens of MPa) of single root tensile strength for an average root diameter of about 0.5-1.5 mm. This issue regarding tensile strength of roots is discussed in depth in Chapter 8, where the contribution of roots on increasing shear strength of reinforced soil is investigated.

The efficiency of roots in increasing soil shear strength depends on how they develop in soil, as discussed in depth in Chapter 4. Indeed, Root Area Ratio (*RAR*), represents one of the plant parameters needed to understand the rooted-soil behavior. It was demonstrated that this ratio depends on the plant species, and typically decreases with depth. As already introduced in previous Chapter, this generally occurs despite of the complex geometry of the root system which presents a great variability, depending on plant species, soil properties and chemical composition (nutrient availability, pH, soil salinity) and environmental conditions.

Cecconi et al. (2012) proposed a geometrical model, typical of fasciculate root system (Fig. 5.2), to simply calculate the root distribution along

depth of *Graminae* species, like those used by Prati Aramati technology. It consisted of a truncated cone with opening angle, β, surface radius, r, and maximum radius R attained at maximum depth z_{max}. In such configuration, every single root has diameter, d_i, and cross section, $a_{r,i}$. The *RAR* in this study was considered as ratio between rooted area (A_r) and the soil cross section (A_s).

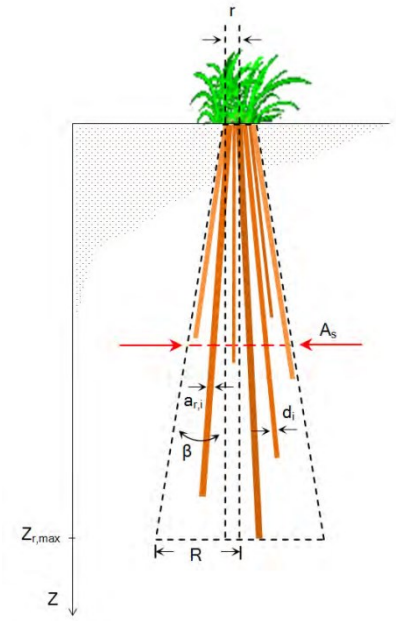

Figure 5.2 Simplified model for the definition of the root area index Ar/As (Cecconi et al., 2012).

At any depth z from the ground, the rooted area A_r, is given by:

$$A_r(z) = \sum_{i=1}^{n} n(z, d_i) \cdot a_{r,i} \tag{5.1}$$

where $n(z,d_i)$ is the number of roots with diameter d_i.
The soil cross section A_s, for geometrical considerations, is given by the following equation:

$$A_s(z) = \pi(z \cdot \tan\beta + r)^2 \tag{5.2}$$

with surface radius *r* expressed as:

$$r = \sqrt{\frac{A_r(z=0)}{RAR_{\max}}} \cdot \frac{1}{\pi} \tag{5.3}$$

The maximum value of Root Area Ratio *(RAR_{max})* was found at ground surface, and the opening angle β varying in the range 10° - 15°.
With these simple equations Cecconi et al. (2013) evaluated the *RAR* profile with depth by first dividing the root depth in layers of around 10 cm of thickness each, then assigning for each layer, ten classes of diameters. From the available experimental evidence, reasonable values of n vary from n_{max} = 40 in the top layer, down to n_{min} = 10 at 2-3 m of depth. With the help of a random function which generates the number of roots for each discretized layer, was finally obtained the *RAR* distribution, under the hypothesis that this latter decreases along depth. As an example, Figure 5.3 shows for Eragrass species deep-roots the estimated *RAR* profile: although the longest roots could even reach 3 m of depth, the *RAR* value becomes negligible at much smaller depths, between 1.5 and 2 m (Cecconi et al., 2013).
The analytical function proposed to plot the *RAR* profile obtained was the following:

$$RAR = e^{-\left(\frac{z}{c} + f\right)} \tag{5.4}$$

where z is the depth of the rooted-soil, *c* and *f* are parameters fixed respectively equal to 0.6 and 1.3.
As observed, the *RAR* calculated becomes negligible from depth of 2 m on, highlighting that the peculiarity of these *graminae* species is the root system, which grows longer than the foliage (Fig. 5.1a).
Some authors investigated the mechanical contribution of these species on increasing the Factor of Safety (FS) of an unsaturated infinite slope by considering both the additional reinforce offered by roots as an increment of cohesion (Gray & Ohashi, 1983), proportional to root tensile strength and the *RAR*, and the increasing of suction offered by root water uptake (Rettori et al., 2010; Cecconi et al., 2013).

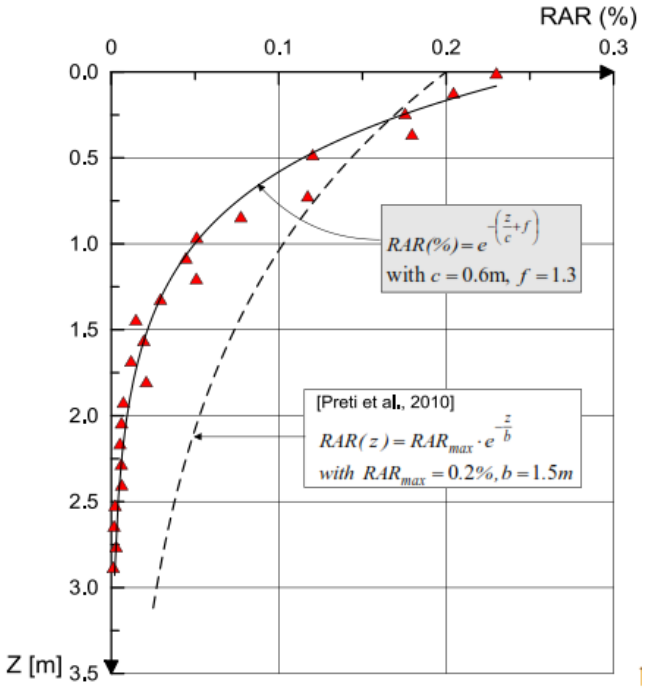

Figure 5.3 Fasciculate deep roots of Eragrass species: numerical results showing the RAR profile (Cecconi et al., 2013). In figure is also plotted the analytical function proposed by Preti et al (2010), which results in poor agreement with that proposed by Cecconi et al., (2013).

They concluded that the positive role of roots on soil mechanical reinforcement is limited to quite shallow slope covers (1 – 2m), but still lack of contributions are present in literature for quantifying the effect of roots on hydro-mechanical behavior of unsaturated soil.

5.1.2 Examples of main applications

As abovementioned, Prati Armati technology was born as bio-engineering practice aimed to prevent erosion phenomena on slopes. The positive effect of these bio-engineering practices on contrasting erosive phenomena and modifying surface water regime was widely recognized by scientific literature (e.g. Popescu & Sasahara, 2009). The vegetation reduces the runoff speed on ground surface. In case of

intense precipitation an important fraction of rainfall flows above the aerial portion of vegetation, also when the plants are seasonally dried up. The erosive action of rain drops is smoothed because of the reduction of their kinetic energy after the impact with the aerial portion of plants.
Furthermore, the implantation of these grass species, made of roots with high tensile strength, may represent an interesting technique also for the improvement of slope equilibrium conditions, limitedly to shallow and potentially unstable soil masses. In order to assess the additional important role played by slope vegetation, the soil-roots interaction needs to be specifically analyzed from a hydro-mechanical point of view. The roots may assimilated to linear cylindrical fiber of high tensile strength and they act like a mechanical soil reinforcement in the rooted-soil. On the other hand they change the pore water pressure regime in unsaturated rooted-soil with an increase of suction and thus shear strength (Vanapalli et al., 1996; Wan et al., 2011; Ng & Menzies, 2007; Ng & Leung, 2012).
This technology was applied in different contexts, such as for road embankments (Fig. 5.4a), for streambanks stability (Fig. 5.4b), for dams (Fig. 5.4c), for landfills, caves or mines (Fig. 5.4d) and contaminated soils, in Italy but also in other parts of the world, such as South America, Central America and Northern Africa.
In other cases, Prati Armati technology is combined to traditional active control works, such as gabions (Fig. 5.5a), erosion control mats (Fig. 5.5b), woody fences (Fig. 5.5c) and reinforced soils (Fig 5.5d), in order to enhance the effectiveness of the whole system, as well as to reduce visual impact and facilitate slope revegetation. No investigation has been conducted on the efficiency of this technology on stabilizing slopes susceptible to shallow landslides, like those triggered by rainfall infiltrating the unsaturated pyroclastic slopes, as discussed in Chapter 3. In fact experimental studies on the quantification of the hydro-mechanical reinforcement of these grass species are still missing.
In next paragraphs the experimental set-up created at University of Salerno for quantifying the role of roots on hydraulic behavior of unsaturated pyroclastic soils is explained, and in the next Chapter the experimental results are discussed.

Figure 5.4 Examples of Prati Armati technology on a) road embankment, b) streambank, c) dam and d) calcareous cave applied in Italy (www.pratiarmati.it).

Figure 5.5 Examples of combined Prati Armati technology and active control works such as a) gabions, b) erosion control mat, c) woody fences and d) reinforced soil applied in Italy (www.pratiarmati.it).

5.2 SET UP DESCRIPTION

5.2.1 Test set-up and instrumentation

Figure 5.6 shows the schematic set-up of the vegetated soil column. The apparatus consisted of a hollow plexiglass column with inner and outer diameter respectively of 192 mm and 200 mm, with a height of 200 cm. The height of the column was chosen high enough to have a visible growing of roots and thus to investigate the effects of roots within a typical thickness of pyroclastic soils in Campania region usually affected by slope instability turning into debris-flows, as discussed in Chapter 3. Furthermore, the columnar shape, typical of infiltration columns, makes flow paths long enough to reproduce infiltration process and evapotranspiration process. In addition, pore-water pressures and water contents can be measured continuously and automatically, and all the boundary conditions can be controlled (Yang et al, 2004). Side boundaries were impermeable and top boundary was exposed to the environment. Free drainage was allowed through 3 mm diameter holes at the bottom of the column, where a geosynthetic layer was also placed to avoid the lack of fine particles through the holes during infiltration tests.
The column was divided in 4 equal blocks of 50 cm height, linked each other by flanged bases, for a practical choose discussed in the next section. The blocks were called A, B, C, D starting from the bottom.
Four different holes respectively at 30 cm, 60 cm, 120 cm and 180 cm from the top were created for the installation of the sensors.
Soil was compacted in the column, as described in detail in the next section, up-to 190 cm depth.
Four mini-tensiometers (T5 pressure transducer Tensiometer, UMS) were installed in the holes to measure negative pore water pressure (PWP) at the central zone of the column at different depths. The tensiometers were previously fully saturated with deaired water and then installed in soil column passing through the holes.
Each minitensiometer has a sensor body incorporated with a piezoelectric pressure sensor that measures the soil water tension against atmospheric pressure in a range from -100 kPa (water pressure/level) to +85 kPa (suction/soil water tension) and with an accuracy of ±0.5 kPa. The acrylic glass shaft is 10 cm length and is equipped with a high grade porous ceramic cup. When installed, each tensiometer was put into the

hole for the entire length of the shaft so that the porous ceramic cup was placed exactly in correspondence of the central vertical of the column (10 cm). Usually the measurement range of suction is limited by water cavitation (Appendix A) in the sensor when negative pore-water pressure in soil approaches 80–90 kPa (Fredlund & Rahardjo, 1993), but in this study the first cavitation process was observed already when negative pore-water pressure approaches 60-70 kPa, as discussed in the next chapter.

Four soil moisture sensors (SM100, Waterscout) were also placed at the same depths mentioned before, to measure the volumetric water content (VWC) in vegetated soil in a range of measurement from 0% to 100% with an accuracy of ±3%. Each soil moisture sensor was calibrated in laboratory with the same soil used for the experimental study (Appendix A).

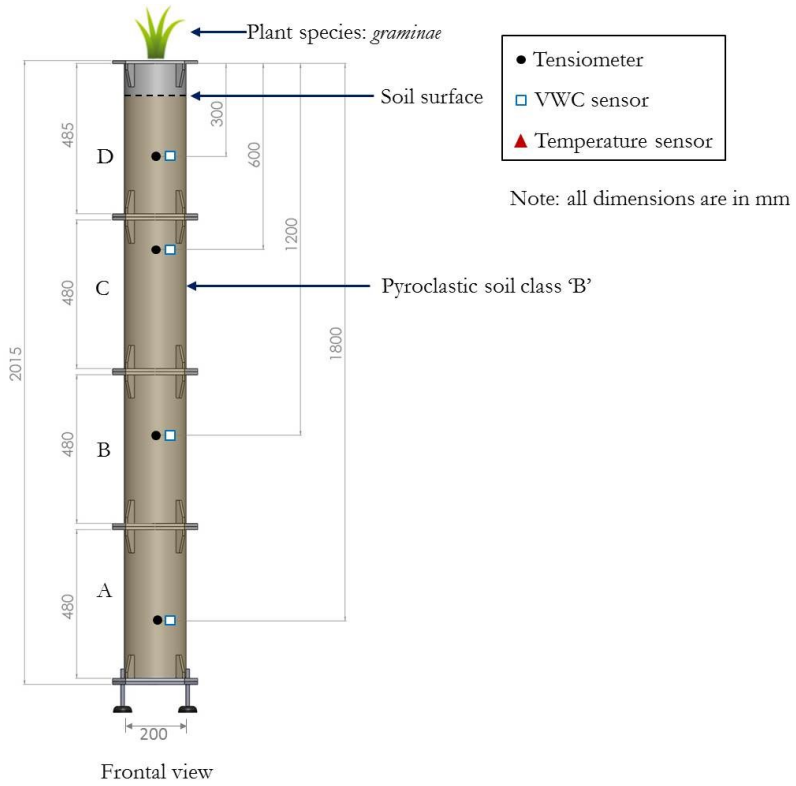

Figure 5.6 Schematization of experimental set-up and instrumentation of vegetated column: frontal view. All dimensions are in mm.

Furthermore, a thermal sensor (109, Campbell Scientific) was placed on the top surface to measure continuously the temperature of the soil in contact with the atmosphere. The sensor consists of a thermistor encapsulated in an epoxy-filled aluminum housing. This design allows the probe to be buried or submerged in water to 15 m. The temperature range varies from –55 °C to +70°C with an accuracy of ±0.3 °C.
In addition, a second soil column without vegetation was designed and constructed in order to compare the hydraulic response of vegetated soil with bare soil. Along the bare soil column, three mini-tensiometers and three soil moisture sensors were installed respectively at 30 cm, 60 cm and 180 cm depths from the top. Those depths were the same of the vegetated column, except for the 120 cm depth, because of the limited number of the available sensors in the laboratory. All sensors were linked trough cables to the Campbell Scientific LTD data logger for collecting data with an acquisition frequency of 10 minutes. The data logger was connected to a personal computer to further process the recorded data through the PC400 (Campbell Scientific) support software (Fig. 5.7).

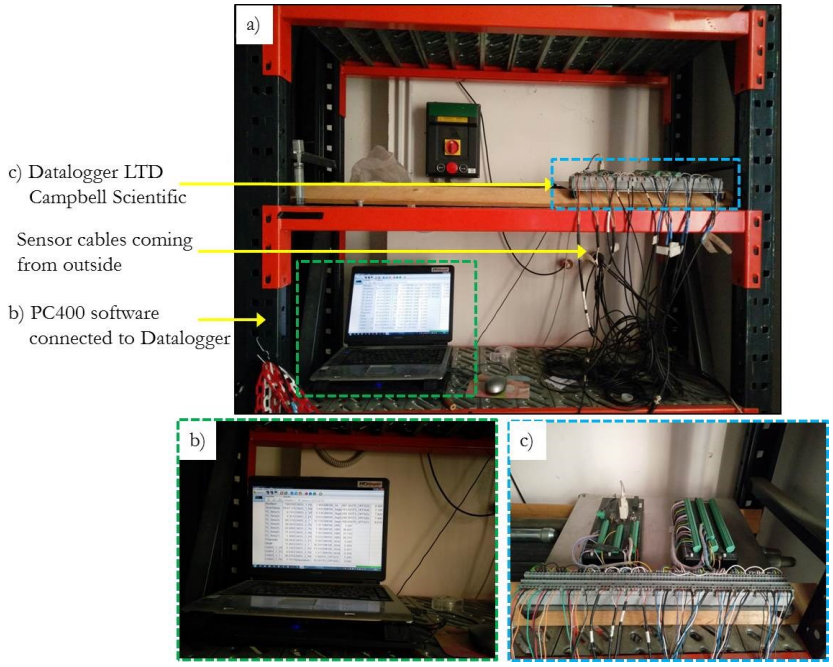

Figure 5.7 a) Data acquisition system: b) PC400 support software on persona computer for data process; c) data logger for data collection.

The vegetated and no-vegetated columns were covered with aluminum reflective panel to protect the soil from the direct sunlight and then were placed outside the Laboratory of Geotechnics "Giuseppe Sorbino" of the University of Salerno (40°46'14.5" N, 14°47'21.4 E).
The columns were exposed to climate conditions (Temperature and Relative Humidity) under a rainout shelter to protect the columns and the sensors from rainfall. Climate data were monitored by the meteorological station of the University of Salerno, not far from the experimental set-up.Vegetation was placed in one column, as discussed in the next section, and for simplicity two ID names were chosen to recognize the vegetated column rather then the no-vegetated column (Tab. 5.1).

Table 5.1 ID of the columns in the experimental study.

Column	**ID**	**Vegetation**
Vegetated	V	*graminae species (Prati Armati)*
Bare	NV	No vegetation

Figure 5.8 shows the place outside the Laboratory selected for the installation of columns and sensors. No column soil replicates were contemplated for this experimental study.

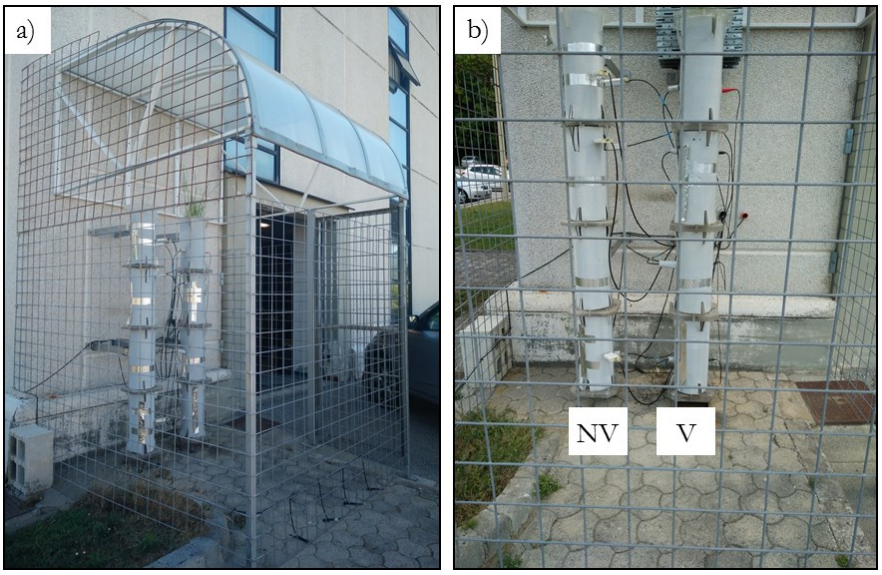

Figure 5.8 Experimental set-up: a) global view of the rainout shelter and two plexiglas columns covered by alluminium panels; b) frontal view of the no-vegetated column (NV) and vegetated column (V).

5.2.2 Soil type and preparation method

The soil used in the experimental study was collected from the pyroclastic soil deposit covering of Pizzo D'Alvano massif, in the source area of one of the several debris flows occurred in May 1998 which caused loss of lives and huge damages to the towns at its piedmont (Chapter 3). Such deposit consists of alternation of several ash and pumice layers (Cascini, 2004). According to Bilotta et al. (2005) the ashy soils can be classified in two main classes called 'A' and 'B'.

On the basis of strati graphical settings of most of the pyroclastic mantles on volcanic rock slopes (Revellino et al., 2004; Bilotta et al., 2005; Cascini et al., 2008; Ferlisi et al., 2016), it was observed that coarser ashy soils of class 'B' generally belong to the superficial layers (1 – 2 m) and overlay those of class 'A', with some presence of inter – bedded pumice layers .

The soil was collected from a dig excavated in the Tuostolo Basin, near to the source area of the so-called Tuostolo debris flow occurred in May 1998 (Fig. 5.9). The soil was collected until a depth of around 2.5 m excluding the first centimeters from the ground surface, because of the

presence of roots and organic matter. A visual observation of the excavation pointed out a quite homogenous stratigraphy of class 'B' pyroclastic soil, with an intrusion of a layer of coarser fragments (Fig. 5.10c). After putting the material in different pots (Fig. 5.10b), the material was transported to the Laboratory for determining physical properties and grain size distribution.

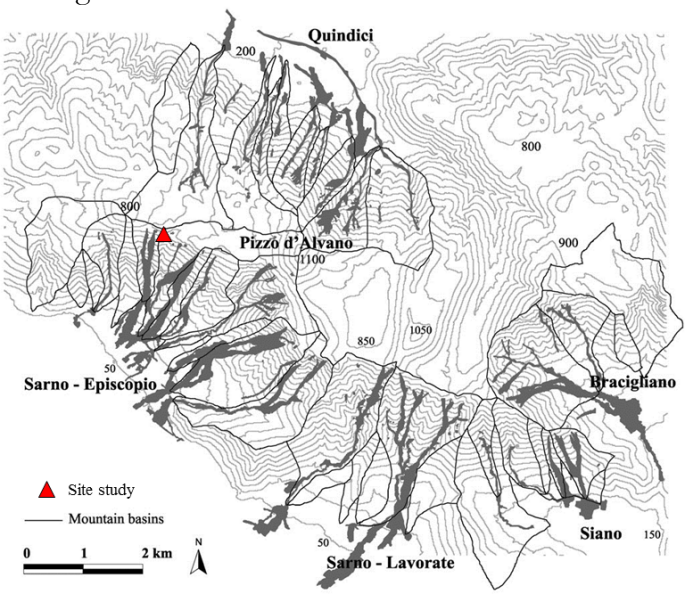

Figure 5.9 Overview of the main flow-like mass movements in May 1998; the red triangle points the site where material was collected, in Tuostolo basin, close to the source area of the Tuostolo debris flow (on the left side of the triangle). (Cascini et al., 2008 modified).

Figure 5.10 The material collected in Tuostolo Basin: a) excavation; b) pots for the transporting the material collected and c) observed stratigraphic setting of the excavation.

The soil investigated belongs to the class 'B' of pyroclastic soils with contents of gravel, sand, silt and clay of 8.09%, 60.20%, 30.61% and 1.1% respectively (Fig. 5.11) and can be classified as silty sand according to Unified Soil Classification System USCS (ASTM, 2010).

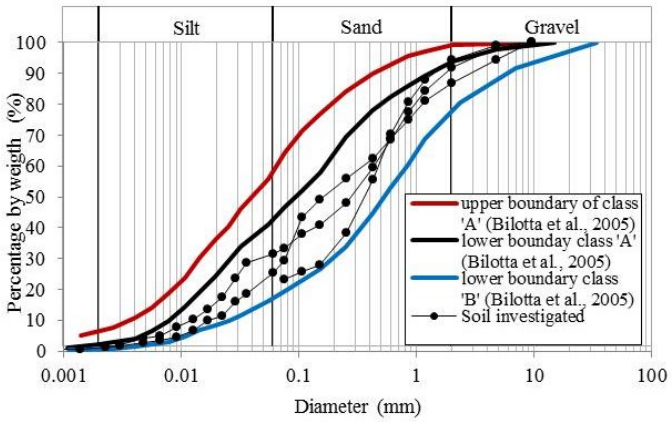

Figure 5.11 Grain size distributions of the investigated soil and boundaries of main pyroclastic classes introduced by Bilotta et al. (2005).

The specific gravity (*Gs*) was found equal to 2.59, which is included in the typical range of specific gravity values for class 'B' materials from 2.45 to 2.70 (Bilotta et al., 2005). The porosity (n) in situ varies from 53% and 69% (Bilotta et al., 2005).
In order to avoid the formation of preferential ways both for the growth of roots and water flow paths, the grains with d > 9.525 mm were removed from the class 'B' soil used in the experimental study.
The two plexiglas columns were divided in 4 blocks of 50 cm height in order to facilitate the filling procedure. Starting from the first block at the base, the moist tamping method (Ladd, 1977) was used to compact the soil by fixing the target bulk density (γ_d) 12.03 kN/m^3 and the gravimetric water content (*w*) of 10%.
The porosity (*n*) obtained from the fixed bulk density is 53.5%, which corresponds to the lowest boundary of the porosity range found in situ for class 'B' materials (Bilotta et al., 2005), as abovementioned. This is because of the collapsibility behavior of the soil investigated, as discussed in Chapter 2, and by choosing a low porosity the potential collapse is reduced. The soil was compacted in 10 layers of 5 cm depth each, up to 50 cm. After the compaction of each layer, the horizontal soil surface was scarified to provide better contact with the subsequent layer. This procedure was followed also for the remaining three 50 cm blocks, connected each other when the previous part was totally filled, until the entire column was constructed and filled (Figs 5.12).

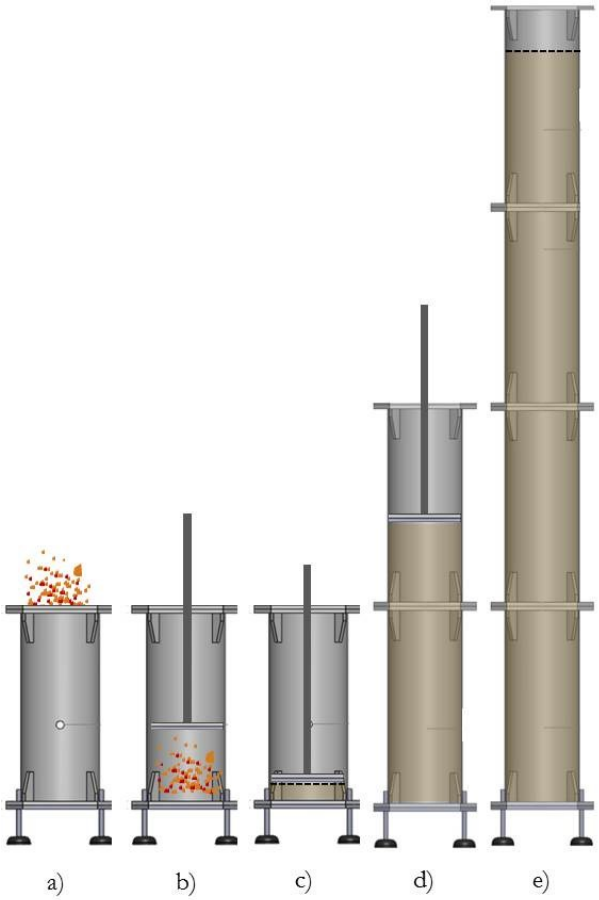

Figure 5.12 Schematization of the main steps followed for filling the column: a) pluviation of soil in the blocks(50 cm height), b) compaction with piston and c) reaching of 5 cm of thickness of the layer; d) example of on-going compaction in the second block; d) final configuration of the column.

Each Plexiglas column was filled until 190 cm of depth, so that the top 10 cm remaining part of the column was used for the protection of the foliage and for water application during infiltration tests. It was found that by using this method for the design of man made slopes in Completely Decomposite Granite in Hong Kong for vegetative restoration, a reasonable uniform dry density profile can be obtained, and the maximum deviation from the targeted value was less than 2% along the box depth (Ng et al. 2013b).

5.3 VEGETATION SPECIES AND ROOT GROWING

5.3.1 Selected species and growth conditions

The vegetation type selected belongs to the perennial *graminae* grasses, commonly involved in bio-engineering practices as well as in ecological restoration in Asia and sub-tropical regions of the world. These bushy perennial *graminae* have a radial vegetative growth and a fascicle root system capable to reach great depths even during the first vegetative seasons, as discussed in previous sections.

These *graminae* belong to the *microthermal* species, commonly known as "evergreen", because of their strength to the medium humid climates, by surviving during winter at low temperatures (<0° C) and during summer at high temperatures (>35°C). The climate conditions in Italy are favorable to their growth, by ensuring a quite amount of water available with rainfall and air humidity.

During the growth of the microthermal species two peaks of growth are usually observed: the highest peak of growth during the spring season and another during the fall season. Roots are able to reach depths of 2 – 3 m, and their leaves are long, erect and able to grow up to 1 m. The *graminae* have been seeded in a small pot, germinated 1 month in a greenhouse with daily water supplying, and then transplanted in the column called vegetated (*V*) in this experimental study (Fig. 5.13a). The transplanting period was on the end of January 2016 and the initial mean root depth was 6.0 ±0.3 cm while the average height of foliage was 8.0 ±0.2 cm. On the soil surface of the column an amount of 3.5 g of seeds was also spread (Fig. 5.13b) in order to increase the vegetation growth along the entire soil surface available, and in conclusion the first irrigation was done (Fig. 5.13c).

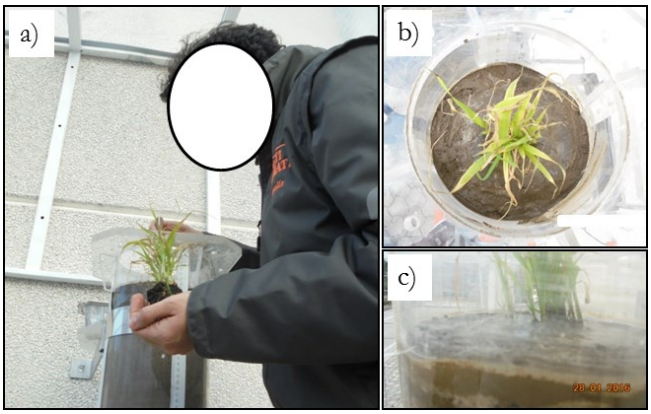

Figure 5.13 Vegetation of the column: a) transplant of sprout in the column, b) spreading of seeds along the soil surface and c) first irrigation.

The column was irrigated with an automatic irrigation system (T 1030 D, Gardena Water Timer electronic) properly programmed for providing the same amount of water every two days, at the same watering time. The irrigation system allows setting different frequencies of watering for different watering times independently of the watering system used (i.e. sprinkler, drip head). It consists in a timer which is manually programmed by selecting the current day, the watering starting time (i.e. Monday), the frequency (i.e. 24 h: 1 watering cycle per day) and the watering duration (i.e. 3 minutes), by turning the pointer B of the control knob A to the correct time pressing the OK button (Fig. 5.14).

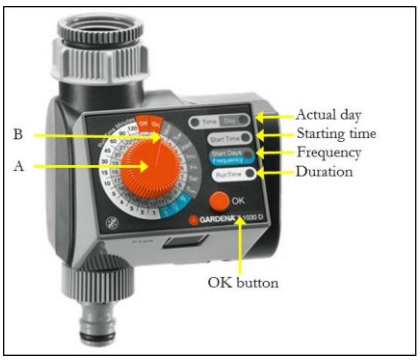

Figure 5.14 T 1030 D, Gardena Water Timer electronic used for watering the vegetated column.

During plant growth the average root depth and height of foliage have been monitored every month. The roots were measured at the middle of each month through graduated scales placed on the four sides of the transparent Plexiglas column: the monthly root depth was considered as the average value between the four longest roots observed from the soil surface for each of the four sides (Fig. 5.15). The monthly height of foliage was calculated as the average value of direct measurements for five different leaves chosen randomly among all the leaves.

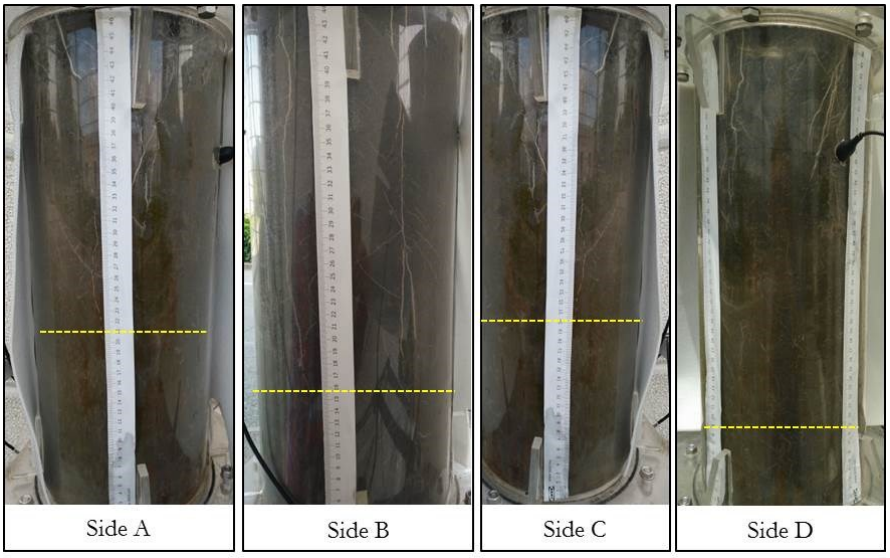

Figure 5.15 Graduated scales placed on the four sides of the vegetated column: the yellow dashed lines are referred to the monthly maximum root depth observed for each side. The average of the four maximum length of the four sides is the root depth.

Figure 5.16 shows the monthly average of height of foliage and root depth during the monitoring period, which was of 12 months starting from month 0 corresponding to January 2016 when the transplant of vegetation occurred. The dimensions were measured and expressed in centimeters.

The height of foliage, shown in Figure 5.16a, increased during the first months of growth, from 8.0 ±0.2 cm in January up to 29.9 ±3.0 cm recorded in May, because of the high rate of growth recognized during the first vegetative season of the microthermal species. From June to September, the height of foliage increased with lower rate of growth

from 36.3 ±6.2 cm up to 52.5 ±1.8 cm. From September, the height of foliage increased quite slowly up to 55.7 ±2.4 cm in November, after that, during winter it remained quite the same. On the other hand, the monthly average of root depth (Fig. 5.16b) increased exponentially from 6.0 ±0.3 cm up to 95.7 ±2.6 cm during the first spring vegetative season (January – May), consistent with the growth of the foliage, because of the growth behavior of microthermal species. After the first period, the monthly root depth increased about linearly during the summer season from 112.2 ±8.9 cm (in June) up to 181.1 ±4.4 cm (in September). In this study the second peak of growth, typically observed during fall season for microthermal species, was recorded between September and November, eventhough it was negligible. In fact, the monthly root depth increased from 181.1 ±4.4 cm up to 185.6 ±2.0 cm during these months, reaching the bottom of the column.

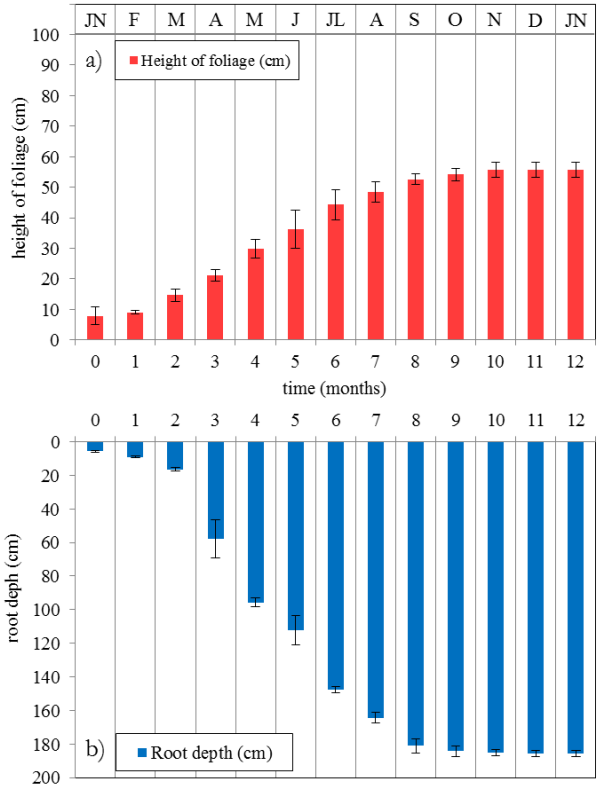

Figure 5.16 Monthly average of a) height foliage and b) root depth during first 12 months of plant growth.

During winter the root growth was inhibited both because of the season and the limit of the height of the column, and no differences in monthly root depths between November and January of the next year were observed.
A positive linear correlation of height of foliage and root depth during the first vegetative year was observed. In Figure 5.17 the values of height of foliage recorded each month were plotted against the corresponding root depth. It can be aimed that, by only having a visual observation of the foliage is possible to know the expected root depth along the vertical direction, when 1Dimensional conditions exist.

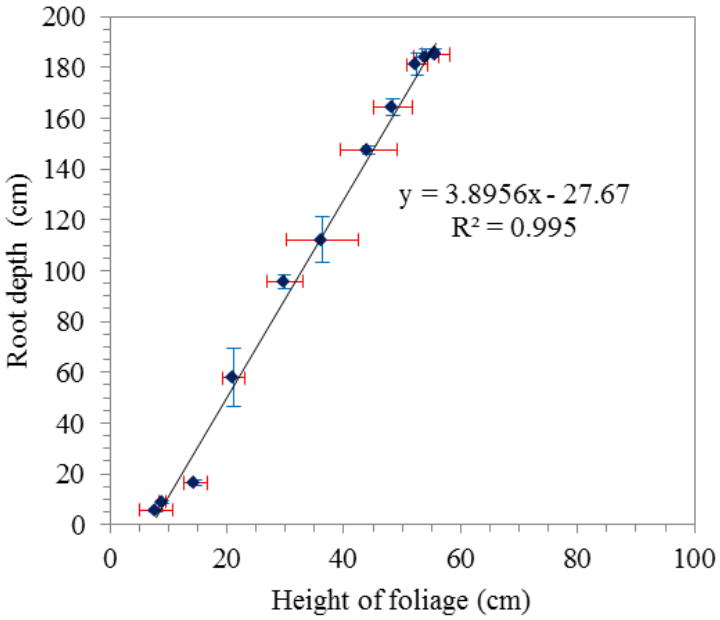

Figure 5.17 Relationship of Height of foliage with Root depth recorded during the first vegetative year.

These results are consistent with agronomical considerations regarding the ratio between the hypogeum (roots) part and the part above the ground level (foliage), which is demonstrated to be more than 3 in this experimental study.

5.3.2 Observed root characteristics

At the end of the experimental study root characteristics, such as Root Area Ratio (*RAR*), root mean diameter, and root dry biomass (*RM*) along depth, were measured. The 1D vegetated soil column (*V*) was divided by the 4 modulus undisturbed rooted soils were sampled from the 1D vegetated column (*V*) at different depths by following a sampling procedure designed for the specific case, that can be exported for sampling of undisturbed soils in physical models.

For each 50 cm block belonging to the soil column (Fig. 5.7), two 20 cm high and one 10 cm high of rooted soil samples were extruded. The extrusion has been conducted for each block starting from the bottom of the column (Fig. 5.18a). The entire soil column was positioned along an horizontal plane (Fig.5.18b) and the soil at the interface between two adjacent blocks was cut with a plain steel string of 0.28 mm diameter (Fig. 5.18c,d).

After isolated the block, it was positioned vertically and with the help of a piston the soil was extruded in plexiglas cylinders of respectively 10 cm and 20 cm height. In addition, for each soil surface cut, high definition pictures were taken in order to measure the percentage of soil surface occupied by roots through ImageJ software.

The 20 cm height plexiglas cylinders destined to triaxial tests were taken in laboratory for the sampling procedure, whereas the remaining cylinders have been covered at both the base and the upper part and opportunely sealed in order to maintain the initial soil water content and to preserve roots from imminent decaying. The sampling procedure of undisturbed root-soil specimens for triaxial tests is discussed in Chapter 8.

ImageJ analysis (Rasband, 2011), already introduced in previous Chapter, was conducted for *RAR* measurements, even if the procedure adopted in this study has been different from that used during the experimental study conducted at HKUST (Garg et al., 2015). In fact, in this study roots were not separated from soil through water by using the principle of hydro-pneumatic elutriation, because root-soil composites were needed for laboratory experiments. Furthermore, the roots of *graminae* species were thinner than those of *Schefflera heptaphylla* and also they reached almost 2 m of length, thus the separation procedure would be onerous.

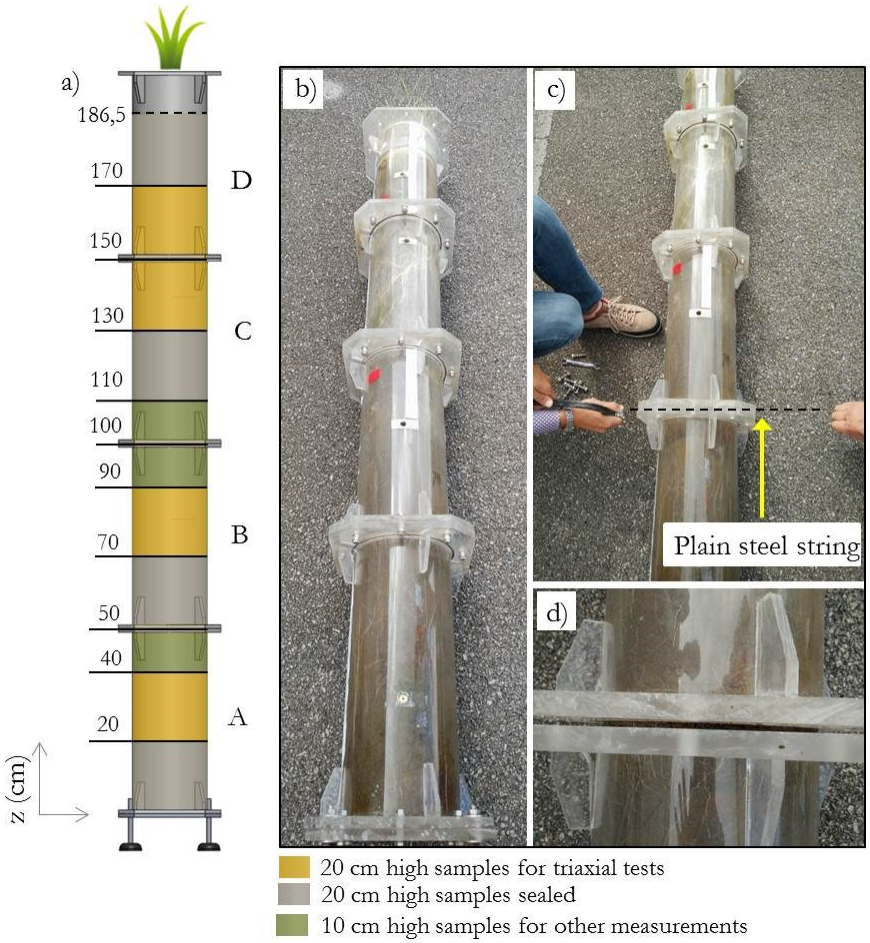

Figure 5.18 a) schematization of the vegetated soil column and the z where soil was cut; pictures of: b) soil column placed in horizontal plane for the cutting, c) cutting phase of modulus A, d) particular of the soil interface between modulus A and B.

High-resolution images were taken at different depth of the soil column during extrusion process, in correspondence of each cut surface (Fig. 5.18a). Before taking the image, the cut surface was exposed to atmosphere in order to dry roots which became white and more visible for image analysis.

Each image in ImageJ had grid with known pixel size (i.e. 12 pixels per unit mm of length) and was converted in binary image, thus the total number of pixels corresponding to root surface (A_r) along the soil cross

section (A_s) was easily recognized (white pixels) and then converted in mm^2.
Finally, *RAR* at any depth within the root zone was determined by dividing the root surface A_r by the soil cross section A_s, which in this study was constant and equal to the surface of the soil column.
RAR measurements were then plotted by using the same exponential function proposed by Cecconi et al. (2013), with empirical parameters c and f fixed respectively equal to 0.45 and 1.5 (Fig. 5.19).

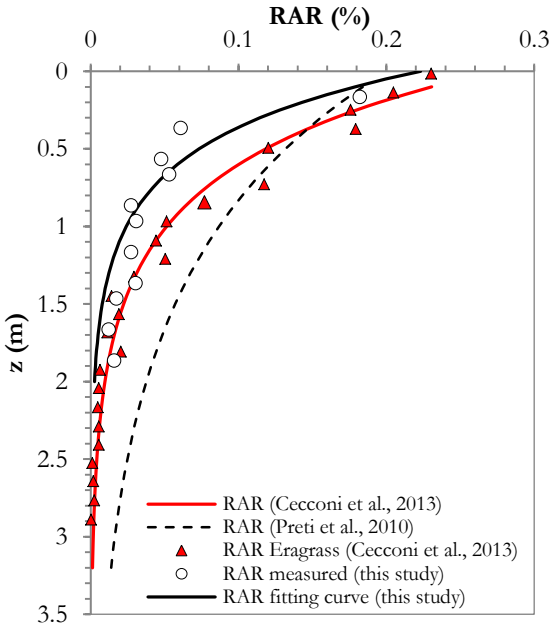

Figure 5.19 *RAR* measurements of graminae species used in this study (white circles) and its analytical function (black line), compared with *RAR* measurements of Eragrass (red triangles) and its analytical function (red line) proposed by Cecconi et al. (2013), and analytical funcion proposed by Preti et al. (2010).

In order to measure the mean root diameters, separation of roots from the soil matrix was needed. To this aim, after triaxial tests on undisturbed root-soil samples taken at different depth from soil column, as described in Chapter 8, 250 roots have been used to carry out the statistical distribution of diameters.

A caliper monoblock with an accuracy of 0.05 mm has been used for measuring the diameter of each root. Root diameters were divided in 4 classes from the lower (0-0.55 mm) to the higher (1.65-2.20 mm).The frequency of all diameters was then computed (Fig. 5.20).

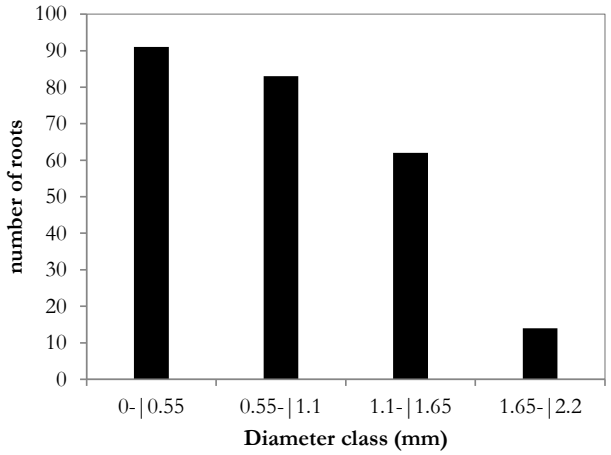

Figure 5.20 Number of roots for each diameter class.

The lower diameter class (0-0.55mm) showed the maximum frequency, while the highest diameter class (1.65-2.2mm) showed the minimum frequency. This result confirms the typical fibrous system of roots belonging to grass species, which is characterized by numerous fine and light roots. Fine roots in literature are widely recognized to have diameters less than 2 mm, which is a size often used to distinguish between fine and coarse roots (Stokes et al. 2009).

5.4 CONCLUDING REMARKS

This Chapter describes the experimental set-up constructed within the PhD activity at University of Salerno and the investigated vegetation species. The growth period of this *graminae* species was consistent with that of microthermal species, showing two peaks of growth during the first vegetative year. Root and shoot lengths were monitored during the growth period showing a linear correlation. Measured *RAR* along depth was in accordance with previous studies and the analytical function for

predicting *RAR* depending on depth was carried out. The root diameters measurements confirmed the typical fibrous system of roots belonging to grass species, which is characterized by numerous fine and light roots. In conclusion, roots of Prati Armati technology in pyroclastic soils reached 2 m depth during the first vegetative year and the foliage was florid, with healty and numerous green leaves. This is likely due to the soil properties and climate conditions, which enhanced the plant growth. These results confirmed the conclusions pointed out in previous Chapter regarding the importance of nutrient availability in soil on plant growth and encourage the use of natural based solutions in pyroclastic soils, widely known as rich in nutrients.

6 HYDROMECHANICAL BEHAVIOR OF ROOTED SOILS

A literature review on the hydraulic behaviors of different vegetated soils is carried out in this Chapter.
In particular, the effect of roots on induced soil suction during evapotranspiration process and infiltration process are deeply discussed.
Then, the experimental study soils is introduced with an accurate description of the experimental programme followed, in order to quantify the hydro-mechanical response of vegetated pyroclastic.
Results of wetting tests and drying tests during different seasons are interpreted and discussed in depth.

6.1 INTRODUCTION

Plant roots have been widely used as a sustainable and environment friendly engineering practice for stabilizing slopes and landfill covers (Cazzuffi et al., 2006; Sinnathamby et al., 2013). It is well known that vegetation enhances evapotranspiration (ET) process governed by plants, which decreases volumetric water content (VWC) and increases soil suction with a consequent reduction in soil permeability and increase in soil shear strength (Ng & Menzies, 2007; Ng & Leung, 2012).
Furthermore, during plant growth, roots occupy soil pore spaces and thus modify the whole soil structure with a modification of both soil water retention curves and soil hydraulic conductivity (Buczko et al. 2007; Scanlan and Hinz 2010).
Volumetric water content (VWC) and soil suction, which are affected by ET, are the main soil hydraulic properties governing the transient seepage of unsaturated soils. As consequence, the presence of vegetation in a transient seepage problem would vary the pore water pressure regime by changing the initial condition before rainfall infiltration.
During a rainstorm, infiltration of vegetated soils can be reduced by i) the leaf interception, which reduces the net rainwater, ii) the change of

water flux within the rooted soil because the soil water retention and soil hydraulic conductivity are modified (Inoue et al., 2000; Vogel et al., 2000) iii) the change of initial pore water pressure regime because of the higher induced soil suction by ET.
The effects of vegetation on soil responses during ET process and rainwater infiltration process have been widely studied for different soil types vegetated with different plants. However there is a lack of contribution on the hydrological response of pyroclastic soils vegetated with long root grasses as those used by Prati Armati technology, introduced in Chapter 5.
In fact, experimental studies recently conducted on hydraulic response of pyroclastic soils to atmospheric forcing (Rianna et al., 2014; Pagano et al., 2014) did not considered the presence of vegetation.
The consequence is that i) the possible increase of ET related to water uptake by roots is not taken in to account, ii) the possible effects relating to evapotranspiration persistency are neglected, that may result over long periods in significant amounts of cumulative water loss from the soil, iii) the possible change of infiltration due to the presence of vegetation in soil is not evaluated.
In this Chapter, a literature review on the hydraulic behaviors of different vegetated soils was carried out and then an experimental study has been conducted in order to quantify the hydro-mechanical response of pyroclastic soils vegetated with long root grasses to atmospheric conditions.

6.2 LITERATURE REVIEW

In the recent years the attention on the effects of plant roots on hydraulic properties of soil, have been focused by some researchers from different fields.
In geotechnical engineering problems, water infiltration rate and hydraulic conductivity of vegetated soil are two important parameters governing surface runoff, soil suction and volumetric water content in the vadose zone of unsaturated soils. The knowledge of these parameters is important to analyze suction distribution for stability problems of vegetated soil slopes (Indraratna et al., 2006; Genet et al., 2010).

In agricultural problems, these parameters are also crucial to determine the availability of soil moisture for accurately fix an irrigation schedule and assessing crop yields (Wetzel and Chang, 1987; Zhang et al., 2004). The hydro-mechanical response of rooted soils can be studied in two different ways depending on the interaction between the soil surface and the atmosphere: i) if water is entering in soil there is an infiltration process which usually leads to a reduction of soil suction and the increasing of VWC; ii) if the water is exiting from the soil there is an Evapotranspiration process which leads to the increasing of induced soil suction and consequently the reduction of VWC by root water uptake.

6.2.1 Effect of vegetation on infiltration rate

Several past studies have been conducted to quantify the infiltration rate in natural soil vegetated with different vegetation species. Furthermore, in many of these studies suction regime was simultaneously monitored because is well-recognized as one of the key stress-state variables (Coleman, 1962) governing the behavior of unsaturated soil. Several field studies have been conducted by geotechnical researchers to investigate suction on vegetated slopes comprising of residual soils (Huat et al., 2006; Rahardjo et al., 2008; Ishak et al., 2012), decomposed soils (Leung et al., 2011), non-expansive clay (Smethurst et al., 2006; Heppell et al., 2014), expansive clay (Zhan et al., 2007) and silty sand pyroclastic soils (Comegna et al., 2013).
Nevertheless the results obtained seem to be limited because of many factors affecting the hydraulic response of rooted permeated soil, but some considerations based on previous studies can be done.
One factor affecting the hydro-mechanical response of root permeated soil is the state of roots: actively growing or decaying. It was found that actively growing plants could reduce infiltration rate and saturated permeability of the soil (Huat et al. 2005, 2006; Rahardjo et al. 2014; Leung et al. 2015b, 2015c). On the other hand, for grass-covered soil, if the roots are actively growing the infiltration rate can be lower than those in bare soil (Gish and Jury, 1983; Huat et al., 2006; Ng et al., 2014); whereas, if roots are decaying the infiltration rate can be higher than those in bare soil (van Noordwijk et al., 1991; Mitchell et al., 1995).
Moreover, plant roots effects on soil, such as the creation of network of preferential flow (Ghestem et al., 2011) or conversely the clogging of soil pore (Gabr et al., 1995; Scanlan and Hinz, 2010), influence also the

hydraulic response of soil and these effects are currently not well understood.

The infiltration rate in vegetated soils was studied through tests conducted in different manners (i.e. by applying artificial rainfall with rainfall simulators, or by monitoring natural rainfall) and in different contexts (i.e. in-situ vegetated soil or laboratory-vegetated soil experiments).

Some studies on infiltration rate and suction have been conducted on natural vegetated soil slopes (Fig. 6.1) by applying artificial rainfall or real rainfall, but the suction recorded can be potentially affected by three-dimensional water flow, from which is not easy to isolate the vegetation effects on infiltration rates (Rahardjo et al., 2005; Huat et al., 2006). Rahardjo et al. (2005) conducted a study on a vegetated slope made of residual soil and concluded that the percentage of rainfall contributing to infiltration decreases with rainfall (Fig. 6.2), even though there are not comparisons with bare soil.

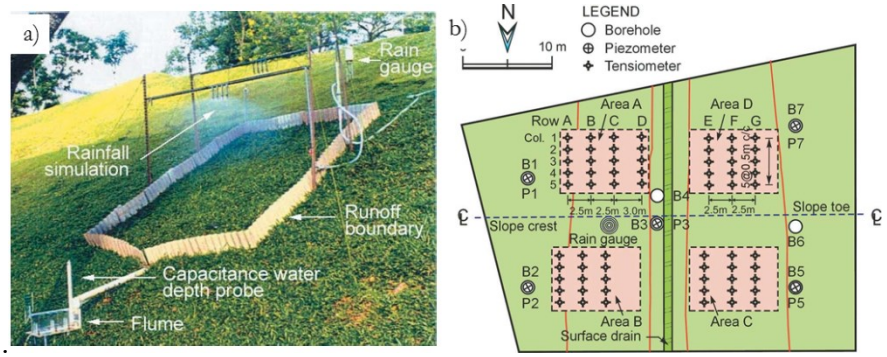

Figure 6.1 Example of in situ infiltration test: a) Experimental Setup for rainfall simulation on vegetated slope and b) plan view of slope with layout of instruments for pore water pressure measures (Rahardjo et al., 2005).

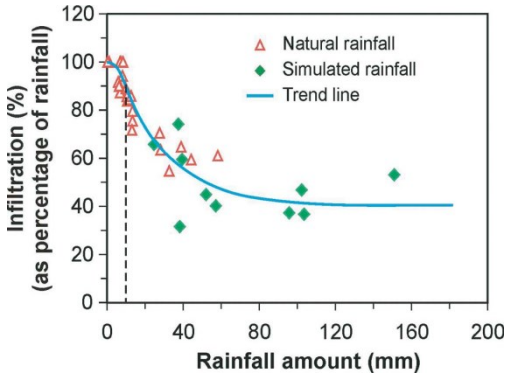

Figure 6.2 Percent infiltration as a function of rainfall amount (Rahardjo et al., 2005).

On the other hand, Leung et al. (2015c) conducted in situ double ring infiltration test (Fig. 6.3) in Completely Decomposed Granite soils, typically found in Hong Kong territories. The infiltration test consisted in applying a ponding with constant head, to measure the effect of Schefflera heptaphylla plant species and Cynodon dactylon grass species on infiltration rate and suction reduction compared with bare soil. They concluded that infiltration rate in vegetated soil is lower than those measured in bare soil, even the lower infiltration rate is observed for soil covered with plant species (Schefflera heptaphylla) (Fig. 6.4a).

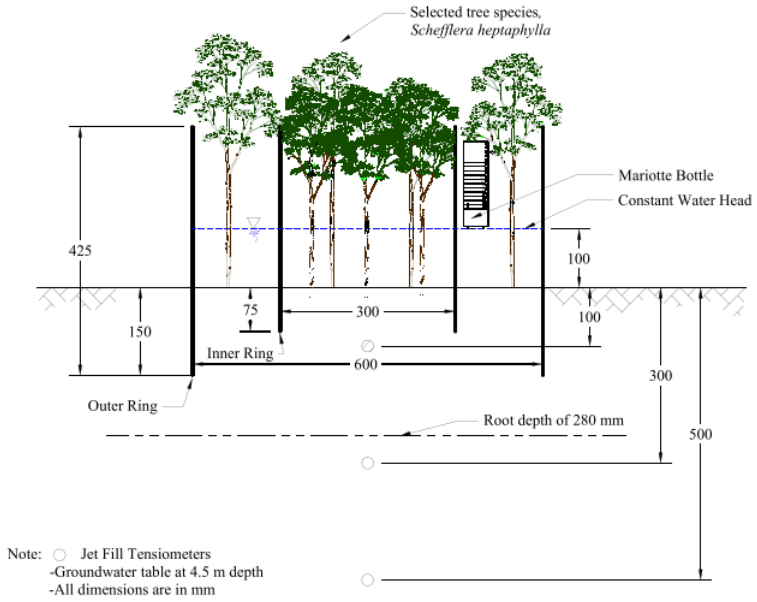

Figure 6.3 A schematic diagram showing test setup and instrumentation for vegetated soil in double ring infiltration test (Leung et al., 2015c).

The reduction of suction due to water infiltration was observed to decrease as depth increases: at shallowest depth the suction reached zero value in the same time both in bare and grass-covered soil, while it went to zero in delay for soil covered by plants. Hence, they concluded that the depths of influence of suction in both vegetated soil were below the root zones between 0.3 and 0.5m depths and the suction reduction is less evident in soil covered by plants (Fig. 6.4b).

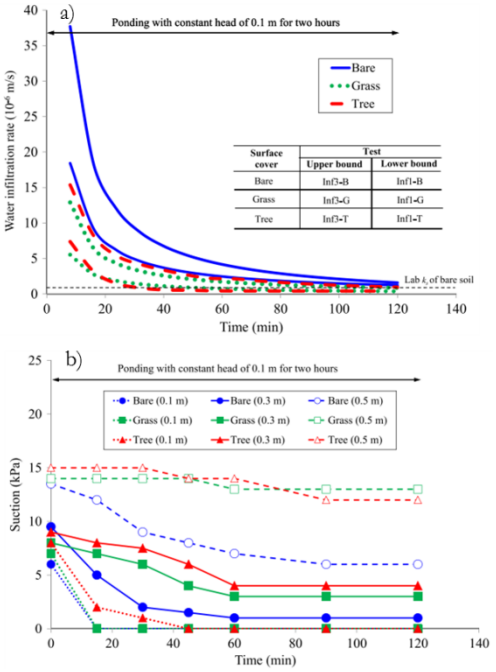

Figure 6.4 a) Comparisons of upper and lower bounds of infiltration rates for grass-covered soil (Cynodon Dactylon grass species), plant-covered soil (Schefflera heptaphylla species), and bare soil series; b) Comparisons of suction responses at 0.1-, 0.3- and 0.5-m depths between bare, grass-covered and tree-covered soil during ponding (Leung et al., 2015c).

For grass-covered (Cynodon dactylon) soil the infiltration rate was also indirectly obtained in laboratory by water balance calculation (Ng et al., 2013) from rainfall simulation (Fig. 6.5).

In this latter study, they confirmed that by calculating indirectly the infiltration rate with water balance, it results always lower in vegetated soil than in bare soil (Fig. 6.6a), in agreement with previous studies. Furthermore, the effect of soil density on grass growth and infiltration rate was also investigated, with the conclusion that for denser soil the reduction of suction due to water infiltration is lower and consequently the infiltration rate is reduced (Fig. 6.6b).

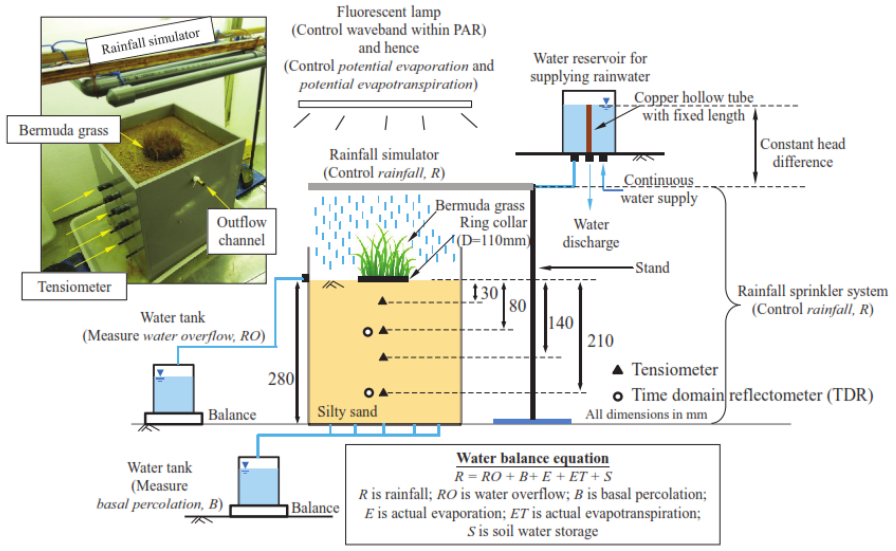

Figure 6.5 A Schematic diagram showing test setup and rainfall simulator for simulating constant rainfall intensity for 1D infiltration test on grass-covered soil square box: the infiltration rate was obtained from water balance equation shown in the figure (Ng et al., 2013).

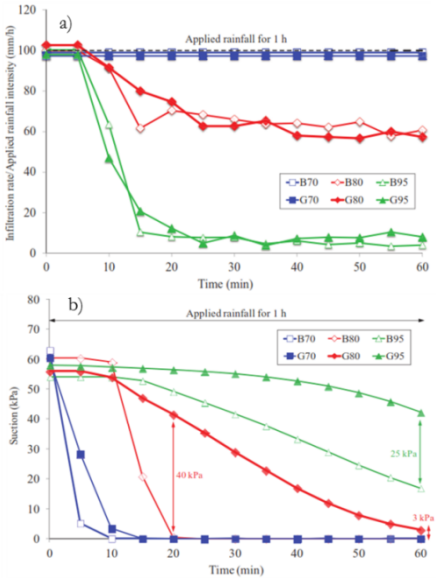

Figure 6.6 a) Measured variations of infiltration rate with time for bare and vegetated silty sand; b) Comparisons of variations of induced suction at 30 mm depth with time for bare and vegetated silty sand (Ng et al., 2013).

It can be claimed that generally the vegetation reduces the infiltration rate, but this reduction depends on: vegetation species (i.e. plant species or grass species), state of roots (i.e. actively growing or decaying), rainfall amount, and type of hydraulic boundary condition (ponding, rainfall simulation, natural rainfall). Furthermore, soil suction is usually influenced by vegetation species, rainfall amount, soil depth and soil density.
However, it was revealed from field investigation that soil suction in unsaturated slopes shows a seasonal trend due to the soil-atmosphere interaction and this is reflected on different initial suction values that should be considered before a rainfall event. This latter aspect is not always considered in infiltration tests.
In conclusion, infiltration tests are useful to understand the response of unsaturated vegetated soil in terms of suction reduction.

6.2.2 Effect of vegetation on induced soil suction

Some studies have been conducted to monitor the suction increase due to soil-atmosphere interaction (i.e. evapotranspiration process) in field and in laboratory experiments.
The soil suction in vegetated slopes induced by Evapotranspiration process (ET) shows a seasonal trend which has a high peak during summer, when temperature is higher and vegetation is more florid, and decreases in wet season, when evaporation is reduced by lower temperature and the transpiration is vanishing because vegetation is quiescent.
The suction induced by ET was observed as 5-20 kPa during wet season and up to 200 kPa (Leung et al., 2011) or 400 kPa (Smethurst et al., 2006) during dry season in decomposed soil and clayey soil, respectively.
Garg et al. (2015) conducted a field investigation on the effect of grass-covered soil and plant-covered soil on the induced suction during evapotranspiration process, compared with bare soil (Fig. 6.7).
They concluded that, in agreement with the seasonal variation of suction values observed by previous studies, in all slopes peak suction occurs during relatively dry seasons when rainfall is less frequent.
Furthermore, slope vegetated with plant species (Schefflera heptaphylla) is observed to induce the highest suction within their root zone, which is around 41% and 72% higher than the bare slope and grass-covered slope (Cynodon Dactylon), respectively.

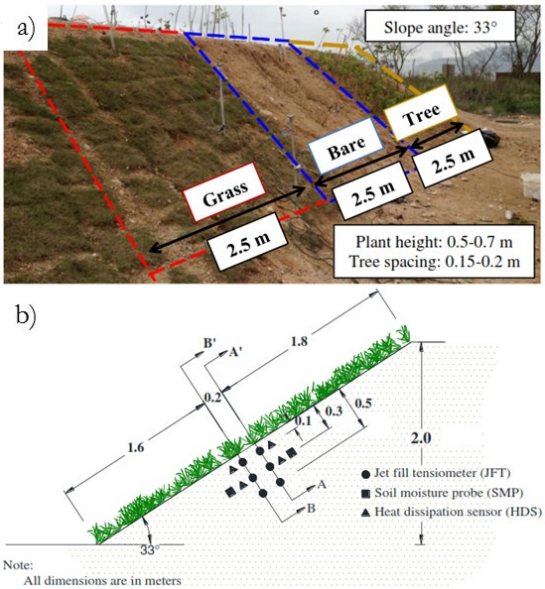

Figure 6.7 a) Side view of 33° slope with two different vegetation species (i.e. Cynodon dactylon (Grass) and Schefflera heptaphylla (Plant) and bare soil;b) Typical layout of instrumentation on the grass vegetated slope (Garg et al., 2015).

Lim et al. (1996) monitored matric suction in a residual soil slope with 3 types of surface covers (canvas-covered grassed surface, grass-covered surface and bare surface). They showed that the variations of matric suction profile were the least significant under the canvas-covered section as compared to those measured under the grass-covered and the bare sections of the slope.

Recently some authors tried to correlate the main plant characteristics to induced soil suction in order to understand the way plant foliage and roots influences the soil response. Laboratory investigations were carried out to correlate the suction induced by evapotranspiration process with plant traits and characteristics in environment controlled room, with temperature and relative humidity fixed.

Ng et al. (2016) found a positive linear correlation between *RAI* and mean peak suction (Difference between suction measured in vegetated soil and suction in bare soil) after 2 days of drying, as well as between *LAI* and mean peak suction (Fig. 6.8), as observed also in the experimental study conducted in Hong Kong during this PhD research program and discussed in depth in Chapter 4.

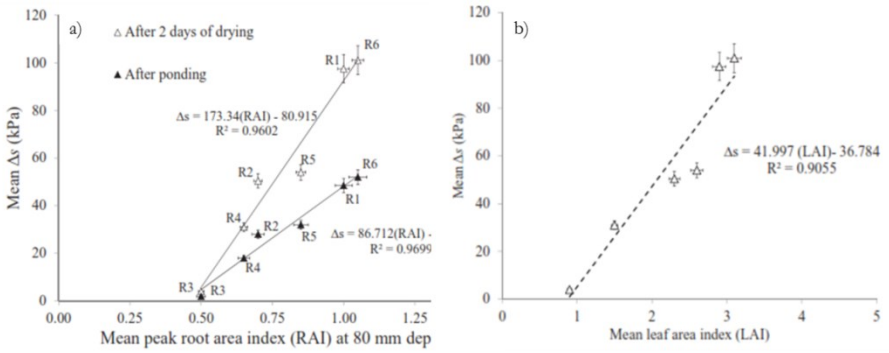

Figure 6.8 Relationships of mean peak of suction (Δs) and mean peak RAI at a depth of 80 mm before and after ponding and b) Relationships between mean LAI and peak of suction (Δs) during drying (Ng et al., 2016).

6.3 THE EXPERIMENTAL PROGRAMME

6.3.1 Test plan and procedures

The aim of this study is to quantify the effects of root growth on hydraulic response of unsaturated pyroclastic soil involved in wetting and drying tests, simulating respectively infiltration and evapotranspiration processes, in the real-size 1D physical model introduced in the previous sections. The experimental program was organized in two test series, the first one consisted in drying tests (D) to investigate the effect of root growth on suction during Evapotranspiration process, and the second one including wetting tests (W) to investigate the effect of roots on suction during Infiltration process.

All test series were conducted on both vegetated (V) and no-vegetated (NV) soil columns in order to quantify the effectiveness of roots in changing the hydro-mechanical response of soil.

Drying tests (D) were conducted in two seasons of the year, respectively, spring (Apr) and summer (Jul), during the root growth.

Before D test, each soil column was saturated by applying water from the upper part of the column, even if soil full saturation was never reached because of the lack of an additional water pressure involved in saturation process. The not full saturation of the soil column is representative of in situ condition, where usually any soil near the ground

surface, present in an environment where the water table is below the ground surface, is in unsaturated condition (Fredlund, et al., 2012). Furthermore, in situ measurements of suction in pyroclastic covers of Campania region, as discussed in depth in Chapter 2, even during the wetting season, indicate the minimum values around 5 kPa, highlighting the soil unsaturated condition (Cascini et al., 2014; Cascini & Sorbino 2002; Damiano et al., 2012; Pirone et al., 2015; Comegna et al., 2016).
On the other hand, wetting tests (W) were conducted after root growth by applying an artificial rainfall through a rainfall system up to reach the saturation. Two wetting tests were conducted, one on vegetated soil column and one on no-vegetated soil column, in order to investigate the effect of vegetation on hydraulic response under a rainfall intensity pattern.
Details on rainfall intensity selected in this study are explained in Chapter 6 where results of infiltration tests are discussed in depth. The test programme followed in this experimental study was summarized in Table 6.1.

Table 6.1 Summary of the test programme followed for the investigation of the hydraulic response of rooted-soil.

Objectives	Test ID	Vegetation	Root age (months)	Month	Root lenght (cm)	Drying	Wetting
Effect of root growth on increasing suction during evapo-transpiration	V_D_A1	Grass	3	April (2016)	57.8	ET	
	V_D_A2	Grass	15	April (2017)	185.6		
	NV_D_A2	Bare	-	April (2017)	-	ET	
	V_D_Jul1	Grass	6	July (2016)	147.6	ET	
	V_D_Jul2	Grass	18	July (2017)	185.6		
	NV_D_Jul2	Bare	-	July (2017)	-	ET	
Effect of roots on decreasing suction during Infiltration	V_W	Grass	15	April (2017)	185.6		Artificial Rainfall
	NV_W	Bare	-		-		

6.3.2 Climatic conditions monitoring data

The experimental set up consisted of two 1D soil columns, as introduced in previous Chapter, exposed to atmospheric conditions (Temperature and Relative Humidity) under a rainout shelter to protect them from direct rainfall. Temperature and Relative Humidity data were hourly monitored by the official meteorological station of University of Salerno, placed around 200 m far from the experimental set up (Fig. 6.9).

Figure 6.9 The map of University of Salerno Campus with the position of the experimental set –up and meteorological station for monitoring climate data during the programme.

Climate data provided hourly within the monitoring period were: Maximum and minimum external air Temperature (°C), wind Temperature (°C), Atmospheric pressure (bar), wind velocity (Km/h), wind direction, Relative Humidity (%), Solar radiation (W/m^2) and UV index. Furthermore, soil temperature in contact with the atmosphere was monitored by a sensor placed on soil surface of each soil column, as previously explained in Chapter 5. Daily and monthly average of the external air Temperature (*Te, Monthly Te)* and Relative Humidity (*RH, Monthly RH*), together with daily soil temperature (*Ts*) were monitored from March 2016, when the sensors were installed in soil columns, until the end of July 2017, corresponding to the end of the hydraulic tests (Fig. 6.10).

Within the monitoring period the *Monthly Ts* trend showed seasonal fluctuations, in particular it increased starting from the lowest peak recorded in January (5.5 °C), and reached the maximum peak (25.1 °C) in July (Fig. 6.10), in the middle of the summer. On the other hand, *Monthly RH* trend was quite constant, even decreased in summer season, with the lowest peak in July (57.3%), while showed the maximum peak of value in the middle of winter (78.3%). This means that wet season, when in Campania Region usually occurred Debris Flows, is the period of the year when temperatures are low and the humidity is quite high, and this is reflected with a low contribution by the plants to the Evapotranspiration process (Comegna et al., 2013; Napolitano et al., 2016).

In addition, it can be observed that values of soil temperature (*Ts*) differed very slightly from external air temperature values (*Te*), in particular the maximum difference was found to be at least 4 °C. This means that climatic data provided by meteorological station of University of Salerno were consistent with the data needed in this PhD research.

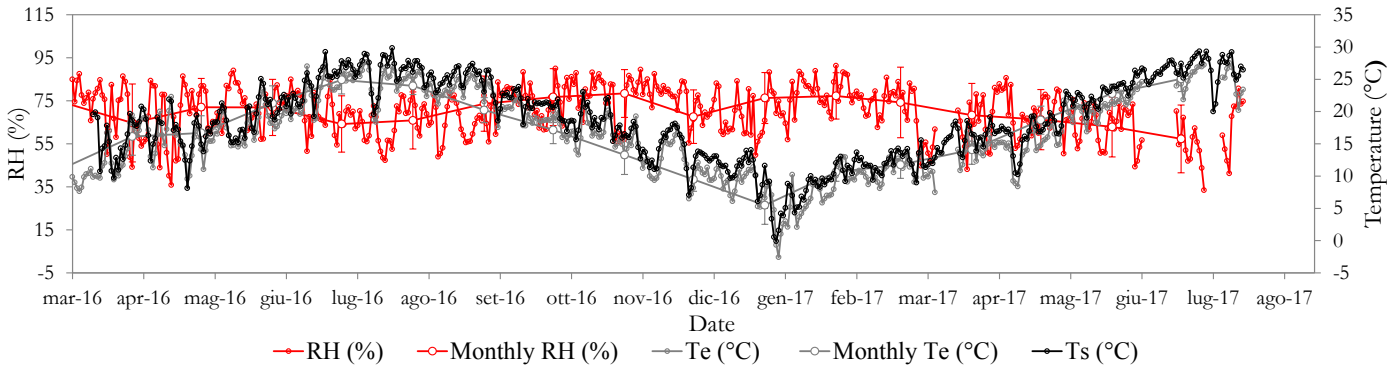

Figure 6.10 Climatic monitoring data: Daily and monthly average of external air Temperature (T_e) and Relative Humidity (RH) measured at the meteorological station; daily soil Temperature measured in the soil columns (T_s).

6.3.3 Soil suction and VWC monitoring data

Soil suction and VWC monitoring started on March 2016 and has been done continuously until the end of July, when tests on hydraulic behavior of rooted-soil concluded and vegetated soil column (V) was used for sampling specimens for laboratory tests.
The depths of investigation were 4 and they were called respectively row A at 0.3 m, row B at 0.6 m, row C at 1.2 m and row D at 1.8 m from the upper part of the column.
Figure 6.11 shows the monitoring data for all the rows of vegetated soil column divided in terms of soil suction (Fig. 6.11a) and VWC (Fig. 6.11b).
Both soil suction and VWC measurements were depurated from unreliable values (i.e. VWC<0%).
In fact, the soil suction monitoring period was occasionally interrupted by 1-2 days of maintenance, in which mini-tensiometers have been re-saturated because air bubbles were observed in the plastic body (Appendix A). In addition, at the end of each drying test, all mini-tensiometers have been re-saturated because most of them (in particular those placed on superficial layers) reached high suction values and thus became desaturated.
On the other hand, VWC sensors must be tightly connected to the soil and occasionally this did not happened, thus many measurements have been lost in particular in the first stage of the monitoring period.
During first year, irrigation process occurred every two days (see Chapter 5). Nevertheless, it was quite difficult to observe daily fluctuations of suction due to irrigation. Slight fluctuation trend was observed at all depths in Figure 6.11a, and this is due to the variation of suction due to the temperature. Comparing the suction values measured during first year to those of the second year it is possible to observe a clear increase of values in the second year, because vegetation had grown and thus its influence on soil suction increased.
On the other hand, the trend of VWC values decreased from the first year to the second year, because of the growth of roots, which reduced VWC through root water uptake.
After the drying test conducted in July 2016 (V_D_Jul1) the irrigation frequency has been changed to 2 times per day, because summer started and vegetation required more water to survive. In fact, during this period

suction was maintained quite low, ranging from 0 to 10 kPa (Fig. 6.11a), while VWC was quite constant (Fig. 6.11b).
Starting from October 2016 the irrigation frequency was reset again to 2 days, however the suction values did not change because of the lower temperatures, while VWC showed an increasing trend, and this might be due to the reduction of root water uptake in the so called 'dormant' stage of roots.
The high suction variation on row A was clearly evident because of the direct interaction between superficial layer and atmosphere, through evapotranspiration process. In fact, suction fluctuations are higher on this layer compared to those measured at deeper depths.
This variation is slightly observed also for VWC measurements.
The drying tests conducted during the monitoring period (Tab.6.1) are also reported because they lasted 15 days and it is possible to see the increasing in soil suction at all depths investigated and, conversely a decreasing in VWC due to both evaporation from soil and root water uptake (transpiration from roots).
However, wetting tests were not reported due to their short duration (few hours), thus would be impossible to recognize them within the whole monitoring period.

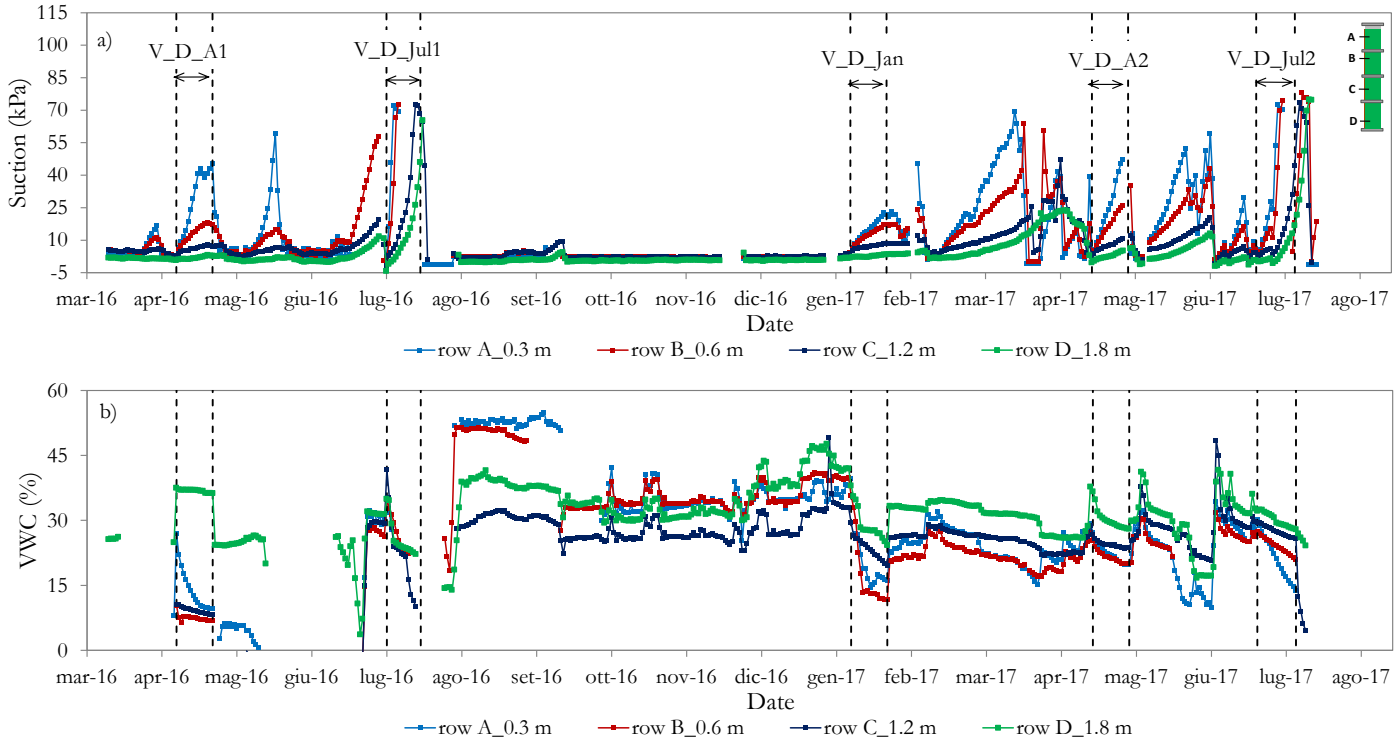

Figure 6.11 a) Soil suction and b) VWC monitoring data at 4 depths of the vegetated soil column (V): row A (blue line) at 0.3 m depth, row B (red line) at 0.6 m depth, row C (dark blue line) at 1.2 m depth and row D (green line) at 1.8 m depth..

6.4 HYDRO-MECHANICAL RESPONSE DURING EVAPOTRANSPIRATION

6.4.1 Drying test results in wet season

In Campania region, wet season typically goes from October to May and rainfall events are frequent (Cascini et al., 2014).
The drying test in wet season was conducted in April (Tab. 6.1), because at that time the roots had already grown and effects of roots on suction were observable. The aim of this study was to quantify the effectiveness of perennial graminae on increasing soil suction, and conversely decreasing volumetric water content, through evapotranspiration and root water uptake. As discussed in previous paragraph, both vegetated (V) and no-vegetated (NV) have been saturated and then drying tests have been conducted for 15 days.
In order to quantify the effect of root growth on soil response, for V column two different drying tests have been conducted, the first in April 2016, when have reached 0.58 m of length, and the second during April 2017 when roots were completely grown and have reached 1.85 m of length. On the contrary, for NV column only the drying test conducted in April 2017 is reported because the soil hydraulic response was the same within the two years.
The monthly Temperature in April 2016 was 16.1 ±2.9°C, while in April 2017 was 14.1 ±2.3°C.
Figure 6.12 shows the soil suction (s) and volumetric water content (VWC) daily values and their fluctuations during drying tests conducted in April 2016 and April 2017 on vegetated and no-vegetated soil columns, which have been called in Table 6.1 respectively V_D_A1 (Fig. 6.12b,e), V_D_A2 (Fig. 6.12c,f) and NV_D_A2 (Fig. 6.12a,d).
For each test result, the schematization of soil column with root length and depths of 4 monitoring points was reported.
Furthermore the daily suction increment (Δs), as the average of the amount of soil suction increased day by day (kPa/d), was calculated for each depth and reported for each test.

It can be observed that soil suction increased more quickly in the superficial layers (row A and row B) in all soil columns, even if the Δs in correspondence of row A of V_D_A1 (3.1 kPa/d) and V_D_A2 (3.5 kPa/d) were almost the double of that recorded in NV column (1.7 kPa/d). The daily suction increment at row B was the same between NV_D_A2 and NV_D_A1 (Fig. 6.12a,b), while in V_D_A2 slightly increased. This might be due to the length of roots in V_D_A1, which did not yet reached the depth of row B. As consequence, no root water uptake occurred at that depth and thus the daily suction increment was similar, even smaller, to that recorded in NV column.

On the other hand, the daily suction increment referred to row B in V_D_A2 test was higher than that of V_D_A1, due to the presence of roots along the entire column. As it concerns the lowest depths (1.2 m to 1.8 m from the upper part of column), the effect of roots on suction increase during drying was negligible. In fact, daily suction at row C for both V_D_A1 and V_D_A2 tests was quite the same (Fig. 6.12b,c).

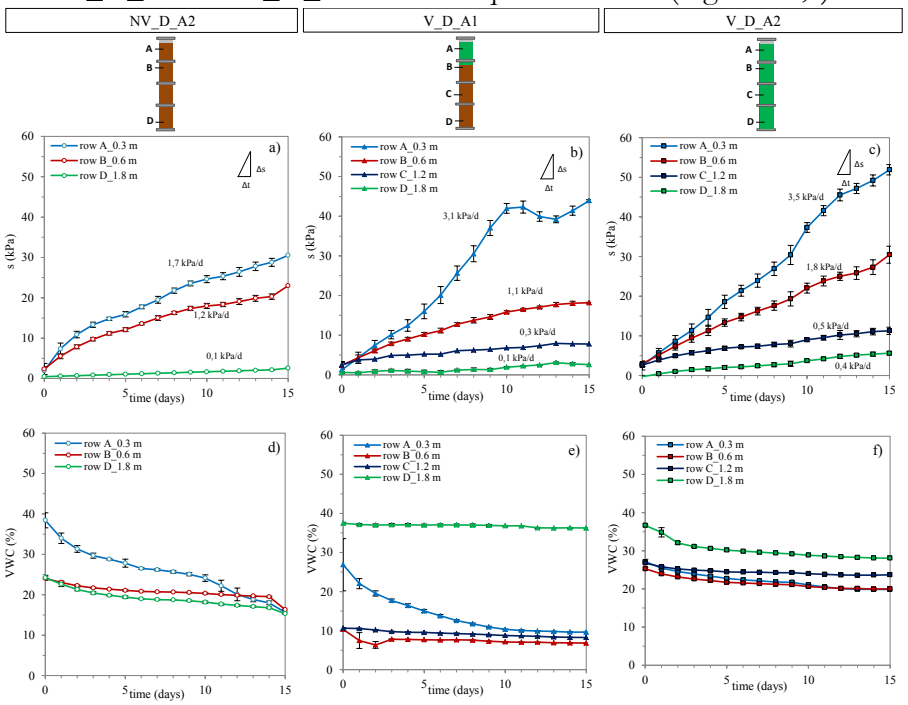

Figure 6.12 15 days drying test results for wet season during April. Daily soil suction (s) with time for a) NV_D_A2 test, b) V_D_A1 and c) V_D_A2 tests. Daily Volumetric Water content (VWC) with time for d) NV_D_A2 test, e) V_D_A1 and f) V_D_A2 tests (modified by Capobianco et al., 2017).

In correspondence of row D a slight difference was observed between in daily suction increment values, in fact it increased from a minimum of 0.1 kPa/d recorded in NV_D_A2 test to 0.3 kPa/d for V_D_A1 test, up to 0.5 kPa/d in V_D_A2 test. In conclusion, bigger differences in soil suction increments can be observed at shallowest depths where both roots are more numerous and the soil is closer to the atmosphere for water exchange due to evaporation (Capobianco et al., 2017).
Volumetric Water Content measurements were slight comprehensive during all tests, in particular at row A and row B of V_D_A1 tests values recorded have been too low and thus no reliable for fair comparisons (Fig. 6.12c).
However, the general behavior of VWC during drying can be easily recognized for all tests, in fact VWC decreased as the soil suction increased. For a fair comparison, VWC measured at row A in all tests showed a decreasing trend, nevertheless it slowed down in vegetated column. This is due to the presence of roots, as observed in Chapter 4 for *Schefflera heptaphylla*, which occupied the soil pore spaces and this reduced the size of soil pores. Reduction in size of soil pores means that suction increases quickly because of capillary pressure, while VWC decreases slowly.
Furthermore, roots are very light elements similar to initially empty capillary tubes, which become full of water during water uptake. Thus VWC measurements in vegetated soil column take into account as the volume of water between soil pore spaces, as the volume of water contained into the roots.
This is reflected in VWC-time curve as flatter as the roots increase (Fig. 6.12e,f), compared to that observed in no-vegetated soil column.
Figure 6.13 shows the correlation between the daily suction values measured during drying in V column when the roots were completely grown (V_D_A2) and those recorded in NV column (NV_D_A2). At shallowest layers (row A, B) soil suction measured was the same of NV column until it reached 15 kPa. This means that during first days (3 days) of drying no differences have been observed in soil suction increment between V and NV column. After that, the suction showed a more pronounced increasing trend with time. This is reflected in a bigger difference between soil suction measured in V column and that measured in NV column. In particular, at row A, the difference between soil suction in V and NV column was 20 kPa at the end of the test.

This difference became smaller with the increase of depths investigated, in particular resulted equal to 7 kPa at row B and 3 kPa at row D.

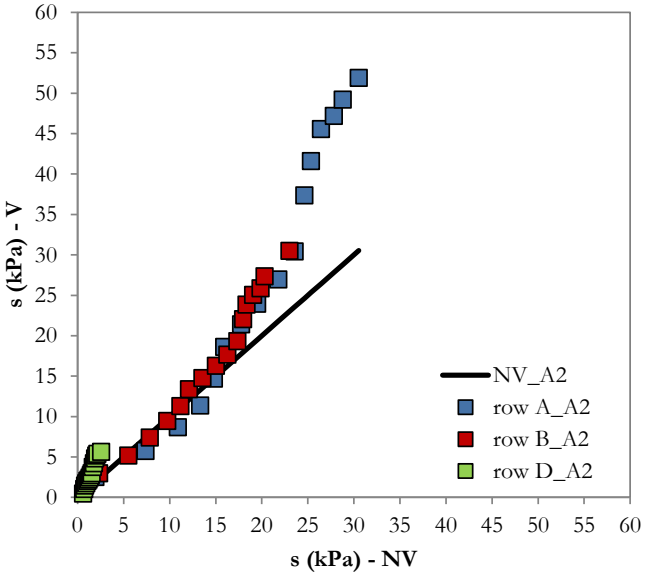

Figure 6.13 Soil suction values in NV column recorded in NV_D_A2 tets vs Soil suction values in V column recorded in V_D_A2 test.

Hydraulic head profiles at different days of drying test are showed in Figure 6.14.

A down flow direction of water can be observed in all tests at the initial condition, while after 5 days the flow direction was changed because evaporation process started in NV column and evapotranspiration process started in V columns.

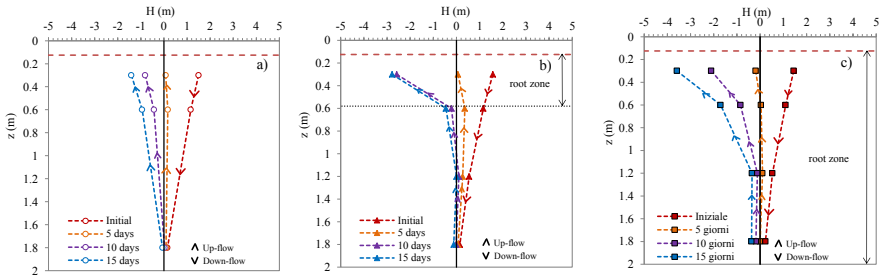

Figure 6.14 Hydraulic Head profiles for a) NV_D_A2 test, b) V_D_A1 test and c) V_D_A2 test (modified by Capobianco et al., 2017).

The slope of water head profile indicates the hydraulic gradient. Thus, the higher is the inclination, the higher is the hydraulic gradient.
The inclination of water head profiles is steeper in both V columns compared to that of NV column. This is because in rooted zones the water flow was facilitated by both evaporation and transpiration processes (Capobianco et al., 2017).

6.4.2 Drying test results in dry season

The positive effect of plant evapotranspiration on induced soil suction in summer season is widely recognized, because of the high temperatures and the lack of rainfall events. During this period the vegetation is florid and plants need water for their vital functions. In Campania Region the dry period goes from May to September (Cascini et al., 2014).
In order to quantify the effect of root growth on soil hydro-mechnical response, for V column two different drying tests were conducted, the first in July 2016, when roots were 1.47 m long, and the second during July 2017 when roots were completely grown and 1.85 m long. On the contrary, for NV column only the drying test conducted in July 2017 is reported because the soil hydraulic response was the same within the two years.
Figure 6.15 shows the daily suction and VWC values measured during 15 days drying respectively in NV_D_Jul2 test (Fig. 6.15a,d), V_D_Jul1 (Fig. 6.15b,e) and V_D_Jul2 (Fig.6.15c,f) tests.
The monthly Temperature in July 2016 was 24.9 ±2.2°C, while in July 2017 was 25.0 ±1.9°C.
At shallowest layer (row A) the soil suction increased almost linearly in NV column, as observed in previous tests, even if the daily suction increment was 2.6 kPa/d, higher than in wet season.
Daily suction increments observed at row A in both V columns were definitely higher than that in NV columns, indeed they varied from 8.7 kPa/d up to 22.8 kPa/d. Furthermore, in V_D_Jul1 test, both tensiometers at row A and row B went to cavitation on fifth day of drying (Fig. 6.15b). This means that plant transpiration induced a soil suction of about 70 kPa in 5 days of drying, compared to NV column, where suction reached at least 15kPa (Fig. 6.15a).

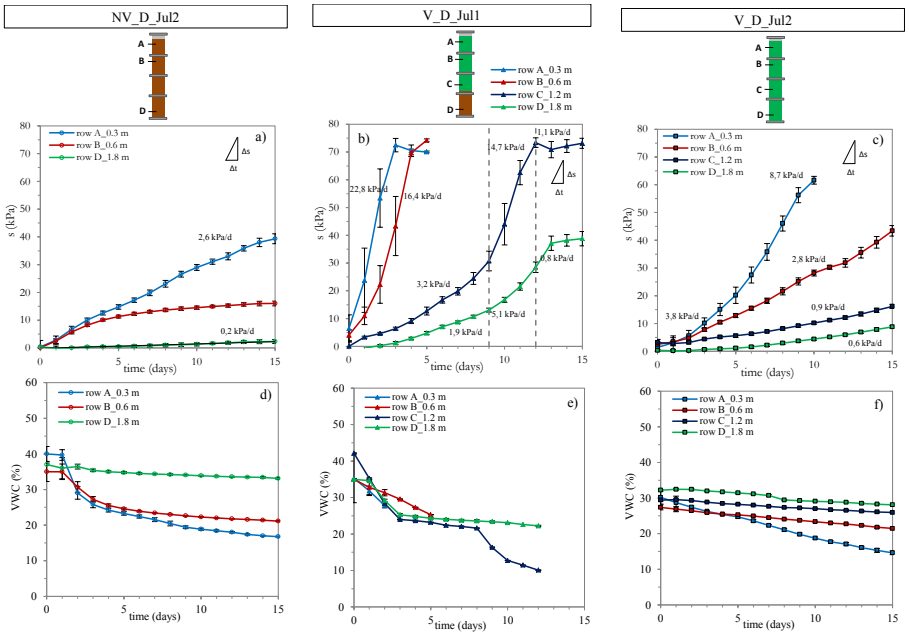

Figure 6.15 15 days drying test results for wet season during July. Daily soil suction (s) with time for: a) NV_D_Jul2 test, b) V_D_Jul1 and c) V_D_Jul2 tests. Daily Volumetric Water content (VWC) with time for d) NV_D_Jul2 test, e) V_D_Jul1 and f) V_D_Jul2 tests.

Cavitation occurred also in correspondence of row A in V_D_Jul2 test, in fact the last reliable suction value recorded was 63 kPa after 10 days of drying (Fig. 6.15c). In general, final suction values recorded along V column in July 2016 were considerably higher than those measured in July 2017 along the same column. This might be due to the different stage of growth between July 2016 and July 2017. In fact, in July 2016 the graminae was in its first stage of growth and it required more water to grow and to face with high temperatures during its first dry season. Differently, in July 2017 it was already 1.5 years, thus it required less water to survive and this was reflected in lower daily suction increment (Fig. 6.15c). Furthermore, in April 2017 some leaves have been cut for infiltration tests and this influenced the evapotranspiration occurred in July 2017, because is widely known that it depends on *LAI* (Monteith, 1965). As direct consequence, *LAI* influences the suction increment (Fig.6.8).

However, drying test results obtained in July 2017 are more reliable and they can represent the hydraulic response of vegetated soil in dry season. VWC values showed a decreasing trend during time , as observed in wet season. The slope of VWC curve with time was flatter in V_D_Jul2 test compared to that of V_D_Jul1 test. This might be due to the effect of roots on soil aggregation, as discussed for drying test conduced in April 2017. In conclusion, roots concur to the hydraulic response of pyroclastic soils with two effects: transpiration by root water uptake and increment of soil aggregation. As consequence of the first effect, root water uptake is reflected as a reduction of VWC and thus an increment of soil suction. On the other hand, as consequence of the second effect the structure becomes denser with more soil aggregates.
Figure 6.16 shows the correlation between the daily suction values measured during drying in V column when the roots were completely grown (V_D_Jul2) and those recorded in NV column (NV_D_Jul2). At shallowest layers (row A, B) soil suction in V column was equal to that measured in NV column until it reached 5 kPa, after that it increased more quickly. After 10 days of drying, the difference between soil suction in V and NV column was 33 kPa at row A and 14 kPa at row B.

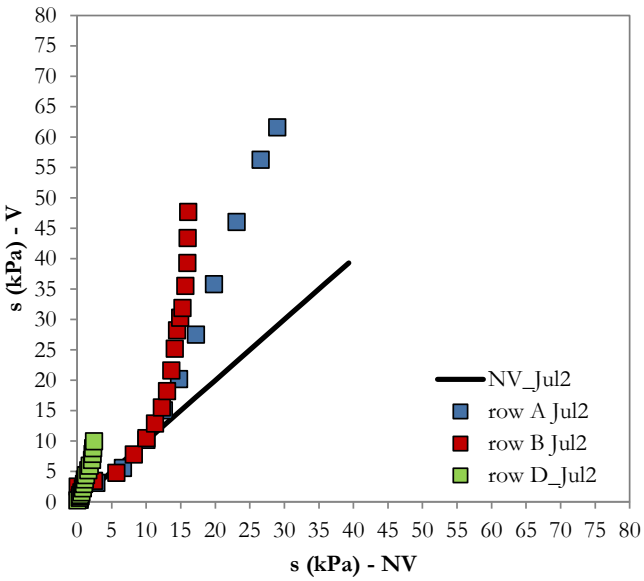

Figure 6.16 Soil suction values in NV column recorded in NV_D_Jul2 test vs Soil suction values in V column recorded in V_D_Jul2 test.

At the end of the test, since tensiometer at row A of V column reached cavitation, the difference in soil suction recorded at row B between V and NV column was 32 kPa.
Hydraulic head profiles at different days of drying test are showed in Figure 6.17.
A down flow direction of water was guaranteed at initial condition, while after 5 days the flow direction was changed because evaporation process started in NV column and evapotranspiration process started in V columns. In addition, hydraulic gradients in V columns, as expected, were higher in root zone because of root water uptake (Fig. 6.17b,c).

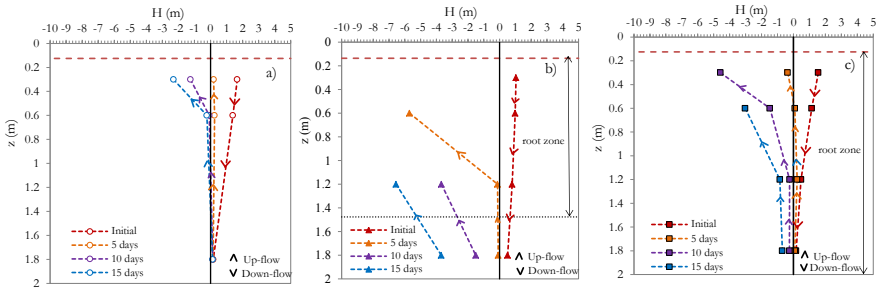

Figure 6.17 Hydraulic Head profiles for a) NV_D_Jul2 test, b) V_D_Jul1 test and c) V_D_Jul2 test.

6.4.3 Prediction of induced suction by vegetation in pyroclastic soils

The results of drying test on both NV and V soil columns represent the base for a prediction of the amount of soil suction induced by graminae species during two period of the years.
Figure 6.18 shows the experimental points of soil suction measurements after 5 days of drying in NV column and V column for both wet season and dry season tests conducted in 2017, when roots were grown.
It is possible to quantify the change of suction induced by graminae transpiration as the difference between the experimental point and the value along the bisector of the graph, which corresponds to the amount of soil suction measured in NV column. In wet season, at 30 cm of depth (row A) for a suction of 16 kPa in NV soil, the expected suction in V soil is 18 KPa, while in dry season for 15 kPa of suction in NV soil, 22

kPa of suction are expected in vegetated soil. This difference increases with time, as showed in Figure 6.19.

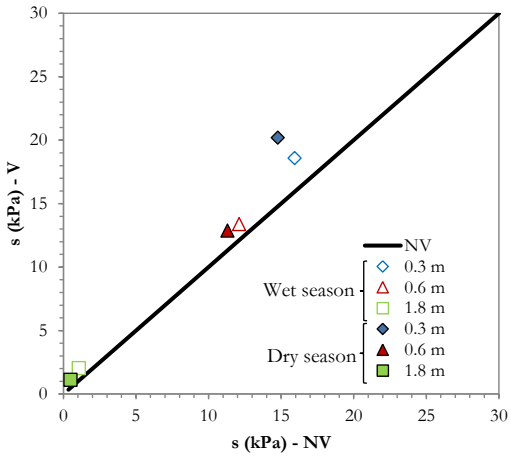

Figure 6.18 Soil suction in V column after 5 days of drying vs soil suction in NV column.

After 10 days of drying the expected suction in V soil at 0.3 m in wet season was 37 kPa for 25 kPa of soil suction in NV column. On the other hand, in dry season when the suction in NV is equal to 28 kPa, the expected suction in V soil is 62 kPa.

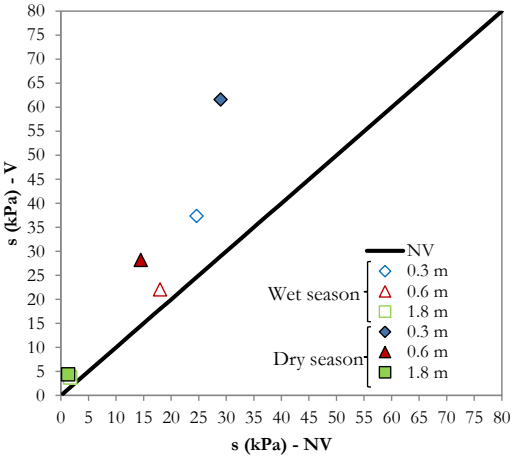

Figure 6.19 Soil suction in V column after 10 days of drying vs soil suction in NV column.

6.4.4 The effects of roots on soil water retention ability

The hourly measurements of soil suction (s) and volumetric water content (VWC) obtained by drying tests represent the soil water retention ability of soil column when external stress induces the water flux to exit from the soil.

Figure 6.20 shows experimental points of SWRCs carried out from drying tests conducted on April 2017, when roots were completely grown, on NV and V soils at 0.3 m and 0.6 m depths (respectively row A and row B).

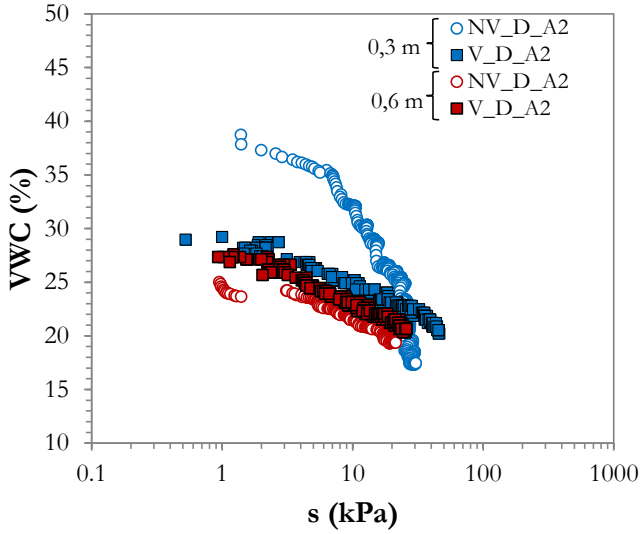

Figure 6.20 Measured SWRCs of NV and V soil along the drying path of April 2017 at 0.3 m and 0.6 m depth.

In any case the saturated volumetric water content (θs), which corresponds to VWC when the soil is fully saturated (Sr=100%), was not reached even if the soil suction was equal to 0 kPa, because occluded air in pore spaces usually requires positive pressure to dissolve (Lu et al., 2014; Jotisankasa & Sirirattanachat, 2017).

However, the VWC near to saturation in V soil was lower than that measured in NV soil, in accordance with that observed by Jotisankasa & Sirirattanachat (2017), who concluded that the saturated VWC decreases as the root biomass increases.

As consequence, the presence of roots incremented apparently the soil density and this is clearly reflected in a reduction on VWC for a fixed

amount of suction value, compared to NV soil. In fact, the SWRC at 0.3 m depth of V soil is flattered than that of NV soil.
For a fixed suction value lower than 10 kPa, the VWC in V soil is almost 10% less than that measured in NV soil, and this difference decreases with soil suction increasing. On the other hand, at 0.6 m depth the soil water retention behavior is quite similar between V and NV soil.
Figure 6.21 shows the SWRCs at 0.3 m and 0.6 m for both V and NV soil during drying path occurred in July 2017. At any depth, VWC measured in V column in correspondence to low suction values, is lower than for NV soil. Furthermore, the shape of the experimental curve in V soil is flatter than for NV soil, as for the drying path in April 2017. Differences in soil water retention ability can be explained as different stress history to which soils were subjected. In fact, the flat trend and the low VWC near saturation of SWRC for V soil is typical of compacted materials (Fredlund et al., 2012).

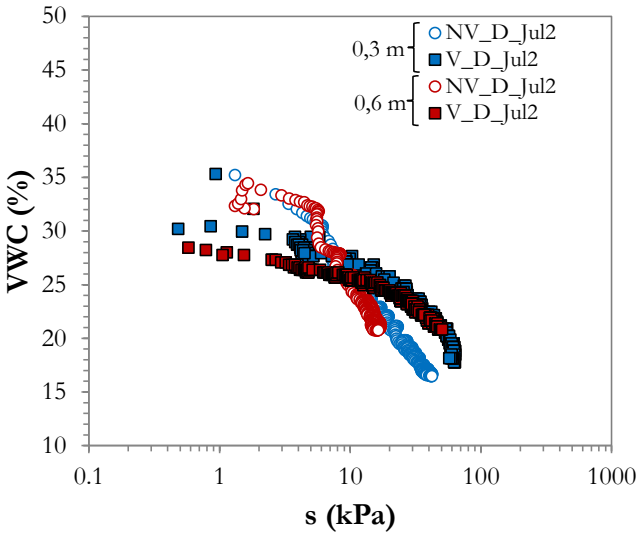

Figure 6.21 Measured SWRCs of NV and V soil along the drying path of July 2017 at 0.3 m and 0.6 m depth.

The presence of roots, as discussed previously, facilitates soil aggregations and thus the soil behaves like a compacted material. This is reflected in a change of the soil matric structure, in which roots provide

a bonding among the soil particles trough capillary pressure as well as through the cellulose and the exudates produced by roots.
Moreover, the exudates produced by roots tend to enhance the water retention around roots (e.g. Grayston et al. 1997; Traoré et al. 2000; Kroener et al. 2014; Tian et al. 2015).
In V soil for high suction values the slope of SWRC increased. As consequence a small increment in soil suction is matched with high VWC reduction. This might be due to the increasing of root water uptake when soil goes to dry condition, so roots need more water to survive.

6.5 HYDRO-MECHANICAL RESPONSE DURING INFILTRATION

6.5.1 Infiltration test procedure

The aim of this study was to quantify the hydro-mechanical response of vegetated soil, in terms of soil suction reduction, to atmospheric action such as rainfall during wet season. Wetting tests consisted in applying an artificial rainfall at the top of soil columns. The effect of roots was quantified by comparing the soil suction reduction observed in V column with that recorded in NV column subjected to the same rainfall intensity.
The artificial rain system was essentially a rain simulator and a water tank. The rain simulator was constructed with a main plastic pipe with an inner diameter of 3.0 mm forming a ring with 6 T-joints. Each T-joint was connected to a secondary plastic tube with the same inner diameter with a needle holed, from where the rain comes out. In total 6 holes were available to allow the water to be discharged as rainfall. The dimension of the holes can vary from almost nil to about 7 mm in diameter depending on rainfall intensity to simulate (Meyer, 1979).
In this study the diameter of the holes, close to 1 mm, was consistent with the rainfall intensity to simulate. The rain simulator was connected to the water reservoir through a cable used in medical treatments for intra venous (IV) applications and then was mounted on a circular support standing at a specified height above soil surface. The IV cable consisted of a drip system linked to the tap of the water reservoir and a

water flux regulator. The water reservoir of 6 l capacity was adopted and placed on a shelf to maintain constant hydraulic head difference relative to the rainfall simulator.
The rainfall intensity selected was the most frequent rainfall intensity occurred from 2001 to 2011 in a test site placed in Campania region (Cervinara test site) where pyroclastic soils cover the calcareous bedrock, and it was in a range between 1 mm/h and 4 mm/h (Comegna et al., 2016).
Before the wetting test, leaves exiting the column were cut in order to guarantee that rainfall applied was equal to net rainfall infiltrated, by avoiding that rain drops intercept by leaves would not infiltrate the soil.
The variable investigated in this study was soil suction, which undergoes significant drops due to rainfall, with consequent reduction of soil shear strength and potential slope failure (Anderson and Sitar 1995; Alonso et al. 1995). In particular, in this study the soil suction reduction ($\Delta s<0$) due to rainfall infiltration was measured as the difference between the soil suction measured at initial condition (s_0) before rainfall and the soil suction at the end of the event.
In order to study the effect of rainfall duration on soil suction reduction, 4 different rainfall events were simulated with a duration (D) respectively equal to 3 h, 6 h, 9 h and 12 h. The 3-6 hours rainfall events were considered short events, while 9-12 hours were considered long events, based on the study conducted by Comegna et al. (2016).
The rainfall events have been conducted for different initial soil suction (s_0) values, to quantify the influence of initial soil suction on Δs.
Since soil suction reduction due to all rainfall events simulated was negligible at deeper layers of both NV and V columns, considerations on soil suction reduction have been done considering shallowest layers.

6.5.2 Wetting test results

Figure 6.22 shows the Δs variation with s_0 for V and NV columns at 0.3 m and 0.6 m depth (respectively row A and row B in column) for D= 3-6 hours (Fig. 6.22a,b) and for D= 9-12 hours (Fig. 6.22c,d). Furthermore, in situ measurements of Δs at 0.6 m depth at Cervinara test site (Comegna et al., 2016) are showed in Figure 6.22c,d. Initial soil suction s_0 for V and NV columns were not the same because was

difficult to reproduce the same initial condition in soil columns subjected to atmospheric conditions.

At shallowest depth the hydraulic response in term of suction reduction for both NV and V soil was quite similar when s_0 was low, in particular less than 15 kPa (Fig.6.22a).

When s_0 is higher than 15 kPa, for a rainfall event of 3 hours the Δs recorded was lower in V column compared to NV column and this difference increased with increasing of s_0. In fact, it was observed that for short rainfall event the infiltration process in V column is delayed because rain drops first were intercepted by leaves and then infiltrated in soil. This effect is reduced with increasing of rainfall duration (D=6 hour). When initial soil suction was high (40 kPa), for short event (D= 3, 6 h) reduction in suction less than 5 kPa (in absolute value) was recorded in V column compared with those recorded in NV column, which ranged from 5 to 15 kPa.

Regarding rainfall events of long duration (D=9,12 h), no differences between Δs recorded in V and NV soil were observed for any given initial soil suction, furthermore Δs in V soil after 12 hours of rainfall were higher than those measured in NV (Fig. 6.22b).

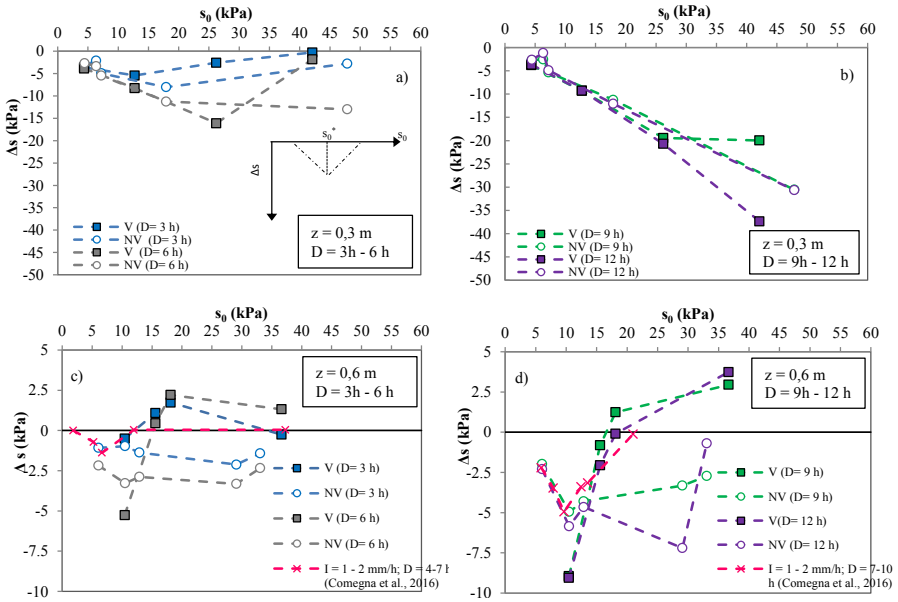

Figure 6.22 Soil suction reduction Δs versus initial suction s0 in V and NV colum at row A (z =0,3 m) and row B (z=0,6 m) for rainfall intensity 1-4 mm/h (Capobianco et al., 2017).

At 0.6 m depth the hydraulic response to rainfall events of 3,6 h (Fig. 6.22c) and 9,12 h (Fig. 6.22d) are below discussed.
For 3 hour rainfall event (Fig. 6.22c), when the initial suction is less than 10 kPa, the response in V column in terms of Δs was negligible as that observed in NV column. On the other hand, the increasing of rainfall duration from 3 to 6 hours was reflected in an increasing of Δs for both NV and V columns.
When s_0 increased, independently on the duration of the event, two different behaviors were observed between V and NV column. In V column the Δs recorded seemed to be not influenced by rainfall infiltration because it was at least 0 kPa (for s_0=37 kPa) or, in some cases, it showed positive values. Positive values of Δs represent a suction increasing trend during rainfall event instead of decreasing, as for NV column. This means that when initial soil suction was higher than 10 kPa, the rainwater did not reached 0.6 m depth. Furthermore the increasing in suction value might be due to the transpiration process which probably continued during the rainfall event.
The same behavior was observed for longer duration of rainfall event (9, 12 h) when initial soil suction was higher than 10-15 kPa (Fig. 6.22d).
These results are consistent with those observed by Comegna et al. (2016) for the test site of Cervinara, even if differences between this experimental study and the study conducted by Comegna et al. (2016) are reported in Capobianco et al. (2017).

6.5.3 Discussion

Wetting tests conducted on vegetated (V) and no vegetated (NV) soil columns highlighted the positive effect of perennial graminae on reducing infiltration process for ordinary rainfall events. In conclusion, some general considerations can be done for this experimental study.
1. The initial soil suction influences the hydro-mechanical response of soil, in particular with decreasing of initial soil suction the reduction of soil suction increases.
2. The soil suction reduction, independently on rainfall duration, decreases with depth.
3. At shallowest layer (0.3 m) in presence of vegetation, the infiltration process is delayed with the occurrence of short rainfall events because of the leaves interception, and this effect is enhanced with increasing of initial soil suction.

4. As consequence of the delay of infiltration process, at deeper layer (0.6 m) the suction reduction is negligible and when initial soil suction is higher than 10 kPa, increasing in soil suction can occur due to the transpiration process of vegetation.
Starting from these considerations, a general interpretation of the hydromechanical response of vegetated pyroclastic soils during low intensity rainfall events can be conducted depending on the typical soil suction values in dry season and wet season.

6.6 CONCLUDING REMARKS

Some final considerations can be done regarding the effects of long root grasses, such as those of perennial graminae used in this experimental study, on the hydraulic response of pyroclastic soil under both wetting and drying cycles. These effects are highlighted in shallowest layers, up to 1.2 m depth.
During drying, the presence of roots enhances the soil suction increment in both wet and dry season and this increment increases with the elongation of the duration of drying. Starting from these considerations, it is possible to predict that seasonal suction trend, as introduced in Chapter 2, may change in presence of vegetation covering pyroclastic soils of Campania region.
During wetting, the presence of roots leads to a delay in infiltration process for small duration events and this effect tends to disappear with the increase of rainfall duration. On the other hand, this effect is enhanced when the soil suction before the event is high and is reflected as a delay of water infiltration at deeper depths.
Soil water retention ability of vegetated pyroclastic soils is different from that observed in no vegetated soils. In particular, the volumetric water content near full saturation is reduced in accordance with others authors, even if in general more water is retained in vegetated soil during drying path, due to the chemical products of roots which provide aggregation among the soil particles. This latter evidence is reflected in a flatter drying path of SWRC, which is typical of compacted soils. In conclusion, the presence of roots in unsaturated pyroclastic soils change its hydraulic response to drying and wetting cycles, by changing its structure and, as consequence, by changing the water flow in soil.

In order to fully characterize this new composite material made of pyroclastic soil and roots of pereniall graminae species, a further work can be the laboratory investigation of SWRC of vegetated soil samples, through volume extractor or suction controlled oedometer tests. These properties can then be used for modeling seepage problems to the aim of knowing the ground water regime behavior in presence of roots.

7 THE COLLAPSIBILITY BEHAVIOR OF ROOTED SOILS

Unsaturated pyroclastic soils, as discussed in Chapter 2, show collapsible behavior upon wetting with a consequent reduction in volume and a rearrangement of soil particles.
This Chapter investigates the collapsibility of pyroclastic soils through standard odeometer tests conducted on reconstituted specimens of class 'B' (Bilotta et al., 2005). Tests on both bare and vegetated soil samples have been carried out in order to identify the range of porosity in which they show a collapsible behavior. This preliminar investigation allows to quantify the effect of root growth on the occurrence of this phenomenon.

7.1 INTRODUCTION

Pyroclastic soils of class 'B' generally belong to the shallowest layers of pyroclastic deposits (1-2 m) and overlay those of class 'A', with some presence of inter – bedded pumice layers (Revellino et al., 2004; Bilotta et al., 2005; Cascini et al., 2008; Ferlisi et al., 2016), so they first experiment saturation due water infiltration during a rainfall event.
Neverthless, the collapsibility behavior of these soils is not deeply investigated in the scientific literature.
In order to quantify the magnitude of volumetric collapse due to wetting, the double oedometer procedure is usually adopted (Jennings and Knight 1957). This procedure is based on the assumption that the deformations induced by wetting are independent on the loading-wetting sequence. To this aim, two oedometer tests are performed using nominally identical samples. In one test, the specimen remains in unsaturated condition with a specific water content, whereas in the other test the sample, is saturated under a small seating load. The loading sequence applied during the test is the same for both specimens. The difference in void ratio between the

vertical deformation in unsaturated and saturated specimens, at any vertical stress, is assumed to represent the volume change related to collapsibility. Since the accuracy of results in oedometer apparatus is related to the computation of volumetric deformation, which is assumed to be equal to the axial deformation, the technique has been extended to three-dimensional testing known as double-triaxial test. However, Lawton et al. (1991a) claimed that no significative differences in terms of magnitude of collapse have been observed between these two methods.
In next sections, the results obtained by recent studies on collapsibility behaviour of undisturbed pyroclastic soils of class 'B' are first discussed (Lancellotta et al., 2012), then the experimental program followed in this study is introduced.
Since there is a lack of contribution in literature on the effect of roots on the collapsible behavior of unsaturated soils, the results obtained in this study must be considered as first contribution to this challenging topic as it concerns pyroclastic soils. The aim of this study was firstly to investigate the range of porosity within pyroclastic soils of class 'B' show a collapsible behaviour and then the quantification of changing in collapsibility of same soils permeated by roots.
The test program for studying collapsibility of rooted soils is hereafter explained, as well as the experimental set up and the sampling method. Then, results of collapse tests on root-soil samples are discussed and compared with those obtained in bare samples.

7.2 LITERATURE REVIEW

7.2.1 Suction controlled and standard oedometer tests on undisturbed samples

Lancellotta et al. (2012) carried out four suction controlled oedometer tests with a constant suction of 20 kPa on undisturbed soils of class 'B' at different initial specific volume (v). Results obtained are compared with those observed in oedometer tests in saturated conditions (Fig. 7.1). However, in this study the double oedometer procedure was not adopted to get insight of magnitude of collapse, because the initial specific volume (v) of samples was not the same.

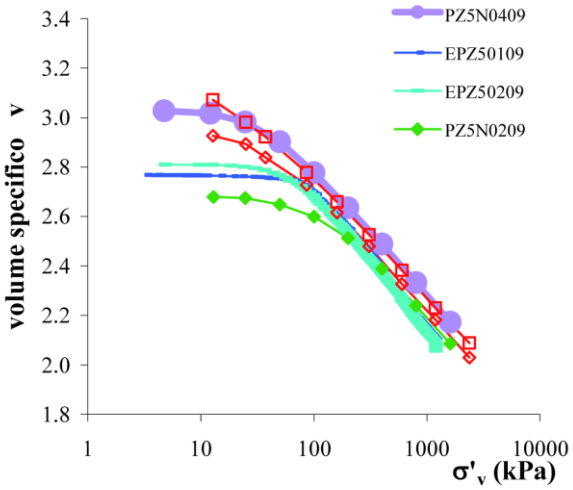

prova	campione	u_a-u_w (kPa)	v_0
PZ5N0409	PZ5 inf.	20	3.049
EPZ50109	PZ5 sup.	20	2.866
EPZ50209	PZ5 sup.	20	2.830
PZ5N0209	PZ5 sup.	20	2.718

Figure 7.1 Results of suction controlled oedometer tests on undisturbed soils of class 'B' and comparison with results of two oedometer tests on saturated samples (red curves) (Lancellotta et al., 2012).

On the other hand, Figure 7.2 shows results of two standar oedometer tests conducted on undisturbed samples of pyroclastic soils of class 'B' with similar initial specific volume (v), in this case expressed in terms of of void ratio (e), since they are related each other by the following equation:

$$v = 1 + e \tag{7.1}$$

The first oedometer test was carried out by maintaining the natural water content of the soil specimen by adopting a non-conventional procedure explained in Lancellotta et al. (2012), while the second one was conducted on undisturbed soil in saturated condition, by following the same loading sequence.

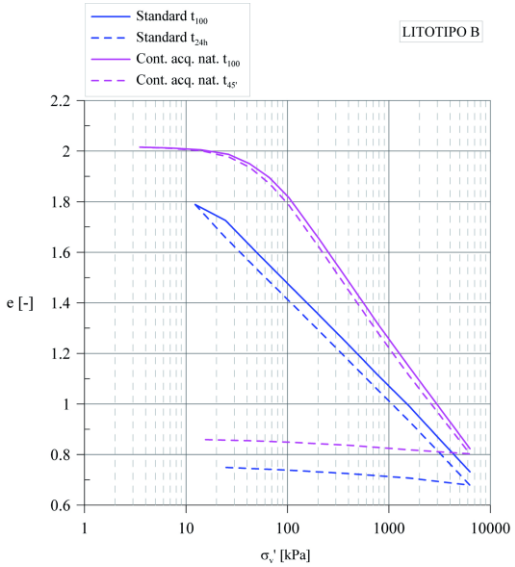

Figure 7.2 Results of standard oedometer test on unsaturated sample with constant natural water content (violet curve) and on saturated sample (blue curve). Dashed lines are referred to the void ratio of samples after 45 minutes (Lancellotta et al., 2012).

It can be observed that the magnitude of potential collapse increases with vertical net stress up to 100 kPa, where it attained the maximum value (12%). After that, the potential collapse decreases with increasing in vertical net stress and the compressibility curve of unsaturated soil became closer to that of saturated soil for very high loads (more than 1000 kPa). These results are consistent with those obtained for pyroclastic soils of class 'A' in suction controlled oedometer tests, even if in that case the maximum collapse of (9%) was attained in correspondence of 160 kPa of vertical net stress (Bilotta et al., 2008).

7.3 MATERIAL AND METHODS

7.3.1 Oedometric apparatus and test program

Standard oedometric apparatus has been used in this experimental program and the double oedometer procedure was adopted (Jennings and Knight 1957).
All oedometer tests have been conducted at Geotechnical Laboratory of University of Salerno. The oedometric apparatus consisted of a stainless steel rigid ring of 50 mm of diameter and 20 mm high, placed into a containing cell. This latter was opportunely filled of distilled water during the wetting phase of collapse tests. The vertical load is applied through a frontal loading frame with a lever system where the load is charged. This load is then transferred through the lever to the upper surface of the sample where is uniformly distributed by a loading head.
The axial deformation is measured by a LVDT (Linear Variable Differential Transducer) which is connected to a computer for data.

7.3.2 Bare soil investigated

Physical characteristics and grain size distribution of the investigated soil are already described in Chapter 5.
Reconstituted specimens have been formed in laboratory by adopting the same moist tamping technique (Ladd, 1977) used for filling the soil columns described in depth in Chapter 5, except for the target bulk density (γ_d), which varied for each sample in order to obtain different initial porosity (n_0). The compaction procedure was conducted directly in the oedometer ring, in order to obtain the soil sample to test in oedometer apparatus. Five standard oedometer tests have been conducted on soil samples at five different γ_d which corresponds to an initial porosity respectively of 51.7%, 54.0%, 56.4%, 59.4% and 64.3% (Tab. 7.1). The initial saturation degree (S_r) was about 0.2 for all soil samples in order to investigate the effect of porosity on the volumetric collapse of soil. The double oedometer procedure was adopted and test results were compared with those obtained by samples tested in saturated condition.

Table 7.1 Details of double oedometer tests on reconsituted bare samples.

type	ID	γ_d	v_0	e_0	n_0
	#	kN/m³	-	-	(%)
Bare unsaturated	SO_B1	12.50	2.072	1.072	51.7
	SO_B2	11.92	2.173	1.173	54.0
	SO_B3	11.29	2.293	1.293	56.4
	SO_B4	10.51	2.465	1.465	59.4
	SO_B5	9.25	2.799	1.799	64.3
Bare saturated	SO_B1_sat	12.31	2.103	1.103	52.5
	SO_B2_sat	11.86	2.184	1.184	54.2
	SO_B3_sat	11.19	2.314	1.314	56.8
	SO_B4_sat	10.40	2.490	1.490	59.8
	SO_B5_sat	9.68	2.676	1.676	62.6

7.3.3 Test set up for vegetated soil

Four plexiglas cylinders 200 mm high, with inner and outer diameter respectively of 192 mm and 200 mm, have been filled with pyroclastic soils of class 'B' abovementioned, by adopting the moist tamping method (Ladd, 1977). Four different initial γ_d (12.3 kN/m^3, 11.18 kN/m^3, 10.93 kN/m^3 and 10.62 kN/m^3) were adopted, corresponding respectively to 56%, 59% 60% and 62% of initial porosity n_0 (Table 7.2).

Table 7.2 Details of the soil characteristics in plexiglas cylinders.

type	Column	γ_d	v_0	e_0	n_0
	#	kN/m³	-	-	(%)
Vegetated	C_1	12.30	2.273	1.273	56
	C_2	11.18	2.439	1.439	59
	C_3	10.93	2.500	1.500	60
	C_4	10.62	2.632	1.632	62

A mix of 3.5 g of graminae seeds was applied on the soil surface of each cylinder and the samples were maintained in a greenhouse during the sprouting (3 weeks) and then were placed outside the geotechnical laboratory of University of Salerno, under the rainout shelter devised and constructed for this experimental study, as described in Chapter 5.

After 10 weeks of root growth, the height of soil in each cylinder was measured, so the porosity reduction due to vegetation was computed.

7.3.4 Soil sampling for vegetated soil

After 20 weeks of growth, undisturbed root-soil samples were taken from each of the 20 cm high cylinder trough a rigid sampler of 70 mm diameter and 210 mm in length. First the extra-leaves spreading out from the cylinder were cut in order to guarantee a good contact between the top of the sampler and the soil surface. After that, the sampler was introduced in rooted soil with a low penetration velocity to gently cut the lateral roots and to prevent that the soil would be dragged by lateral roots not yet broken.
From each sampler, extrusion process have been adopted (Fig. 7.3a) and undisturbed root-soil samples with 50 mm diameter and 20 mm high were obtained. During the sampling trough oedometer ring extra roots outing from the sample were cut (Fig. 7.3b) and both top surface and bottom surface have been carefully smoothed (Fig. 7.3c).

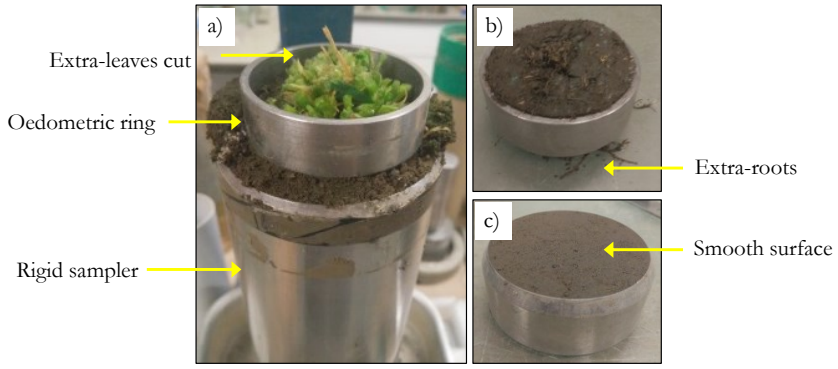

Figure 7.3 Root-soil sampling procedure adopted: a) extrusion process from the sampler with rigid oedometer ring, b) sample with extra-roots and c) sample with smooth surface after cutting of extra-roots.

For each cylinder one sampling has been conducted, from which 4 different root-soil specimens have been taken respectively at 30 mm, 80 mm, 120 mm and 150 mm of depth, except for cylinder C_1 and C_2, in which soil samples at 150 mm of depth were not taken due to a disturb during sampling. After collapse tests, root parameters of each sample have been measured, as discussed in next paragraph.

7.4 EXPERIMENTAL TEST RESULTS

7.4.1 Bare soil

Results of both standard oedometer tests (Fig. 7.4) in unsaturated and saturated samples highlight that the porosity range obtained in reconstituted samples is lower than that of undisturbed samples (Lancellotta et a., 2012). This is essentially related to the difficulty in the laboratory to reproduce very opened structure, similar to those typically found in pyroclastic covers as a consequence of their natural deposition process.

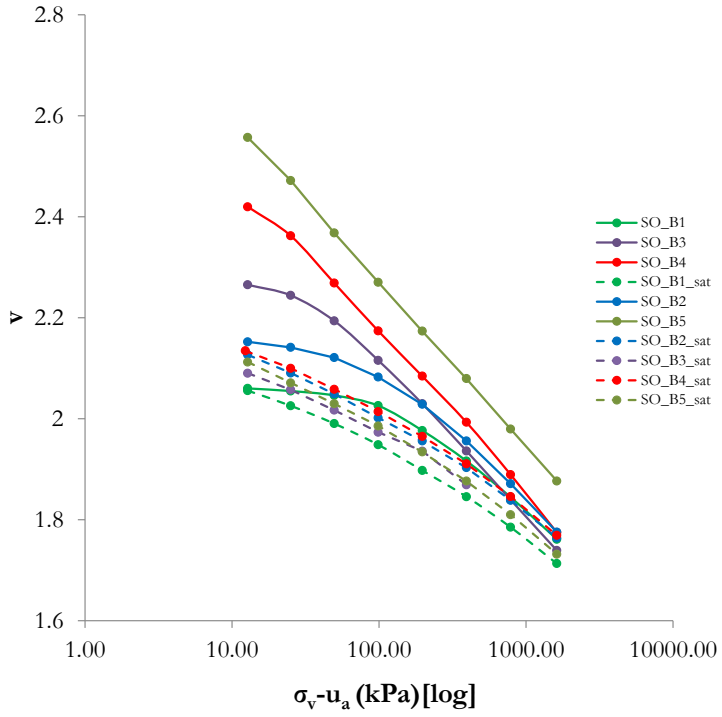

Figure 7.4 Results of standard oedometer test on unsaturated sample with constant gravimetric water content (continues curves) and on saturated sample (dashed curves).

Figure 7.5 shows the magnitude of collapse, calculated for each vertical net stress applied. The potential collapse increases with increasing in

initial porosity and it decreases with increasing in net vertical stress applied. Moreover, the range of collapse varies between a maximum of 0.17, in correspondence of the lowest vertical net stress for the sample with the highest porosity, and a minimum of 0.02, in correspondence of the lowest vertical net stress for the sample with lowest porosity (Figure 7.5).

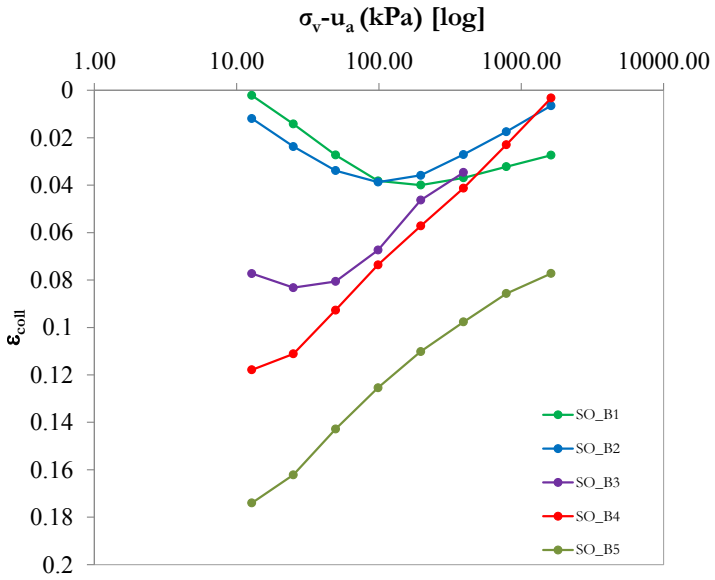

Figure 7.5 Results of double oedometer procedure.

Since pyroclastic soils of class B usually belong to the shallowest layers of pyroclastic deposits (1- 2 m), the effect of initial porosity on soil collapse was investigated in laboratory for a low vertical net stress applied (13 kPa).

Figure 7.6 shows results of oedometer tests in correspondence of the lowest vertical net stress (13 kPa). The initial void ratio and the void ratio after collapse due to wetting are reported, as well as the corresponding magnitude of collapse (ε_{coll}). Initial void ratio corresponds to a collapse equal to 0.

It can be observed that the amplitude of collapse reduces with the reduction of initial void ratio and it become negligible($\varepsilon_{coll} < 0.02$) for void ratio lower than 1.20, corresponding to 54.5% of porosity (SO_B1 test in Figure 7.5) .

This information was used for filling the 2 m high soil columns introduced in previous Chapters, since the study was aimed to investigate on the hydro-mechanical behavior of rooted soil, by not suffering the collapse as consequence of wetting. Hence, the porosity of soil columns was selected as equal to 53.5%, as discussed in Chapter 5, for which Fig. 7.5 highlighted a negligible collapse.

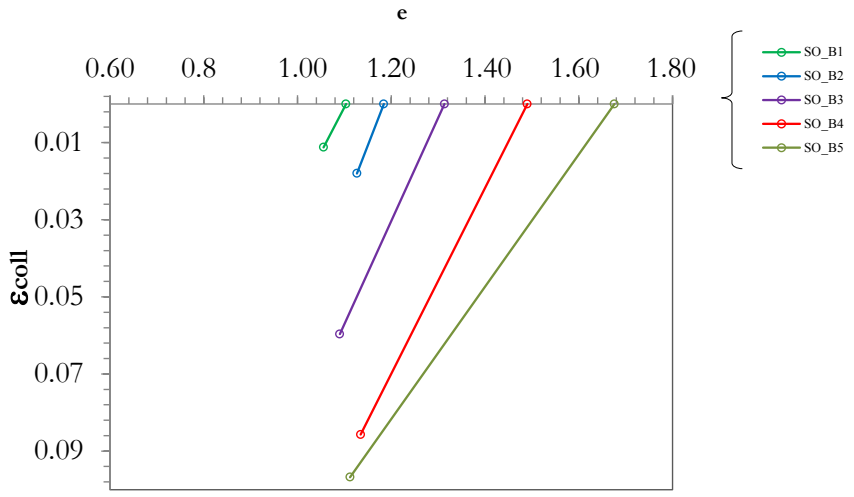

Figure 7.6 Void ratio before and after collapse for 13 kPa of vertical net stress; magnitude of collapse for each oedometer test.

7.4.2 Vegetated soil

The effect of root growth on soil porosity for all cylinders is showed in Figure 7.7, where the porosity (n) computed at three different growth stages is reported: stage 1 corresponding to initial condition, stage 2 after 10 weeks of growing, and stage 3 corresponding to the average void ratio of root-soil samples taken from each cylinder after 20 weeks.

It can be observed that he initial porosity of rooted soil was progressively reduced compared to the initial condition in all cylinders. This might be due to several factors that can be summarized as follows: i) roots occupy pores and enhance soil aggregation, ii) the dense and clustered root network produces exudates and this facilitates a reduction in soil porosity through links between soil particles, iii) sampling disturbs.

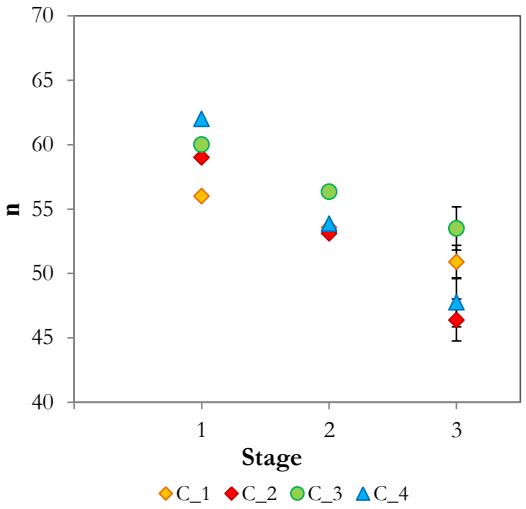

Figure 7.7 porosity at three stages of root growth.

Standard oedometer tests for vegetated samples after 20 weeks of growth taken by four cylinders at different depths have been conducted. The magnitude of collapse for 13 kPa of vertical net stress applied was investigated. The standard oedometer test consisted in first applying the vertical net stress, then the collapse was induced by flooding specimens with distilled water until reaching the saturation.
14 tests were performed and details of the samples are reported in Table 7.3, in which first part of the ID of root-soil sample represents the name of the cylinder from which was taken, V is for "vegetated" and the last numbers correspond to its depth.
At the end of each test root parameters, such as root dry biomass (*RM*) and Root Mass Density (*RMD*), were measured.
The root dry biomass (*RM*) was found to decrease with depth (Fig. 7.8), because root distribution and their biomass in soil tends to decrease going far from the soil surface, where the maximum root biomass is usually found (Leung et al., 2015b). *RM* value ranges from a maximum of 0.6 g at the shallowest layer (30 mm) to a minimum of 0.02 g at the deepest depth (180 mm). Moreover, *RM* value is strictly related to initial soil porosity at the third stage of growth (n_{ini}) and it increases as n_{ini} decreases. Conversely, considering the initial soil porosity at the first stage (n_0) the *RM* increases proportionally with n_0.

Table 7.3Details of root-soil samples for oedometer test.

type	Column #	ID #	γ_d kN/m³	e_{ini} -	n_{ini} (%)	n_{ini} (%)
Vegetated	C_1	C_1_V30	12.28	1.110	52.6	50.9
		C_1_V80	13.09	0.979	49.5	
		C_1_V120	12.83	1.018	50.5	
	C_2	C_2_V30	13.37	0.937	48.4	46.4
		C_2_V80	13.91	0.862	46.3	
		C_2_V120	14.32	0.797	44.4	
	C_3	C_3_V30	11.79	1.169	53.9	53.5
		C_3_V80	12.04	1.145	53.4	
		C_3_V120	12.67	1.042	51.0	
		C_3_V150	11.47	1.257	55.7	
	C_4	C_4_V30	12.58	1.033	50.8	47.7
		C_4_V80	13.55	0.902	47.4	
		C_4_V120	13.79	0.876	46.6	
		C_4_V150	14.03	0.845	45.8	

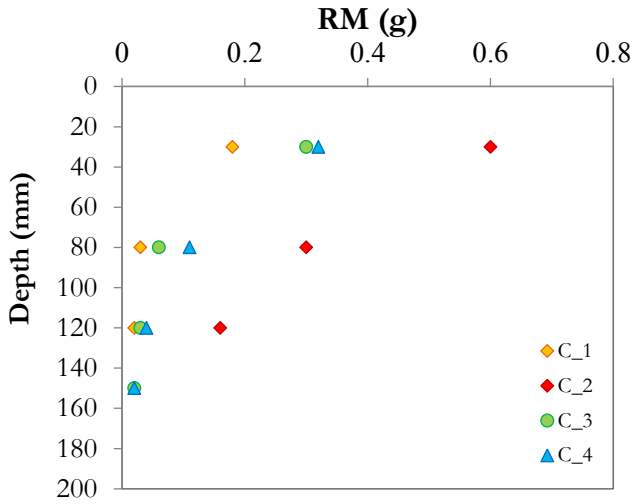

Figure 7.8 Root dry biomass (RM) along depth for each cylinder.

This means that roots are able to grow better within a more porous initial soil structure, and this leads to a reduction of the soil structure during their growth (stage 3 Figure 7.7).
This means that the as the initial soil structure is more porous, the root biomass increases, and consequently the soil structure at the end of root growth is reduced proportionally.
In Figure 7.9 *RMD,* which represents the amount of roots (in percentage) contained in the root-soil sample relative to the soil dry mass (M_s), showed the same trend of RM and decreased with depth.
Thus, *RMD* was also influenced by the initial porosity of soil before root growth (n_0), according with Zhu & Zhang (2016), who found that the higher the compaction of soil the lower was *RMD*. Moreover, *RMD* for grass roots used in bio engineering purposes was found to be typically less than 0.210 % in correspondence of 60 mm far from soil surface (Zhu & Zhang, 2016).
In this study, *RMD* reached values between 0.4% and 1% at shallowest layer (30 mm), consistent with those measured by Zhu & Zhang (2016), considering the different depth of investigation. Furthermore, *RMD* resulted quite nil at deepest depth (180 mm).

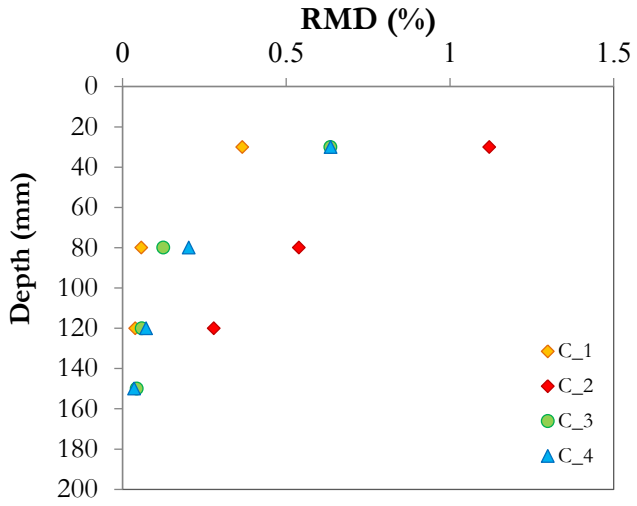

Figure 7.9 Root Mass Density (RMD) along depth for each cylinder.

Starting from void ratio of root-soil samples already reduced due to root growth, the magnitude of collapse was investigated for 13 kPa of vertical net stress applied, and compared with that obtained in bare soils (Fig. 7.10).

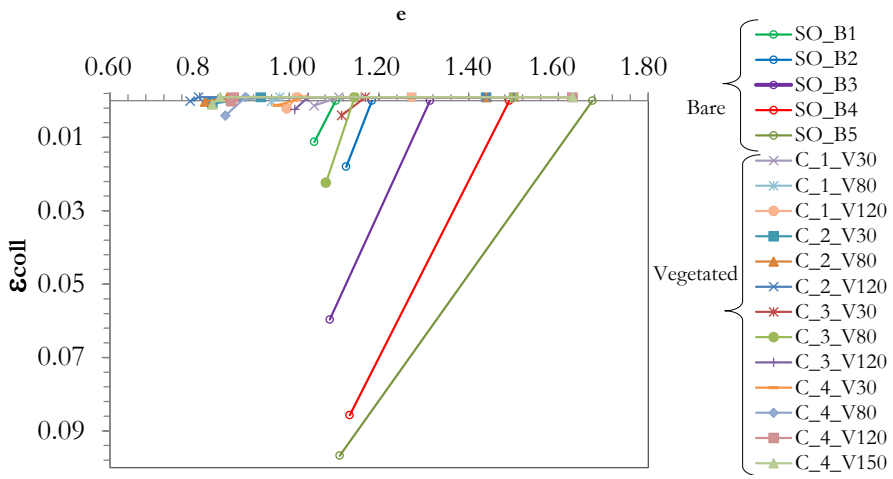

Figure 7.10 Void ratio before and after collapse for 13 kPa of vertical net stress and magnitude of collapse for vegetated samples, compared with bare samples.

The entity of collapse is highly reduced in root-soil samples because of the initial void ratio. In particular, the biggest collapse occurred in sample with 1.081 of initial void ratio, which corresponded to the highest void ratio among all root-soil samples investigated. Anyway, referring to the same initial void ratio of the tested sample, a comparable magnitude of collapse is obtained for both bare and rooted soils. This means that in general roots in high porous structure do not reduce the collapsibility of unsaturated soil, while they can reduce the porosity during their growth.

7.5 CONCLUDING REMARKS

This Chapter studies the collapsibility of reconstituted specimens of pyroclastic soils of class 'B' and the role played by the presence of roots on the behavior of soil matrix undergoing a saturation process.
Since there is a lack of contribution in literature on the effect of roots on the collapsible behavior of unsaturated soils, the results obtained in this

chapter must be considered as first contribution to this challenging topic as it concerns pyroclastic soils.
This topic is a key issue in the analysis of the post-failure stage of rainfall induced landslides that is strictly related to the soil collapsibility. As introduced in Chapter 2, during post-failure stage of unsaturated loose soils, rainfall infiltration originates a significant increase of the pore water pressures with a consequent volume collapse of the soil structure.
Regarding this phenomenon, the obtained results highlight that for bare soils collapse is experimented independently on soil porosity or vertical net stress applied and its magnitude changes according with these two conditions. In particular, the higher initial porosity of the structure, the higher the magnitude of collapse observed due to wetting for each vertical net stress. On the other hand, loads reduce the collapsibility due to wetting.
Under low vertical net stress (13 kPa), the collapse was found to be negligible when the porosity is less than 54 %.
Regarding the effect of roots on collapsibility of soils during post-failure stage under wetting, there is a lack of contributions in literature. Thus, on the basis of the experimental results obtained in this preliminary study, some hypotheses on rooted soil collapsible behavior can currently be formulated. Particularly, it can be argued that roots growing in highly porous pyroclastic soils tend to aggregate the soil particles and thus reduce the porosity of the whole root-soil matrix. In fact, numerous roots can develop in highly porous structure instead of denser soil, because they have more space available to move and grow.
This means that despite the high porosity of pyroclastic soils, the roots can easily grow and enhance soil aggregation. Moreover, roots produce exudates and other chemical products able to create soil aggregates, denser than those observed in bare soils.
However, the experimental results show that roots are only able to reduce the collapsibility of pyroclastic soils but further investigations are required as it concerns the post-failure stage of shallow landslides.

8 THE CONTRIBUTION OF ROOT GRASSES ON SOIL SHEAR STRENGTH

The effect of soil properties (nutrient availability) on root growth and consequently on induced hydraulic properties of root permeated soil was investigated in previous Chapter in the case study of Hong Kong CDG soil.
The effect of long root grasses on hydro-mechanical response of unsaturated pyroclastic soils have been systematically analyzed during the experimental study conducted at the geotechnical laboratory of University of Salerno. The collateral effect of roots on modifying collapsibility behavior of these loose soils was also investigated and discussed in Chapter 7.
As conclusion of this PhD research, this Chapter evaluates the reinforcing effect of roots by comparing the shear resistance of soil with and without roots, in drained and undrained conditions. To this aim several triaxial tests were conducted in no-rooted and rooted pyroclastic soils and results are hereafter discussed.

8.1 INTRODUCTION

Is widely known that the way vegetation affects slope stability is through root reinforcement of soil. Roots in soil create a new soil–root composite system in which root fibers with strong tensile strength but weak compressive strength are embedded in soil. This reinforcement is considered as additional soil strength via root cohesion (Wu et al. 1979, 2013; Nilaweera and Nutalaya 1999; Cazzuffi et al., 2006; Leung et al. 2015a).
Some authors in the past investigated on the role of vegetation roots on slope stability with in situ shear tests performed on soil blocks containing roots and they concluded that shear strengths of rooted-soils were substantially larger than those of soils without roots (Endo and

Tsuruta 1969; Ziemer 1981; Nilaweera 1994). Later, laboratory shear tests and in situ shear tests on root-reinforced soil blocks have been conducted by several researchers (Endo and Tsuruta, 1969; Wu et al., 1988; Tobias, 1995; Wu and Watson, 1998; Operstein and Frydman, 2000), that provided substantial insight into the role of roots in the shear strength of soils. Furthermore, analytical models have also been developed to evaluate soil-root interaction and employed to analyze laboratory and in situ shear tests results (Waldron 1977; Wu et al. 1979; Gray and Ohashi 1983; Wu et al. 1988).

Despite the direct shear test is often adopted for the assessment of shear strength of root-reinforced soils, the limitation of using this method is given by the failure plane assumed. Actually, stress and strain in a sample are not regular and the shear plane assumed may not to be the actual weakest surface. Direct shear tests performed for determining soil-root composite shear strength show that roots provide increase of cohesion, while the internal friction angle is slightly affected by roots (Waldron, 1977). On the other hand, in triaxial tests the failure surface is generated along the weakest surface and also different (drained, undrained, consolidated, unconsolidated) conditions can be simulated to closely reproduce the in situ conditions (Zhang et al., 2010).

In recent years few triaxial tests were conducted on root-soil composite samples, which claimed the positive role of roots on increasing the shear strength of reinforced soil.

However, conflicting results were carried out: in loess soil roots increase shear strength through root cohesion (Zhang et al., 2010), while in moraine soil was observed that the presence of roots increased the internal friction angle due to the increase in soil density (Graf et al., 2009). On the other hand, Hu et al. (2013) conducted triaxial tests on silty soil permeated by roots of shrubs typically used in China for reducing shallow landslides and erosion phenomena, and they found that roots reinforced the soil through both root cohesion and increasing in internal friction angle.

Root-soil composite is usually reproduced in laboratory: few roots of selected plant species (trees or plants) with the same diameter and same length, are placed in a fixed geometry (i.e. horizontal direction, cross direction, vertical direction) in the reconstituted soil sample (Zhang et al., 2010; Hu et al., 2013). These adopted preparation methods can affect results since the root distribution is not well reproduced. Moreover, grass roots contribution on shear strength is still not clear since their

distribution can be hardly reproduced in soil sample, because of their small diameters and the dense bundle provided during growth. Furthermore, grass roots can change the whole soil matrix by creating a dense root network extremely light and indirectly stabilizing soil aggregates via the production of exudates and microbial communities (Jastrow et al. 1998; Eisenhauer et al. 2010). This can reflect in a change of the soil structure in soils with metastable structure, such as pyroclastic soils that, during post-failure stage in undrained conditions, can experience static liquefaction phenomena (Musso and Olivares, 2004; Bilotta et al., 2005; Olivares et al., 2007), this is essentially due to the rise of pore water pressure, which drastically reduces shear resistance by decreasing the effective normal stress (Bishop, 1973).
However, the role of roots on soil composite behavior during post-failure stage is still unclear and their effects on the occurrence of static liquefaction during undrained tests is not yet investigated. Indeed, drained and Undrained triaxial tests on both rooted and bare pyroclastic soils were conducted in order to better understand the influence of grass root network on mechanical behavior of the soil.

8.2 THE EFFECTS OF ROOTS ON SOIL SHEAR RESISTANCE

8.2.1 Failure mechanisms and root cohesion

The failure criteria of a soil-root composite system is expressed by the Mohr Coulomb's law in this way:

$$\tau_f = \sigma \tan\phi + C \tag{8.1}$$

where ϕ is the internal friction angle and C is the cohesion, nevertheless the meanings of internal friction angle and cohesion of a root composite soil are different from those of bare soil. In fact, the composite soil permeated by roots has a reinforced matrix, similar to the concrete reinforced by steel, and thus the stresses produced during loading variation are transferred differently trough the reinforced matrix. In this way the cohesion C of a composite is an integrated cohesion, because is not only the soil cohesion but it takes into account also the cohesion

between soil particles and roots, and the anchorage of roots. In a similar manner, the internal friction angle of a composite can be also defined as its integrated internal friction angle.
Since in the majority of literature roots are considered to provide increase of cohesion to the composite soil, the integrated cohesion is generally accepted as equal to the summary of soil cohesion and root cohesion.
In this way the integrated cohesion *C* is given by:

$$C = C_s + C_r \tag{8.2}$$

where *Cs* is the soil cohesion and *Cr* the root cohesion.
In order to obtain the root additional cohesion, the tensile strength (*Tr*) of the roots involved as well as the 'breaking' mechanisms must be known. Some authors provided 'breaking' predicting models to calculate the reinforcement of roots as additional cohesion for soil shear strength.
The W&W model (Wu, 1976 and Waldron 1977) assumed that the increase in shear strength provided by roots as additional cohesion into Coulomb's law is accepted for the schematic soil root-interaction model showed in Figure 8.1. The failure plane is assumed horizontal and the roots are subjected to tensile stress due to their elongation trough the sliding surface.

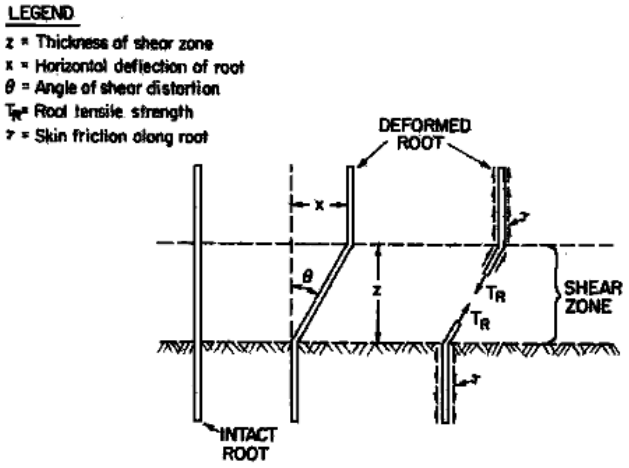

Figure 8.1 Schematic diagram of perpendicular root-fiber reinforcement model (Gray and Ohashi, 1983).

The tensile stress generated in root *Tr* has two components, called *Tn* and *Tt*, acting respectively on the horizontal and the vertical directions.
Tn is given by the following equation:

$$T_n = T_r \cos\theta \tan\phi' \tag{8.3}$$

where θ is the angle between the deformed root and the initial vertical root and ϕ' is the internal friction angle. This normal component increases the confining stress on the failure plane. On the other hand, the tangential component *Tt* is equal to:

$$T_t = T_r \sin\theta \tag{8.4}$$

and it directly acts as shear resistance force.
In this model, the increase in shear resistance provided by the individual root as additional cohesion is equal to:

$$C_r = T_r(\sin\theta + \cos\theta \tan\phi') = T_r k' \tag{8.5}$$

where *k'* depends on the value of θ and ϕ', as discussed in depth in next paragraph. In this model is assumed that all roots break simultaneously and thus the tensile strength of root fibers per unit area of soil (*Tr*) is given by the following equation:

$$T_r = \sum_{n=1}^{N} T_{r,n} \cdot RAR_n \tag{8.6}$$

where the roots are grouped in *N* diameter classes, *Tr,n* is the tensile strength referred to the root class and *RARn* is the root area ratio of the root class.
In this way the root cohesion at each depth of soil can be calculated since both root classes and *RARn* change along depth.
This 'breaking' model is usually used for predicting the soil shear strength of soil permeated by grass roots since the root class diameters for bundle and fasciculate systems are more homogeneous than those of plants or trees. The limitation of this model is the assumption that all

roots break simultaneously and pull out does not occur, as consequence it overestimates the root reinforcement.
The Fiber Bundle Model (FBM) was proposed by Pollen and Simon (2005) and it assumed that all roots have the same elastic properties but they break at different instants depending on the way the load is distributed by the fibers. In this way when the weakest roots broke, the stress can redistribute among the remaining unbroken roots since pull out does not occur. The roots are ordered from the strongest to the weakest and, by calling j the index of the weakest root that is still unbroken upon loading, *RARj* is the *RAR* of the root j and *Tr,j* the tensile strength of that root. The resistance is equal to the product of the number of weakest roots (*j*) and their tensile strength (*Tr,j*).
Schwarz et al (2010b) proposed an extension of the FBM model, called Root Bundle Model (RBM), where a more realistic strain step loading approach is used (Vergani et al., 2014). A displacement is imposed equally in all root composing the bundle and for each displacement increment, the load is distributed among roots as the sum of the stresses in all roots, only if it does not exceed their maximum tensile strength.
Therefore the total force in the bundle (*Ftot*) for Δx displacement is given by the following equation:

$$F_{tot}(\Delta x) = \sum_{i=1}^{N} F_i(\Delta x) \cdot n_i \tag{8.7}$$

where Fi(Δx) is the maximum pull out force allowed in the root belonging to the i-class of diameter, *N* is the number of diameter classes and n_i is the number of roots belonging to i-class of diameter. Later, Schwartz et al. (2013) introduced a statistical approach for RBM, called RBMs, in order to take into account the variability of tensile strength within a root diameter class. For these models proposed, root tensile strength is required in order to compute the shear resistance offered by a bundle in root-soil composite. In the next paragraph a literature review of root tensile test results is provided for different plant species.

8.2.2 Root tensile strength and root characteristics

Root tensile strength is one of key factors recognized to affect mechanical reinforcement of slopes. In particular, it was found that root

tensile strength of single root is affected by root diameter, root species, state of root (living or decaying) (Schmidt et al., 2001; Preti, 2013), as well as rate of displacement of test (Cofie & Koolen, 2001), season of the year, and environmental conditions. Indeed, laboratory results show a great variability among different species and for the same species. The root diameter affects mechanical properties of individual root in terms of tensile strength, in particular it was found that this latter decreases via a power relationship as root diameter increases. Several contributions are available in literature regarding tensile strength of roots for different plant species and root diameters (Nilaweera and Nutalaya, 1999; Operstein and Frydman, 2000; Abernethy and Rutherfurd, 2001; Gray and Barker, 2004; Pollen et al., 2004; Bischetti et al., 2005; Mattia et al., 2005; Tosi, 2007; De Beats et al., 2008; Cecconi et al., 2012).
The vegetation species investigated were classified in three main types: tree species, most of them belonging to conifer species and deciduous species (Genet et al., 2005; Bischetti et al., 2005; Nilaweera et al., 1999), plant species (Mattia et al., 2005) and grass species, consisting on perennial graminae and leguminose (Loades et al., 2010; Cecconi et al., 2012; Zhong et al., 2016). All results have been summarized in the same graph (Fig. 8.2) where tensile strength of single root (*Tr*) is related to the root diameter (*D*). According to Gray and Sotir (1996) a non-linear relationship between *Tr* and root diameter was observed in all the vegetation species studied, in particular *Tr* decreases significantly with increasing root diameter following a power law equation:

$$T_r = \alpha D^{\beta} \tag{8.8}$$

where α and β are empirical constants depending on species, in particular α can be considered as a scale factor and β as the rate of strength decrease.
The typical root diameters of grass species are smaller than those of plant species and tree species, in fact they can vary between 0.1 and 3 mm (Fig. 8.2), with an average value of 1.5 mm.
The tensile strength of some variants of perennial graminae grass species used in this research activity (Prati Armati technology), was carried out from Cecconi et al. (2012) and the range of *Tr* equations where they are included is showed in red region of Figure 8.2.

It can be observed that for small diameters of 0.1 mm, *Tr* can vary in a wide range between 500 MPa and 50 MPa for all vegetation species, whereas in general, for grass species *Tr* are smaller than those observed for both tree and plant species. This means that small roots strength behavior is quite similar for all species, but for higher diameters, grass roots are less resistant than other species roots to tensile stresses.

The dependency of stress-strain relationship on diameter of single root is also influenced by root moisture content and cellulose content (Genet et al., 2005; Wang et al., 2006; Yang et al., 2016).

Genet et al. (2005) concluded that the percentage of cellulose content increases linearly with a decrease in root diameter, consequently tensile strength and cellulose quantity are significantly correlated, in particular the higher cellulose content the higher tensile strength was observed. Yang et al. (2016) investigated the effect of root moisture content on stress-strain curve of single root of different tree species, and concluded that the roots with higher moisture content showed an elastoplastic behavior with higher deformations, differently from dry roots, which showed an elastic behavior with weak elasticity. The maximum rooting depth is another factor influencing root reinforcement function in slopes, because root length exerts considerable influence on the amount of displacement needed to engage its maximum tensile strength. The length of roots is often restricted by bedrock layers, soil porosity and structure, nutrients availability, as discussed in previous sections and by climatic conditions (Tobin et al., 2007). Some authors found that that root length is linearly correlated with root diameter (Waldron and Dakessian, 1981; Wu et al., 1988). Moreover, the spatial distribution of roots influences the intensity of soil reinforcement by roots, in particular the most efficient branching pattern is generated when many roots are spread deep into the soil (Stokes et al. 1996; Fan et al. 2010).

In conclusion, the effects of roots reinforcing soil are closely related to root number, root diameter, root shape (architecture), root tensile strength, and root-soil interaction (Wu et al. 1979; Stokes et al. 1996; Dupuy et al. 2007; Mickovski et al. 2007; Reubens et al. 2007).

However, studies showed that structure-related root factors such as root mass density (RMD), root length density (RLD), root area index (RAI), number of roots, maximum root depth and branching pattern are likely to exert a greater impact upon hillslope stability than factors such as root tensile strength (Reubens et al. 2007; Genet et al. 2005; Fattet et al. 2011; Mao et al. 2012; PollenBankhead et al. 2009).

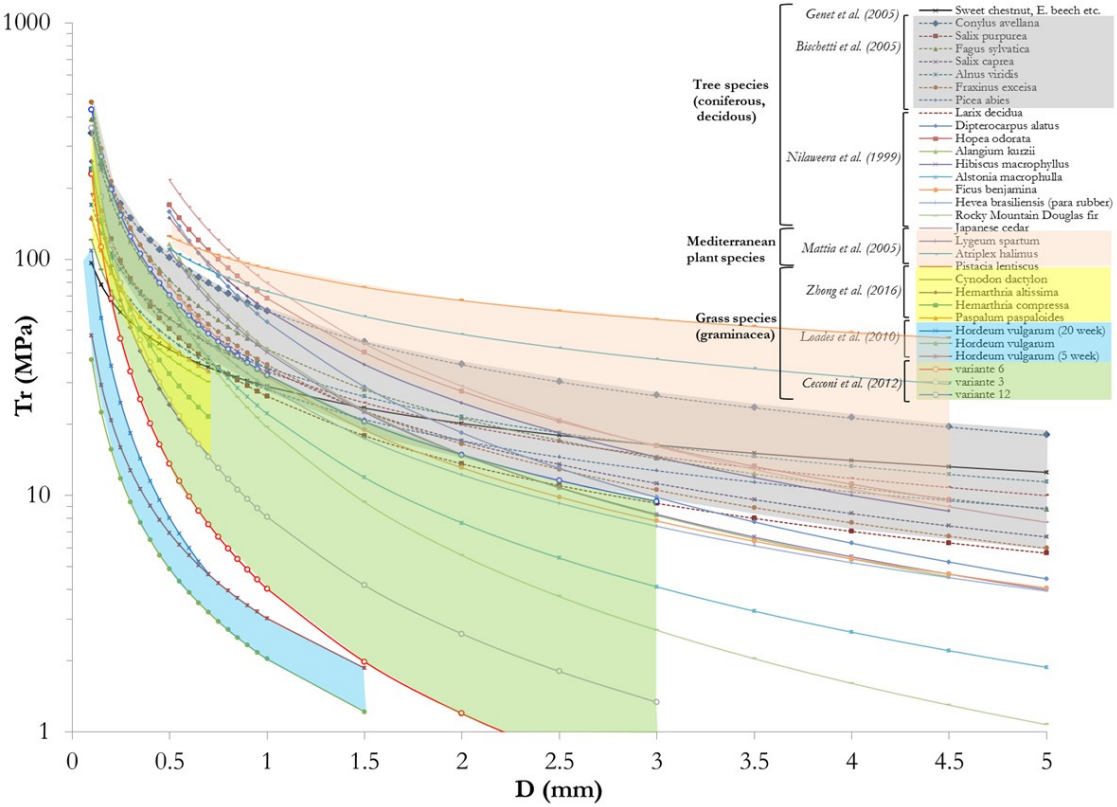

Figure 8.2 Experimental results of tensile strength tests on different plant species: tree roots, Mediterranean and grass species

8.3 MATERIAL AND METHODS

8.3.1 Soil type and sampling procedure

Soil type investigated in this work has been already introduced in previous Chapters, because it belongs to pyroclastic soils used for the filling of the 1D soil column in Chapter 5, and for the study of the effects of root grasses on hydro-mechanical response of root-soil composite (Chapter 6). In fact, undisturbed rooted soils were sampled from the 1D vegetated column (V) at different depths as described in Chapter 5.

Undisturbed root-soil samples were taken from the 20 cm high cylinder trough a rigid plastic sampler of 36.4 mm diameter and 210 mm in length. The sampling procedure was the same adopted in Chapter 7, except for the dimension of the sampler used. In this case, there were no extra-leaves, thus the sampler was directly introduced in rooted soil. Furthermore the penetration velocity was low to gently cut the lateral roots and to prevent that the soil would be dragged by lateral roots not yet broken. From each sampler 2 undisturbed soil samples were extruded of 79.3 mm height and 36.4 mm diameter each. In total, 6 undisturbed root-soil samples were obtained for each 20 cm height cylinder.

8.3.2 Triaxial apparatus and test programme

Isotropic consolidated drained and undrained compression triaxial tests (ASTM D 4767-95, 2000) were conducted at geotechnical laboratory of University of Salerno.

At an initial confining pressure of 12kPa, the specimen was subjected to filtration (from toe vs head of specimen) using de-aired water under a back-pressure of 7kPa until a clear water flow was observed through the upper boundary (no entrapped air bubble). Then the saturation degree was improved by simultaneously increasing confining water pressure and back pressure up to a target value of 205 kPa and 200 kPa respectively (Bishop and Henkel, 1957). Finally, a B-Test was performed and the

specimen was assumed fully saturated if the B –value was checked to be greater than 0.98.
For each group of 6 root-soil samples, 3 consolidated drained and 3 consolidated undrained triaxial tests were conducted with confining pressure of 10, 30 and 50 kPa. For comparison purposes, both drained and undrained triaxial tests on reconstituted bare soil were performed at the same consolidation pressures (10, 30 and 50 kPa) used in triaxial tests of root-soil samples, as discussed in next paragraph. 24 hours was sufficient time to complete the consolidation stage.
After consolidation, the shear stage was conducted in strain-controlled conditions with a rate of 0.06 mm/min. During shear, axial stress, height and volume/pore water pressure variations were recorded.
The list of triaxial tests on both rooted (Vegetated) and no-rooted (Bare) soil samples is reported in Table 8.1. The ID of each sample is composed of 8 characters where: first two letters (TX: triaxial test) describe the type of test, third letter correspond to the soil condition (U: undisturbed; R: reconstituted), fourth and fifth letter are the abbreviation of the type of soil investigated (PB: pyroclastic soil belongs to class 'B' for Bilotta et al., 2005), then the letter which describes if the soil is vegetated or not (B: bare soil; V: vegetated soil) and latter two characters (letter or number) which represent the number of sample. In particular, for root-soil samples, the second last character is a letter and represents the modulus of the soil column from which was taken the sample (i.e.: A). _Examples of bare soil sample and root-soil sample ID are respectively TXRPBB01 and TXUPBVA1.
In order to check the comparability of soil sample subjected to triaxial tests, the initial bulk density (γ_d) of both bare and rooted soil was calculated. A value of 11.9±0.03 kN/m^3 was obtained for bare specimens while a value of 12.1±0.41 kN/m^3 was obtained for vegetated soil. It can be observed that the value of initial γ_d for vegetated soil varied within a higher range than bare soil, likely due to the presence of different volume of roots within the rooted specimens.

Table 8.1 Details of the triaxial compression tests (TX).

type		ID	test	v_0	γ_d	p'*cons*	v *cons*	γ_d *cons*
		#	-	-	kN/m^3	kPa	-	kN/m^3
Bare	B_D	TXRPBB05	D	2.170	11.9	8	2.001	12.9
		TXRPBB10	D	2.171	11.9	31	1.905	13.6
		TXRPBB11	D	2.172	11.9	51	1.949	13.3
	B_U	TXRPBB08	U	2.162	12.0	10	2.104	12.3
		TXRPBB13	U	2.170	11.9	31	2.015	12.9
		TXRPBB12	U	2.175	11.9	51	1.946	13.3
Vegetated	VA_U	TXUPBVA1	U	2.111	12.3	51	2.058	12.6
		TXUPBVA2	U	2.104	12.3	31	2.066	12.5
		TXUPBVA3	U	2.129	12.2	11	2.124	12.2
	VA_D	TXUPBVA4	D	2.070	12.5	50	2.030	12.8
		TXUPBVA5	D	2.088	12.4	31	2.056	12.6
	VB_U	TXUPBVB1	U	2.015	12.9	51	1.978	13.1
		TXUPBVB2	U	2.057	12.6	31	2.011	12.9
		TXUPBVB3	U	2.134	12.1	11	2.130	12.2
	VB_D	TXUPBVB4	D	2.085	12.4	51	2.024	12.8
		TXUPBVB5	D	2.065	12.5	10	2.069	12.5
		TXUPBVB6	D	2.226	11.6	31	2.186	11.8
	VC_U	TXUPBVC1	U	2.276	11.4	51	2.180	11.9
		TXUPBVC2	U	2.130	12.2	30	2.081	12.4
		TXUPBVC3	U	2.257	11.5	10	2.248	11.5
	VC_D	TXUPBVC4	D	2.113	12.3	51	2.039	12.7
		TXUPBVC5	D	2.283	11.3	32	2.250	11.5
		TXUPBVC6	D	2.182	11.9	11	2.197	11.8
	VD_U	TXUPBVD1	U	2.196	11.8	50	2.140	12.1
		TXUPBVD2	U	2.052	12.6	31	2.012	12.9
		TXUPBVD3	U	2.192	11.8	10	2.188	11.8
	VD_D	TXUPBVD4	D	2.093	12.4	51	1.996	13.0
		TXUPBVD5	D	2.188	11.8	12	2.181	11.9
		TXUPBVD6	D	2.098	12.3	31	2.051	12.6

Bulk density after consolidation process (γ_d*cons*) was also calculated and it was observed to be higher in bare specimens compared to vegetated specimes. In fact, in bare soil γ_d*cons* was 13.2±0.48 kN/m^3, compared to

12.4±0.47 kN/m^3 in vegetated soil. This means that during both filtration and consolidation stages of the performed tests, roots maintained almost unchanged the bulk density of vegetated soils by contrasting the volumetric deformation of the entire root-soil system.

8.4 TRIAXIAL TEST RESULTS

8.4.1 Measurements of root parameters

In order to find a correlation between mechanical parameters of integrated root-soil and root characteristics, after each compression triaxial test, root dry biomass was measured in accordance with the method proposed by Liang et al. (1989). Each sample was weighed and oven-dried at 60° C for 24 h. After that, different sieves with decreasing diameter of the network were used to retain any roots contained in soil specimen. Furthermore, a tweezer was used to remove roots from soil retained at each sieve. Finally, the root dry biomass (*RM*) was weighed.
In addition, Root Mass Density (*RMD*) and Root Volume Density (*RVD*) were calculated (Zhu & Zhang, 2016). Root Mass Density is a dimensionless index describing the ratio between the root dry biomass (*RM*) and the dry mass of the root-permeated soil sample (M_s). Since the dry roots contained in each sample was very small, this index is expressed in percentage, so:

$$RMD(\%) = \frac{RM}{M_s} \times 100 \tag{8.9}$$

On the other hand, RVD is the ratio between the total volume occupied by roots (V_r) and the total volume of root-permeated soil sample (V). The same choice on considering *RMD* as percentage has been done also for *RVD* index, so:

$$RVD(\%) = \frac{V_r}{V} \times 100 \tag{8.10}$$

The root volume was calculated as the ratio between the root dry biomass *RM* and the root density (γ_r). The procedure adopted for

measuring the root density was the following: i) 100 g of dry roots have been mixed to distilled water, ii) the mixture was boiled to remove the air and the measurement was done after cooling. In this way, without forcing the saturation of possible internal voids of roots the root density (γ_r) was equal to 6,18 kN/m^3, consistent with that provided by Gray and Sotir (1996). Values of *RM*, *RMD* and *RVD* for each root-soil sample taken from different soil depths from vegetated column are summarized in Table 8.2.

Table 8.1 Root parameters measured for each root-soil sample of triaxial tests.

column zone	ID	z (from the bottom)	RM	RMD	RVD
	#	m	g	(%)	(%)
A	TXUPBVA2	0.25	0.07	0.063 ± 0.005	0.125 ± 0.005
	TXUPBVA3		0.06		
	TXUPBVA1	0.35	0.09	0.067 ± 0.021	0.135 ± 0.021
	TXUPBVA4		0.08		
	TXUPBVA5		0.04		
B	TXUPBVB2	0.75	0.07	0.062 ± 0.008	0.122 ± 0.008
	TXUPBVB3		0.07		
	TXUPBVB6		0.05		
	TXUPBVB1	0.85	0.12	0.088 ± 0.023	0.180 ± 0.023
	TXUPBVB4		0.1		
	TXUPBVB5		0.06		
C	TXUPBVC2	1.35	0.09	0.115 ± 0.021	0.225 ± 0.040
	TXUPBVC4		0.12		
	TXUPBVC6		0.14		
	TXUPBVC1	1.45	0.06	0.09 ± 0.026	0.167 ± 0.026
	TXUPBVC3		0.08		
	TXUPBVC5		0.12		
D	TXUPBVD2	1.55	0.13	0.121 ± 0.020	0.244 ± 0.020
	TXUPBVD4		0.1		
	TXUPBVD6		0.15		
	TXUPBVD1	1.65	0.1	0.137 ± 0.020	0.263 ± 0.020
	TXUPBVD3		0.15		
	TXUPBVD5		0.16		

The root dry biomass *RM,* as expected after results obtained in previous Chapter, was found to decrease with depth (Fig. 8.3)

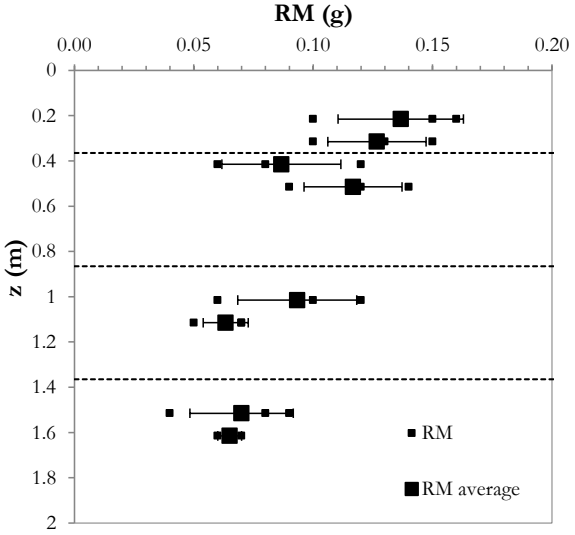

Figure 8.3 *RM* with depth of root-soil samples (small black squares) and *RM* average for those at the same depth (big black squares). The dashed black lines correspond to the interfaces between two different column zones.

The *RM*s measured were always quite small for all root-soil samples, and lower than those measured in root-soil samples taken from cylinders used in Chapter 7 for the investigation of collapsibility because the investigation depth was lower. Indeed, the maximum *RM* measured was equal to 0.16 g, from the sample placed on the upper part of the column investigated in triaxial tests (zone D, z= 1.65 m from the bottom), in correspondence of about 300 mm from the soil surface.
In general, low values of *RM* always found for these grass species can be attributed to the fine and fibrous root system of grass roots in nature (Metcalfe & Nelson, 1985), which thus results very light. In this study *RMD* trend decreased with depth (Fig. 8.4), in accordance with *RM* measurements, and the maximum value observed was equal to 0.137%, consistent with *RMD* measures obtained in previous Chapter.

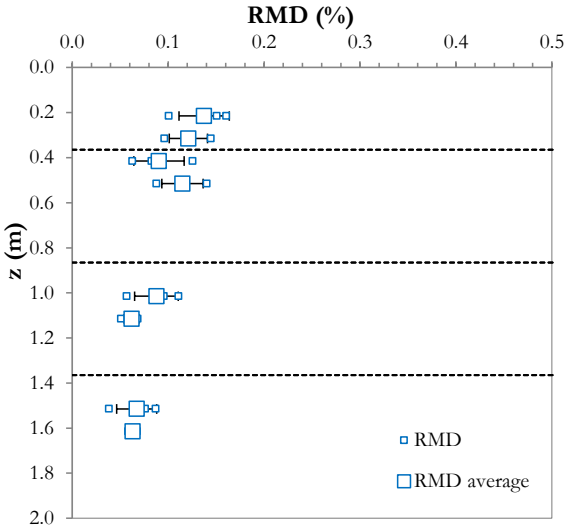

Figure 8.4 *RMD* with depth of root-soil samples (small blue squares) and *RMD* average for those at the same depth (big blue squares).

The *RVD* represents the percentage of root-soil volume occupied by roots and it can be considered as a 'root-porosity'. It showed the same trend of *RMD*, and its maximum value was recorded to be equal to 0.263% at shallowest depth (Fig. 8.5).

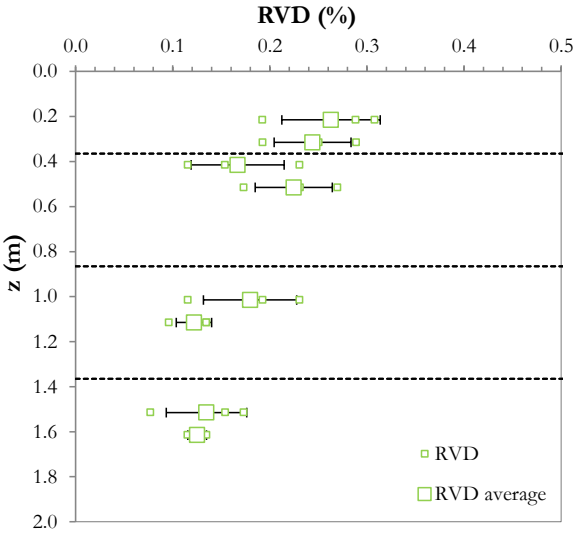

Figure 8.5 *RVD* with depth of root-soil samples (small green squares) and *RVD* average for those at the same depth (big green squares).

The *R\D* values recorded in this study were not in accordance with those found by Zu & Zhang (2016) and this might be from the different way to measure the root volume. In fact Zu & Zhang (2016) measured indirectly the volume of wet roots as the volume of the displaced water during separation process of roots from soil mass, without measuring the root density (γ_r).

8.4.2 Test results

In order to understand the effect of roots on increasing shear strength of composite soil, the saturated shear envelopes were drawn by a linear regression of (q-p') points at critical state. Five different envelopes have been carried out, one for bare soil and the rest for root-soil samples taken from different depths of the vegetated column (Fig. 8.6). It was observed that critical state envelope of bare soil is lower than those carried out from tests of vegetated soils.
This is because both intercept of the enveloping equation (a) and the stress ratio (M), which are related to cohesion and internal friction angle, resulted smaller than those of vegetated soils. In fact, a and M are also expressed as function of cohesion (C) and internal friction angle (ϕ') by the following general equations in triaxial conditions:

$$a = \frac{6 \cdot C \cdot \cos(\phi')}{3 - \sin(\phi')} \; ; \; M = \frac{6 \cdot \sin(\phi')}{3 - \sin(\phi')} \tag{8.11}$$

Vegetated soils showed a trend to increase their shear resistance moving from zone A to zone D of the vegetated column. This might be due to the denser network of roots observed in shallower depths compared to deeper layers.
From the linear regression (q-p') in bare soil the deviatoric stress at the critical state qf_{bare} can be obtained for each p'. Similarly, for each vegetated layer the qf_{rooted} corresponds to the deviatoric stress at the critical state related to a specific p' considered.
As consequence, the qf_{rooted}/qf_{bare} ratio corresponds to the ratio between the deviatoric stress at critical state for vegetated soil and that of bare soil for the same mean effective stress p'.
This ratio expresses the percentage of deviatoric stress at critical state increased due to the presence of roots in soil.

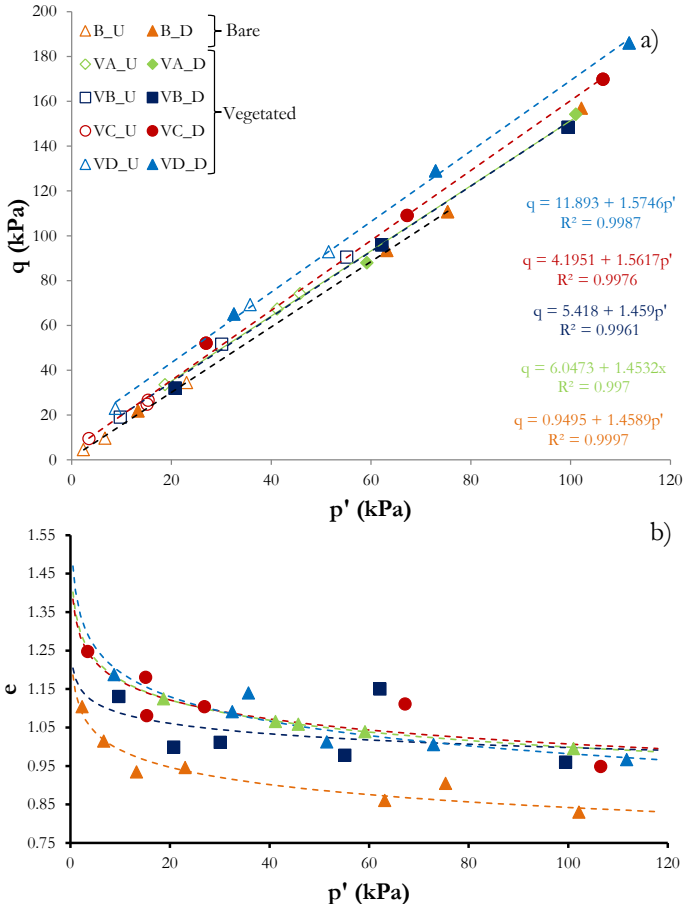

Figure 8.6 a) (q-p') points at critical state and envelopes (dashed lines) of consolidated triaxial tests undrained and drained for bare (B_U, B_D) samples and vegetated samples taken from zone A (VA_U,VA_D), zone B (VB_U, VB_D), zone C (VC_U, VC_D) and zone D (VD_U, VD_D); b) (e-p') points and critical state line of triaxial tests

The ratio qf_{rooted}/qf_{bare} equal to the unity corresponds to the condition in which the presence of roots does not change the shear strength of root-soil composite, since the deviatoric stress at the critical state is coincident with that would be showed from bare soil.
The qf_{rooted}/qf_{bare} ratio has been computed within the domain of *p'* ranging from 10 kPa to 100 kPa for the four different vegetated parts of the column abovementioned, respectively *VA*, *VB*, *VC* and *VD*.

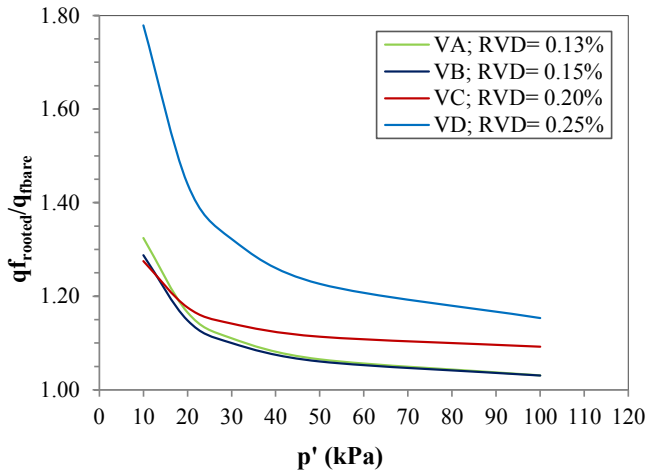

Figure 8.7 qf_{rooted}/qf_{bare} ratio vs mean effective stress p' for vegetated soils.

In Figure 8.7 qf_{rooted}/qf_{bare} ratio vs mean effective stress p' are reported. It can be observed that qf_{rooted}/qf_{bare} decreases as *p'* increases, and its magnitude depends on the volume of roots within the soil (*RVD* in Fig. 8.7).

As example, the qf_{rooted}/qf_{bare} ratio for *p'* equal to 10 kPa varies from a minimum of 1.32 (*VA)* up to a maximum of 1.78 (*VD),* while it varies from 1.03 (*VA)* to 1.15 for (*VD)* when *p'* is equal to 100 kPa.

The role of roots in enhanching the soil shear strength is interpreted as the amount of extra deviatoric stress sustained by the soil-root composite at the critical state for a specific mean effective stress *p'*.

As consequence, for qf_{rooted}/qf_{bare} equal to 1.32, the presence of roots increased the deviatoric stress at the critical state of 32% compared to that observed in bare soil.

Mechanical parameters obtained from triaxial tests are summarized in Table 8.3. From each group of triaxial tests have been determined the cohesion *C* and the internal friction angle ϕ' by inverting the equations (8.11).

For bare soil, *C* and ϕ' are properly the soil cohesion (*Cs*) and the internal friction angle of soil particles, thus *C* results to *Cs* .

On the other hand, for vegetated soil, as discussed in previous paragraph, both internal friction angle and cohesion of a root-soil composite are more properly defined as integrated parameters, because they are referred not only to the solid skeleton but to the entire root-soil

matrix. Integrated cohesion (*C*) takes into account both soil cohesion and the so called root cohesion (*Cr*). As consequence, the root cohesion for vegetated soils was obtained as the difference between the integrated cohesion (*C*) and the soil cohesion *Cs*.

Table 8.2 Soil cohesion (Cs), integrated cohesion (C) and internal friction angle of bare and vegetated soils obtained from isotropic consolidated triaxial tests drained and undrained. Root cohesion (Cr) obtained as difference between C and Cs.

type	***ID***	*Cs* kPa	*C* kPa	*Cr* kPa	*ϕ'* (°)
Bare	B	0.47	0.47	0	35.93
Vegetated	VA		3.00	2.53	35.80
	VB		2.69	2.22	35.93
	VC		2.12	1.65	38.29
	VD		6.03	5.55	38.58

It can be observed that the increasing in cohesion by roots varied from a minimum of 1.65 kPa up to a maximum of 5.55 kPa. In particular the maximum root cohesion was observed in vegetated soil taken from zone D, which corresponds to the upper part of the soil column. In this zone root biomass was high as well as the volume occupied by roots in soil sample (Figs 8.3, 8.5). On the other hand, internal friction angle did not change in vegetated soils belonging to deepest zones (VA, VB), while it increased almost 3° in shallowest zones (VC,VD).
A diffused volumetric failure, for all the tested specimens, was observed without any formation of a well-defined shear plane.

8.4.3 Consolidated drained test results

Drained test results after consolidation with 30 kPa of confining pressure on both bare soil and vegetated soils are showed in Figure 8.8. In particular, 5 drained triaxial tests are compared, and test condition of each sample before the application of deviatoric stress are summarized in Table 8.4. Differences in terms of specific volume after consolidation have been observed (v_{cons}) in all tests. However, some consideration can be done by the comparison of bare soil with vegetated soils. Both bare soil and vegetated soils showed a contractive behavior, provided by an increasing volumetric deformation during the application of deviatoric

stress (Fig. 8.8c). However, the critical state was different between bare soil and vegetated soils. Bare soil reached the critical state for a deviatoric stress q= 90 kPa while vegetated soils, except for TXUPBVA5 (green in Fig. 8.8), showed a positive hardening constitutive behavior and the deviatoric stress at critical state resulted up to 40 kPa higher than that observed in bare soil (Fig. 8.8b). In conclusion in drained conditions roots enhanced the shear resistance of composite soil-root system.

Table 8.3 Test condition of drained triaxial tests at 30 kPa.

type	ID	test	p'cons	v cons
	#	-	kPa	-
Bare	TXRPBB10	D	31	1.905
Vegetated	TXUPBVA5	D	31	2.056
	TXUPBVB6	D	31	2.186
	TXUPBVC6	D	32	2.250
	TXUPBVD6	D	31	2.012

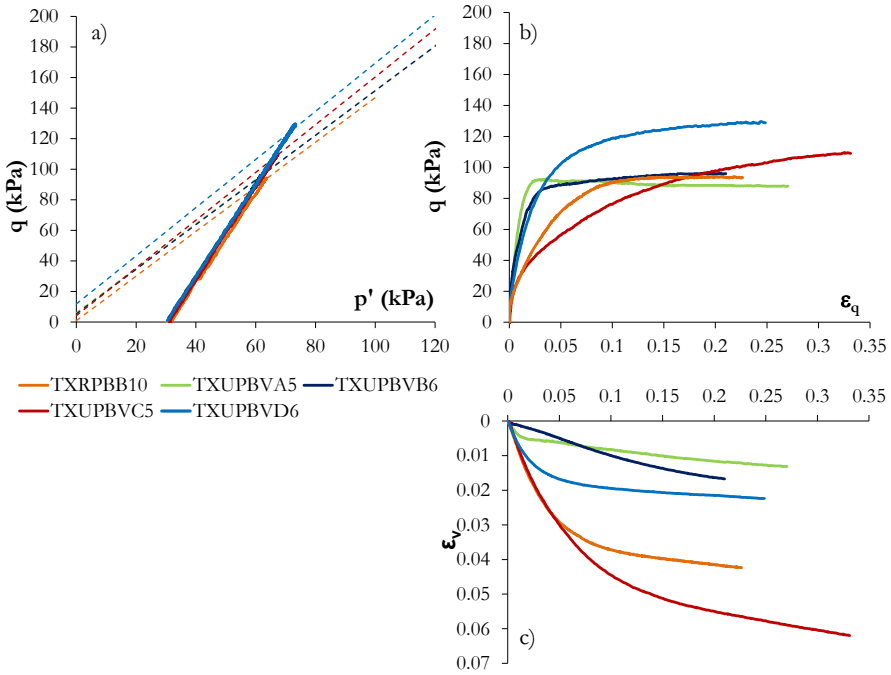

Figure 8.8 a) Stress-path, b) constitutive behavior and c) deformations on bare soil (orange) and vegetated soils at 30 kPa of confining pressure.

8.4.4 Consolidated undrained test results

For a fair comparison, undrained test results after consolidation under about 30 kPa of confining pressure, on both bare soil and vegetated soils, are showed in Figure 8.9. In particular, 5 undrained triaxial tests are compared, and test condition of each sample before the application of deviatoric stress are summarized in Table 8.5.
However small differences in terms of specific volume after consolidation (v_{cons}) were observed in all 5 tests. For a fair comparison, triaxial tests on bare soil were compared with triaxial test conducted on the vegetated sample with the v_{cons} closer to that of bare soil, which resulted the TXUPBVD2.
The bare soil (orange in Fig. 8.9) showed a contractive tendency with mean effective stress (p') decreasing along the stress path (Fig. 8.9a) thus showing a continuous increase of pore water pressure during the entire undrained shear stage (Fig. 8.9c).

Table 8.4 Test condition of undrained triaxial tests at 30 kPa.

type	ID	test	p'cons	v cons
	#	-	kPa	-
Bare	TXRPBB13	U	31	2.015
Vegetated	TXUPBVA2	U	31	2.066
	TXUPBVB2	U	31	2.011
	TXUPBVC2	U	30	2.081
	TXUPBVD2	U	31	2.012

On the other hand, in vegetated soil (blue in Fig. 8.9) p' increased with increasing in deviatoric stress (q) (Fig. 8.9a) by showing a dilatant tendency of the root-soil composite, which was reflected in a lower increasing of pore water pressure as long as the critical state was approached (Fig 8.9c). This trend can be also observed in its positive hardening constitutive behavior (Fig. 8.9b).
Furthermore, similar trend was observed for TXUPBVA2 test, nevertheless its constitutive behavior was not positive hardening.
Though remaining vegetated soil did not show the same dilatant tendency of TXUPBVD2, they all reach the critical state with a continuous increase of the mean effective stress p', except for

TXUPBVC2, which shows a behavior similar to bare soil specimen (Fig. 8.9a).

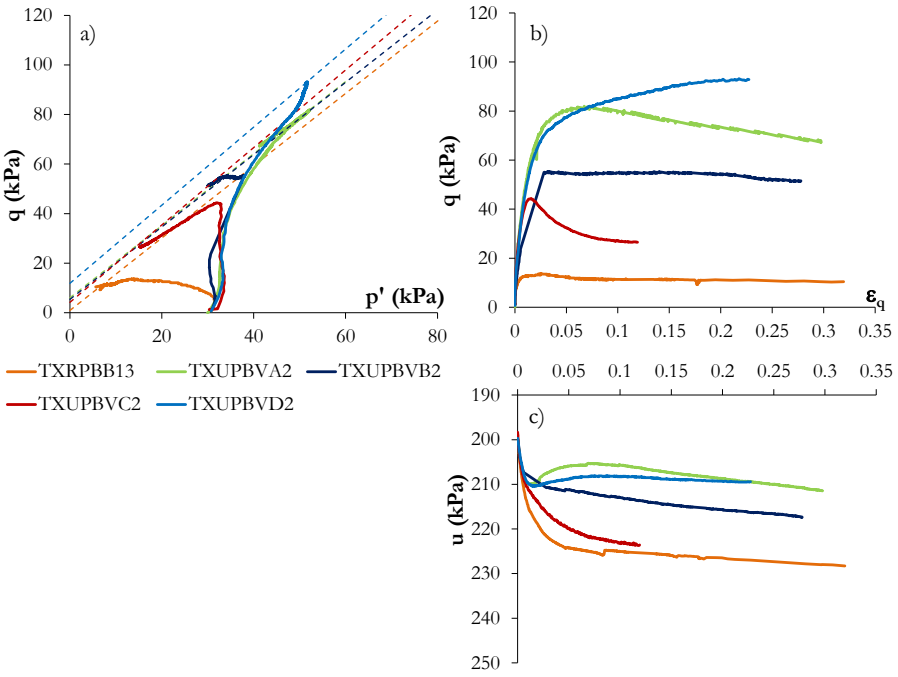

Figure 8.9 a) Stress-path, b) constitutive behavior and c) Pore Water Pressure of undrained triaxial tests on bare soil (orange) and vegetated soils at 30 kPa of confining pressure.

However, pore water pressure increment recorded during all the tests performed on vegetated soils have been lower than those recorded in bare soil (Fig. 8.9c).

The presence of roots in pyroclastic soil seems to create a composite system with a structure different from that usually observed in bare pyroclastic soils.

In fact, with the same specific volume, rooted specimens showed a modified behavior compared to that showed by bare specimens probably caused by the very light root network created within the porous spaces, which might behaves as a bonding between particles and thus make soil and/or soil-root aggregates.

It has been already discussed in previous Chapters that soil aggregates are maintained by exudates directly produced by roots. As consequence

the behavior showed in these tests can disappear with root decaying and this aspect would be investigated in future works.

8.4.5 Mechanical parameters and root parameters

Figure 8.10 shows the variation of mechanical parameters such as integrated cohesion *C* and friction angle ϕ' with Root Volume Density (*RVD*) variation.
As expected, starting by *RVD*=0, which corresponds to bare soil, both *C* and ϕ' increase with *RVD* increasing, without following a clear correlation law. However, it was observed that for *RVD* < 0.2% both *C* and ϕ' showed a slight increasing in their values, while for *RVD* >0.2% the increasing trend changed.

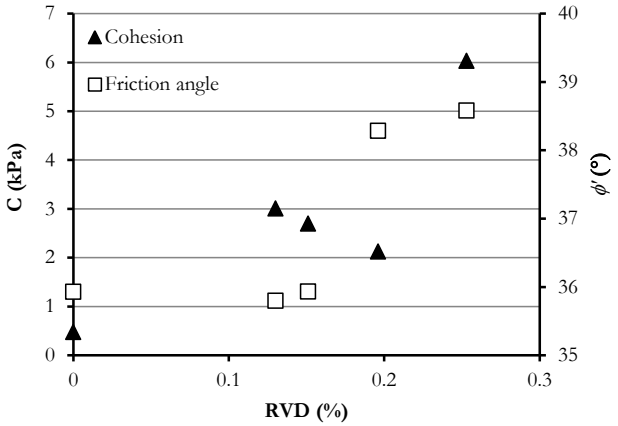

Figure 8.10 Cohesion C (black triangles) and friction angle □' (white squares) of pyroclastic soils at different RVD (%).

In conclusion, drained shear strength (τ) increases positively with *RVD* and its variation at 3 different confining pressures (10, 30, 50 kPa) is showed in Figure 8.11.

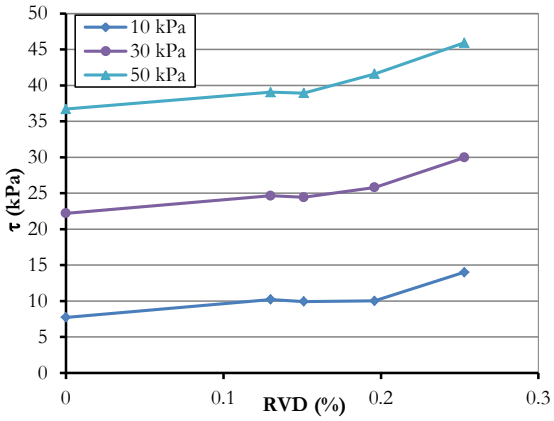

Figure 8.11 Shear strength variation with RVD of root-soil composite at confining pressures of 10, 30 and 50 kPa.

8.5 W&W MODELING OF ROOT COHESION

8.5.1 Root cohesion evaluation

In this study a comparison between the experimental root cohesion and its predicted values by W&W breaking model has been discussed.
Among different breaking models, W&W model, which assumes that all roots during shearing break simultaneously, was selected. The root cohesion was computed by applying the equation (8.5), as the product of the tensile strength of root fibers per unit area of soil (Tr) and an experimental parameter (k') which takes into account the decomposition of root tensile strength according to the bending angle of roots with respect to the shear plane. This empirical parameter is function of the internal friction angle of soil (ϕ') and the inclination of roots (θ) on the shear soil surface. It ranges around 1-1.3 but usually is assumed equal to 1 (Thomas and Pollen-Bankhead, 2010).
Tensile strength of root fibers Tr is given by equation (8.6) hereafter reported:

$$T_r = \sum_{n=1}^{N} T_{r,n} \cdot RAR_n \tag{8.6}$$

where, as previously introduced, the roots are grouped in N diameter classes, Tr,n is the tensile strength referred to the root class and $RARn$ is the root area ratio of the root class.
In this study the total RAR, independently on root class diameters, was measured along depth of the vegetated soil column, as explained in depth in Chapter 5. At each depth RAR was computed by applying the fitting equation carried out from experimental measurements. The fitting curve was the following:

$$RAR(\%) = e^{-\left(\frac{z}{c} + f\right)} \tag{8.11}$$

where c and f are respectively equal to 0.45 and 1.5.
Since RAR was computed independently on root diameter class, the evaluation of the tensile strength of root fibers was obtained by assuming the presence of only one root diameter class. In total three different evaluations of root cohesion have been conducted, considering a root diameter class respectively of 0.5 mm, 1 mm and 1.5 mm, based on their frequency in measurements of root diameters carried out in this experimental study, as discussed in Chapter 5.

8.5.2 Comparison between model results and experimental results

The tensile strength Tr,n referred to each root diameter class selected was easily calculated by applying the power law equation (8.8), where the empirical constants of the species used in this study are respectively α=21.146 and β=-1.266 (Tab. 8.6).
The tensile strength of the entire root fiber Tr was calculated considering RAR computed by equation (8.11) along depth. Then root cohesion along depth (Fig. 8.12) was obtained as product of Tr and k', in this study assumed to be equal to 1 (Thomas and Pollen-Bankhead, 2010).
As expected, the increment of cohesion due to the tensile strength of roots decreases with depth because of the reduction of RAR. On the other hand, at the same depth it increases with decreasing of root class diameter.

Table 8.5 Root diameter class selected and their relative tensile strength.

Root diameter class	D	*Tr,n*
	mm	MPa
1	0.5	50.9
2	1.0	21.1
3	1.5	12.7

Root cohesion obtained from triaxial tests on root-soil samples is also reported along depth. Experimental results are lower than those obtained by W&W model. Moreover, this difference in root cohesion is highlighted at shallowest depths, where the experimental value of Cr resulted equal to 6 kPa, compared to 16 kPa, 27 kPa and 65 kPa computed by the model for each class (respectively class 3, class 2 and class 1).

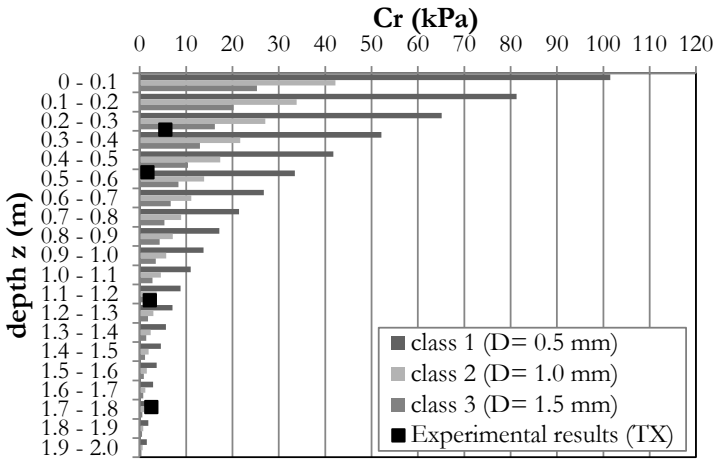

Figure 8.12 Root cohesion along depth computed with W&W model for three root diameter classes, and experimental values obtained by triaxial tests.

It can be clamed that the W&W model overestimates the increment in cohesion provided by roots for triaxial consolidated tests. This is due to the different failure mechanisms occurring in triaxial tests, where no share surface is generated but a volumetric failure occurs.
Moreover, the W&W model assumes that contribution of roots on cohesion is provided by their tensile strength offered simultaneously during their breaking. This means that roots in triaxial conditions do not

break simultaneously and thus their contribution on shear strength is less than that given by considering their simultaneous breaking. Hence, probably during volumetric failure some roots have been involved in breaking at different instants or some other have been involved in pull out mechanisms.

8.5.3 Discussion

The aim of this study was to apply the W&W model in prediction of root cohesion expressed during volumetric failure as that observed in consolidated triaxial tests in both drained and undrained conditions.
Evaluated root cohesion by W&W model was compared with experimental results in order to quantify the effectiveness of the model on failure occurring in triaxial conditions.
Results shows that the W&W model overestimates root cohesion in triaxial conditions even if it showed the same trend in decreasing root cohesion along depth as that observed in experimental results. During volumetric failure in triaxial tests it can be argued that not all roots experiment the breakage simultaneously, since a not well defined share surface is created and some roots can experiment the pull out.
Despite W&W model is particularly indicated for fasciculate grass roots with similar diameter classes, the Fiber Bundle Model (FBM), which takes into account that roots break in different instants depending on the load and the elastic properties of each root, can be more appropriate for the evaluation of root cohesion in triaxial tests.
Moreover, during failure in triaxial conditions, pull-out mechanisms can be experimented by some roots and their contribution in enhancing shear resistance depends on their pull-out resistance.

8.6 CONCLUDING REMARKS

In this Chapter the effect of roots on the behavior of pyroclastic soils under shearing was investigated through a comparison with mechanical behavior of bare soil. The mechanical parameters (C, ϕ) of both bare soil and vegetated soils were obtained from isotropic consolidated triaxial tests in drained and undrained conditions.

In drained condition, highly rooted soils (high *RVD*) show a reduction of volumetric deformation, which is reflected on the shear strength parameters of vegetated soils. In particular, both *C* and ϕ' increase as the percentage of root volume within the soil increases. In undrained condition, experimental results show that pore water pressure increment is reduced during shearing. Thus the mean effective stress does not decrease with increasing of deviatoric stress, so liquefaction can not occur. Moreover, this effect is enhanced by the root biomass, in particular when *RVD* increases, the pore water pressure increment during shearing is reduced.

Finally, W&W model results were compared with experimental results in order to verify the possibility to use the model in predicting root cohesion in pyroclastic soils during triaxial consolidated drained tests. The W&W model overestimates the root cohesion measured in this study and the reasons can be imputed to several factors in triaxial condition: not simultaneous breaking of roots, different failure mechanisms, root pull-out mechanisms. Despite W&W model is the most appropriated for fasciculate grass roots, in this experimentaly study it resulted not appropriated for predicting the root cohesion in triaxial conditions. In fact, in experimental results it was observed an increasing of both *C* and ϕ' parameters during shearing, while the model W&W only contemplates the increasing in cohesion due to the presence of roots.

This study claims that the presence of roots in pyroclastic soils (widely known as loose soils) during post-failure stage in undrained conditions can strongly reduce the probability of occurrence of static liquefaction, by changing the rheology of root-soil composite material.

These innovative results confirm the important role played by roots on changing the metastable structure of pyroclastic soils that do not experience the liquefaction in undrained conditions because of the dense network of fine roots.

In order to enhance the knowledge obtained in this experimental work, further works can concern the investigation on the effect of root growth on *RVD* and thus on soil shear strength, by conducting an experimental test on root growth during the years. In this way, the effects of aging and decaying on roots and thus on mechanical characteristics of root permeated soil can be clarified.

Further works could regard the quantification of root cohesion by conducing direct shear tests and by comparing experimental results in drained conditions with W&W model results and triaxial test results.
Moreover, pull-out tests on grass roots could be useful for predicting the pull-out resistance experimented during failure.

9 CONCLUSIONS

The experimental investigation on the effect of roots on hydro-mechanical behavior of unsaturated pyroclastic soils points out a preliminary conclusion on the effectiveness of using vegetation as natural-based solution for stabilizing slopes in Campania region.

Firstly, the effect of nutrients in soil on plant growth and thus on the hydro-mechanical response of soil was investigated. Experimental results showed that additional nitrogen rich NPK water soluble fertilizer supply during irrigation of vegetated soil could stimulate plant growth which increases plant induced soil suction that can increase shear strength, reduce permeability effectively during rainfall and reduce the probability of failure of bio-engineered treed slopes.
This means that initial soil properties can strongly affect the efficiency of plants on hydro-mechanical reinforcement, and this factor should be taken into account when a bio-engineering practice is chosen for stabilizing slopes.
These results encouraged to investigate on the effect of vegetation on pyroclastic soils, which are widely recognized as fertile soils rich in nutrients.

Then, the effectiveness of the vegetation on pyroclastic soils was studied firstly by monitoring the stress state variables of unsaturated soils (suction) together with volumetric water content of soil permeated by roots in order to quantify the role of roots in changing hydro-mechanical response of soil during evapotranspiration (drying) and infiltration (wetting).
As concluded in Chapter 6, in both drying and wetting conditions, the effect of roots is highlighted in shallowest layers, up to 1.2 m depth.
During drying, the presence of roots enhances the soil suction increment in both wet and dry season and this increment increases with the elongation of the duration of drying. Starting from these considerations, it is possible to predict that seasonal suction trend, as introduced in

Chapter 2, may change in presence of vegetation covering pyroclastic soils of Campania Region.
During wetting, the presence of roots leads to a delay in infiltration process for small duration events and this effect tends to disappear with the increase of rainfall duration. On the other hand, this effect is enhanced when the soil suction before the event is high and is reflected as a delay of water infiltration at deeper depths.
In conclusion, the presence of roots in unsaturated pyroclastic soils change its hydraulic response to drying and wetting cycles, by changing its structure and, as consequence, by changing the water flow in soil.

The results on the study of the collapse behavior of unsaturated reconstituted pyroclastic soils highlight that for bare soils collapse is experimented independently on soil porosity or vertical net stress applied and its magnitude changes according with these two conditions. In particular, the higher initial porosity of the structure, the higher the magnitude of collapse observed due to wetting for each vertical net stress. On the other hand, loads reduce the collapsibility due to wetting.
Under low vertical net stress (13 kPa), the collapse was found to be negligible when the porosity is less than 54 %.
It can be preliminarily argued, as discussed in Chapter 7, that roots growing in highly porous pyroclastic soils tend to aggregate the soil particles and thus reduce the porosity of the whole root-soil matrix. In fact, numerous roots can develop in highly porous structure instead of denser soil, because they have more space available to move and grow.
This means that despite the high porosity of pyroclastic soils, the roots can easily grow and enhance soil aggregation. Moreover, roots produce exudates and other chemical products able to create soil aggregates, which concur to make the soil structure more stable under wetting.
In conclusion, the magnitude of collapse due to wetting, for low vertical net stress, is reduced.

Finally, the effect of roots on the behavior of pyroclastic soils under shearing was investigated in the last Chapter. In general, the presence of roots change the mechanical parameters of root soil composite, in both drained and undrained conditions. In particular, in drained conditions, the volumetric deformations are reduced and both C and ϕ increase as the percentage of root volume within the soil increases.

Standing on the results obtained in consolidated undrained triaxial tests it can be claimed that the presence of roots in pyroclastic soils (widely known as loose soils) during post-failure stage in undrained conditions can strongly reduce the probability of occurrence of static liquefaction, by changing the rheology of root-soil composite material. The pore water pressure increment is reduced during shearing as the biomass in soil increases, and thus liquefaction can not occur.
Finally W&W model results have been compared with experimental results in order to verify the possibility to use the model for the prediction of root cohesion in pyroclastic soils during triaxial consolidated drained tests. The W&W model overestimates the root cohesion and the reasons can be imputed to several factors: not simultaneous breaking of roots, different failure mechanisms, root pull-out mechanisms.
In conclusion, despite W&W model is the most appropriated for fasciculate grass roots, in this experimentaly study it resulted not appropriated for predicting the root cohesion in triaxial conditions.

Further works on the hydro-mechanical characterization of pyroclastic soils permeated by graminae species could regard the laboratory investigation of SWRC of vegetated soil samples, through volume extractor or suction controlled oedometer tests. These properties can then be used for modeling seepage problems to the aim of knowing the ground water regime behavior in presence of roots.

As it concerns the investigation on the collapsibility of rooted soils, further collapse tests in suction controlled oedometer apparatus can improve the knowledge gained in this study.

Finally, as it concerns the role of roots on soil shear resistance, an experimental test on root growth during the years could be started in order to investigate the effects of aging and decaying of roots on mechanical characteristics of rooted soils.
Direct shear tests can provide mechanical parameters in drained tests to compare with W&W model results and triaxial test results.
Moreover, pull-out tests on grass roots could be useful for predicting the pull-out resistance experimented during failure.

Starting from these further developments, it will be possible to point out a complete characterization of a new composite material made of 4 phases (air, pore water, soil skeleton and living roots), which can represent a natural-based solution for slope stabilization in pyroclastic covers This means that, after several centuries, a new sustainable practice, integrated to passive control works, can be considered as natural-based solution for contrasting the triggering of shallow flow-like landslides.

REFERENCES

Abernethy, B., & Rutherfurd, I. D. (2001). The distribution and strength of riparian tree roots in relation to riverbank reinforcement. *Hydrological processes*, 15(1), 63-79.

Albaladejo Montoro, J., Alvarez Rogel, J., Querejeta, J., Diaz, E., & Castillo, V. (2000). Three hydro-seeding revegetation techniques for soil erosion control on anthropic steep slopes. *Land degradation and development*, 11(4), 315-325.

Allen, R. G., Pereira, L. S., Raes, D. & Smith, M. (1998). Crop evapotranspiration: guidelines for computing crop water requirements. *Food and Agriculture Organization's Irrigation and Drainage* paper no. 56. Rome, Italy: Food and Agriculture Organization.

Alonso, E., Gens, A., Lloret, A., & Delahaye, C. (1995). Effect of rain infiltration on the stability of slopes. In *Proceedings of the first International Conference on unsaturated Soils*/ Unsat'95/Paris/France/6-8 September 1995. Volume 1

Ambrozic T., Fairbank H., Grelle G., Guadagno F.M., Houghton J., Leroi E., Logar J., Marsden P., Revellino P., Turk G. (2009). "Guidelines on relevant criteria to assess vulnerability and risk". FRANE Future Risk Assessment as a New European approach to landslide hazards. Guidelines & Relevant Reports. Guadagno F.M., Revellino P. (eds.), European Commission, Directorate General Environment, Directorate A – Governance, Communications and Civil Protection, Unit A5 – Civil Protection.

Anderson, S. A., & Sitar, N. (1995). Analysis of rainfall-induced debris flows. *Journal of Geotechnical Engineering*, 121(7), 544-552.

Arredondo, J. T., & Johnson, D. A. (1999). Root architecture and biomass allocation of three range grasses in response to nonuniform supply of nutrients and shoot defoliation. *The New Phytologist* 143(2), 373-385.

Arrieta, C., Busey, P. & Daroub, S. H. (2009). Goose grass and Bermuda grass competition under compaction. *Agronomy Journal* 101, No. 1, 11–16.

Arrighi, S., Principe, C., & Rosi, M. (2001). Violent strombolian and subplinian eruptions at Vesuvius during post-1631 activity. *Bulletin of Volcanology*, 63(2), 126-150.

ASTM Committee D-18 on Soil and Rock. (2011). *Standard Practice for Classification of Soils for Engineering Purposes* (unified Soil Classification System). ASTM International.

ASTM, D4767-95, (2000): *Standard test methods for consolidated undrained triaxial compression tests for cohesive soils*, Ann. b. ASTM standards, sect. four: constr., Volume 04.08: 882–891.

Belfiore, G., & Urciuoli, G. (2004). Analisi del contributo meccanico delle radici alla resistenza del terreno (Interpretation of the root mechanical contribution to the soil shear strength). In *Proceedings of the Annual Meeting of the Geotechnical Researchers* 2004.

Beverage, J. P., & Culbertson, J. K. (1964). Hyperconcentrations of suspended sediment. *Journal of the Hydraulics Division*, 90(6), 117-128.

Bilotta, E., Cascini, L., Foresta, V., & Sorbinow, G. (2005). Geotechnical characterisation of pyroclastic soils involved in huge flowslides. *Geotechnical and Geological Engineering*, 23(4), 365-402.

Bilotta, E., Foresta, V., & Migliaro, G. (2006). Suction controlled laboratory tests on undisturbed pyroclastic soil: stiffnesses and volumetric deformations. In *Unsaturated Soils 2006* (pp. 849-860).

Bilotta, E., Foresta, V., & Migliaro, G. (2008, June). The influence of suction on stiffness, viscosity and collapse of some volcanic ashy soils. In *1st European Conference on Unsaturated Soils, Durham, England* (Vol. 1, pp. 349-354).

Bischetti, G. B., Chiaradia, E. A., Simonato, T., Speziali, B., Vitali, B., Vullo, P., & Zocco, A. (2005). Root strength and root area ratio of forest species in Lombardy (Northern Italy). *Plant and soil*, 278(1), 11-22.

Bishop, A. W. (1973). The influence of an undrained change in stress on the pore pressure in porous media of low compressibility. *Geotechnique*, 23(3).

Bishop, A. W., & Henkel, D. J. (1957). *The measurement of soil properties in the triaxial test*. Edward Arnold (Publishers) Ltd; London.

Bo, M. W., Fabius, M., Arulrajah, A., & Horpibulsuk, S. (2015). *Environmentally friendly slope stabilization using a soil nail and root system in Canada. Ground Improvement Case Histories: Chemical, Electrokinetic, Thermal and Bioengineering Methods*. Edited by Indraratna, B., Chu, J., and Rujikiatkamjorn, C. Butterworth-Heinemann, 629-654.

Boldrin, D., Leung, A. K., & Bengough, A. G. (2017). Correlating hydrologic reinforcement of vegetated soil with plant traits during establishment of woody perennials. *Plant and Soil*, 1-15.

Bonfanti, F., & Bischetti, G. (2001). *Resistenza a trazione delle radici e modello di interazione terreno-radici*. Istituto di Idraulica Agraria, Milano–Rapporto interno.

Borja, R. I., & White, J. A. (2010). Continuum deformation and stability analyses of a steep hillside slope under rainfall infiltration. *Acta Geotechnica*, 5(1), 1-14.

Brady, N. C., & Weil, R. R. (2002). *Soil phosphorus and potassium*. The Nature and Properties of Soils (13th Ed.). Upper Saddle River, NJ: Prentice-Hall, Inc.

Briaud, J. L., Chen, H. C., Govindasamy, A. V., & Storesund, R. (2008). Levee erosion by overtopping in New Orleans during the Katrina Hurricane. *Journal of Geotechnical and Geoenvironmental Engineering*, 134(5), 618-632.

Buczko, U., Bens, O., & Hüttl, R. F. (2007). Changes in soil water repellency in a pine–beech forest transformation chronosequence: influence of antecedent rainfall and air temperatures. *Ecological Engineering*, 31(3), 154-164.

Budetta, P., Calcaterra, D., CoRNIELLO, A., De Riso, R., Ducci, D., & Santo, A. (1993). Appunti di Geologia dell'Appennino meridionale. *Ist. Geol. Appl*, 332, 1-39.

Bull, W. B. (1964). *Alluvial fans and near-surface subsidence in western Fresno County, California* (Vol. 437). US Government Printing Office.

Calcaterra, D., De Riso, R., Evangelista, A., Nicotera, M. V., Santo, A., & Scotto di Santolo, A. (2003, May). Slope instabilities in the pyroclastic

deposits of the Phlegraean district and the carbonate Apennine (Campania, Italy). *In Proc. Intern. Workshop on Occurrence and Mechanisms of Flows in Natural Slopes and Earthfills*, Sorrento, Italy (pp. 61-75).

Campbell, K. A., & Hawkins, C. D. (2003). Paper birch and lodgepole pine root reinforcement in coarse-, medium-, and fine-textured soils. *Canadian journal of forest research*, 33(8), 1580-1586.

Capobianco, V., Cascini, L., Cuomo, S., Foresta, V., (2017). Sperimentazione sulla risposta idraulica di terreni piroclastici radicati con graminacee. Atti *Incontro Annuale dei Ricercatori di Geotecnica IARG 2017*, Matera 5-7 Luglio (Italy).

Capra, L., Lugo-Hubp, J., & Borselli, L. (2003). Mass movements in tropical volcanic terrains: the case of Teziutlán (México). *Engineering Geology*, 69(3), 359-379.

Cascini, L. (2006). *La gestione scientifica dell'emergenza idrogeologica del maggio 1998 nella Regione Campania*. Rubbettino Editore srl.

Cascini, L. (2004). The flowslides of May 1998 in the Campania region, Italy: the scientific emergency management. *Ital Geotech J*, 2, 11-44.

Cascini, L., Cuomo, S., & Guida, D. (2008a). Typical source areas of May 1998 flow-like mass movements in the Campania region, Southern Italy. *Engineering Geology*, 96(3), 107-125.

Cascini, L., Cuomo, S., & Sorbino, G. (2005). Flow-like mass movements in pyroclastic soils: remarks on the modelling of triggering mechanisms. *Italian Geotechnical Journal*, 4, 11-31.

Cascini, L., Ferlisi, S., & Vitolo, E. (2008b). Individual and societal risk owing to landslides in the Campania region (southern Italy). *Georisk*, 2(3), 125-140.

Cascini, L., & Sorbino, G. (2002). Soil suction measurement over large areas: a case study. *In Proc. 3rd International Conference on Unsaturated Soils,* Recife (Brasil), Balkema (Vol. 2, pp. 829-834).

Cascini, L., & Sorbino, G. (2003, May). The contribution of soil suction measurements to the analysis of flowslide triggering. In *Workshop "Flows* (pp. 77-86).

Cascini, L., Sorbino, G., Cuomo, S., & Ferlisi, S. (2014). Seasonal effects of rainfall on the shallow pyroclastic deposits of the Campania region (southern Italy). *Landslides*, 11(5), 779-792.

Cazzuffi, D., Corneo, A., & Crippa, E. (2006). Slope stabilisation by perennial "gramineae" in southern Italy: plant growth and temporal performance. *Geotechnical and Geological Engineering*, 24(3), 429-447.

Cecconi, M., Pane, V., Napoli, P., & Cattoni, E. (2012). Deep roots planting for surface slope protection. *Electronic Journal of Geotechnical Engineering* U, 17, 2809-2820.

Cecconi, M., Pane, V., Napoli, P., & Zarotti, C. (2013, July). Mechanical and hydraulic effects of deep roots planting on slope stability. In TC 215 CPEG 2013 *Symposium, Coupled Phenomena in Environmental Geotechnics*, Torino, Italy(pp. 1-3).

Cechin, I. & Fumis, T. (2004). Effect of nitrogen supply on growth and photosynthesis of sunflower plants grown in the greenhouse. *Plant Science* 166, 1379-1385.

Chu, J., Leroueil, S., & Leong, W. K. (2003). Unstable behaviour of sand and its implication for slope instability. *Canadian Geotechnical Journal*, 40(5), 873-885.

Cibelli, M. P. (2014) *Le opere idrauliche di origine borbonica del Somma–Vesuvio: antiche funzioni ed esigenze conservative*. Academia.edu (In Italian)

Cioni, R., Civetta, L., Marianelli, P., Metrich, N., Santacroce, R., & Sbrana, A. (1995). Compositional layering and syn-eruptive mixing of a periodically refilled shallow magma chamber: the AD 79 Plinian eruption of Vesuvius. *Journal of Petrology*, 36(3), 739-776.

Cioni, R., Santacroce, R., & Sbrana, A. (1999). Pyroclastic deposits as a guide for reconstructing the multi-stage evolution of the Somma-Vesuvius Caldera. *Bulletin of Volcanology*, 61(4), 207-222.

Cioni, R., Levi, S., & Sulpizio, R. (2000). Apulian Bronze Age pottery as a long-distance indicator of the Avellino Pumice eruption (Vesuvius, Italy). *Geological Society, London, Special Publications*, 171(1), 159-177.

Cioni, R., Bertagnini, A., Santacroce, R., & Andronico, D. (2008). Explosive activity and eruption scenarios at Somma-Vesuvius (Italy): towards a new classification scheme. *Journal of Volcanology and Geothermal Research*, 178(3), 331-346.

Cofie, P., & Koolen, A. J. (2001). Test speed and other factors affecting the measurements of tree root properties used in soil reinforcement models. *Soil and Tillage Research*, 63(1), 51-56.

Cole, P. D., Guest, J. E., & Duncan, A. M. (1993). The emplacement of intermediate volume ignimbrites: a case study from Roccamonfina Volcano, Southern Italy. *Bulletin of Volcanology*, 55(7), 467-480.

Coleman JD. 1962. Correspondence: stress/strain relations for partly saturated soils. *Geotechnique* 12(4): 348–350.

Comegna, L., Damiano, E., Greco, R., Guida, A., Olivares, L., & Picarelli, L. (2013). Effects of the vegetation on the hydrological behavior of a loose pyroclastic deposit. Procedia Environmental Sciences, 19, 922-931.

Comegna, L., Damiano, E., Greco, R., Guida, A., Olivares, L., & Picarelli, L. (2016). Field hydrological monitoring of a sloping shallow pyroclastic deposit. *Canadian Geotechnical Journal*, 53(7), 1125-1137.

Committee on Methodologies for Predicting Mudflow Areas (1982). *Selecting a Methodology for Delineating Mudslides Hazard Areas for the National Flood Insurance Program*. Nat. Res. Counc., Nat. Acad. Press, Washington, D.C.

Coppin, N. J., & Richards, I. G. (1990). *Use of Vegetation in Civil Engineering Butterworths London*. UK Google Scholar.

Costa, J. E. (1988). Rheologic, geomorphic, and sedimentologic differentiation of water floods, hyperconcentrated flows, and debris flows. *Flood Geomorphology. John Wiley & Sons New York*. 1988. p 113-122. 5 fig, 2 tab, 54 ref.

Coussot, P., & Meunier, M. (1996). Recognition, classification and mechanical description of debris flows. *Earth-Science Reviews*, 40(3), 209-227.

Crosta, G. B., & Dal Negro, P. (2003). Observations and modelling of soil slip-debris flow initiation processes in pyroclastic deposits: the Sarno 1998 event. *Natural Hazards and Earth System Science*, 3(1/2), 53-69.

Chu, J., Leroueil, S., and Leong, W. K. (2003). Unstable behaviour of sand and its implications for slope instability. *Can. Geotech.* J., 40, 873–885.

Cronin, S. J., Lecointre, J. A., Palmer, A. S., & Neall, V. E. (2000). Transformation, internal stratification, and depositional processes within a channelised, multipeaked lahar flow. *New Zealand Journal of Geology and Geophysics*, 43(1), 117-128.

Cruden D.M., Varnes D.J. (1996). Landslide types and processes. In *Turner A.K.and Schuster R.L. eds., Landslides Investigation and Mitigation, Transportation Research Board, US National Research Council, Special Report* 247, Washington, DC pp. 36-75.

Dahlgren, R. A., Saigusa, M., & Ugolini, F. C. (2004). The nature, properties and management of volcanic soils. *Advances in Agronomy*, 82, 113-182.

Dai, F., Lee, C. F., Wang, S., & Feng, Y. (1999). Stress–strain behaviour of a loosely compacted volcanic-derived soil and its significance to rainfall-induced fill slope failures. *Engineering Geology*, 53(3), 359-370.

Damiano, E. (2004). Meccanismi di innesco di colate di fango in terreni piroclastici.

Damiano, E., Olivares, L., & Picarelli, L. (2012). Steep-slope monitoring in unsaturated pyroclastic soils. *Engineering Geology*, 137, 1-12.

Das, G. K., Hazra, B., Garg, A., & Ng, C. W. W. (2018). Stochastic hydro-mechanical stability of vegetated slopes: An integrated copula based framework. Catena, 160, 124-133.

Day, R. W. (1993). Surficial slope failure: a case study. *Journal of performance of constructed facilities*, 7(4), 264-269.

De Baets, S., Poesen, J., Reubens, B., Wemans, K., De Baerdemaeker, J., & Muys, B. (2008). Root tensile strength and root distribution of typical Mediterranean plant species and their contribution to soil shear strength. *Plant and soil*, 305(1-2), 207-226.

De Chiara, G. (2014). Quantifying the risk to life posed by hyperconcetrated flows. *PhD Thesis, University of Salerno, Italy*.

Dellino, P., Isaia, R., & Orsi, G. (2001). Statistical analysis of textural data from complex pyroclastic sequences: implications for fragmentation processes of the Agnano-Monte Spina Tephra (4.1 áka), Phlegraean Fields, southern Italy. *Bulletin of Volcanology*, 63(7), 443-461.

Dellino, P., Isaia, R., La Volpe, L., & Orsi, G. (2004). Interaction between particles transported by fallout and surge in the deposits of the Agnano–Monte Spina eruption (Campi Flegrei, Southern Italy). *Journal of Volcanology and Geothermal Research*, 133(1), 193-210.

DeRose, R. O. N. A. L. D. (1994, October). Effect of rainfall intensity on the spatial density of shallow landslides in a small watershed, Taranaki, New Zealand. In *Proceedings of the International Symposium on Forest Hydrology*, Tokyo, Japan (pp. 391-398).

Desnos, T. (2008). Root branching responses to phosphate and nitrate. *Current opinion in plant biology* 11(1), 82-87.

de Vallejo, L. I. G. (2005). *Geoingegneria*. Pearson Italia Spa.

Di Crescenzo, G., Rotella, M., & Santo, A. (2007). Il contributo della geologia per lo studio dei meccanismi di innesco di colate rapide di fango al campo sperimentale di Monteforte Irpino (AV). *Piattaforme Evolute di Telecomunicazioni e di Information Technology per l'Offerta di Servizi al settore Ambiente, Progetto PETIT-OSA*. Aracne Edizioni, Rome, 263-272.

Dietrich, W.E., Reneau, S.L., Wilson, C.J., (1986). Hollows, colluvium and landslides in soil-mantled landscapes. In: Abrahamas, A.D. (Ed.), *Hillslope processes*. Allen and Unwin, pp. 361–388.

Dudley, J. H. (1970). Review of collapsing soils. *Journal of Soil Mechanics & Foundations* Div, 97(SM1).

Duncan, A. M., Chester, D. K., & Guest, J. E. (1981). Mount Etna Volcano: environmental impact and problems of volcanic prediction. *Geographical Journal*, 164-178.

Eamus, D., Huete, A., & Yu, Q. (2016). *Vegetation dynamics*. Cambridge University Press.

Eckersley, D. (1990). Instrumented laboratory flowslides. *Geotechnique*, 40(3), 489-502.

Ekanayake, J. C., & Phillips, C. J. (2002). Slope stability thresholds for vegetated hillslopes: a composite model. *Canadian Geotechnical Journal*, 39(4), 849-862.

Eisenhauer, N., Beßler, H., Engels, C., Gleixner, G., Habekost, M., Milcu, A., & Weigelt, A. (2010). Plant diversity effects on soil microorganisms support the singular hypothesis. *Ecology*, 91(2), 485-496.

Endo, T., & Tsuruta, T. (1969). *The effect of the tree's roots on the shear strength of soil, Annual Report, 1968*. Hokkaido Branch, For. Exp. Stn., Sapporo, Japan, 167-182.

EPA (2003). *Summary of state fertilizer laws*. The Fertilizer Institute's (TFI) Product Quality & Technology Committee, Washington, D.C.

Evangelista, A., Nicotera, M. V., Papa, R., & Urciuoli, G. (2008). Field investigation on triggering mechanisms of fast landslides in unsaturated pyroclastic soils. Toll, et al.(eds.) Unsaturated Soils: Advances in Geo-Engineering, 909-915.

Evangelista E., Pellegrino A., Urcioli G. (2008). "Mitigazione del rischio di frana". In: Strategie di intervento per la mitigazione del rischio di frana, L. Picarelli editor, Progetto di ricerca P.R.I.N. 2001 – 2003, Ministero dell'Istruzione, dell'Università e della Ricerca Scientifica (M.I.U.R.).

Farley, R. A. & Fitter, A. H. (1999). The responses of seven co-occurring woodland herbaceous perennials to localized nutrient-rich patches. *Journal of Ecology* 87(5), 849-859.

Fedi, M., Nunziata, C., & Rapolla, A. (1991). The Campania-Campi Flegrei area: a contribution to discern the best structural model from gravity interpretation. *Journal of Volcanology and Geothermal Research*, 48(1), 51-59.

Fell, R., Hungr, O., Leroueil, S., & Riemer, W. (2000, November). Keynote lecture-geotechnical engineering of the stability of natural slopes, and cuts and fills in soil. In *ISRM International Symposium. International Society for Rock Mechanics*.

Ferlisi, S., De Chiara, G., & Cascini, L. (2016). Quantitative risk analysis for hyperconcentrated flows in Nocera Inferiore (southern Italy). *Natural Hazards*, 81(1), 89-115.

Fiengo G. (1988). *I Regi Lagni e la Bonifica della campania Felix durante il viceregno Spagnolo*, Firenze: Leo S. Olschki editore. (In Italian)

Fiorillo, F., Guadagno, F., Aquino, S., & De Blasio, A. (2001). The December 1999 Cervinara landslides: further debris flows in the pyroclastic deposits of Campania (southern Italy). *Bulletin of Engineering Geology and the Environment*, 60(3), 171-184.

Francour, P. & Semroud, R. (1992). Calculation for the root area index in Posidonia oceanica in the Western Mediterranean. *Aquatic Botany* 42, No. 3, 281–286.

Fredlund, D. G., & Rahardjo, H. (1993). *Soil mechanics for unsaturated soils*. John Wiley & Sons.

Fredlund, D. G., Rahardjo, H., & Fredlund, M. D. (2012). *Unsaturated soil mechanics in engineering practice*. John Wiley & Sons.

Fredlund, D. G., Rahardjo, H., Leong, E. C. and Ng, C. W. W. (2001). Suggestions and recommendations for the interpretation of soil-water characteristic curves. *Proc. Int. Conf. on Geotechnical Engineering*, 14 503-508.

Fredlund, D. G., and Xing, A. (1994). Equations for the soil-water characteristic curve. *Canadian Geotechnical Journal*, 31(4), 521 - 532.

Gabr MA, Akran M, Taylor HM. 1995. Effect of simulated roots on the permeability of silty soil. *Geotechical Testing Journal, ASTM* 18(1): 112–115.

Gadi, V. K., Bordoloi, S., Garg, A., Kobayashi, Y., & Sahoo, L. (2016). Improving and correcting unsaturated soil hydraulic properties with plant parameters for agriculture and bioengineered slopes. *Rhizosphere*, 1, 58-78.

Gagoshidze M.S. (1969). *Mudflows and floods and their control*. Sov Hydrol. 4, 188 pp. 410-422

Garg, A., Coo, J. L., & Ng, C. W. W. (2015a). Field study on influence of root characteristics on soil suction distribution in slopes vegetated with Cynodon dactylon and Schefflera heptaphylla. *Earth Surface Processes and Landforms*, 40(12), 1631-1643.

Garg, A., Leung, A. K., & Ng, C. W. W. (2015b). Comparisons of soil suction induced by evapotranspiration and transpiration of S. heptaphylla. Canadian Geotechnical Journal, 52(12), 2149-2155.

Garg, A., Leung, A. K., & Ng, C. W. W. (2015c). Transpiration reduction and root distribution functions for a non-crop species Schefflera heptaphylla. Catena, 135, 78-82.

Gates, D. M. (1980). *Biophysical ecology*. New York, NY, USA: Springer-Verlag.

GCO (Geotechnical Control Office) (2000). *Geotechnical manual for slopes*. Hong Kong, China: Geotechnical Control Office.

Genet, M., Stokes, A., Fourcaud, T., & Norris, J. E. (2010). The influence of plant diversity on slope stability in a moist evergreen deciduous forest. *Ecological engineering,* 36(3), 265-275.

Genet, M., Stokes, A., Salin, F., Mickovski, S. B., Fourcaud, T., Dumail, J. F., & Van Beek, R. (2005). The influence of cellulose content on tensile strength in tree roots. *Plant and soil*, 278(1), 1-9.

GEO (Geotechnical Engineering Office) (2011). Technical guidelines on landscape treatment for slopes. Hong Kong, China: Geotechnical Engineering Office.

Gersani, M., & Sachs, T. (1992). Development correlations between roots in heterogeneous environments. *Plant, Cell and Environment* 15(4), 463-469.

Gerson R. (1977). Sediment transport for desert watersheds in erodible materials. *Earth Surface Processes*, 2, pp. 343-361.

Ghestem, M., Sidle, R. C., & Stokes, A. (2011). The influence of plant root systems on subsurface flow: implications for slope stability. *BioScience*, 61(11), 869-879.

Giordano, G. (1998). Facies characteristics and magma–water interaction of the White Trachytic Tuffs (Roccamonfina Volcano, southern Italy). *Bulletin of volcanology*, 60(1), 10-26.

Gish, T. J., & Jury, W. A. (1983). Effect of plant roots and root channels on solute transport. *Transactions of the ASAE*, 26(2), 440-0444.

Goldsmith, W. (1998). Soil reinforcement by river plants: progress results. In *Engineering Approaches to Ecosystem Restoration* (pp. 169-174).

Goldsmith, W., Gray, D., & McCullah, J. (2013). *Bioengineering case studies: Sustainable stream bank and slope stabilization*. Springer Science & Business Media.

Graf, F., Frei, M., & Böll, A. (2009). Effects of vegetation on the angle of internal friction of a moraine. *Forest Snow and Landscape Research*, 82(1), 61-77.

Gray, D. H., & Barker, D. (2004). Root-Soil Mechanics and Interactions. *Riparian vegetation and fluvial geomorphology*, 113-123.

Gray, D. H., & Leiser, A. T. (1982). *Biotechnical slope protection and erosion control*. Van Nostrand Reinhold Company Inc

Gray, D. H., & Ohashi, H. (1983). Mechanics of fiber reinforcement in sand. *Journal of Geotechnical Engineering*, 109(3), 335-353.

Gray, D. H., & Sotir, R. B. (1996). *Biotechnical and soil bioengineering slope stabilization: a practical guide for erosion control*. John Wiley & Sons.

Grayston, S. J., Vaughan, D. & Jones, D. (1997). Rhizosphere carbon flow in trees, in comparison with annual plants: the importance of root exudation and its impact on microbial activity and nutrient availability. *Applied Soil Ecology* 5, No. 1, 29–56.

Greenwood, J.R., Norris, J.E., and Wint, J. (2004). Assessing the contribution of vegetation to slope stability. Proceedings of the ICE - *Geotechnical Engineering*, 157(4): 199–207. doi:10.1680/geng.2004.157.4.199.

Guadagno, F. M., Forte, R., Revellino, P., Fiorillo, F., & Focareta, M. (2005). Some aspects of the initiation of debris avalanches in the Campania Region: the role of morphological slope discontinuities and the development of failure. *Geomorphology*, 66(1), 237-254.

Guida, D., (2003). The role of the zero-order basin in flowslide-debris flow occurrence and recurrence in Campania (Italy). Proc. Int. Conference on *Fast Slope Movements — Prediction and Prevention for Risk Mitigation*, vol. 1. Patron Editore, Napoli, pp. 255–262.

Gurioli, L., Sulpizio, R., Cioni, R., Sbrana, A., Santacroce, R., Luperini, W., & Andronico, D. (2010). Pyroclastic flow hazard assessment at Somma–Vesuvius based on the geological record. *Bulletin of Volcanology*, 72(9), 1021-1038.

Hau, B. C., & Corlett, R. T. (2003). Factors affecting the early survival and growth of native tree seedlings planted on a degraded hillside grassland in Hong Kong, China. *Restoration Ecology* 11(4), 483-488.

He, Y., Guo, X., & Wilmshurst, J. F. (2007). Comparison of different methods for measuring leaf area index in a mixed grassland. *Canadian Journal of Plant Science*, 87(4), 803-813.

Heppell, J., Payvandi, S., Zygalakis, K. C., Smethurst, J. A., Fliege, J., & Roose, T. (2014). Validation of a spatial-temporal soil water movement and plant water uptake model. *Geotechnique*, 64(7), 526-539.

Hetherington, A. M., and F. I. Woodward (2003), The role of stomata in sensing and driving environmental change. *Nature*, 424, 901–908.

Hillel, D., Krentos, V. D., & Stylianou, Y. (1972). Procedure and test of an internal drainage method for measuring soil hydraulic characteristics in situ. *Soil Science*, 114(5), 395-400.

Hodge, A. (2004). The plastic plant: root responses to heterogeneous supplies of nutrients. *New phytologist* 162(1), 9-24.

Hu, X. S., Brierley, G., Zhu, H. L., Li, G. R., Fu, J. T., Mao, X. Q., ... & Qiao, N. (2013). An exploratory analysis of vegetation strategies to reduce shallow landslide activity on loess hillslopes, Northeast Qinghai-Tibet Plateau, China. *Journal of Mountain Science*, 10(4), 668-686.

Huat, B. B., Ali, F. H., & Low, T. H. (2006). Water infiltration characteristics of unsaturated soil slope and its effect on suction and stability. *Geotechnical and Geological Engineering*, 24(5), 1293-1306.

Hungr, O., Evans, S.G., Bovis, M., and Hutchinson, J.N., (2001). Review of the classification of landslides of the flow type. *Environmental and Engineering Geoscience*, VII:221238.

Hungr O., Leroueil S., Picarelli L. (2012). *Varnes classification of landslide types, an update*. In: Eberhardt E, Froesse C, TurnerAK, Leroueil S (eds) Landslides

and engineered slopes: protecting society through improved understanding, vol 1. CRC Press, Boca Raton, pp. 47–58.

Hutchinson, J. H. (1988). Morphological and Geotechnical Parameters of Landslides in Relation to Geology and Hydrogeology, Landslides. In *Proceedings of the fifth international symposium on landslides* (pp. 3-35).

Hutchinson J.N. (2003). Review of flow-like mass movements in granular and fine-grained materials. *Proc. of the Int. Workshop "Flows 2003 - Occurrence and Mechanisms of Flows in Natural Slopes and Earthfill"*, pp. 3-16, Sorrento.

Indraratna B, Fatahi B, Khabbaz H. 2006. Numerical analysis of matric suction effects of tree roots. *Proceedings of the Institution of Civil Engineers—Geotechnical Engineering* 159(2): 77–90.

Inoue, M., Šimůnek, J., Shiozawa, S., & Hopmans, J. W. (2000). Simultaneous estimation of soil hydraulic and solute transport parameters from transient infiltration experiments. Advances in Water Resources, 23(7), 677-688.

Ishak, M. F., Ali, N., & Kassim, A. (2012). Tree induce suction for slope sustainability. *In Applied Mechanics and Materials* (Vol. 170, pp. 1334-1338). Trans Tech Publications.

Iverson, R. M. (2000). Landslide triggering by rain infiltration. *Water resources research*, 36(7), 1897-1910.

Iverson, R. M., Reid, M. E., & LaHusen, R. G. (1997). Debris-flow mobilization from landslides. *Annual Review of Earth and Planetary Sciences*, 25(1), 85-138.

Jasso-Chaverria, C., Hochmuth, G. J., Hochmuth, R. C. & Sargent, S. A. (2005). Fruit yield, size, and color responses of two greenhouse cucumber types to nitrogen fertilization in perlite soilless culture. *Horticulture Technology* 15(3), 565-571.

Jastrow, J. D., Miller, R. M., & Lussenhop, J. (1998). Contributions of interacting biological mechanisms to soil aggregate stabilization in restored prairie. *Soil Biology and Biochemistry*, 30(7), 905-916.

Jennings, J. E., & Knight, K. (1957, September). The prediction of total heave from the double oedometer test. In Proc. *Symposium on Expansive clays* (Vol. 7, No. 9, pp. 13-19).

Johnson, K. A., & Sitar, N. (1990). Hydrologic conditions leading to debris-flow initiation. *Canadian Geotechnical Journal*, 27(6), 789-801.

Johnston, D. M. (1997). Physical and social impacts of past and future volcanic eruptions in New Zealand: a thesis presented in partial fulfilment of the requirements for the degree of Doctor of Philosophy in Earth Science, Massey University, Palmerston North, New Zealand (Doctoral dissertation, Massey University).

Jotisankasa, A., & Sirirattanachat, T. (2017). Effects of grass roots on soil-water retention curve and permeability function. *Canadian Geotechnical Journal*, (ja).

Kelliher, F. M., Leuning, R., Raupach, M. R., & Schulze, E. D. (1995). Maximum conductances for evaporation from global vegetation types. *Agricultural and Forest Meteorology*, 73(1-2), 1-16.

Kitao, M., Yoneda, R., Tobita, H., Matsumoto, Y., Maruyama, Y., Arifin, A., Azani, A. M. & Muhamad, M. N. (2006). Susceptibility to photoinhibition in seedlings of six tropical fruit tree species native to Malaysia following transplantation to a degraded land. *Trees* 20(5), 601-610.

Kostaschuk, R., Terry, J., & Raj, R. (2003). Suspended sediment transport during tropicalcyclone floods in Fiji. *Hydrological Processes*, 17(6), 1149-1164.

Kostler, J. N., Bruckner, E., & Bibelriether, H. (1968). *Die Wurzeln der Waldbaume. Untersuchungen zur Morphologie der Waldbaume in Mitteleuropa*. Verlag Paul Parey: Hamburg & Berlin, 284, 3-4.

Kröner, E. (2016). Water dynamics in the rhizosphere: How mucilage affects water flow in soils (Doctoral dissertation, Göttingen, Georg-August Universität, Diss., 2016).

Kurdin R.D. (1973). *Classification of mudflows*. Sov. Hydrol. 4, pp. 310-316.

Ladd, R.S. (1977). Specimen preparation and cyclic stability of sands. *Journal of the Geotechnical Engineering Division*, ASCE, 103(6): 535–547.

Lade, P. V. (1992). Static instability and liquefaction of loose fine sandy slopes. *Journal of Geotechnical Engineerin*g, 118(1), 51-71.

Lampitiello, S. (2004). Resistenza non drenata e suscettività alla liquefazione di ceneri vulcaniche della Regione Campania. *Unpublished PhD thesis, Seconda Università di Napoli* (in Italian).

Lancellotta, R., Di Prisco, C., Costanzo, D., Foti, S., Sorbino, G., Buscarnera, G., Cosentini, R.M., Foresta V., (2012). Caratterizzazione e modellazione geotecnica. In: Criteri di zonazione della suscettibilità e della pericolosità da frane innescate da eventi estremi (piogge e sisma)/Leonardo Cascini. Composervice srl, Padova, pp. 266– 319. ISBN 9788890687334 (in Italian).

Laronne, J. B., Reid, I., Yitshak, Y., & Frostick, L. E. (1994). The non-layering of gravel streambeds under ephemeral flood regimes. *Journal of Hydrology*, 159(1-4), 353-363.

Lawson, D. E. (1982). Mobilization, movement and deposition of active subaerial sediment flows, Matanuska Glacier, Alaska. *The Journal of Geology*, 90(3), 279-300.

Lawton, E. C., Fragaszy, R. J., & Hardcastle, J. H. (1991a). Stress ratio effects on collapse of compacted clayey sand. *Journal of Geotechnical Engineering*, 117(5), 714-730.

Leamy, M. L. (1984). International Committee on the Classification of Andisols (ICOMAND) Circular letter No. 6. New Zealand Soil Bureau, DSIR, Lower Hutt.

Lee, Y. S., Cheuk, C. Y., & Bolton, M. D. (2008). Instability caused by a seepage impediment in layered fill slopes. *Canadian Geotechnical Journal*, 45(10), 1410-1425.

Leroueil, S. (2004). *Geotechnics of slopes before failure*. Landslides: evaluation and stabilization, 1, 863-884.

Leung, A. K., Garg, A., & Ng, C. W. W. (2015b). Effects of plant roots on soil-water retention and induced suction in vegetated soil. *Engineering Geology*, 193, 183-197.

Leung, A. K., Garg, A., Coo, J. L., Ng, C. W. W., & Hau, B. C. H. (2015c). Effects of the roots of Cynodon dactylon and Schefflera heptaphylla on water infiltration rate and soil hydraulic conductivity. *Hydrological processes*, 29(15), 3342-3354.

Leung, F. T., Yan, W. M., Hau, B. C., & Tham, L. G. (2015a). Root systems of native shrubs and trees in Hong Kong and their effects on enhancing slope stability. *Catena*, 125, 102-110.

Leung, A. L. A., Sun, H. S. H., Millis, S. M. S., Pappin, J. P. J., Ng, C. N. C., and Wong, H. W. H. (2011). Field monitoring of an unsaturated saprolitic hillslope. *Canadian Geotechnical Journal*, 48(3), 339-353.

Liang, Y. M., Hazlett, D. L. & Lauenroth, W. K. (1989). Biomass dynamics and water use efficiencies of five plant communities in the shortgrass steppe. *Oecologia* 80, No. 2, 148–153.

Lirer, L., Pescatore, T., Booth, B., & Walker, G. P. (1973). Two plinian pumice-fall deposits from Somma-Vesuvius, Italy. *Geological Society of America Bulletin*, 84(3), 759-772.

Lo, D. O. K. (2000). Review of natural terrain landslide debris-resisting barrier design. Geotechnical Engineering Office, Civil Engineering Department.

Loades, K. W., Bengough, A. G., Bransby, M. F., & Hallett, P. D. (2010). Planting density influence on fibrous root reinforcement of soils. *Ecological Engineering*, 36(3), 276-284.

López-Bucio, J., Cruz-Ramırez, A., & Herrera-Estrella, L. (2003). The role of nutrient availability in regulating root architecture. *Current opinion in plant biology* 6(3), 280-287.

Lourenço, S. D., Sassa, K., & Fukuoka, H. (2006). Failure process and hydrologic response of a two layer physical model: implications for rainfall-induced landslides. *Geomorphology*, 73(1), 115-130.

Lu, N., Alsherif, N., Wayllace, A., & Godt, J. W. (2014). Closing the Loop of the Soil Water Retention Curve. *Journal of Geotechnical and Geoenvironmental Engineering*, 141(1), 02814001.

Maizels J. (1989). Sedimentology, paleoflow dynamics and flood hystory of jökulhlaup deposits: Paleohydrology of Holocene sediment sequences in southern Iceland sandur deposits. Journal of Sedimentary Petrology, 59, pp. 204-223.

Mattia, C., Bischetti, G. B., & Gentile, F. (2005). Biotechnical characteristics of root systems of typical Mediterranean species. *Plant and soil*, 278(1), 23-32.

Major, J. J., Iverson, R. M., McTigue, D. F., Macias, S., & Fiedorowicz, B. K. (1997). Geotechnical properties of debris-flow sediments and slurries. In Proceedings of the 1997 1st *International Conference on Debris-Flow Hazards Mitigation: Mechanics, Prediction, and Assessment* (pp. 249-259).

McCully, M. E. (1999). Roots in Soil: Unearthing the complexities of roots and their rhizospheres. *Annual Review of Plant Physiology and Plant Molecular Biology* 50, 695-718.

McElrone, A. J., Choat, B., Gambetta, G. A. & Brodersen, C. R. (2013). Water Uptake and Transport in Vascular Plants. *Nature Education Knowledge* 4(5), 6.

Metcalfe, D. S., & Nelson, C. J. (1985). The botany of grasses and legumes. In *Forages*, 4th edn, Heath ME et al. (eds). Iowa State University Press: Ames; 52–63.

Meyer, L. D. (1979). Methods for attaining desired rainfall characteristics in rainfall simulators. *Proceedings of the Rainfall Simulator Workshop*, U.S. Department of Agriculture Science and Education Administration Agricultural Reviews and Manuals, 35-44

Mickovski, S. B., Hallett, P. D., Bransby, M. F., Davies, M. C., Sonnenberg, R., & Bengough, A. G. (2009). Mechanical reinforcement of soil by willow roots: impacts of root properties and root failure mechanism. *Soil Science Society of America Journal* 73(4), 1276-1285.

Migliaro, G. (2008). *Il legame costitutivo nei terreni piroclastici per la modellazione di scavi in ambiente urbanizzato ed influenza della parziale saturazione*. PhD thesis, University of Salerno (in Italian).

Miller, C. R., Ochoa, I., Nielsen, K. L., Beck, D. & Lynch, J. P. (2003). Genetic variation for adventitious rooting in response to low phosphorus availability: potential utility for phosphorus acquisition from stratified soils. *Functional Plant Biology* 30(9), 973-985.

Mitchell, A. R., Ellsworth, T. R., & Meek, B. D. (1995). Effect of root systems on preferential flow in swelling soil. *Communications in Soil Science & Plant Analysis*, 26(15-16), 2655-2666.

Monteith, J. L. (1965). Evaporation and environment. The state and movement of water in living organisms. Symposium of the society of experimental biology, Vol. 19 (pp. 205-234).

Morgan, J. B. & Connolly, E. L. (2013). *Plant-Soil Interactions: Nutrient Uptake*. Nature Education Knowledge 4(8), 2.

Morgan, R. P., & Rickson, R. J. (2003). *Slope stabilization and erosion control: a bioengineering approach*. Taylor & Francis.

Musso, A., & Olivares, L. (2004). Post-failure evolution in flowslide: Transition from static liquefaction to fluidization. In *Patron, Proc. Int. Workshop on Occurrence and Mechanisms of Flow-Like Landslides in Natural Slopes and Earthfills*, Sorrento(pp. 117-128).

Nanzyo, M., Dahlgren, R., & Shoji, S. (1993). Chemical characteristics of volcanic ash soils. *Developments in Soil Science*, 21, 145-187.

Napolitano, E., Fusco, F., & De Vita, P. (2016). Control of Hydrological Seasonal Variability of Ash-fall Pyroclastic Deposits on Rainfall Triggering Debris Flows in Campania (Southern Italy). *Procedia Earth and Planetary Science*, 16, 118-127.

Ng, C.W.W. (2009). What is static liquefaction failure of loose fill slopes? In The *First Italian Workshop on Landslides*, Napoli, 8-10 June 2009. NAPOLI Doppiavoce. Studio editoriale. Vol. 1, pp. 43–51. ISBN:9788889972120.

Ng, C. W., Garg, A., Leung, A. K., & Hau, B. C. H. (2016). Relationships between leaf and root area indices and soil suction induced during drying–wetting cycles. *Ecological Engineering*, 91, 113-118.

Ng, C. W. W., & Leung, A. K. (2012). Measurements of drying and wetting permeability functions using a new stress-controllable soil column. *Journal of Geotechnical and Geoenvironmental Engineering*, 138(1), 58-68.

Ng, C. W. W., Leung, A. K., & Woon, K. X. (2013). Effects of soil density on grass-induced suction distributions in compacted soil subjected to rainfall. *Canadian Geotechnical Journal*, 51(3), 311-321.

Ng, C. W. W., Leung, A. K. & Woon, K. X. (2014). Effects of soil density on grass-induced suction distributions in compacted soil subjected to rainfall. *Canadian Geotechnical Journal* 51, No. 3, 311–321.

Ng, C. W. W. & Menzies, B. (2007). Advanced Unsaturated Soil Mechanics and Engineering. Taylor and Francis, USA.

Ng, C. W. W., Tasnim, R., Capobianco, V., Coo, J.L. (2018) Influence of soil nutrients in heavily compacted soil on plant characteristics and soil hydrological responses. Geotechnique letters. *In press*

Ng'etich, Niyokuri, O. K. A. N., Rono, J. J., Fashaho, A. & Ogweno, J. O. (2013). Effect of different rates of nitrogen fertilizer on the growth and yield of zucchini (Cucurbita pepo cv. Diamant L.) Hybrid F1 in Rwandan high-altitude zone. *International Journal of Agricultura and Crop Sciences* 5, No. 1, 54-62.

Nicotera, M. V. (1998). Effetti del grado di saturazione sul comportamento di una pozzolana del napoletano. PhD Thesis, Università di Napoli Federico II (Italy).

Nicotera, M. V., & Papa, R. (2008). Comportamento idraulico e meccanico della serie piroclastica di Monteforte Irpino. *Piattaforme Evolute di Telecomunicazioni e di Information Technology per l'Offerta di Servizi al settore ambiente PETIT-OSA*. Centro Specializzato Monitoraggio Frane, Aracne Editrice, 272-280.

Nicotera MV, Papa R, Urciuoli G (2010) An experimental technique for determining the hydraulic properties of unsaturated pyroclastic soils. *Geotech Test J* 33(4):263–285

Nilaweera, N. S. (1994). Effects of tree roots on slope stability-The case of Khao Lunag Mountain Area, Southern Thiland. Doctor thesis No. GT-93-2, 452.

Nilaweera, N. S., & Nutalaya, P. (1999). Role of tree roots in slope stabilisation. *Bulletin of engineering geology and the environment*, 57(4), 337-342.

Norton, J., Smith, J. & Firestone, M. (1990). Carbon flow in the rhizosphere of Ponderosa pine seedlings. *Soil Biology and Biochemistry* 22, No. 4, 449–455.

O'Connor, J. E., Hardison, J. H., & Costa, J. E. (2001). Debris flows from failures of Neoglacial-Age moraine dams in the Three Sisters and Mount Jefferson wilderness areas, Oregon (No. 1606). US Department of the Interior, US Geological Survey.

Olivares, L., Andreozzi, L., Damiano, E., Lampitiello, S., & Picarelli, L. (2003). Hydrological response of a steep slope in unsaturated pyroclastic soils. Fast Slope Movements. In *Fast Slope Movements* (Vol. 1, pp. 391-397). Patron.

Olivares, L., & Damiano, E. (2007). Postfailure mechanics of landslides: laboratory investigation of flowslides in pyroclastic soils. *Journal of geotechnical and geoenvironmental engineering*, 133(1), 51-62.

Olivares, L., & Picarelli, L. (2001). Susceptibility of loose pyroclastic soils to static liquefaction-some preliminary data. In International Conference on Landslides: *Causes, Impacts and Countermeasures* (Vol. 1, pp. 75-85). VGE.

Olivares, L., & Picarelli, L. (2003). Shallow flowslides triggered by intense rainfalls on natural slopes covered by loose unsaturated pyroclastic soils. *Géotechnique*, 53(2), 283-287.

Olivares, L., Picarelli, L., Andreozzi, L., Avolio, B., Damiano, E., & Lampitiello, S. (2002). Scenari di pericolosità di frana in terreni sciolti di natura piroclastica. In *XXI Convegno Nazionale di Geotecnica* (Vol. 1, pp. 173-182). Patron Editore.

Olivares, L., Picarelli, L., Andreozzi, L., Damiano, E., & Lampitiello, S. (2004). Meccanismi di innesco delle colate di fango in terreni piroclastici sciolti: il caso di Cervinara. In *Workshop Internazionale su Convivere con le Frane: Effetti su Infrastrutture e Insediamenti Urbani. Strategie di Intervento per la Mitigazione del Rischio* (Vol. 1, pp. 205-223). Hevelius.

O'Loughlin, C. 1974. The effect of timber removal on the stability of forest slopes. *Journal of Hydrology, New Zealand*, 13: 121–134.

Operstein, V., & Frydman, S. (2000). The influence of vegetation on soil strength. *Proceedings of the Institution of Civil Engineers-Ground Improvement* 4(2), 81-89.

Orsi, G., De Vita, S., & Di Vito, M. (1996). The restless, resurgent Campi Flegrei nested caldera (Italy): constraints on its evolution and configuration. *Journal of Volcanology and Geothermal Research*, 74(3-4), 179-214.

Orsi, G., Civetta, L., Del Gaudio, C., De Vita, S., Di Vito, M. A., Isaia, R., ... & Ricco, C. (1999). Short-term ground deformations and seismicity in the resurgent Campi Flegrei caldera (Italy): an example of active block-

resurgence in a densely populated area. *Journal of Volcanology and Geothermal Research*, 91(2), 415-451.

Pagano, L., Reder, A., & Rianna, G. (2014). Experiments to investigate the hydrological behaviour of volcanic covers. *Procedia Earth and Planetary Science*, 9, 14-22.

Papa, R. (2008). Indagine sperimentale sulla coltre piroclastica di un versante della Campania. *PhD thesis, Università degli Studi di Napoli Federico II* (in Italian).

Papa, R., Evangelista, A., Nicotera, M. V., & Urciuoli, G. (2008, July). Mechanical properties of unsaturated pyroclastic soils affected by fast landslide phenomena. In *Unsaturated Soils, Advances in Geo-Engineering, Proceedings of the 1st European Conference,* E-UNSAT (pp. 917-923).

Papa, R., & Nicotera, M. V. (2011, February). Calibration of TDR probes to measure water content in pyroclastic soils. In *5th Asia-Pacific Conference on Unsaturated Soils*, Pattaya, Thailand.

Papa R, Pirone M, Nicotera MV, Urciuoli G (2013) Seasonal groundwater regime in an unsaturated pyroclastic slope. *Geotechnique* 63(5):420–426

Pastor, M., Quecedo, M., Fernández Merodo, J. A., Herrores, M. I., Gonzalez, E., & Mira, P. (2002). Modelling tailings dams and mine waste dumps failures. *Geotechnique*, 52(8), 579-591.

Picarelli, L., Evangelista, A., Rolandi, G., Paone, A., Nicotera, M. V., Olivares, L., ... & Rolandi, M. (2006, December). Mechanical properties of pyroclastic soils in Campania Region. In Invited paper, *2nd Int. Workshop on Characterisation and Engineering Properties of Natural Soils*, Singapore.

Picarelli, L., Urciuoli, G., & Olivares, L. (2006). Interazione tra movimenti di versante, infrastrutture e centri abitati. In: Instabilità di Versante. Interazioni con le infrastrutture, i centri abitati e l'ambiente. In *XI Ciclo di conferenze di Meccanica e Ingegneria delle Rocce* (Vol. 1, pp. 9-40).

Pierson, T. C. (1986). Flow behavior of channelized debris flows Mount St. Helens Washington. *Hillslope processes*, 269-296.

Pierson T.C. and Scott K.M.(1985). Downstream dilution of a lahar: transition from debris flow to hyperconcentrated streamflow. *Water Resources Research*, 21 pp. 1511-1524.

Pierson T.C., Daag A.S., delos Reyes P.J., Regalado M.T.M., Solidum R., and Tubianosa B.S. (1996). Flow and deposition of posteruption hot lahars on the east side of Mount pinatubo, July-October 1991. In: C.G. Newhall, and R.S. Punungbayan (eds), Fire and Mud: Eruptions and Lahars of Mount Pinatubo, Philippines pp. 921-950. Philippines Institute of Vulcanology and Seismology, Quezon City and University of Washington Press, Seattle.

Piochi, M., Mastrolorenzo, G., & Pappalardo, L. (2005). Magma ascent and eruptive processes from textural and compositional features of Monte Nuovo pyroclastic products, Campi Flegrei, Italy. *Bulletin of Volcanology*, 67(7), 663-678.

Pirone, M., Papa, R., Nicotera, M. V., & Urciuoli, G. (2015). In situ monitoring of the groundwater field in an unsaturated pyroclastic slope for slope stability evaluation. *Landslides*, 12(2), 259-276.

Pirone, M., & Urciuoli, G. (2012). Seasonal effects in the groundwater regime of unsaturated slopes. *Unsaturated Soils: Research and Applications*, 359-365.

Pollen, N., Simon, A., & Collison, A. (2004). Advances in assessing the mechanical and hydrologic effects of riparian vegetation on streambank stability. *Riparian vegetation and fluvial geomorphology*, 125-139.

Pollen-Bankhead, N., & Simon, A. (2010). Hydrologic and hydraulic effects of riparian root networks on streambank stability: Is mechanical root-reinforcement the whole story?. *Geomorphology*, 116(3), 353-362.

Popescu, M. E., & Sasahara, K. (2009). Engineering measures for landslide disaster mitigation. In *Landslides–Disaster Risk Reduction* (pp. 609-631). Springer Berlin Heidelberg.

Preti, F. (2013). Forest protection and protection forest: tree root degradation over hydrological shallow landslides triggering. Ecological engineering, 61, 633-645.

Principe, C., Tanguy, J. C., Arrighi, S., Paiotti, A., Le Goff, M., & Zoppi, U. (2004). Chronology of Vesuvius' activity from AD 79 to 1631 based on archeomagnetism of lavas and historical sources. *Bulletin of Volcanology*, 66(8), 703-724.

Rahardjo, H., Lee, T. T., Leong, E. C., & Rezaur, R. B. (2005). Response of a residual soil slope to rainfall. *Canadian Geotechnical Journal*, 42(2), 340-351.

Ramírez García, J., Almendros García, P., & Quemada Saenz-Badillos, M. (2012). Ground cover and leaf area index relationship in a grass, legume and crucifer crop. *Plant, Soil and Environment*, 58(8), 385-390.

Rasband, W. S. (2011). ImageJ. Bethesda, MD, USA: US National Institutes of Health.

Reder, A., Rianna, G., & Pagano, L. (2014). Calibration of TDRs and heat dissipation probes in pyroclastic soils. *Procedia Earth and Planetary Science*, 9, 171-179.

Rettori, A., Cecconi, M., Pane, V., & Zarotti, C. (2010). Stabilizzazione superficiale di versanti con la tecnologia Prati Armati®: implementazione di un modello di calcolo per la valutazione del coefficiente di sicurezza. *Accademia Nazionale dei Lincei–X Giornata Mondiale dell'Acqua, Convegno: Frane e Dissesto Idrogeologico*.

Revellino, P., Hungr, O., Guadagno, F. M., & Evans, S. G. (2004). Velocity and runout simulation of destructive debris flows and debris avalanches in pyroclastic deposits, Campania region, Italy. *Environmental Geology*, 45(3), 295-311.

Rianna, G., Pagano, L., & Urciuoli, G. (2014). Rainfall patterns triggering shallow flowslides in pyroclastic soils. *Engineering Geology*, 174, 22-35.

Ritchie, J. T. (1972). Model for predicting evaporation from a row crop with incomplete cover. *Water resources research*, 8(5), 1204-1213

Rodolfo K.S., Umbal J.V., Alonso R.A., Remotigue C.T., Paladio-Melosantos M.L., Salvador J.H.G., Evangelista D., Miller Y. (1991). Two years of lahars on the western flank of Mount Pinatubo: Initiation, flow processes, deposits, and attendant geomorphic and hydraulic changes. In: C.G. Newhall, and R.S. Punungbayan (eds), Fire and Mud: Eruptions and Lahars of Mount Pinatubo, Philippines pp. 989-1013. Philippines Institute of Vulcanology and Seismology, Quezon City and University of Washington Press, Seattle.

Rolandi, G., Bellucci, F., Heizler, M. T., Belkin, H. E., & De Vivo, B. (2003). Tectonic controls on the genesis of ignimbrites from the Campanian Volcanic Zone, southern Italy. *Mineralogy and Petrology*, 79(1), 3-31.

Rolandi, G., Bertollini, F., Cozzolino, G., Esposito, N., & Sannino, D. (2000). Sull'origine delle coltri piroclastiche presenti sul versante occidentale del Pizzo d'Alvano (Sarno-Campania). *Quaderni di Geologia Applicata*, 7(1), 37-48.

Rolandi, G., Mastrolorenzo, G., Barrella, A. M., & Borrelli, A. (1993). The Avellino plinian eruption of Somma-Vesuvius (3760 yBP): the progressive evolution from magmatic to hydromagmatic style. *Journal of Volcanology and Geothermal Research*, 58(1-4), 67-88.

Rolandi, G., Petrosino, P., & Mc Geehin, J. (1998). The interplinian activity at Somma–Vesuvius in the last 3500 years. *Journal of Volcanology and Geothermal Research*, 82(1), 19-52.

Sacco C. (2015). Landslide risk management in Italy: practice and perspectives. *PhD Thesis, University of Salerno, Italy*.

Sassa, K. (1985). The mechanisum of debris flows. In Proc., XI Int'l *Conference on Soil Mechanics and Foundation Engineering*, San Francisco (Vol. 3, pp. 1173-1176).

Sauer, D., Kuzyakov, Y. & Stahr, K. (2006). Spatial distribution of root exudates of five plant species as assessed by 14C labelling. *J. Plant Nutr. Soil Sci.* 169, No. 3, 360–362.

Scanlan CA, Hinz C. 2010. Insights into the processes and effects of root-induced changes to soil hydraulic properties. *In Proceedings of the 19th World Congress of Soil Science*, 2.: Brisbane, Australia; 41– 44.

Schiechtl, H. M., & Stern, R. (1996). *Ground bioengineering techniques for slope protection and erosion control.*

Schmidt, K. M., Roering, J. J., Stock, J. D., Dietrich, W. E., Montgomery, D. R., & Schaub, T. (2001). The variability of root cohesion as an influence on shallow landslide susceptibility in the Oregon Coast Range. *Canadian Geotechnical Journal*, 38(5), 995-1024.

Schmincke, H. U. (2004). *Volcanic Hazards, Volcanic Catastrophes, and Disaster Mitigation. n Volcanism* (pp. 229-258). Springer Berlin Heidelberg.

Schwarz, M., Lehmann, P., & Or, D. (2010). Quantifying lateral root reinforcement in steep slopes–from a bundle of roots to tree stands. *Earth Surface Processes and Landforms*, 35(3), 354-367.

Signorelli, S., Vaggelli, G., Romano, C., & Carroll, M. (2001). Volatile element zonation in Campanian Ignimbrite magmas (Phlegrean Fields, Italy): evidence from the study of glass inclusions and matrix glasses. *Contributions to Mineralogy and Petrology*, 140(5), 543-553.

Sigurdsson, H., Carey, S., Cornell, W., & Pescatore, T. (1985). The eruption of Vesuvius in AD 79. *National Geographic Research*, 1(3), 332-387.

Simon, A., & Collison, A. J. (2002). Quantifying the mechanical and hydrologic effects of riparian vegetation on streambank stability. *Earth Surface Processes and Landforms*, 27(5), 527-546.

Sinnathamby, G., Phillips, D. H., Sivakumar, V. & Paksy, A. (2013). Landfill cap models under simulated climate change precipitation: impacts of cracks and root growth. *Géotechnique* 64, No. 2, 95–107.

Smethurst, J. A., Clarke, D., & Powrie, W. (2006). Seasonal changes in pore water pressure in a grass covered cut slope in London Clay. *Géotechnique*, 56(8), 523-537.

Soil Survey Staff (1999). *Soil Taxonomy, Second edition. USDA-NRCS, Agriculture Handbook* No.436.

Stokes, A., Atger, C., Bengough, A. G., Fourcaud, T. & Sidle, R. C. (2009). Desirable plant root traits for protecting natural and engineered slopes against landslides. *Plant and soil* 324(1-2), 1-30.

Stokes, A., & Mattheck, C. (1996). Variation of wood strength in tree roots. *Journal of Experimental Botany*, 47(5), 693-699.

Stulen, I. & Hertog, J. D. (1993). Root growth and functioning under atmospheric CO2 enrichment. *Plant Ecology* 104, No. 1, 99-115.

Swanston, D. N. (1974). Slope stability problems associated with timber harvesting in mountainous regions of the western United States. *Gen. Tech.*

Rep. PNW-21. Portland, OR: U.S. Department of Agriculture, Forest Service, Pacific Northwest Forest and Range Experiment Station. pp 14.

Takahashi, T., & Shoji, S. (2002). Distribution and classification of volcanic ash soils. *Global Environmental Research-English Edition*, 6(2), 83-98.

TDOT (Tennessee Department of Transportation) (1981). Subgrade construction and preparation: specifications for road and bridge construction. Kingsport, TN, USA: Tennessee Department of Transportation (TDOT) Bureau of Highways.

Thomas, R. E., & Pollen-Bankhead, N. (2010). Modeling root-reinforcement with a fiber-bundle model and Monte Carlo simulation. *Ecological Engineering*, 36(1), 47-61.

Thornthwaite, C. W. (1946). *The moisture factor in climate*. Eos, Transactions American Geophysical Union, 27(1), 41-48.

Tingey, D. T., Johnson, M. G., Phillips, D. L., Johnson, D. W. & Ball, J. T. (1996). Effects of elevated CO2 and nitrogen on the synchrony of shoot and root growth in ponderosa pine. *Tree Physiology* 16, 905-914.

Tobias, S., 1995. *Shear strength of the soil root bond system*. In: Vegetation and Slopes. Thomas Telford, London, pp. 280–286.

Tobin, B., Čermák, J., Chiatante, D., Danjon, F., Di Iorio, A., Dupuy, L., ... & Nadezhdina, N. (2007). Towards developmental modelling of tree root systems. *Plant Biosystems*, 141(3), 481-501.

Todesco, M., Neri, A., Ongaro, T. E., Papale, P., Macedonio, G., Santacroce, R., & Longo, A. (2002). Pyroclastic flow hazard assessment at Vesuvius (Italy) by using numerical modeling. I. Large-scale dynamics. *Bulletin of Volcanology*, 64(3-4), 155-177.

Tosi, M. (2007). Root tensile strength relationships and their slope stability implications of three shrub species in the Northern Apennines (Italy). *Geomorphology*, 87(4), 268-283.

Traoré, O., Groleau-Renaud, V., Plantureux, S., Tubeileh, A. & Boeuf-Tremblay, V. (2000). Effect of root mucilage and modelled root exudates on soil structure. *European Journal of Soil Science* 51, No. 4, 575–581.

Unger, L. (1953). Rural settlement in the Campania. *Geographical Review*, 43(4), 506-524.

Vacca, A., Adamo, P., Pigna, M., & Violante, P. (2003). Genesis of tephra-derived soils from the Roccamonfina volcano, south central Italy. *Soil Science Society of America Journal*, 67(1), 198-207.

Vaciago, G. (2013). The SafeLand compendium of landslide risk mitigation measures. *In Landslide Science and Practice* (pp. 683-689). Springer Berlin Heidelberg.

Van Asch, T. W., Malet, J. P., & Van Beek, L. P. H. (2006). Influence of landslide geometry and kinematic deformation to describe the liquefaction of landslides: some theoretical considerations. *Engineering geology*, 88(1), 59-69.

VanDine, D. F. (1996). Debris flow control structures for forest engineering. Res. Br., BC Min. For., Victoria, BC, Work. Pap, 8, 1996.

Van Genuchten, M. T. (1980). A closed-form equation for predicting the hydraulic conductivity of unsaturated soils. *Soil science society of America journal*, 44(5), 892-898.

Vanapalli, S. K., Fredlund, D. G., Pufahl, D. E., & Clifton, A. W. (1996). Model for the prediction of shear strength with respect to soil suction. *Canadian Geotechnical Journal*, 33(3), 379-392.

Vanapalli, S. K., Sillers, W. S., & Fredlund, M. D. (1998). The meaning and relevance of residual state to unsaturated soils. In *Proceedings of the 51st Canadian Geotechnical Conference*, Edmonton, Alta (pp. 4-7).

Van Noordwijk, M., Heinen, M., & Hairiah, K. (1991). Old tree root channels in acid soils in the humid tropics: important for crop root penetration, water infiltration and nitrogen management. *Plant and Soil*, 134(1), 37-44.

Veihmeyer, F. J. & Hendrickson, A. H. (1931). The moisture equivalent as a measure of the field capacity of soils. *Soil Science* 32, No. 3, 181–193.

Vergani, C., Schwarz, M., Cohen, D., Thormann, J. J., & Bischetti, G. B. (2014). Effects of root tensile force and diameter distribution variability on root reinforcement in the Swiss and Italian Alps. *Canadian journal of forest research*, 44(11), 1426-1440.

Versace, P., Caruso, A., Cassetti, M., & Capparelli, G. (2008). Il presidio territoriale e la gestione dell'emergenza a Sarno. *Quad CAMIlab*, 3(3), 55-84.

Waldron, L. J. (1977). The shear resistance of root-permeated homogeneous and stratified soil. *Soil Science Society of America Journal*, 41(5), 843-849.

Waldron, L. J., & Dakessian, S. (1981). Soil reinforcement by roots: calculation of increased soil shear resistance from root properties. *Soil science*, 132(6), 427-435.

Wan, Y., Xue, Q., & Zhao, Y. (2011). Mechanism study and numerical simulation on vegetation affecting the slope stability. *Electronic Journal of Geotechnical Engineering*, 16.

Wang, Z., Guo, D., Wang, X., Gu, J., & Mei, L. (2006). Fine root architecture, morphology, and biomass of different branch orders of two Chinese temperate tree species. *Plant and Soil*, 288(1-2), 155-171.

Wang, F. W., Sassa, K., & Wang, G. (2002). Mechanism of a long-runout landslide triggered by the August 1998 heavy rainfall in Fukushima Prefecture, Japan. *Engineering Geology*, 63(1), 169-185.

Wang, G., & Sassa, K. (2001). Factors affecting rainfall-induced flowslides in laboratory flume tests. *Geotechnique*, 51(7), 587-599.

Watson, D. J. (1947). Comparative physiological studies on the growth of field crops: I. Variation in net assimilation rate and leaf area between species and varieties and within and between years. *Annals of Botany* 11, No. 1, 41–76.

Watt, S. F., Pyle, D. M., Mather, T. A., Martin, R. S., & Matthews, N. E. (2009). Fallout and distribution of volcanic ash over Argentina following the May 2008 explosive eruption of Chaitén, Chile. *Journal of Geophysical Research: Solid Earth*, 114(B4).

Wetzel, P. J., & Chang, J. T. (1987). Concerning the relationship between evapotranspiration and soil moisture. *Journal of climate and applied meteorology*, 26(1), 18-27.

Wu, T. H. (1976). Investigations of landslides on Prince of Wales Island, Alaska, *Geotech. Eng.* Rep 5, Columbus, OH: Dept. Civ. Eng,, Ohio State Univ. 94 p.

Wu, T. H. (2013). Root reinforcement of soil: review of analytical models, test results, and applications to design. *Canadian Geotechnical Journal*, 50(3), 259-274.

Wu, T. H., Bettadapura, D. P., & Beal, P. E. (1988). A statistical model of root geometry. *Forest Science*, 34(4), 980-997.

Wu, T. H., McKinnell III, W. P., & Swanston, D. N. (1979). Strength of tree roots and landslides on Prince of Wales Island, Alaska. *Canadian Geotechnical Journal*, 16(1), 19-33.

Wu, T. H., & Watson, A. (1998). In situ shear tests of soil blocks with roots. *Canadian Geotechnical Journal*, 35(4), 579-590.

Yamamuro, J. A., & Lade, P. V. (1998). Steady-state concepts and static liquefaction of silty sands. *Journal of Geotechnical and Geoenvironmental Engineering*, 124(9), 868-877.

Yang, Y., Chen, L., Li, N., & Zhang, Q. (2016). Effect of root moisture content and diameter on root tensile properties. *PloS one*, 11(3), e0151791.

Yang, H., Rahardjo, H., Wibawa, B., & Leong, E. C. (2004). A soil column apparatus for laboratory infiltration study.

Yasufuku, N., Ochiai, H., and Hormdee, D. 2005. An empirical relationship for evaluating collapsible settlements of volcanic ash sandy soil. *In Advanced experimental unsaturated soil mechanics*. Edited by Tarantino, Romero and Cui. pp. 265–272

Young, R. F. 1989. *Cavitation.* McGraw-Hill, London.

Zarotti, C. (2014). L'interazione pendio atmosfera: piante erbacee a radicazione profonda per la protezione dei versanti in caso di fenomeni metereologici intensi. XXV Convegno Nazionale di Geotecnica: la geotecnica nella difesa del territorio e delle infrastrutture dalle calamità naturali, Baveno (Lago Maggiore), giugno 2014, Atti.

Zhan, T. L., Ng, C. W., & Fredlund, D. G. (2007). Field study of rainfall infiltration into a grassed unsaturated expansive soil slope. *Canadian Geotechnical Journal*, 44(4), 392-408.

Zhang, C. B., Chen, L. H., Liu, Y. P., Ji, X. D., & Liu, X. P. (2010). Triaxial compression test of soil–root composites to evaluate influence of roots on soil shear strength. *Ecological Engineering*, 36(1), 19-26.

Zhang, Y., Kendy, E., Qiang, Y., Changming, L., Yanjun, S., & Hongyong, S. (2004). Effect of soil water deficit on evapotranspiration, crop yield, and water use efficiency in the North China Plain. *Agricultural Water Management,* 64(2), 107-122.

Zhong, R. H., He, X. B., Bao, Y. H., Tang, Q., Gao, J. Z., Yan, D. D., ... & Li, Y. (2016). Estimation of soil reinforcement by the roots of four post-dam prevailing grass species in the riparian zone of Three Gorges Reservoir, China. *Journal of Mountain Science*, 13(3), 508.

Zhu, H., & Zhang, L. M. (2016). Field investigation of erosion resistance of common grass species for soil bioengineering in Hong Kong. *Acta Geotechnica*, 11(5), 1047-1059.

Ziemer, R.R. 1981. Roots and the stability of forested slopes. In Erosion and sediment transport in Pacific Rim Steeplands. Pub. No. 132. *International Association of Hydrological Sciences*. pp. 343-361.

10 APPENDIX A

10.1 INSTRUMENTATION: CALIBRATION AND INSTALLATION

10.1.1 Soil Suction measurements: Mini-tensiometers T5 (UMS)

Mini-tensiometer T5 (UMS) is specifically designed for accurate measurements and is typically used for suction measurements in soil columns, lysimeters or soil pots. It has a small ceramic tip of 5 mm diameter and the active surface is only 0.5 cm^2, this ensures a minimal disturbance and rapid response at the contact with soil (5 seconds with appropriate filling). The T5 consists of a water tank that in contact with the soil through a ceramic tip, which creates a continuous interface between soil and inner water of the sensor (Fig. 10.1). Soil water pressure is thus directly transmitted to a transducer inside the tensiometer from which a proportional electrical signal is issued.

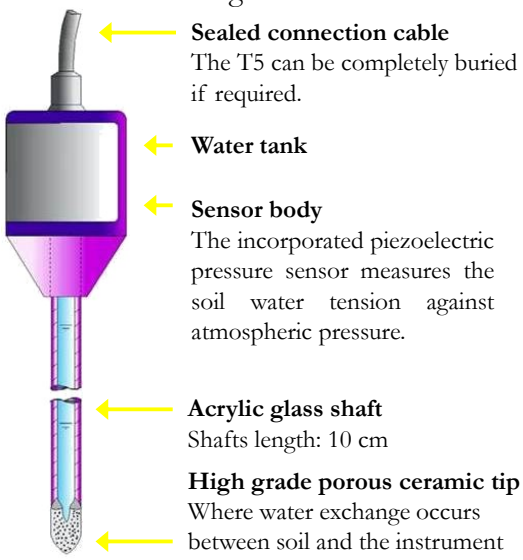

Figure 10.1 Schematization of mini-tensiometer T5 (UMS) (Official T5 manual).

Measurements are compensated by atmospheric pressure: the dry side of the transducer is in contact with the atmospheric pressure through a teflon filter for more accurate measurements. The T5 can be installed in any position and orientation because any cavitation process can be easily recognized from its plastic body.
This mini-tensiometer is ideal for laboratory experiments but can be also installed in field for small-scale measurements, by guaranteeing a good covering from frost or wind.
In this experimental study 7 mini-tensiometers T5 were used, respectively 4 installed in vegetated column (V) and 3 installed in no-vegetated column (NV), see Chapter 5.
Connecting cables of T5 were connected to the data-logger for data acquisition without requiring any other power supply, and the output signal was directly converted in pressure (kPa).
The installation process was the following: i) saturating all T5s with deaired water (Fig. 10.2a), ii) drilling holes at the design depths along the column (Fig. 10.2b) and iii) horizontal installation of each T5 in the corresponding hole (Fig. 10.2c).

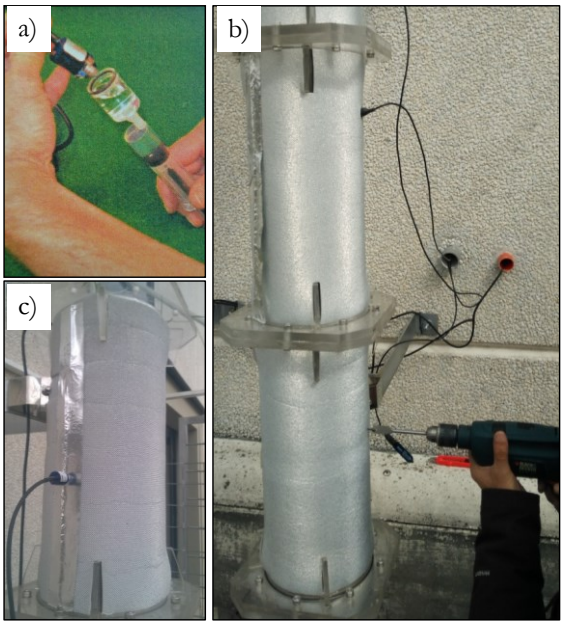

Figure 10.2 Phases of the installation process of mini-tensiometers T5: a) saturation of tensiometer; b) picture of drilling a designed hole along plexiglass column; c) T5 installed in hole.

T5 characteristics:
Range of pore water pressure measures: -100 kPa to +85 kPa (suction values are positive);
Accuracy: ±0.5 kPa;
Ceramic tip: Al_2O_3 sintered of 5mm diameter and 6mm length;
Connecting cable: 1.5m of length.
Mini-tensiometers do not need calibration process, nevertheless cavitation problems needed to be avoided during monitoring period. Cavitation is the creation of a new cavity or the expansion of a preexisting cavity in a liquid (Young, 1989). When soil suction is quite high, air bubbles can enter trough the ceramic tip inside the body of tensiometer and thus suction measurements become not more reliable.
Frequently mini-tensiometers were pulled out from the corresponding hole in order to check the degree of saturation and, if air bubbles were observed, the tensiometer were re-saturated.

10.1.2 Volumetric Water Content measurements: SM100 sensors (Waterscout)

Soil volumetric water content (VWC) is indirectly measured with two different methods called respectively Time Domain Reflectometry (TDR) and Frequency Domain Reflectometry (FDR).
TDR probe transmits electromagnetic waves to a probe, which reflects them to a receiver that records the velocity of propagation and amplitude of the signal. The instrument provides a moisture content reading in units of volume. The instrumentation is quite expensive and specific calibration is required for organic and saline soils. Additionally, special measures have to be taken to install the probes (e.g. by digging trenches) when measuring at depths of more than 50/60 cm, especially in clay soils.
Frequency domain reflectometry (FDR) is a precise, automated and easy method for measuring soil water content by measuring the capacitance and conductivity at a fixed frequency. A sine-wave current is passed through a resistance made up of two electrodes and the soil acts as the dielectric medium. The dielectric properties of the soil are estimated on the basis of the tension measured between two electrodes and the phase difference between the current and the tension. The electrodes may be of various shapes (laminar, ringed or cylindrical).

FDR probes, were selected for this experimental study because they resulted an economical and user friendly solution.
SM100 (Waterscout) is a very compact capacitive probe, suitable for measuring the soil volumetric water content (VWC), both on field or in soil column. The sensor is composed of two electrodes that function as a capacitor, with the surrounding soil serving as the dielectric. An 80 MHz oscillator drives the capacitor and a signal proportional to the dielectric permittivity of soil is converted to an output signal that is then converted to volumetric water content. The probe itself converts this signal into a continuous voltage, compatible with the majority of data-loggers. The SM100 combines affordability and accuracy into a sensor that is easy to install due to its pointed laminar shape (Fig. 10.3).

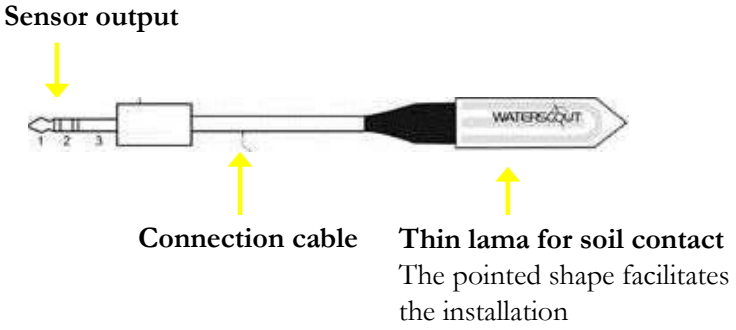

Figure 10.3 Schematization of SM100 sensor (Waterscout).

In this experimental study 7 SM100 sensors were used, respectively 4 installed in vegetated column (V) and 3 installed in no-vegetated column (NV), the same as mini-tensiometers.
The installation process was the same adopted for mini-tensiometers, as previously described in depth.
SM100 characteristics:
Range of VWC measures: 0% to saturation ;
Resolution: 1% VWC;
Accuracy: ±3%;
Oscillator frequency: 80MHz;
Dimensions: 6cm x 2cm x 0.3cm
Connecting cable: 6m of length.

Despite SM100s were provided already with calibration, they have been re-calibrated because of the many uncertainties associated with reliability and representativeness of measurements.
Some authors in past have calibrated TDR probes in unsaturated pyroclastic soils for field monitoring (Papa & Nicotera, 2011; Reder et al., 2016).
However, no literature contributions on the calibration of SM100 probes (FDR) in pyroclastic soils were available since they have not been used on field, hence they were opportunely calibrated on pyroclastic soils used in this experimental study.

10.1.3 SM100 sensors (Waterscout) calibration

The Calibration procedure adopted was opportunely designed for this study taking into account the peculiarities of pyroclastic soils and the dimension of sensors as well as their shape.
A plastic cylinder with inner diameter of 59.5 mm and an height of 85.0 mm was filled with pyroclastic soil used in this experimental study at different volumetric water content values and thus each sensor was introduced for reading the electrical signal in output (η).
First, the sensor was introduced in the cylinder full of water to obtain the upper boundary of the signal (η_w) and then was left in the air to obtain the lower boundary (η_a).
Then, the cylinder was filled with the moist tamping method (Ladd, 1977) by fixing the target bulk density equal to that used for soil columns in Chapter 5, and by changing the volumetric water content. For each sensor 8 specimens with different VWC values have been realized and a correlation between η and the VWC has been carried out Figure A.4a shows a correlation between readings of η and the fixed VWC during calibration of sensor number 1 (SM100_1), where also lower and upper value of η are reported. During calibration of all sensors it was observed that only the sensor SM100_1 had different boundaries compared to those of remaining sensors. In fact in Figure 10.4b are reported the calibration points η-VWC for other 3 sensors (SM100_2, SM100_3, SM100_4). Hence, two calibration curves have been carried out: the first related to sensor SM100_1 and the second for remaining sensors.

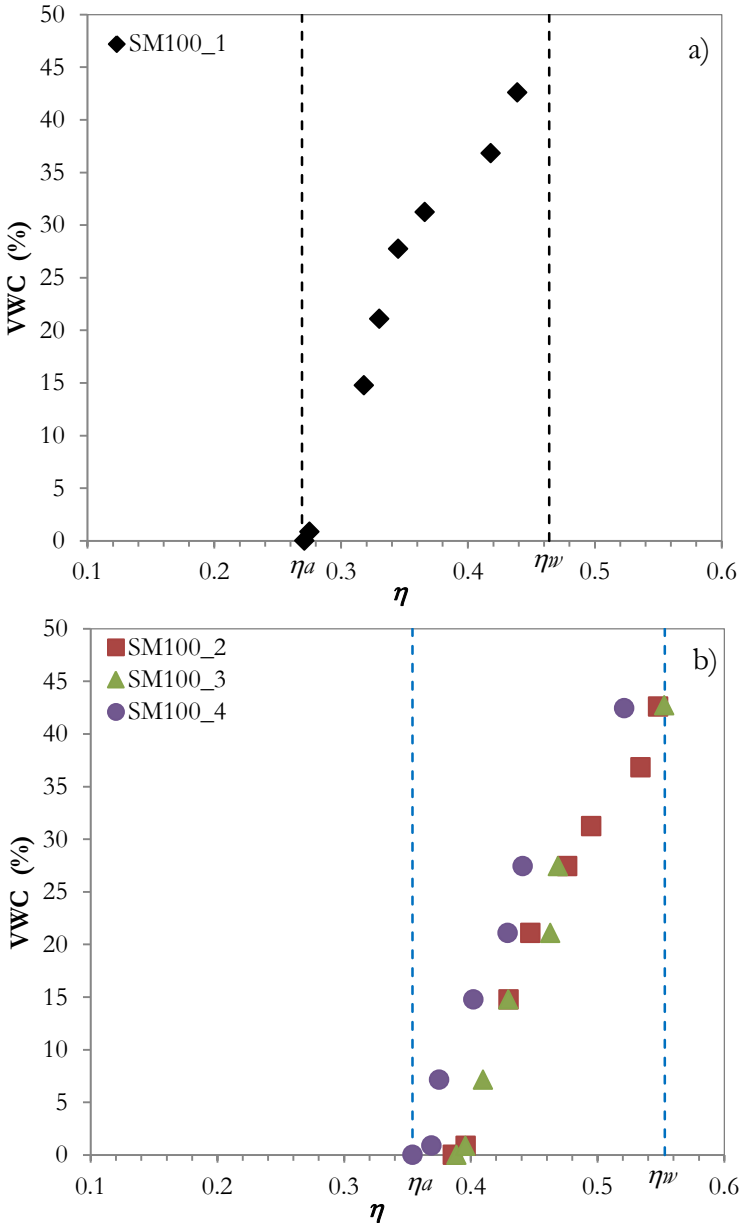

Figure 10.4 Calibration points for sensor a) SM100_1 and b) SM100_2, SM100_3, SM100_4 where η is the output electrical signal with η_a its lower boundary and η_w upper boundary, VWC is the fixed volumetric water content.

For a fair comparison, the relative electrical signal (η_{rel}) was introduced. This parameter varies between 0 and 1 and it takes into account the differences between boundaries η_w and η_a of electrical signal in output by all sensors. The equation describing η_{rel} is the following:

$$\eta_{rel} = \frac{\eta - \eta_a}{\eta_w - \eta_a}$$

Thus, the volumetric water content readings in terms of η_{rel} can vary from a minimum of 0 up to a maximum of 1. Two Fitting curves were carried out for sensor SM100_1 (Fig. 10.6a) and the remaining sensors (Fig. 10.6b).
The equation of both the fitting curves was a function with 4 calibration parameters and it had this form:

$$VWC(\%) = a \cdot \left(\eta_{rel}\right)^{2.5} + b \cdot \left(\eta_{rel}\right)^{2} + c \cdot \left(\eta_{rel}\right)^{1.5} + d$$

where η_{rel} is the relative electrical signal and *a,b,c,d* are the calibration parameters.
In Table 10.1 are summarized the calibration parameters used.

Table 10.1 Calibration parameters for polynomial fitting equation.

Sensor	Calibration parameters			
ID	**a**	**b**	**c**	**d**
SM100_1	261.71	-566.12	354.84	-0.72
SM100_2				
SM100_3	279.97	-559.64	329.32	-1.15
SM100_4				

In conclusion, each punctual measurement in terms of VWC (%) provided by sensors during monitoring period and during hydraulic tests reported in Chapter 6, was the result of calibration process described in depth in this Appendix.

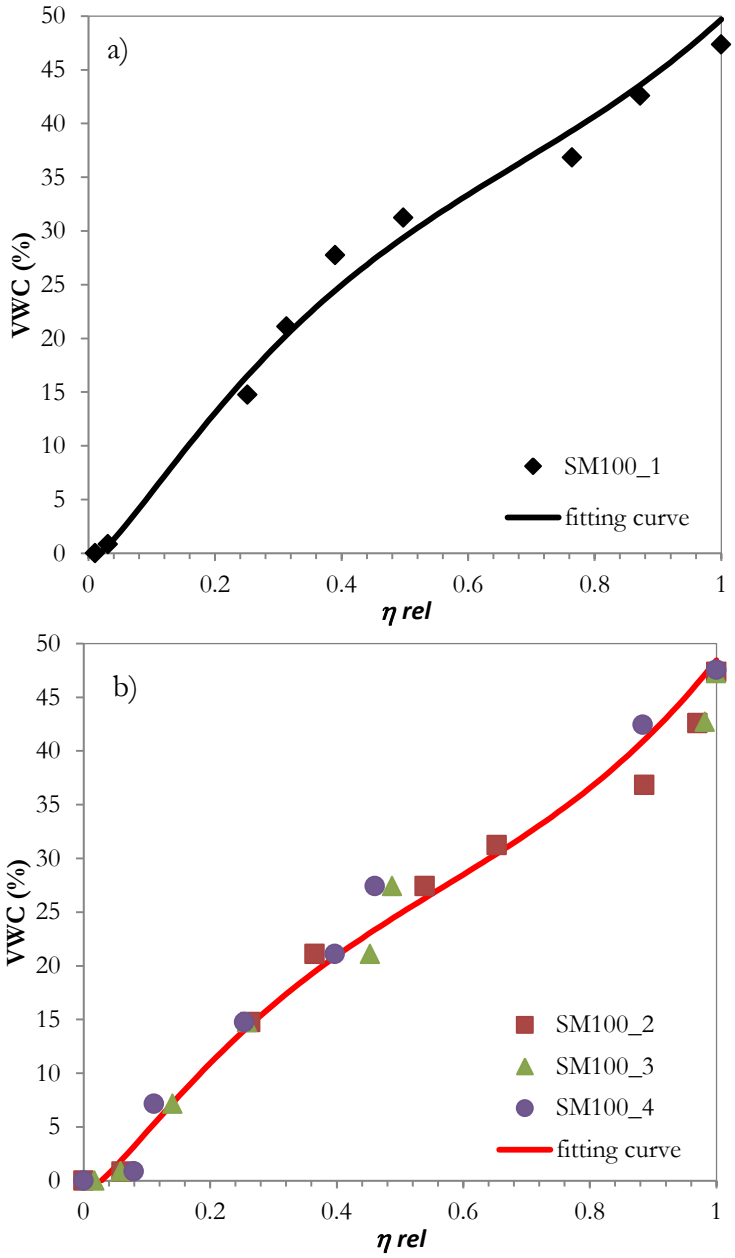

Figure 10.5 Measured points and fitting curves for a) sensor SM100_1 and b) sensors SM100_2, SM100_3, SM100_4.